universität wien

DISSERTATION

Titel der Dissertation

Selective translation of leaderless mRNAs by specialized ribosomes upon MazF-mediated stress response in *Escherichia coli*.

Verfasserin

Martina Sauert

angestrebter akademischer Grad

Doctor of Philosophy (PhD)

Wien, 2015

Studienkennzahl lt. Studienblatt:	A 094 490
Dissertationsgebiet lt. Studienblatt:	Molekulare Biologie
Betreut von:	Assoz. Prof. Mag. Dr. Isabella Moll

Contents

Abstract

During a lifetime bacteria have to deal with a number of stresses due to changes in their environment. Besides the general stress response via reprogramming of the transcriptional machinery, our lab has recently identified a novel post-transcriptional mechanism, which is mediated by a so called toxin-antitoxin (TA) module.

The toxin MazF, whose activity is triggered by various stress conditions, cleaves RNAs at single-stranded ACA sequences. In general, this activity leads to degradation of bulk mRNA. Intriguingly, some distinct mRNAs are cleaved at ACA-sites directly upstream of the start codon and thereby rendered 'leaderless' as they lack the 5'-untranslated region. In addition, MazF targets the 16S rRNA of intact ribosomes, resulting in the removal of its 3'-end harboring the anti-Shine-Dalgarno sequence. Consequently, these specialized ribosomes are selective for translation of leaderless mRNAs. Taken together, activation of MazF under adverse conditions results in the translation of a distinct set of mRNAs, which represents a novel paradigm for a translationally regulated stress response and exemplifies the importance of ribosome heterogeneity for regulation of gene expression.

The major focus of my PhD project is the determination of the 'leaderless mRNA regulon', i.e. the subset of mRNAs, which are selectively translated upon MazF activation. In this course, I also aim to further characterize the physiological relevance of the MazF-mediated stress response and to estimate the extent and functionality of ribosome heterogeneity. To this end, I developed a method to isolate intact and full length mRNAs after mazF over-expression from polysomes which represent the translatome. Comparison of the translatome with the transcriptome after the stress reveals the so far underestimated significance of selective translation as a regulatory mechanism in gene expression during stress.

Zusammenfassung (Abstract in German language)

Bakterien müssen sich fortwährend an die verschiedensten Veränderungen in ihrer Umwelt anpassen. Abgesehen von der gut untersuchten generellen Stressantwort auf Basis der Reprogrammierung der Transkription, wurde in unserem Labor ein neuartiger post-transkriptioneller Mechanismus charakterisiert, welcher durch ein sogenanntes Toxin-Antitoxin (TA) Modul herbeigeführt wird.

Das Toxin MazF, welches durch diverse Stressbedinugngen aktiviert wird, schneidet RNAs an einzelsträngigen ACA-Sequenzen. Prinzipiell führt dies zum Abbau des Großteils aller mRNAs in der Zelle. Erstaunlicherweise werden einige bestimmte mRNAs nur an ACAs kurz vor dem Startkodon geschnitten, wodurch ihre 5‘-nichtranslatierte Region entfernt wird und sie zu sogenannten „leaderless mRNAs“ prozessiert werden. Zusätzlich entfernt MazF auch ein kleines Stück des 3‘-Endes der 16S rRNA von intakten Ribosomen, welches die anti-Shine-Dalgarno-Sequenz beeinhaltet. Die so entstandenen spezialisierten Ribosomen sind dadurch selektiv für die Translation von „leaderless mRNAs“. Zusammenfassend führt die Aktivierung von MazF durch diverse Stressbedingungen zur selektiven Translation einer distinkten Gruppe an mRNAs, welche wir das „leaderless mRNA Regulon“ nennen. Dieser Mechanismus repräsentiert ein neuartiges Modell für eine translational regulierte Stressantwort und ist ein außergewöhnliches Beispiel für die Funktionalität von Ribosomenheterogenität.

Das Hauptaugenmerk meiner Dissertation liegt darauf, erstmals das „leaderless mRNA Regulon“ zu bestimmen und die physiologische Stressreaktion, die durch MazF hervorgerufen wird, weitergehend zu charakterisieren. Dabei untersuche ich auch das Ausmaß und die Bedeutung von Ribosomenheterogenität. Zu diesem Zwecke habe ich eine Methode zur Isolierung von intakten und vollständigen mRNAs aus Polysomen, welche das Translatom repräsentieren, entwickelt. Meine vergleichenden Analysen von Transkriptom und Translatom unter Stressbedingungen zeigen die bisher unterschätzte Bedeutsamkeit selektiver Translation als regulatorisches Element in der Genexpression.

I. Introduction

I.1. Protein synthesis

Gene expression, comprising the selected transcription of a chosen gene by an RNA-polymerase and the subsequent translation of the resulting mRNA into a protein by the ribosomes, is the most essential process in all living cells and represents the central dogma of biology.

I.1.1. Eukaryotic gene expression

I.1.1.a) Eukaryotic transcription

In eukaryotic organisms, from yeast to humans, the genome is organized in linear chromosomes, densely packed with histone proteins into nucleosomes, and localized in the membrane enclosed nucleus. Transcription is performed by three different RNA-polymerases (RNAP) in the nucleus: RNAP I transcribes most of the ribosomal RNAs (rRNA), RNAP III transcribes a small portion of rRNA and transfer RNAs (tRNA), and RNAP II is responsible for messenger RNA (mRNA) transcription and for transcription of small regulatory RNA species. In the last decade, even two additional RNAPs, IV and V, have been identified in plants, playing a role in small interfering RNA (siRNA) pathways and RNA-directed DNA methylation, respectively (Herr et al., 2005; Onodera et al., 2005; Pontes et al., 2009).

Eukaryotic primary transcripts are co- and post-transcriptionally modified by addition of a 5'-terminal cap-structure and a 3'-terminal poly-adenin (poly(A))-tail to ensure their stability. They frequently contain so-called introns, poly-nucleotide stretches that interrupt the protein-coding sequence and whose excision is driven by a process called splicing. Alternative splicing can generate various variants of an RNA by excising different introns from one precursor RNA. Additionally, many RNA molecules are transcribed as pre-mature versions and have to be further processed by site-specific cleavage events and many RNAs have to be edited by the addition of chemical modifications to be fully functional. Completely processed mRNAs are finally exported to the cytoplasm where translation by ribosomes takes place.

I.1.1.b) Eukaryotic translation

Eukaryotic ribosomes are built of a large 60S (S for Svedberg, a unit for sedimentation rate) subunit (LSU) and a small 40S subunit (SSU). The 60S ribosomal subunit is made up by 5S, 5.8S and 28S rRNA and 46 ribosomal proteins (RPs). The 40S subunit consist of one 18S rRNA and 33 RPs, respectively. A crystal structure for the 80S ribosome from

Saccharomyces cerevisiae was solved at 3.0 Å resolution in 2011 by Yusupov and co-workers (Ben-Shem et al., 2011; Yusupova and Yusupov, 2014). Translation is a complex and well regulated process which involves several initiation factors (eIFs), elongation factors (eEFs), release factors (eRFs), and recycling factors (Dever and Green, 2012; Hinnebusch and Lorsch, 2012).

Generally, eukaryotic translation initiation starts with the formation of a ternary complex (TC) in which the initiator tRNA ($tRNA_i$) coupled with methionine ($Met\text{-}tRNA_i^{Met}$) is bound to eIF2, a GTPase in its GTP (guanosine triphosphate)-bound state. *Via* this TC the $tRNA_i$ is recruited to the 40S ribosomal subunit, forming the 43S pre-initiation complex (PIC) (Hinnebusch and Lorsch, 2012). Formation of this 43S PIC is strongly enhanced by additional factors, such as eIF3 (Pestova and Kolupaeva, 2002). Translation initiation is then achieved by binding of the 43S PIC to the capped 5'-end of an eukaryotic mRNA and scanning along the transcript in 5'-3'-direction until it encounters a start codon (Lomakin and Steitz, 2013). Once the PIC is correctly positioned at the start codon, it is joined by the 60S ribosomal subunit to form the translation competent 80S ribosome. These events are accompanied by transient interactions with 12 eIFs and additional auxiliary factors (Jackson et al., 2010). Only under distinct conditions or on certain transcripts eukaryotic translation initiation is not mediated by this scanning mechanism but can occur internally in a cap-independent manner at so called internal ribosome entry sites (IRES) (Jang, 2006).

The step of translation elongation is well conserved in pro- and eukaryotes (Rodnina and Wintermeyer, 2009) and the individual steps can be assigned to distinct tRNA binding sites: The aminoacyl (A)-site, where decoding occurs and the correct aminoacyl-tRNA (aa-tRNA) is selected on the basis of the mRNA codon displayed, the peptidyl (P)-site, which carries the peptidyl-tRNA, and the exit (E)-site, which binds exclusively deacetylated tRNAs that are exiting the ribosome (Burkhardt et al., 1998). Thus, the ribosome translocates from the A-site to the E-site along the mRNA transcript in order to translate the message. The elongation cycle is shown in detail in Figure I.1.1. The aa-tRNA is recruited to the ribosomal A-site by elongation factor eEF1A (Figure I.1.1, purple tRNA) which is subsequently recycled by eEF1B. Next, the growing peptide chain on the tRNA in the P-site (Figure I.1.1, green tRNA) is transferred to the newly bound aa-tRNA by a reaction in the peptidyl-transferase center (PTC) that is exclusively formed by rRNA of the large subunit. This feature earned the ribosome the title ribozyme as the catalytic reaction is performed by RNA. Subsequently, the ribosome translocates one codon downstream on the mRNA assisted by eEF2, which does not require a recycling factor, and the A-site is again available for the next elongation cycle (Dever and Green, 2012).

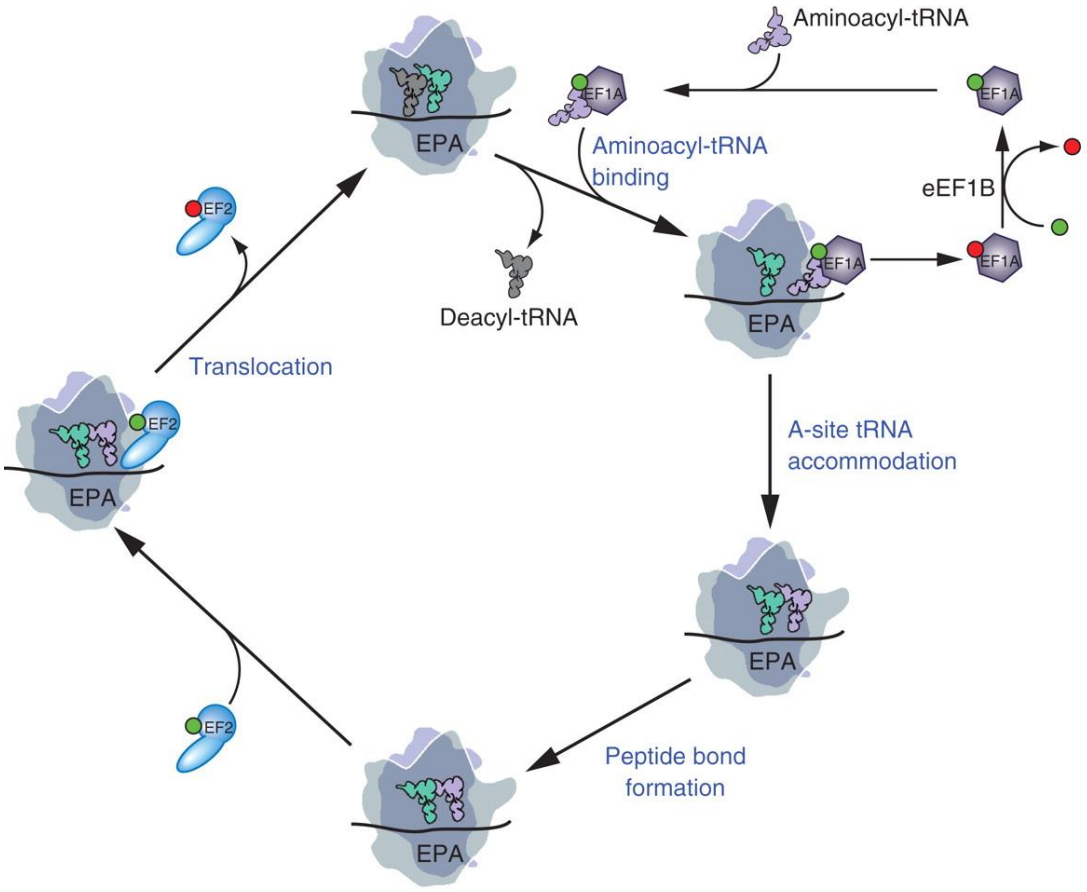

Figure I.1.1: Translation elongation in eukaryotes. The aa-tRNAis recruited to the 80 S ribosome as an eEF1A-GTP-aa-tRNA and positioned in the A-site. Following release of eEF1A-GDP, the aa-tRNA is accommodated into the A-site, and the eEF1A-GDP is recycled to eEF1A-GTP by the exchange factor eEF1B. Peptide bond formation is accompanied by translocation of the A-site tRNA to the P-site promoted by binding of eEF2·and following release of eEF2-GDP, which unlike eEF1A does not require an exchange factor. The ribosome is now ready for the next cycle of elongation. GTP and GDP are depicted as a green and red ball, respectively. Taken from Dever and Green (2012).

Translation elongation continues until the ribosome encounters a stop codon for which no corresponding tRNA exists. Instead of a tRNA the eRF enters the A-site and triggers the dissociation of the two ribosomal subunits from the mRNA to set the subunits and the produced polypeptide free. The recycling process of the two subunits is even more complex and involves the ATPase ABCE1 (Nürenberg and Tampé, 2013).

Eukaryotic transcription and translation are disconnected in space and time since the nucleus restricts the area of transcription. mRNAs, tRNAs, and rRNAs are synthesized in the nucleus and even the assembly of the ribosomal subunits occurs majorly here. Upon export of the ribosomal subunits, their assembly on mRNA 5’-ends and subsequent translation occurs in the cytoplasm. This decoupling of events in gene expression comprises opportunities for a vast variance of regulatory mechanisms.

I.1.2. Prokaryotic gene expression

Prokaryotes do not contain a nucleus or any other membrane enclosed intracellular structure and therefore gene expression is arranged in a “one-pot” reaction. Transcription and translation are tightly coupled, meaning that ribosomes can initiate translation on a nascent mRNA that is still being produced by RNA-polymerase (Miller et al., 1970).

I.1.2.a) Prokaryotic transcription

In contrast to eukaryotes, transcription in prokaryotes is performed by only one RNAP being much less complex than its eukaryotic counterpart. The core RNAP is composed of two α-subunits, two β-subunits, β and β’, and the ω-subunit (Borukhov and Severinov, 2002). The $\alpha_2\beta\beta'\omega$ core is by itself able to perform DNA-dependent RNA synthesis but it cannot bind to DNA promoter regions. For this purpose the core complex is transiently joined by the σ-subunit, the DNA-binding element that guides the RNAP to the desired promoter region. Thus, it comprises an important layer of transcription regulation as alternative σ-factors are available (Burgess et al., 1969, also see chapter I.3.1).

Prokaryotic mRNAs don’t possess extensive terminal structures like the eukaryotic 5’-cap or poly(A)-tail. RNAP produces the primary transcripts with a 5’-triphosphate group and a 3’-hydroxyl group (-OH). As prokaryotic mRNAs do not necessarily require any further modifications they can be used as template for translation while still being transcribed by RNAP. In order to do so ribosomes binds to the mRNA and translate it, even sometimes catching up with RNAP.

I.1.2.b) The prokaryotic ribosome

The ribosome is, as in eukaryotes, the highly conserved molecular machinery that performs the essential process of translation and it is centre of intensive research since the 70ies (Lake, 1976). The tremendous universal significance of the ribosome in all living organisms is also reflected by the joint award of the Nobel Prize in Chemistry 2009 to Venkatraman Ramakrishnan, Thomas A. Steitz and Ada E. Yonath "for studies of the structure and function of the ribosome". The prokaryotic ribosome is smaller and less complex than the eukaryotic one and a crystal structure of the *E. coli* ribosome at 3.5 Å was obtained in 2005 by Schuwirth and co-workers (Schuwirth et al., 2005).

Two unequal subunits with distinct functions in translation built up the bacterial ribosome (Kaczanowska and Rydén-Aulin, 2007). The small 30S subunit is composed of 21 RPs (blue ribbons in Figure I.1.2A) and the 16S rRNA (translucent gray spheres in Figure I.1.2A) and approximately half the molecular weight of the large subunits. Its main function in translation is the initiation of the interaction with the mRNA and the decoding

of the message. The 30S structure can be divided into an upper part, the head domain and a lower part, the body connected by the neck region (denoted as cleft in Figure I.1.2A). Viewed from the interface side, as shown in Figure I.1.2A, one can appreciate the platform where the anti Shine-Dalgarno sequence (see next chapter) is located.

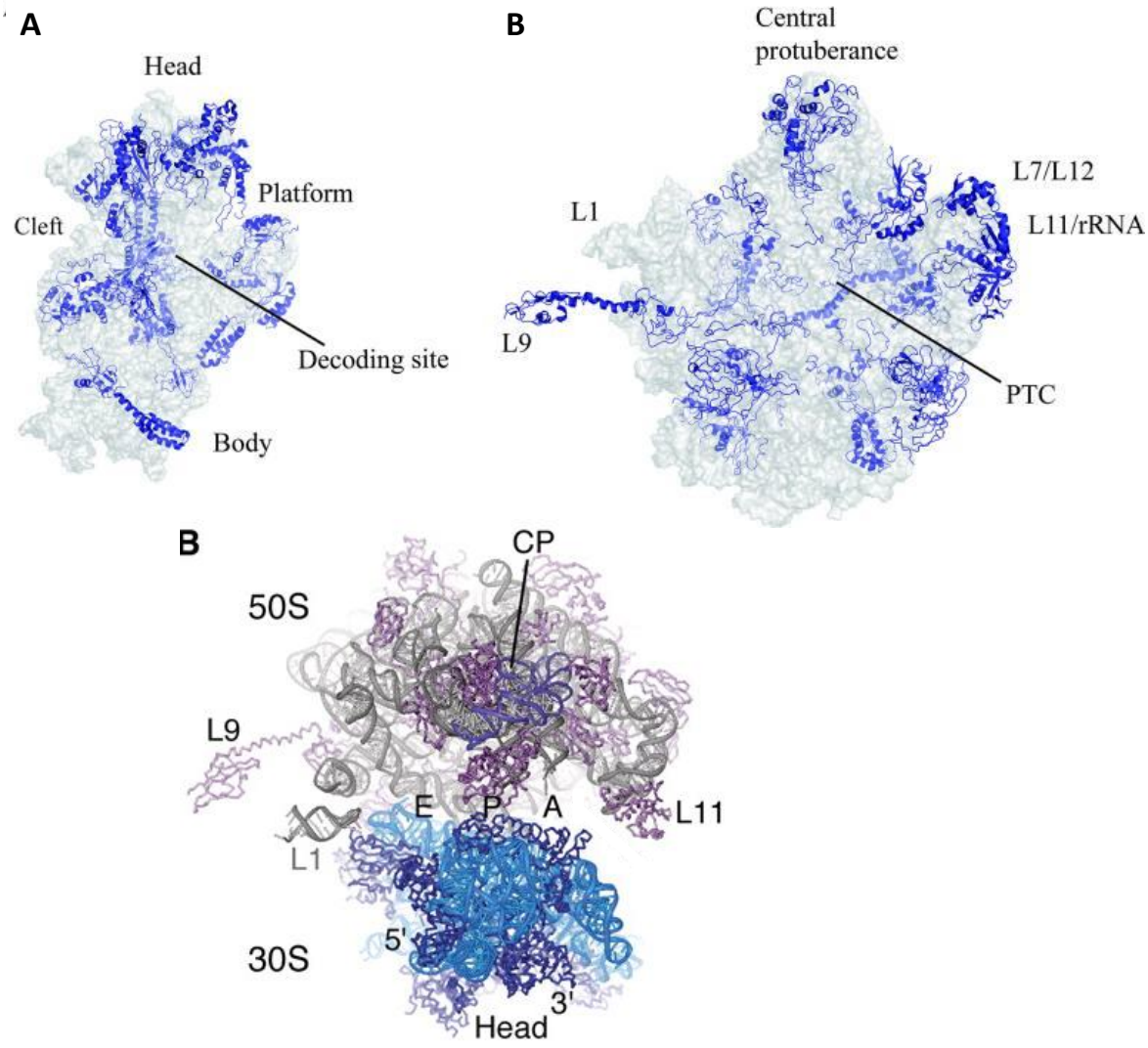

Figure I.1.2: Structure of the 70S ribosome of *Escherichia coli*. Tertiary structures of the 30S (**A**) and 50S (**B**) subunits, seen from the interface side. The structures are adapted from Schuwirth et al. (2005) and were modeled by Kaczanowska and Rydén-Aulin (2007). rRNA is shown as translucent gray spheres, and ribosomal proteins are shown as blue ribbons. The positions of the decoding site in tha 30S subunit and of PTC in the 50S subunit are indicated. (**C**) Tertiary structure of the assembled 70S ribosome, from Schuwirth et al. (2005). rRNA and proteins in the 30S subunit are colored light blue and dark blue, respectively. 23S rRNA and proteins in the 50S subunit are colored gray and magenta, respectively. 5S rRNA is colored purple. The central protuberance (CP) is indicated and the letters mark the approximate alignments of the A-, P-, and E- sites at the subunit interface.

The large 50S subunit, built up by 33 RPs (blue ribbons in Figure I.1.2B), the 5S and 23S rRNA (translucent gray spheres in Figure I.1.2B), is the site of reaction where the peptidyl transfer takes place and the growing polypeptide chain passes through. Viewed again from the interface side three main structural feature become apparent: the central protuberance (CP in Figure I.1.2C), including the 5S rRNA, the left L1 and the right L11/rRNA arm. In Figure I.1.2B the binding site of the L7/L12 tetramer is indicated at the L11/rRNA arm though not visualized in the crystal structure due to its high flexibility. Likewise, the flexible protein L9 is indicated. The PTC is indicated in the middle of the interface side of the 50S subunit, entirely composed of rRNA. Right below the PTC begins the polypeptide exit tunnel, constituting a path for the nascent polypeptide chain out of the ribosome, which can accommodate approximately 40 amino acids (Moore and Steitz, 2003; Yonath et al., 1987).

Figure I.1.2C illustrates the assembled 70S ribosome (Schuwirth et al., 2005) and indicates the A-, P- and E-site at the subunit interface where the translated mRNA will be positioned *via* extensive RNA-RNA interactions (Hennelly et al., 2005; Selmer et al., 2006).

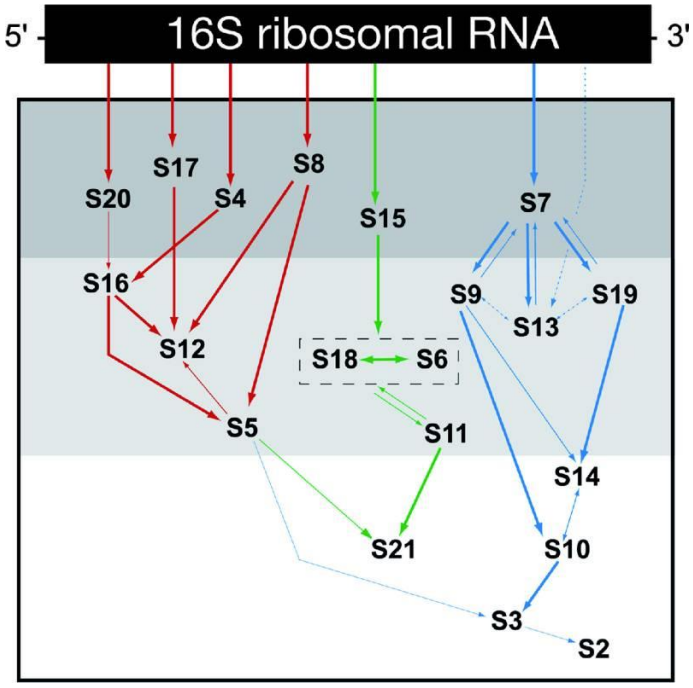

Figure I.1.3: Assembly map of the 30S ribosomal subunit. Taken from Culver (2003) and modified by Kaczanowska and Rydén-Aulin (2007). The binding order of the RPS to the 16S rRNA (black rectangle) is shown. The blue area indicates the primary binding proteins, the light blue area indicates the secondary binding proteins, and the white area indicates the tertiary binding proteins. The thick, thin, and dashed arrows show strong, weak, and very weak interactions between the proteins, respectively. Proteins S6 and S18 bind as a complex and are therefore enclosed in a dashed box. Red arrows indicate the assembly of the body, green arrows indicate the platform, and blue arrows indicate the head.

The assembly and maturation of the ribosomal subunits is a very complex process involving rRNA processing and multiple transient interactions with so-called biogenesis factors. The three rRNAs, 5S, 23S and 16S, are transcribed as one single primary transcript and are separated by guided RNAse III and RNAse E cleavages (Kaczanowska and Rydén-Aulin, 2007). Concomitantly, the rRNAs are further modified at several positions by conversion of uridine to pseudouridine (ψ), methylation or addition of other chemical groups (Decatur and Fournier, 2002). Likewise, RPs are chemically modified by acetylation and methylation (Arnold and Reilly, 1999; Kaczanowska and Rydén-Aulin, 2007).

The hierarchical and cooperative binding of RPs to the rRNA could be fully reconstituted for the bacterial ribosome *in vitro* (Culver and Noller, 1999) and RPs were grouped primary, secondary and tertiary binding proteins. Figure I.1.3 shows the binding hierarchy of RPs of the small subunit to the 16S rRNA. The assembly of the 50S subunit is much more complex and grouping of RPs in dependence of the binding hierarchy is more difficult (Herold and Nierhaus, 1987). *In vivo*, these processes require the supplemental action of additional proteins, so-called biogenesis factors. Biogenesis factors are RNA chaperones, RNA helicases, ribosome-dependant GTPases and others (Kaczanowska and Rydén-Aulin, 2007).

Taken together, ribosome biogenesis is a very complex process that is highly regulated at multiple levels (Kaczanowska and Rydén-Aulin, 2007). rRNA and RP modifications, the various maturation steps and the final RP composition in the ribosome pose an additional regulatory hub in the translation specificity of the ribosomes as heterogeneous ribosomes with variable modifications can emerge as discussed by (Sauert et al., 2014) (chapter 2.4).

I.1.2.c) Prokaryotic translation

Prokaryotic translation initiation

Translation initiation in prokaryotes differs considerably from eukaryotes. Initiation requires only three initiation factors (IF1 to IF3) and is not achieved by binding to the 5'-end of an mRNA and the scanning mechanism, the ribosome rather initiates directly at close proximity of the start codon by direct rRNA-mRNA interaction. Prokaryotic mRNAs possess the so called Shine-Dalgarno (SD) sequence with a consensus sequence of 5'-AGGAGG-3' approximately four to 14 nucleotides upstream of the start codon (Shine and Dalgarno, 1974). The 30S ribosome can bind directly to this SD sequence *via* the anti-Shine-Dalgarno (aSD) sequence (5'-ACCUCCUU-3'), a complement to the SD sequence on the 3'-end of the 16S rRNA. Upon binding of the mRNA to the SSU, the bacteria-specific $tRNA_i$ coupled with a formylated methionine (fMet-$tRNA_i^{fMet}$), herein referred to as $tRNA_i$ is recruited by IF2 and positioned at the ribosomal P-site where it interacts with the start

codon (see Figure I.1.4). Accuracy of the codon-anticodon recognition is controlled by IF3, while IF1 stimulates the activity of IF2. The complex of mRNA, 30S ribosome, IF2, and fMet-tRNA$_i^{fMet}$ presents the prokaryotic PIC. Subsequently, the 50S ribosome joins the PIC and IF3 dissociates to result in the elongation-prone 70S initiation complex (IC) (Simonetti et al., 2009). Interestingly, the exact chronological order of the PIC assembly is still a matter of debate and seems not to be strictly determined, as an alternative initiation mechanism *via* an initial formation of a 30S-IF2-tRNA$_i$-complex prior to mRNA binding has been proposed (Jay and Kaempfer, 1974). Nevertheless, it is generally agreed that prokaryotic translation initiation is achieved by the 30S subunit alone.

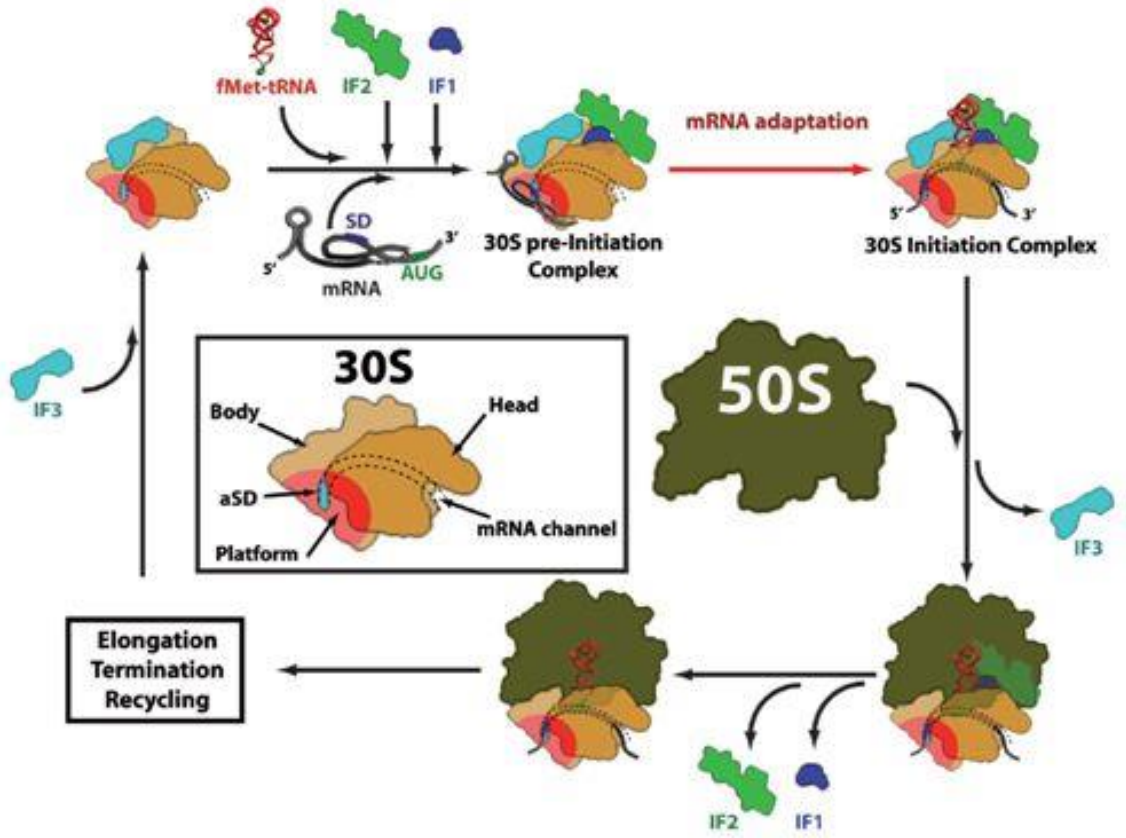

Figure I.1.4: Scheme of bacterial translation initiation. Prokaryotic translation initiation starts with recruitment of the tRNA$_i$ (depicted in red) by IF2 (green), stimulated by IF1 (blue), to the mRNA (gray) bound via SD-aSD interaction to the 30S subunit (light brown) which is kept in its dissociated state from the 50S subunit by binding of IF3 (cyan). This PIC is joined by the 50S subunit (dark green) after dissociation of IF3 if proper positioning of the tRNAi at the start codon was verified. Subsequently elongation starts upon dissociation of IF1 and IF2. Recycling of the ribosomal subunits is amongst others achieved by binding of IF3 to the 30S subunit which is then ready for the next initiation (Simonetti et al., 2009).

Prokaryotic translation elongation, termination and recycling

As introduced in chapter I.1.1.b) the mechanism of translation elongation in principle is well conserved in pro- and eukaryotes. In prokaryotes recruitment of the aa-tRNA to the ribosomal A-site is achieved by EF-Tu (thermo unstable) and translocation assisted by EF-G (Agirrezabala and Frank, 2009). The formation of the first peptide bond is supplementary stimulated by EF-P. It binds the 70S ribosome between the P-site and the E-site where it helps to properly orient the fMet-tRNA$_i^{fMet}$ in the P-site for efficient peptidyl transfer to the second aa-tRNA in the A-site (Blaha et al., 2009). Whereas the process of peptidyl transfer and translocation is in general very similar, termination and recycling differ in prokaryotes. Upon encountering a stop codon, either release factor 1 (RF1) or RF2 recognizes the stop codon and triggers hydrolysis of the ester-bond in the peptidyl-tRNA situated in the P-site resulting in the release of the synthesized polypeptide chain from the ribosome (as shown in Figure I.1.5). Next, the GTPase RF3 stimulates the rapid dissociation of RF1 or RF2 from the ribosome (Zavialov et al., 2001). The two subunits and the mRNA of the post-termination complex are then disassembled with the help of the ribosome recycling factor (RRF) together with IF3 (Korostelev, 2011).

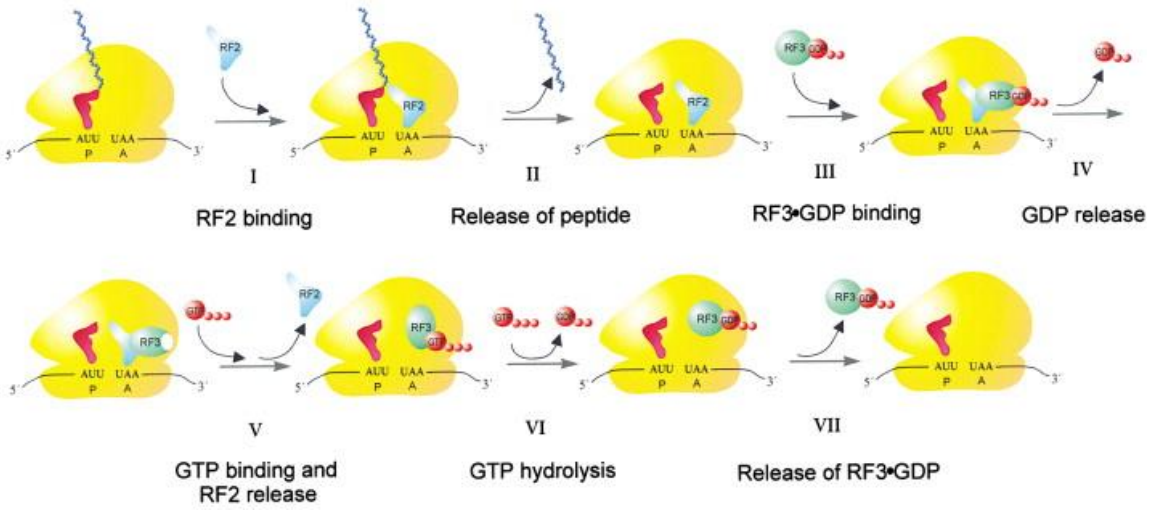

Figure I.1.5: Translation termination in prokaryotes. Binding of RF2 (blue) triggers the release of the polypeptide chain (blue helix) from the preceding tRNA (red) and thus from the ribosome (yellow) (steps I and II). Subsequently, RF3 (green) stimulates the release of RF2 from the ribosome by a series of GDP/GTP (red spheres) binding, hydrolysis and dissociation events (Zavialov et al., 2001).

If a ribosome translates an mRNA that is lacking a proper stop codon it cannot enter into the termination mechanism and is stalled at the actual 3'-end, thus it cannot initiate on another mRNA. At this point a rescue mechanism, named trans-translation, kicks into play involving a molecule that jointly mimics a tRNA and an mRNA: the tmRNA (Moore and Sauer, 2007). The tmRNA is a structural chimer of an alanine-coupled tRNA and a

short mRNA (short stable RNA A, *ssrA*) encoding a degradation tag. The alanyl-tmRNA in complex with EF-Tu-GTP and the protein SmpB (small protein B) binds to the stalled ribosome and the nascent polypeptide chain is transferred to the alanine on the tmRNA (see Figure I.1.6). Subsequently, translation continues on the mRNA provided by the tmRNA, the degradation tag is added to the defective protein (Moore and Sauer, 2007) and RF/RF2-mediated termination releases the peptide and dissociates the ribosomal subunits for a next round of initiation. The SsrA-tagged proteins are immediately degraded by proteolytic complexes (see chapter I.1.3.d).

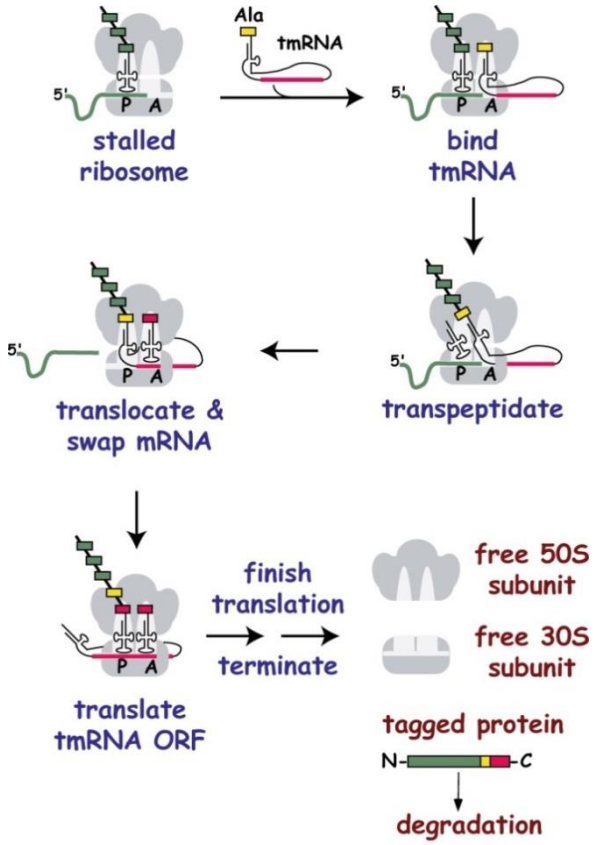

Figure I.1.6: Rescue of stalled ribosomes by trans-translation. The alanyl-tmRNA binds to the stalled ribosome and the nascent polypeptide chain is transferred to the alanine (yellow rectangle). Subsequently, the tmRNA ORF (red) is translated, and termination releases the tagged protein for degradation and liberates the 30S and 50S subunits (Moore and Sauer, 2007).

Translation initiation on leaderless mRNA

Besides the usually occurring mRNAs that contain a 5'-untranslated region (UTR) with a SD sequence, another class of mRNAs has been discovered in all domains of life that lack the 5'-UTR, so-called leaderless mRNAs (lmRNAs) (Moll et al., 2002a). These lmRNAs cannot be translated *via* the conventional SD-aSD-mediated initiation mechanism. However, lmRNAs are translated (Wu and Janssen, 1996) and initiation at the 5'-terminal start codon can be achieved by a proposed 30S-IF2-$tRNA_i$ complex (Grill et al., 2000; Moll et al., 2002a) or by 70S ribosomes (Balakin et al., 1992; Moll and Bläsi, 2002; Moll et al., 2004). Further studies confirmed the lmRNA translation by 70S monosomes (Moll et al., 2002a, 2004; O'Donnell and Janssen, 2002; Udagawa et al., 2004). Furthermore, the 5'-terminal AUG start codon seems to be the sole prerequisite for lmRNA recognition (Brock et al., 2008; Van Etten and Janssen, 1998).

Additionally, several results evidence that IF2 stimulates (Grill et al., 2000) and IF3 antagonizes lmRNA translation initiation (Moll et al., 1998a; Tedin et al., 1999). Thus, the molecular ratio of IF2 to IF3 plays a decisive role whether the ribosome selects a 5'-terminal start codon or not (Grill et al., 2001). In this context Moll and co-workers have hypothesized that relative IF3 deficiency at high growth rate and/or transiently elevated levels of IF2 ,for example during cold shock, lead to an increase in lmRNA translation in response to altered environmental conditions (Grill et al., 2001). Another player in regulation of lmRNA translation seems to be the RP S1 whose binding to the ribosome is dependent of S2 (Byrgazov et al., 2012, 2015; Moll et al., 2002b). S1 is not required for 30S-initiation complex formation on leaderless mRNA *in vitro* (Tedin et al., 1997) but rather mediates the IF3-dependent discrimination of lmRNAs (Moll et al., 1998b).

I.1.3. Regulation of bacterial gene expression

Gene expression can be influenced at every level starting with guided transcription of a specific gene and post-transcriptional modification of the transcript that can influence mRNA stability or localization. Further downstream, translation efficiency can be regulated by interfering RNA or protein factors or by intrinsic mRNA structures. Finally, protein levels are post-translationally influenced by their inherent stability and by regulated degradation.

I.1.3.a) Regulation of transcription

Very direct means to regulate gene expression is provided by operons in which all necessary genes for one particular pathway are controlled by one promoter which can be activated or repressed in response to the presence or absence of specific metabolites. Well known examples are the *lac* or the *trp* operons, responsible for lactose catabolism and tryptophan synthesis, respectively (Beckwith, 1967; Youderian and Arvidson, 1994). As all operons these confer only very constricted responses to very specific needs.

Regulons however, are a collection of genes under joint regulation by the same regulatory factor provide regulatory opportunities for a broader range of adjustments. The SOS response pathway, for example, confers DNA repair mechanisms as a reaction to DNA damage (Shinagawa, 1996). Over 20 genes involved in DNA repair contain a regulatory region that is specifically bound by the SOS repressor LexA leading to repression of those genes under neutral conditions. The second protein in this response mechanism, the co-protease RecA, is activated by binding of single stranded DNA, a signal for DNA damage. Active RecA leads to cleavage of the SOS repressor LexA thus allowing transcription of the SOS inducible genes (Shinagawa, 1996). By this intricate regulon mechanism a manifold reaction is induced by activation of a single protein.

An even broader level of response is provided by the use of alternative σ-factors of RNAP (introduced in chapter I.1.2.a). The canonical σ-subunit is σ^{70} (RpoD) belonging to the σ^{70} family and guiding RNAP to constitutive “housekeeping” promoters which control genes needed during exponential growth (Paget and Helmann, 2003). σ^{70} is the most abundant amongst the σ-factors and the one with the highest affinity to RNAP (Jishage et al., 1996). Yet, bacteria possess several alternative σ-factors, most also belonging to the σ^{70} family, and others belonging to the σ^{54} (RpoN) family. Members of the σ^{54} family differ in their mechanism of promoting transcription initiation from σ^{70} family members in a way that they require an additional activating protein and ATP (Buck et al., 2000). σ^{54}, for example, guides RNAP to σ^{54} specific promoters, controlling genes for nitrogen utilization.

More alternative σ-factors and their functions are summarized in Table I.3.1 of chapter I.3.1.

As the σ-factors play crucial roles in response to environmental cues expression of their mRNAs, mRNA stability or translation efficiency is also tightly regulated. Another means to regulate alternative σ-factor functions is the use of anti-σ-factors that compete for binding to RNAP (Hughes and Mathee, 1998).

Transcription can also be regulated by interference with small RNAs. 6S RNA, for example mimics an open promoter complex and sequesters σ^{70}-containing RNAP, but not σ^{S}-containing RNAP (Wassarman, 2007). As 6S is highly abundant during stationary phase it comprises an additional means to regulate transcription in non-exponential growth conditions.

I.1.3.b) Post-transcriptional regulation

Post-transcriptional control of gene expression was long underestimated and research of the last decade has shown the immense impact of post-transcriptional modifications on final protein synthesis.

mRNA stability and decay

Compared with eukaryotic mRNAs prokaryotic mRNAs have relatively short half lives, usually in the order of a few minutes which is shorter than the organism's doubling time (Bernstein et al., 2002). The high mRNA turnover generally contributes to the ability of bacteria to quickly adapt to changing environmental conditions (Laalami et al., 2014). How exactly mRNA degradation is initiated is still under scientific debate, one model suggesting the endoribonuclease RNase E as a general initiator and scaffold for subsequent degradation. Upon initial endoribonucleolytic cleavage by RNase E the affected mRNA is then quickly degraded by an RNase E associated multi-enzyme complex, the degradasome, consisting of the exoribonuclease, polynucleotide phosphorylase (PNPase), the RNA helicase RhlB, and the glycolytic pathway enzyme, enolase (Carpousis, 2007).

In contrast to mRNAs, rRNAs and tRNA are relatively stable RNA molecules that are only degraded under certain conditions or when they are defective (Deutscher, 2003). Factors conferring to mRNA stability are secondary structure, RNA sequence, translational efficiency and binding by proteins or other RNAs. The only common features of prokaryotic mRNAs conferring relative transcript stability are the 5'-terminal triphosphate (Mackie, 1998) and the 3'-terminator loop-structure. However, the 5'-terminal triphosphate can be converted to a monophosphate by the pyrophosphohydrolase RppH that preferentially acts on single-stranded 5′ termini (Celesnik et al., 2007). The 3'-ends,

protected by secondary structures or not, can be polyadenylated by poly(A) polymerase (PAP I) which marks the respective mRNA for degradation (Régnier and Hajnsdorf, 2009). This multitude of opportunities for regulation makes mRNA decay such a powerful tool in regulation of gene expression by transcript specific degradation in response to external stimuli.

Additionally, binding of sRNAs can target an mRNA for degradation by creating a cleavage site for nucleases, as described in the following chapter.

I.1.3.c) Regulation of translation

Regulation of protein synthesis usually happens during initiation and can be achieved by specific sequence and/or structural features of the respective mRNAs, which influence their translation. More frequently, additional molecules, like RNA-binding proteins or non-coding RNAs (ncRNAs), interact with the mRNA and influence its translation.

mRNA-intrinsic sequence features

A rather simple level of translation regulation is based on the sequence of the mRNA's 5'-UTR. The SD-sequence, responsible for the initial interaction with the ribosome (see chapter I.1.2.c), can be a relatively weak or a relatively strong sequence for translation initiation, depending on the complementarity with the aSD sequence on the 16S rRNA and the distance to the respective start codon (Osada et al., 1999). Likewise, the start codon of the protein-coding region influences the efficiency of translation initiation, in which AUG is usually the strongest start codon (Nie et al., 2006).

Additionally, the mRNA sequence can influence the efficiency of translation elongation. Stretches of codons for a particular amino acid can act as a sensor for the availability of that amino acid and translation of the message is stalled during amino acid deprivation. Likewise, the use of many low-abundant codons in one particular mRNA can slow down translation elongation (Akashi and Gojobori, 2002). Furthermore, the Wilson lab has shown ribosome stalling at polyproline coding regions of mRNAs, due to the property of proline to be a poor donor and acceptor for peptide bond formation (Starosta et al., 2014). Interestingly, stalling at the polyproline site can be rescued by the EF-P (introduced in chapter I.1.2.c) (Doerfel et al., 2013).

Very different examples of mRNA-intrinsic structural features that interfere with their translation are riboswitches. The 5'-UTR is composed of an aptamer region, which binds a ligand (pink in Figure I.1.7), and the so-called expression platform (orange in Figure I.1.7), which folds into a certain structure that either conceals or reveals the ribosome binding site (RBS) to block or allow translation. Direct binding of an effector molecule, which could be a metabolite or an ion, to the mRNA results in a differentially folded structure

that then oppositely reveals (right side in Figure I.1.7) or sequesters (right) the RBS to allow or hinder translation (Breaker, 2012). A well know riboswitch in *E. coli* is the *thiM* riboswitch that binds the coenzyme thiamine pyrophosphate (TPP) in order to negatively control translation of the enzyme hydroxyethylthiazol kinase involved in thiamine metabolism (Rentmeister et al., 2007).

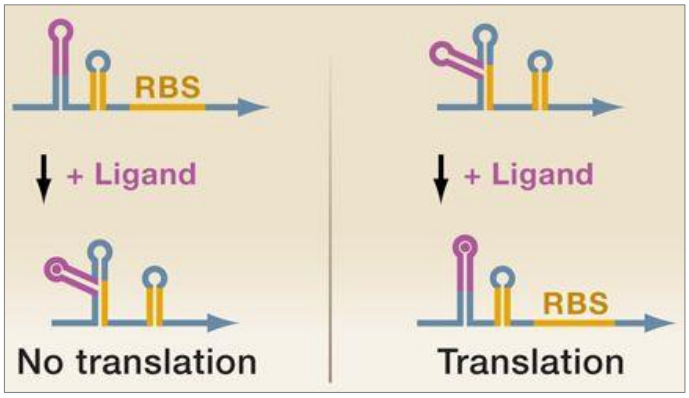

Figure I.1.7: Schematic depictions of the two modes of action of riboswitches. The aptamer region is indicated in pink, the expression platform in orange. Left: In the absence of ligand, the RBS is accessible, but upon ligand binding, is sequestered into an inhibitory stem-loop, preventing translation. Right: In the absence of ligand, the expression platform forms a repressive secondary structure in which the ribosome binding site is occluded. When the ligand binds to the aptamer region, the ribosome binding site is released and translation can initiate (Waters and Storz, 2009).

Translation regulating proteins

In some cases binding of a protein to the RNA can lead to inhibition of translation. This regulatory mechanism is exemplified by the auto-regulation of some RPs. Excess of free RPs that are not incorporated in ribosomes leads to their own translational repression (Dennis et al., 2004). Likewise is the translation of the hexameric Host Factor I (Hfq) negatively auto-regulated by Hfq-binding to its own 5'-UTR (Vecerek et al., 2005).

Regulatory small non-coding RNAs

Regulatory RNAs, like micro RNAs (miRNAs) and siRNAs are a wide spread and common feature in eukaryotes and play pivotal roles in regulation of gene expression. Although the first sRNA to regulate translation in *E. coli* was reported already in 1984 (Mizuno et al., 1984) the high abundance and functional significance of regulatory sRNAs in bacteria has only come to light in the last decade. sRNAs can exert regulatory functions in various manners. They can bind to proteins and thus modulate their activity, as reported for the sRNA GlmY, which titrates a protein factor away from its actual target RNA (Görke and Vogel, 2008) or more frequently they can bind to other RNAs in order to regulate their transcription, stability or translation (Waters and Storz, 2009).

sRNAs that are encoded in *cis* on the opposite strand partially overlapping with their targets act as antisense RNAs by extensive base pairing (Brantl, 2007). Annealing of the antisense RNA to its target can either lead to transcription termination, degradation of the target or to inhibition of translation as described for type I toxin-antitoxin systems (see chapter I.2).

A far better known class of sRNAs is encoded in *trans* and shows less complementarity to their targets (Waters and Storz, 2009). Nevertheless, binding of the sRNA to its target mRNA can either lead to mRNA degradation or obscure the RBS, thus hindering translation initiation (see Figure I.1.8, middle and left panel, respectively). However, stimulation of translation can also occur if binding of the sRNA to its target opens a secondary structure in 5'-UTR that has previously blocked the RBS (right panel in Figure I.1.8,). These sRNA-mRNA interactions in *trans* often need the assistance of the RNA chaperone Hfq (Zhang et al., 2003a).

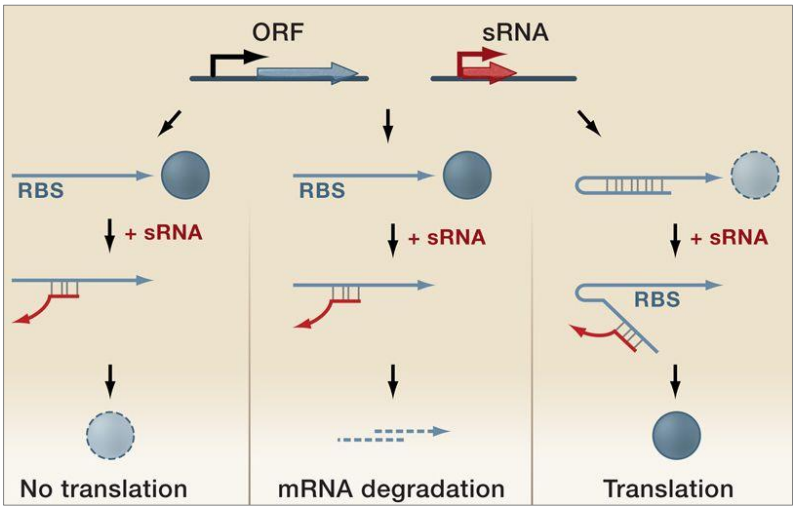

Figure I.1.8: Translational regulation by sRNAs. The *trans*-encoded sRNAs (red) bind to their target RNAs (blue) with different effects. They can block translation by base pairing with the 5' UTR and obscuring the RBS (left panel) or target the sRNA-mRNA duplex for degradation by RNAses (middle panel). Translation stimulation can be achieved by preventing the formation of an inhibitory structure, which would sequester the RBS (right panel) (Waters and Storz, 2009).

For instance, the sRNA RyhB is an intensively studied Hfq dependent sRNA involved in regulation of iron homeostasis. Under iron-rich conditions the expression of RyhB is repressed by the activity of the transcription regulator Fur. Fur however, is inactive during iron-deprivation, thus leading to elevated levels of RyhB in response iron starvation (Massé and Gottesman, 2002; Vecerek et al., 2007). As a result, RyhB represses around 20 different mRNAs encoding iron-dependent proteins by binding to the mRNAs and promoting their recruitment to the degradosome (introduced in chapter I.1.3.b) (Massé

et al., 2003). Thus, RyhB expression during iron starvation contributes to the increase of cellular free iron by reducing the expression of iron-dependent proteins (Jacques et al., 2006). One target of RyhB-mediated mRNA degradation is the *acnB* mRNA as will be discussed in chapter I.4.1.a).

I.1.3.d) Protein turnover

The final level of regulation of protein synthesis is the regulation of the protein levels themselves by controlled degradation. Controlled degradation means energy-dependent proteolysis which is mediated by AAA^+ proteases (ATPases associated with various cellular activities). These proteases combine ATP-consuming unfolding activity (ATPase) with the degradation of proteins. *E. coli* possesses several classes of AAA^+ proteases including Clp proteases, FtsH and Lon.

The main enzymes catalyzing protein degradation are proteases of the caseinolytic protease (Clp) family. In *E. coli* these proteolytic complexes usually consist of two kinds of Clp proteases, one of which is the ATPase (e.g. ClpA or ClpX), the second the protease (e.g. ClpP) and the subunits are arranged in rings forming a barrel-shaped complex (Gottesman, 2003). However, the ATPase itself, can also function as a stabilizing chaperone when not part of the proteolytic complex (Wawrzynow et al., 1995). Targets for degradation by the proteolytic complexes are mainly unfolded proteins and SsrA-tagged proteins resulting from trans-translation (see chapter I.1.2.c). However, some proteases like ClpXP recognize specific peptide motifs (Flynn et al., 2003) and therefore can degrade particular proteins upon activation, like the antitoxin MazE (see chapter I.2.2.a).

FtsH is the only protease essential for viability. Unlike the other proteases it is anchored to the inner membrane but still forms hexameric complexes similar to other proteases (Langklotz et al., 2012; Tomoyasu et al., 1995). FtsH is to a minor extend involved in degradation of SsrA-tagged proteins but seems to play an important role in quality control of membrane proteins (Langklotz et al., 2012). Interestingly, FtsH is involved in the degradation of the heat shock σ-factor σ^{32} (see chapter I.1.3.a) and thus plays an additional role in the fine tuning and recovery from the heat shock response.

The cytoplasmic serine protease Lon also contains an ATPase domain and a proteolytic domain. Lon is less involved in general degradation of unfolded proteins but has regulatory functions in many biological processes in bacteria (Tsilibaris et al., 2006) including degradation of the antitoxin MazE (see chapter I.2.2.a).

I.2. Toxin-antitoxin systems in prokaryotes

Toxin-antitoxin (TA) systems are genetic elements occurring in almost all prokaryotic species (Pandey and Gerdes, 2005). They simultaneously encode a stable toxin and an unstable antitoxin, neutralizing the toxicity of the cognate toxin. Generally, when the expression of the cassette is shut off, the stable toxin remains in the cell, whereas the labile antitoxin is degraded thus leading generally to cell death due to the –now uninhibited– toxic activity of the toxin. TA systems have originally been identified as plasmid encoded cassettes ensuring plasmid maintenance during cell division (reviewed by (Jensen and Gerdes, 1995). In this context, cells that did not receive the plasmid encoding the TA cassette upon division die as they cannot inhibit the toxic proteins by *de novo* synthesis of the neutralizing antitoxins. Homologs of plasmid encoded TA systems have later also been found on the chromosome of many bacteria and archea (Pandey and Gerdes, 2005).

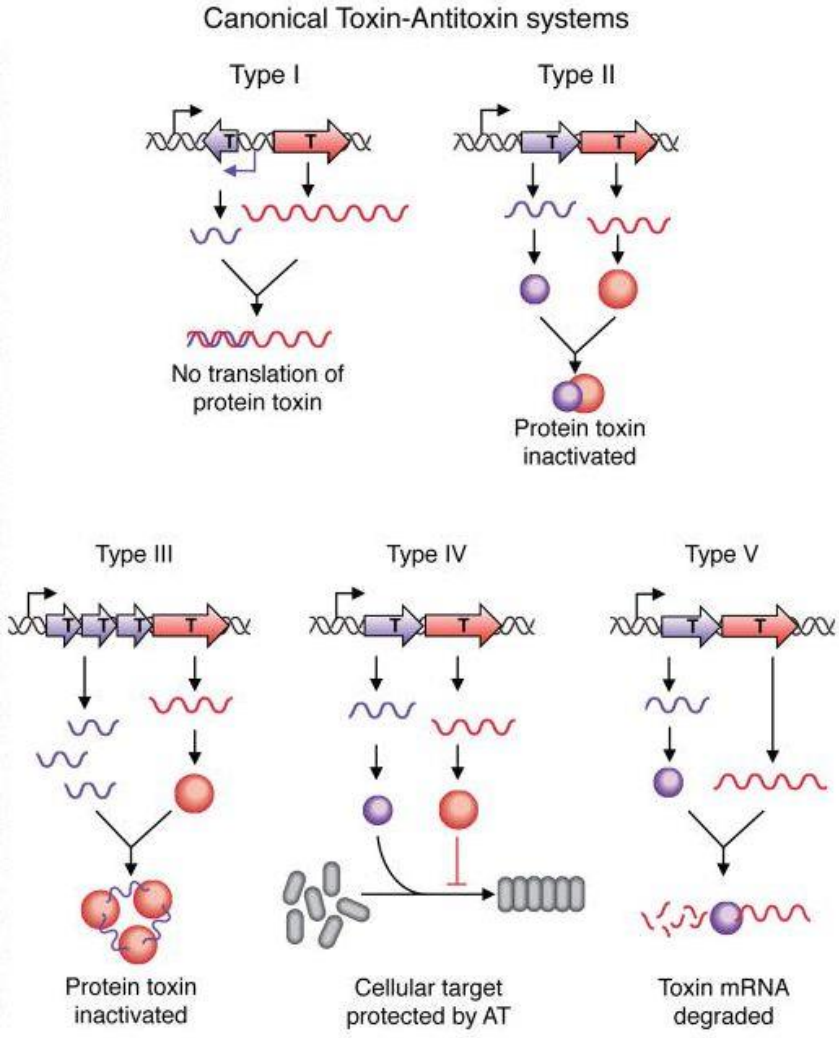

Figure I.2.1: Modes of action of the five classes of TA systems. Antitoxins are depicted in purple, toxins in red. Taken from Markovski and Wickner (2013).

Five types of TA systems have been described so far wherein the toxins in all classes are proteins with various activities and the classification relies on the nature of the antitoxin component. Figure I.2.1 gives a graphical overview over the modes of function of the five types of TA systems.

The antitoxins in type I and III TA modules are ncRNA molecules. In most of the cases of type I TA systems are the genes encoding the toxic protein and the antitoxin RNA located on opposite strands and they often partially overlap (Fozo et al., 2008). Usually, the antitoxin RNA binds to the toxin mRNA and leads either to translation inhibition of the toxin by masking the SD sequence of the toxin mRNA (as introduced in chapter I.1.3.c) and/or to degradation of the toxin mRNA. One example for a type I TA module is the pair Hok (host killing) - Sok (suppressor of host killing), first denoted *par* and originally found on R1-plasmids (Fozo et al., 2008). Later several homologs of Hok-Sok were identified on plasmids in Gram-negative bacteria and also on the chromosome of *E. coli* (Pedersen and Gerdes, 1999) and other species.

In the only recently defined type III class of TA systems the antitoxin ncRNA inhibits the function of the toxin by binding to the protein. As shown for the type III module *toxIN*, originally identified on a plasmid of the Gram-negative phytopathogen, *Pectobacterium atrosepticum,* three molecules of *toxI* antitoxin ncRNA bind three molecules of toxin ToxN protein into a triangular structure, thus inhibiting the toxins (Blower et al., 2011; Fineran et al., 2009).

In types II, IV and V the antitoxin component is a protein. Type II TA systems are the most abundant and most studied ones and types IV and V are each represented only by one example so far. Type IV antitoxin YeeU prevents the toxin YeeV from binding to its targets, the cytoskeleton proteins FtsZ and MreB (Tan et al., 2011) and type V antitoxin GhoS is a ribonuclease cleaving the corresponding toxin mRNA *ghoT* (Wang et al., 2012).

I.2.1. Type II toxin antitoxin systems

Type II TA systems seem to be widespread amongst the prokaryotic classes and are often present in several copies on the bacterial genomes (Pandey and Gerdes, 2005). Here, the antitoxin is an unstable protein that sequesters the toxin by direct protein-protein interaction ((Van Melderen, 2010; Williams and Hergenrother, 2012) and depicted in Figure I.2.2). The toxin and the antitoxin are usually encoded in an operon with the antitoxin gene upstream of the toxin gene and expression of both genes is often auto-regulated by the toxin-antitoxin complex (Bukowski et al., 2011).

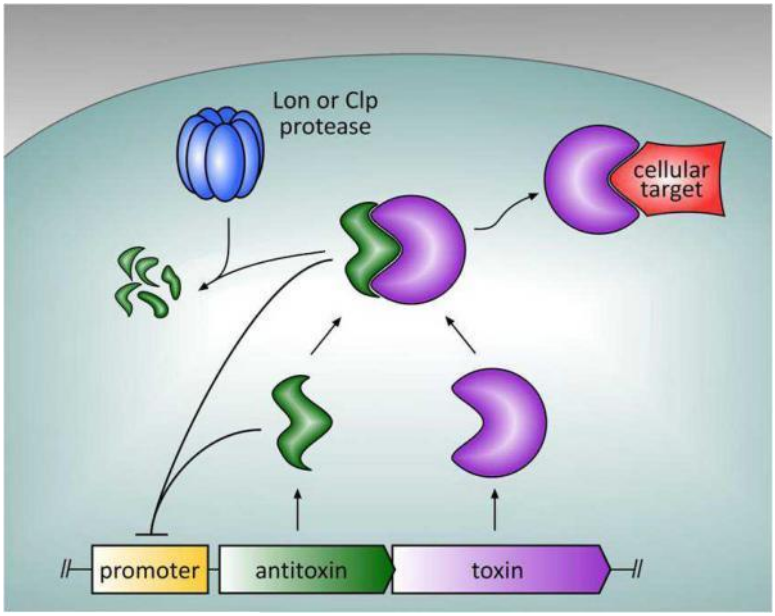

Figure I.2.2: Auto-regulation of type II TA systems. The toxin is depicted in purple, the antitoxin in green. Taken from Williams and Hergenrother (2012).

Exceptions for this genetic organization are the *higAB* locus, where the usual antitoxin-toxin gene order is reverted (Tian et al., 1996) and three-component TA systems like ω-ε-ζ (omega-epsilon-zeta), using ω as an transcriptional regulator instead of the toxin ζ and the antitoxin ε themselves (Zielenkiewicz and Ceglowski, 2005). The toxins of type II TA systems have so far been classified into ten toxin families which are summarized in Table I.2.1. However, several additional putative toxin families have been predicted by bioinformatic approaches (Leplae et al., 2011). This classification by the toxin component has been recently challenged by the observation of hybrid TA systems (Unterholzner et al., 2013) and the prediction of toxins without corresponding antitoxin (Leplae et al., 2011). Structural similarity of the type III toxin ToxN with the type II toxin MazF also lead to speculations about toxin or antitoxin shuffling between the TA types (Blower et al., 2011).

Most toxins target the processes of protein synthesis and the mechanisms by which they act vary from mRNA cleavage to interference with transcription and translation to inhibition of cell wall synthesis. The toxins VapC, MazF, RelE, and HicA are endoribonucleases, in which VapC specifically targets initiator $tRNA_i^{fMet}$ (Winther and Gerdes, 2011) and the others target mRNAs. While HicA does not have a consensus recognition motif (Jørgensen et al., 2009), the toxins of the MazF and RelE families are more specific. MazF and ChpBK, both members of the *mazEF* family, cleave mRNAs specifically at single stranded ACA or ACY (Y is U, A, or G) motifs, respectively (Zhang et al., 2003b, 2005). The members of the *relEB* family, namely RelE, YafQ (of the TA system *yafQ/dinJ*) and YoeB (*yefM/yoeB*) however, target mRNAs during translation in a

ribosome-dependent manner. They cleave the mRNA in the A site of the ribosome, in case of RelE with some preference for codons with G at the third position (Christensen and Gerdes, 2003). Interestingly, the toxicity of RelE can be counteracted by tmRNA (Christensen and Gerdes, 2003). Doc interferes with translation by associating to the 30S ribosome thereby stopping elongation (Liu et al., 2008) and HipA, being a protein kinase, was initially believed to phosphorylate EF-Tu, thus hindering its interaction with the tRNA (Schumacher et al., 2009). By now it has been shown that HipA rather phosphorylates glutamate-bound glutamyl-tRNA synthetase, thus inhibiting translation (Germain et al., 2013). Another kinase is the toxin ζ that phosphorylates a peptidoglycan precursor thus impairing cell wall synthesis (Mutschler et al., 2011). The toxins CcdB and ParE inhibit a subunit of the DNA topoisomerase gyrase leading to accumulation of double strand (DS) breaks and activation of the SOS response (Jiang et al., 2002; Miki et al., 1992).

Toxin	Anti-toxin	Target of toxin	Activity	Cellular process	Reference
CcdB	CcdA	DNA gyrase	Generates DS breaks	Replication	(Miki et al., 1992; Ogura and Hiraga, 1983)
ParE	ParD	DNA gyrase	Generates DS breaks	Replication	(Bravo et al., 1987; Jiang et al., 2002)
VapC	VapB	$tRNA^{fMet}$	Endoribonuclease	Translation	(Pullinger and Lax, 1992; Winther and Gerdes, 2011)
Doc	PhD	Translating ribosome	Induces mRNA cleavage	Translation	(Lehnherr et al., 1993; Liu et al., 2008)
HigB	HigA	Translating ribosome	ribosome-dependent mRNA cleavage	Translation	(Budde et al., 2007; Tian et al., 1996)
MazF (ChpA)	MazE	mRNAs & 16S rRNA	ribosome-independent mRNA cleavage	Translation	(Masuda et al., 1993)
RelE	RelB	Translating ribosome	ribosome-dependent mRNA cleavage	Translation	(Grønlund and Gerdes, 1999)
ζ	ε	UDP-Glc-NAC	Phospho-transferase	Peptido-glycan synthesis	(Meinhart et al., 2001; Mutschler et al., 2011)
HipA	HipB	GltX	Protein kinase	Translation	(Germain et al., 2013)
HicA	HicB	RNAs	ribosome-independent mRNA cleavage	Translation	(Jørgensen et al., 2009)

Table I.2.1: Summary of the ten toxin families of type II TA systems in order of their discovery. The targets, activity and cellular processes targeted by the toxins of the ten toxin families currently described are indicated. DS: double strand. Ccd: coupled cell division. Par: partitioning. Vap: virulent associated protein. Doc: death on curing. Phd: prevent host death. Hig: host inhibition of growth. Chp: chromosomal homologs for plasmid-encoded genes. UDP-Glc-NAC: uridine diphosphate-N-acetylglucosamine. Hip: high in persistence. GltX: glutamyl-tRNA synthetase. Hic: hif contiguous. All ten TA families have plasmid and chromosomally encoded homologs.

In all types of TA systems the antitoxin component is the less stable one and will be quickly degraded by cellular proteases or RNAses. Various external triggers can lead to inhibition of *de novo* expression of the module and/or to activation of antitoxin degrading proteases and RNAses, both resulting in accumulation of the toxin as shown in Figure I.2.2. This makes TA systems responsive to changing conditions in the environment and they can serve as stress response and survival mechanisms, which will be further discussed in chapter I.3.3.

A phylogenetic screen for chromosomal TA loci revealed that TA systems seem to be highly abundant in free-living bacterial cells but mostly devoid in host-associated prokaryotes, arguing that the constant environment of parasitic bacteria does not select for maintenance of the TA modules (Pandey and Gerdes, 2005).

I.2.2. Toxin-antitoxin modules in *Escherichia coli*

The *E. coli* genome encodes at least 36 TA loci (see Figure I.2.3) revealed by bioinformatic or biochemical studies out of which eight type II TA systems are well characterized: MazF–MazE and ChpBK–ChpBI belonging to the *mazE* family; RelE–RelB, YafQ–DinJ, and YoeB–YefM, which belong to the *relE* family and furthermore HipA–HipB, YafO–YafN, and MqsR–MqsA (Yamaguchi and Inouye, 2011). Other bacterial species, in particular pathogenic bacteria like *Mycobacterium tuberculosis* possess many more TA gen loci indicating that they might be of importance for virulence or in survival of the hosts immune response (Pandey and Gerdes, 2005).

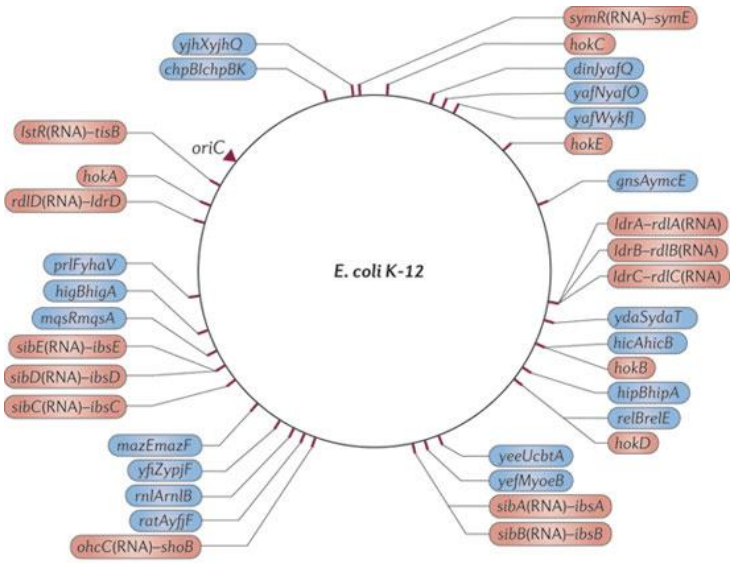

Figure I.2.3: Distribution of type I and II TA modules in the *E. coli* genome. Type I and type II TA modules are shown in orange and blue, respectively. For type I systems, the RNA antitoxin is indicated. Taken from Yamaguchi and Inouye (2011).

I.2.2.a) The toxin-antitoxin module mazEF in Escherichia coli

The type II TA module *mazEF* is one of the best studied TA systems in *E. coli* and is located in the *rel* operon downstream of the *relA* gene encoding the (p)ppGpp synthetase RelA. Amusingly, *mazE* was named after the Hebrew expression for 'what is it', namely "ma-ze", as it was initially identified as an ORF of unknown function downstream of *relA* (Metzger et al., 1988). Expression of *mazEF* is tightly negatively auto-regulated by either MazE alone as well as the MazE-MazF complex (Marianovsky et al., 2001). The auto-regulation mechanism has been further described by the identification of the MazE-MazF structure (Kamada et al., 2003). The MazE antitoxin homodimer inhibits the function of the toxic MazF homodimeric complex by binding of two MazF dimers *via* its unstructured C-terminal regions. This hexameric complex exists in solution and binds to the *mazEF* promoter with additional antitoxin dimers to repress its expression (see Figure I.2.4, (Kamada et al., 2003).

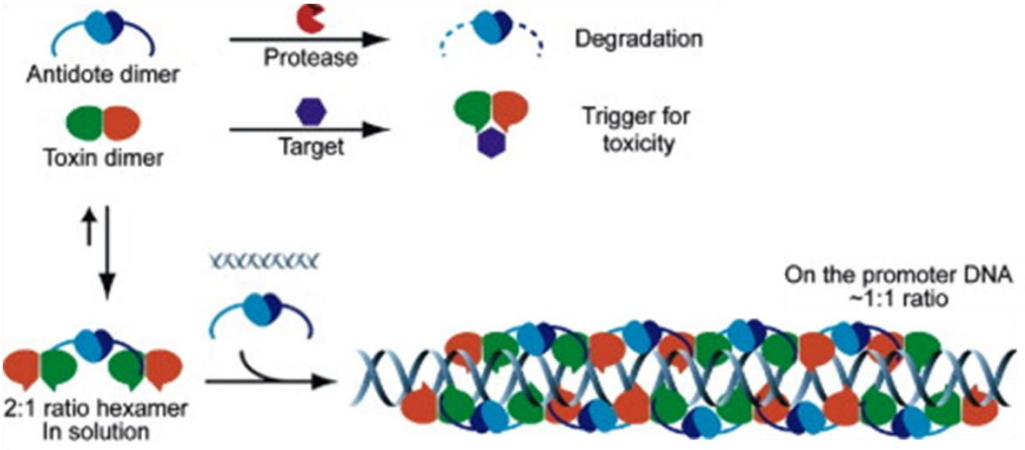

Figure I.2.4: Auto-regulation of *mazEF* expression by the MazE-MazF hetero-hexameric complex. Modified from Kamada et al. (2003).

Besides the transcriptional auto-regulation MazE and MazF levels are regulated in response to environmental stress. Upon diverse stress conditions RelA synthesizes (p)ppGpp subsequently activating ClpPX and Lon proteases which degrade the labile MazE (Aizenman et al., 1996). Degradation of the antitoxin sets the stable toxin MazF free to exert its toxic function (as represented Figure I.2.2). As an ACA-specific endoribonuclease MazF cleaves RNAs at single-stranded ACA-sites (Zhang et al., 2003b). MazF activity can thus be regulated in response to environmental changes and it is conceivable that it plays a role in stress response which will be further discussed in chapter I.3.3.a). However, it is until now under scientific debate if MazF activation leads to programmed cell death (PCD), proposed by the Engelberg-Kulka group (Aizenman et al., 1996) or if it rather induces reversible static conditions by inhibiting translation and replication (Pedersen et al., 2002).

I.3. Stress response in *Escherichia coli*

A bacterial population encounters a frequently changing environment and the cells have to adapt to various conditions like nutrient deprivation or alterations in temperature, osmolarity and pH in order to survive. Thus, bacteria have evolved many mechanisms to regulate gene expression in response to various signals and therefore to adapt protein levels to specific needs.

The prerequisite for regulation of gene expression in response to external signals is the sensing of the stress and the signal transduction into the cell and to the place of adjustment. This task is mainly achieved by two-component systems (TCSs) that are wide spread in bacteria, as well as archea, yeast and also plants. TCSs basically consist of a membrane bound homo-dimeric histidine kinase (HK) with an extracellular sensor domain and of an intracellular response regulator (RR) that can be phosphorylated at an aspartate (Asp) residue by the HK in order to transmit the signal (Casino et al., 2010). As this phosphorylation is reversible, the response can be easily shut on and off. The subsequent signal transduction *via* the phosphorylated RR is mainly accomplished by direct transcriptional regulation of target genes, but can likewise involve the regulation of protein-protein interactions or enzyme activity.

I.3.1. The general stress response

A well known mechanism to adapt to various stressful conditions is the use of alternative σ-factors in order to modulate transcription, introduced in chapter I.1.3.a). *E. coli* features six alternative σ-factors which are summarized in Table I.3.1. Most of them target gene expression in a rather specific manner, inducing transcription of a very distinct set of genes, like for example σ^{32} for the heat shock response (reviewed by (Sharma and Chatterji, 2010). σ^{32} guides transcription to over 20 heat shock response genes encoding the molecular chaperones DnaK, DnaJ, GrpE, GroEL and GroES or proteases (Arsène et al., 2000).

σ-family	σ-factor	gene	Function of regulated genes
σ^{70}	σ^{70}	*rpoD*	Housekeeping functions
	σ^{38}	*rpoS*	General stress response
	σ^{32}	*rpoH*	Heat shock
	σ^{E}	*rpoE*	Cell envelope integrity
	σ^{FecI}	*fecI*	Iron uptake
	σ^{28}	*rpoF*	Flagella synthesis
σ^{54}	σ^{54}	*rpoN*	Nitrogen regulation

Table I.3.1: Summary of alternative σ-factors in *E. coli*.

The general stress response, induced by various conditions such as stationary growth phase, nutrient starvation, low temperature, high osmolarity, and oxidative stress is triggered by σ^{38} (*rpoS*), also referred to as RpoS, the stationary phase or stress σ-factor.

In general, alternative σ-factors are tightly negatively regulated so that they do not compete with σ^{70} for the core RNAP. The same is true for RpoS being very low abundant during exponential growth which is achieved by tight post-transcriptional regulation and rapid protein turnover by proteases such as ClpP (Lange and Hengge-Aronis 1994; Hengge-Aronis 2002). *rpoS* mRNA possesses a 567 nucleotides (nts) long 5'-UTR that folds into a stem-loop structure occluding the SD-sequence thereby generally shutting down *rpoS* translation under normal conditions. This inhibitory structure can be overcome by interaction of *trans*-encoded sRNAs with the help of the RNA chaperone Hfq (reviewed in Battesti, Majdalani et al. 2011). Additionally, RpoS is stabilized and its binding to RNAP favored by high concentrations of (p)ppGpp, the signaling molecule during the stringent stress response (see chapter I.3.2).

Once activated RpoS regulates approximately 500 genes during stress, posing more than 10% of the *E. coli* genome, in a direct or indirect manner (Weber, Polen et al. 2005).

I.3.2. The stringent response

The stringent response is a bacterial survival mechanism in response to amino acid starvation by which the metabolism is reduced to a minimum in order to overcome the nutrient stress until conditions are improved. During the stringent response the transcriptional program is substantially altered leading to shut down of synthesis of DNA, many RNAs, ribosomal proteins and membrane components and to the production of factors that help coping with the stress situation (Potrykus and Cashel 2008).

Key regulators of the stringent response are two unusual phosphorylated derivates of the nucleotides guanosine diphosphate (GDP) and guanosine triphosphate (GTP), called guanosine 3',5'-bis(diphosphate) (ppGpp) and guanosine 3'-diphosphate, 5'-triphosphate (pppGpp), respectively, herein collectively referred to as (p)ppGpp. The so called alarmone (p)ppGpp is generated by two enzymes, RelA and SpoT, from GDP/GTP with consumption of adenosine triphosphate (ATP) in response to amino acid starvation, sensed by RelA (sensing uncharged tRNA at the ribosomal A-site), and phosphate, fatty acid, carbon, or iron starvation and osmotic stress, sensed by SpoT. SpoT, being a bi-functional protein, can reverse the reaction by (p)ppGpp hydrolysis to GDP/GTP and pyrophosphate (PP_i) when nutrient stress is eased (reviewed in Dalebroux and Swanson 2012).

Stress induced high concentration of (p)ppGpp severely influences the bacterial transcription program by multiple mechanisms. Together with the DnaK suppressor (DksA) (p)ppGpp binds to RNAP and guides it directly to particular promoters (Haugen, Ross et al. 2008). Furthermore, (p)ppGpp reduces the affinity of the canonical σ-factor, σ^{70}, to the RNAP thus making the core RNAP available for alternative σ-factor binding and consequently inducing transcription of stress specific genes (Osterberg, del Peso-Santos et al. 2011). The alternative σ-factor RpoS, which induces the general transcriptional stress response (also see chapter I.3.1) is additionally stabilized by high (p)ppGpp levels (Bougdour and Gottesman 2007) and σ^{E}-activity is likewise enhanced (reviewed in Dalebroux and Swanson 2012). Accumulation of (p)ppGpp also leads to activation of the protease Lon which subsequently degrades ribosomal proteins to create a new pool of free amino acids (Kuroda et al., 2001). Activated Lon also connects the (p)ppGpp triggered stress response to the activity of TA systems by degrading the antitoxin component of type II TAs (chapter I.3.3). A scheme of the regulatory network triggered by (p)ppGpp is shown in Figure I.3.1.

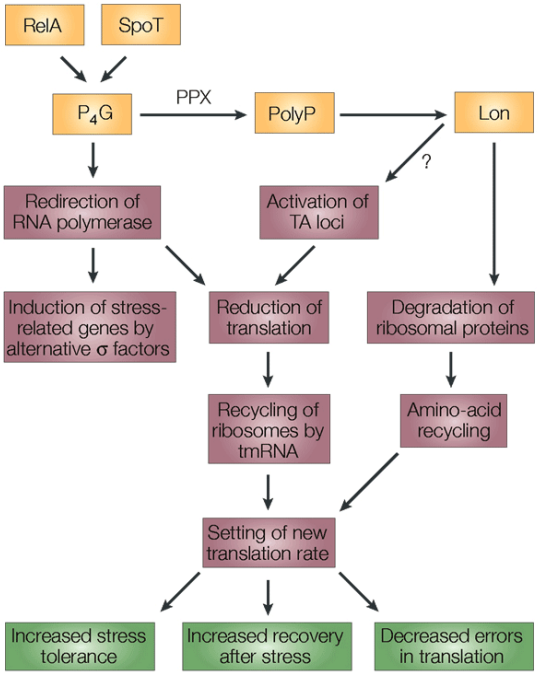

Figure I.3.1: Model integrating the function of TA systems in the stringent stress response network triggered by accumulation of the alarmone (p)ppGpp. P4G: ppGpp. Taken from Gerdes et al. (2005).

In pathogenic bacteria activation of the stringent response by accumulation of (p)ppGpp does not only serve as a stress adaption mechanism but also induces several pathways contributing to the pathogen's virulence (reviewed in Dalebroux and Swanson 2012).

I.3.3. Toxin-antitoxin systems in stress response

As introduced above, elevated levels of the alarmone (p)ppGpp upon perception of stress lead to the activation of proteases that -besides other effects- also degrade the labile antitoxin complement of type II TA pairs. Hence, toxins are activated in response to stress and research of the last years has revealed some striking influences of toxin activity on cell survival.

I.3.3.a) The MazF-mediated stress response in Escherichia coli

mazEF is the best studied example of a TA system involved in stress response in *E. coli*. Upon activation by diverse stress conditions, the endoribonucleolytic activity of MazF leads to rapid degradation of bulk mRNA by ACA-specific cleavage whereby the cell's overall protein synthesis is severely decreased. However, it was observed that not all mRNAs are completely degraded upon MazF activity. Some distinct mRNAs are cleaved at ACA-sites upstream of the translational start-codon, thereby removing the 5'-UTR containing the SD-sequence. These mRNAs are called leaderless mRNA (lmRNAs). Additionally, rRNA is likewise targeted by MazF. The 16S rRNA of the small 30S ribosomal subunit is cleaved at position 1500, removing the last 43 nucleotides from its 3'-end containing the aSD-sequence (Vesper et al., 2011). These so called "stress ribosomes" or herein referred to as 70SΔ43, are incapable to initiate translation on canonical mRNAs harboring 5'-untranslated regions (UTRs) as the SD/aSD interaction, required for canonical translation initiation, cannot take place. However, the 70SΔ43 ribosomes selectively translate lmRNAs (Vesper et al. 2011). Taken together, activation of a single protein, MazF, leads to a general decrease in protein synthesis, but concomitantly to the generation of a distinct subset of lmRNAs which can be selectively translated by the likewise generated 70SΔ43 ribosomes.

Although MazF is the most intensely studied toxin involved in stress response it is very likely that other toxins play additional or complementary roles. Accordingly, it has been shown that the diverse TA systems exert regulatory crosstalk between each other. Kasari and co-workers could show for example that transcription of the *relBEF* operon can be activated by activity of other toxins, such as MazF, and that likewise RelE activity can induce transcription of other TA operons (Kasari et al., 2013). Similarly, endoribonucleolytic toxins can process other toxin mRNAs and thus induce their translation (Kasari et al., 2013).

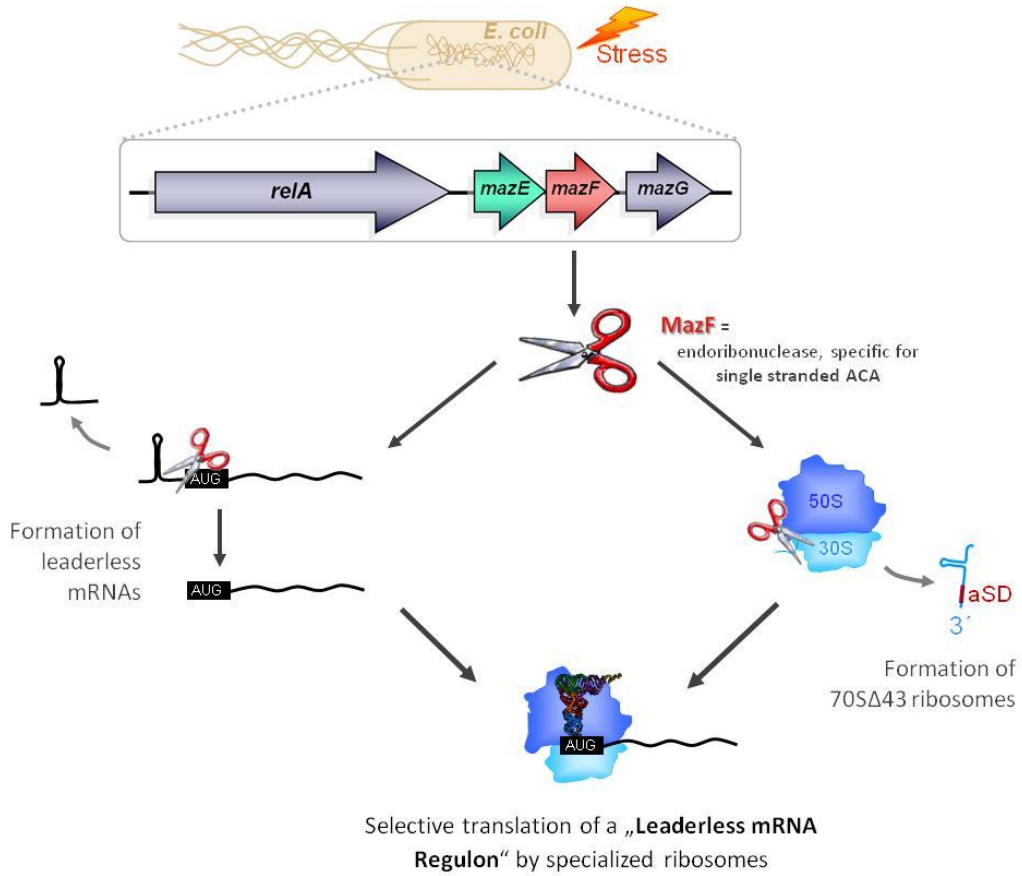

Figure I.3.2: Selective translation of lmRNAs by 70SΔ43 ribosomes upon stress-induced MazF activity. Various stress conditions induce the release of the toxin MazF from its cognate antitoxin. Free MazF on the one hand cleaves mRNAs at single-stranded ACA-sites and leads to the formation of a distinct set of lmRNAs. On the other hand MazF cleaves an ACA-site at the 16S rRNA removing the 3'-terminal 43 nucleotides comprising the aSD sequence. The resulting 70SΔ43 ribosomes are selective for translation of the generated lmRNAs.

I.3.3.b) Reversibility of the MazF-mediated stress response: the RNA ligase RtcB

Activation of MazF upon diverse stress conditions leads to the disruption of canonical ribosomes by removal of the aSD sequence from the 16S rRNA as introduced above. While the stress conditions are still distressing the cells, this mechanism can help to survive by the selective translation of generated lmRNAs. Upon stress release however, the lack of canonical ribosomes poses severe problems in recovery, as *de novo* biogenesis of ribosomes is very costly and synthesis of new proteins by canonical ribosomes is desired. Thus, our lab has recently proposed a ribosome repair mechanism by the RNA ligase RtcB (Temmel et al., manuscript in preparation). RtcB was recently identified as an RNA ligase sealing RNA-5'-hydroxyl ends with 2', 3'-cyclic phosphate ends under

consumption of GTP and manganese (Mn^{2+}) as a cofactor (Tanaka et al., 2011). These are exactly the termini generated by MazF cleavage and as *rtcB* is expressed under stress conditions by regulation *via* σ^{54} (Genschik et al., 1998) it is conceivable that RtcB re-ligates the cleaved 43 nucleotides containing the aSD sequence back to the 70SΔ43 ribosomes to efficiently generate canonical ribosomes (Temmel et al., manuscript in preparation, see Figure I.3.3).

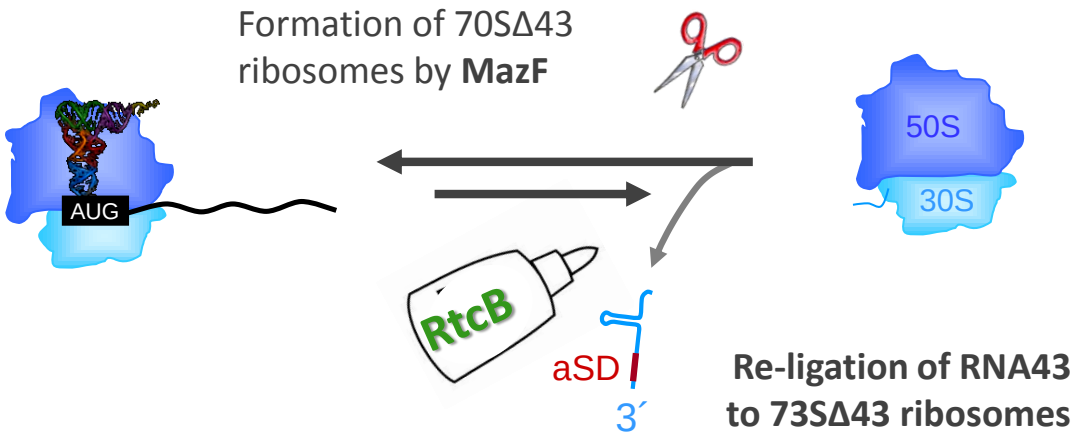

Figure I.3.3: The reversible formation of 70SΔ43 ribosomes. The 70SΔ43 ribosomes generated upon stress can be repaired by the activity of the RNA ligase RtcB.

I.3.3.c) MazF and persister cell formation

Persister cells are supposed to be a metabolically inactive, dormant fraction of a cell population that is - despite being genetically identical to their non-persistent kin- tolerant to otherwise lethal concentrations of antibiotics (Lewis, 2010). Subsequent culturing of isolated persisters yields a population that restores normal growth and reapplication of antibiotic treatment selects for a new population of persisters (Keren et al., 2004). Thus, the phenomenon of persistence poses a severe problem during antibiotic treatment of pathogenic bacteria but its underlying mechanisms are in general poorly understood. It was proposed that persisters arise from a small fraction of cells in mid-exponential growth phase that have experienced stochastic changes in gene expression (Shah et al., 2006). Recent studies have shown that MazF activity is responsible for induction of this physiological switch in a ClpP and Lon protease dependent manner, resulting in increased persister cell formation (Maisonneuve et al., 2011; Tripathi et al., 2014). Other toxins like HipA and RelE also exert positive effects on persister generation (Vázquez-Laslop et al., 2006).

I.4. Aconitase B

I.4.1. Aconitases in *Escherichia coli*

The aconitase is an enzyme driving one of the initial reactions in the central energy metabolism pathway citric acid cycle (also called Krebs cycle, or tricarboxylic acid cycle, herein referred to as TCA cycle, see Figure I.4.1A). The TCA cycle is a universal pathway in most organisms (Smith and Morowitz, 2004) in which the global precursor acetyl-CoA is consumed to generate high energy compounds, like ATP and the reduced form of nicotinamide adenine dinucleotide phosphate (NADPH), or carbon backbones for secondary metabolism pathways. Aconitases are iron-sulfur proteins that catalyze the reversible isomerization of citrate and isocitrate *via* dehydration of citrate to *cis*-aconitate and its rehydration to isocitrate (Cunningham et al., 1997) (see Figure I.4.1B).

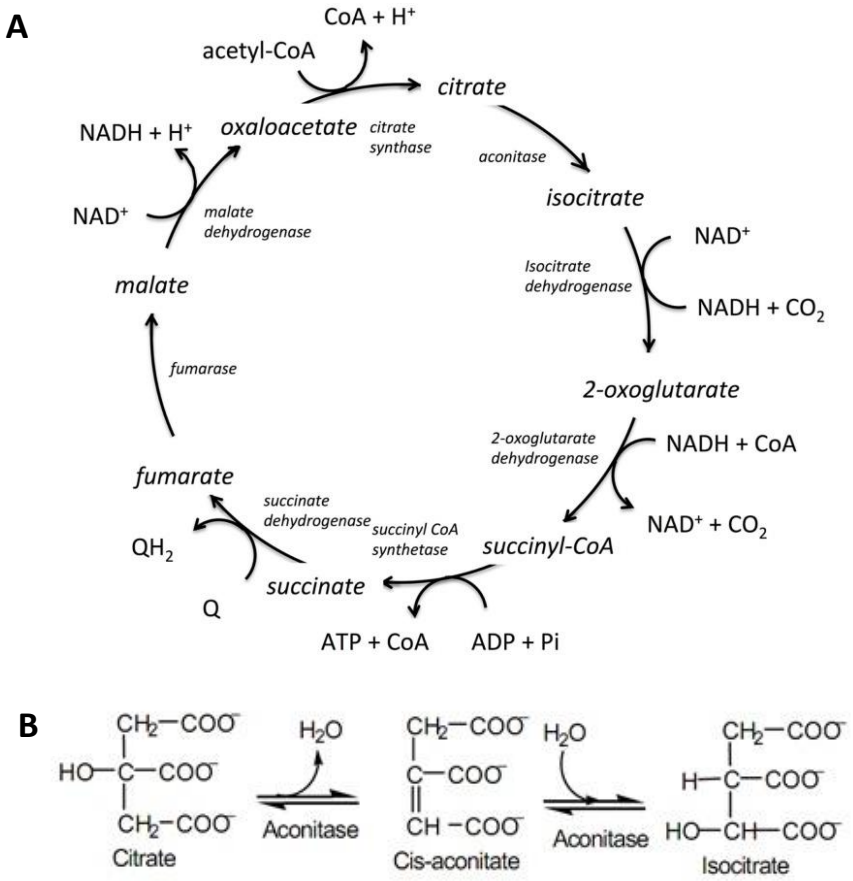

Figure I.4.1: The enzymatic activity of aconitase within the TCA cycle. A) The TCA cycle from *E. coli*. Catalyzing enzymes are shown in italics, co-factors are shown tangentially to each respective reaction, and reaction intermediates are shown in line with the cyclic reaction arrows indicating direction of the cycle. Q and QH2 are electron acceptor/donator pairs and are entry points to the electron transfer chain. Taken from Cannon (2014) **B**) The reaction catalyzed by aconitase. Citrate is dehydrated to cis-aconitate, cis-aconitate is hydrated to isocitrate. The reactions are reversible. Taken from www.tutorsglobe.com.

In *E. coli* three aconitases are known, namely AcnA, AcnB and AcnC (PrpD) (Blank et al., 2002; Gruer et al., 1997a). AcnA and AcnB are the two main aconitases responsible for the enzymatic reaction in the TCA cycle and deletion of *acnA* can be complemented by *acnB+*, whereas deletion of *acnB* can be only partially complemented by *acnA+* (Gruer et al., 1997a). AcnC is encoded in the propionate operon (Brock et al., 2002) and shows only minor isomerization reactivity of below 5% in an *acnAB* double deletion (Gruer et al., 1997a). While *acnA* is expressed during stationary growth and stress, AcnB seems to be the main aconitase, being expressed early during exponential growth from a σ^{70} driven promoter located 95 base pairs (bp) upstream of the GUG start codon (Cunningham et al., 1997; Gruer and Guest, 1994).

I.4.1. Structure and function of *E.coli* AcnB

Aconitases comprise a large protein superfamily with homologs in bacteria as well as in higher organisms (Gruer et al., 1997b). The *E. coli* AcnB protein consists like the other members of the aconitase family of four conserved domains. However, AcnB belongs to a group of Gram-negative bacterial aconitases that exhibit an altered domain structure. Domain 4 precedes domain 1 and is additionally preceded by a HEAT-like domain at the N-terminus (see Figure I.4.2, Williams et al., 2002).

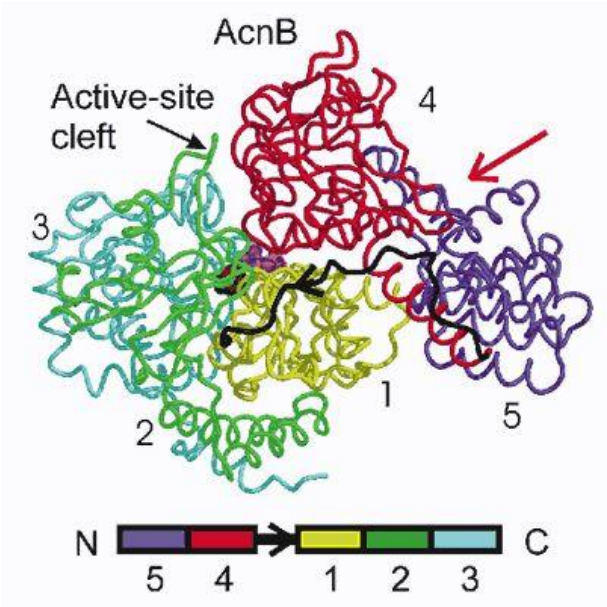

Figure I.4.2: Structure of AcnB. Domains 1, 2, 3, 4 and 5 are yellow, green, cyan, red and purple, respectively, and the linker region is black, with its polarity denoted by an arrow. The [3Fe−4S] / [4Fe−4S] cluster is dark red, with the trans-aconitate in magenta. The position of the tunnel is indicated by a red arrow. A linear representation of the sequential domain arrangement with domain 4 preceding domain 1 and this preceded by the HEAT-like domain 5 is also included (Williams et al., 2002).

Domains 1-4 contribute residues to the active site of AcnB which harbors an iron-sulphur [4Fe−4S] cluster and many of these residues are conserved from bacteria to eukaryotes. Additionally to the enzymatic activity AcnB also confers an RNA binding site, likewise built up by domains 1-4.

The role of the HEAT-like domain in addition to the four others is not yet entirely understood but it makes intensive interactions with domain 4 and together they form a tunnel-structure leading directly to the active site (indicated in Figure I.4.2 by an red arrow) which could improve efficiency of reactions in the TCA cycle by direct substrate channeling from one enzyme to the next (Williams et al., 2002). Tang and co-workers have revealed that domains 4 and 5 can interact with each other to form an AcnB homodimer in dependence of Fe^{2+} levels (Tang et al., 2005).

I.4.1.a) The moonlighting functions of AcnB

As mentioned above, the two isoforms AcnA and AcnB distinct abundances during different states of growth. AcnA is active during stationary phase and under stress and AcnB is the major TCA enzyme during exponential growth (Cunningham et al., 1997). Under certain stress conditions however, both, AcnA and AcnB, are unstable. During oxidative stress or iron starvation the iron sulphur cluster is destroyed, resulting in an apo-protein which has lost its catalytic activity (Gardner and Fridovich, 1991, 1992; Gardner et al., 1997). However, the iron-sulphur cluster of AcnA seems to be more stable than that of AcnB (Varghese et al., 2003) so that the catalytic function of AcnB is more sensitive to iron starvation. On the other hand, apo-AcnB can bind specifically to mRNAs (Beinert et al., 1996; Tang and Guest, 1999; Tang et al., 2002) presumably *via* domains 4 and 5 (Tang et al., 2005). Figure I.4.3 illustrates the switching functions of AcnB *via* protein-protein interactions at the N-terminal domains 4 and 5 in dependence of iron levels.

Subsequently, it has been proposed that AcnB is a moonlighting protein that fulfils additionally post-transcriptional regulatory functions *via* this mRNA binding ability. The mRNA targets of apo-Acns in eukaryotes are iron-responsive elements (IREs) usually located in mRNA's UTRs. Here, apo-Acn binding in response to iron starvation can lead to increased mRNA stability or to inhibition of translation thus classifying aconitases as iron-regulatory proteins (IRPs) (Hentze and Kühn, 1996). One specific target of the *E. coli* apo-AcnB is the 3'-UTR of its own mRNA (Tang et al., 2002, 2004). The *acnB* mRNA is in principle a target for the RyhB sRNA which -in response to iron deprivation- targets *acnB* for degradation (as discussed in chapter I.1.3.b). Binding of apo-AcnB to its own mRNA

protects the *acnB* mRNA from cleavage after RyhB binding thus increasing the stability of the *acnB* transcript during iron deprivation (Benjamin and Massé, 2014).

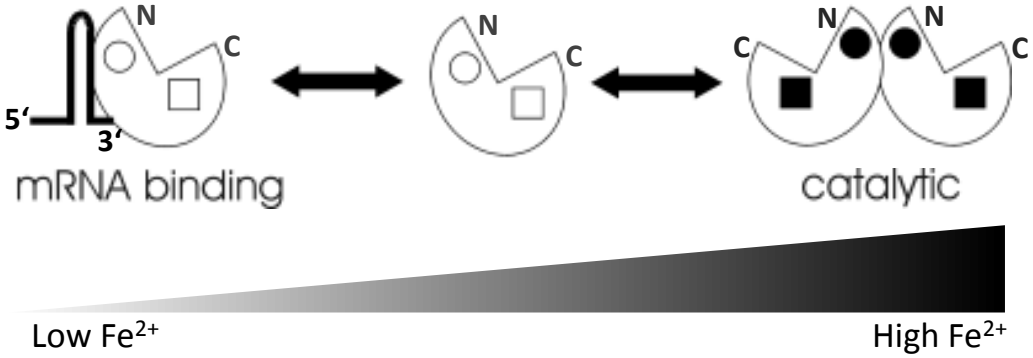

Figure I.4.3. Switching functions of AcnB in dependence of iron levels. High iron levels are sensed at a site (filled circle) distinct from the AcnB iron–sulphur cluster (filled square) and catalytically active AcnB homodimers are formed by interaction between the N-terminal regions of the AcnB subunits (right side). Low iron levels are sensed by the N-terminal region (open circle) and the AcnB iron–sulphur cluster is absent (open square). The AcnB monomers with disrupted iron–sulphur cluster are capable to bind to specific transcripts (stem–loop structure) *via* the domains 4 and 5. Modified from Tang et al. (2005).

I.4.1.b) AcnB and motility

As oxidative stress is of particular relevance for pathogenic bacteria when exposed to marcrophages, Tang and co-workers investigated the effects of *acn*-deletions in *Salmonella enterica* on its interaction with J774 macrophage-like cells (Tang et al., 2004). Surprisingly, they found that deletion of *acnB* leads to impaired mobility of the bacteria due to decreased flagella production by reduced levels of the flagellum protein FliC. It was further shown that apo-AcnB generated in response to oxidative stress binds to *ftsH*, a transcript encoding the protease FtsH. As introduced in chapter I.1.3.d) FtsH is involved in degradation of the alternative σ-factor σ^{32} which subsequently leads to decreased production of the heat shock response chaperones DnaK, DnaJ, GrpE and GroEL (see chapter I.3.1). As these heat shock chaperones have been linked to flagella synthesis and motility in *E. coli* (Shi et al., 1992) Tang and co-workers proposed the regulatory circuit presented in Figure I.4.4 linking the formation of apo-AcnB in response to oxidative stress to reduced motility of affected cells (Tang et al., 2004).

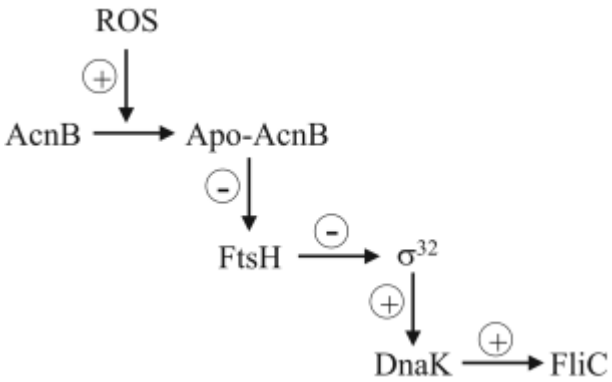

Figure I.4.4: A potential regulatory circuit controlling FliC production in response to oxidative stress. In response to the presence of reactive oxygen species (ROS) apo-AcnB is generated which binds the *ftsH* transcript to inhibit synthesis of the protease FtsH. As FtsH degrades σ^{32}, this transcriptional regulator can no longer stimulate the transcription of *dnaK*. DnaK protein usually enhances FliC production, thus FliC synthesis can be controlled in response to oxidative stress. Taken from Tang et al. (2004).

I.5. Transcriptome and translatome analysis

I.5.1. Methods for transcriptome analysis

In the past, researchers have addressed questions of global cellular adaptations mainly on the transcriptional level by investigating alterations in mRNA abundance under the desired conditions. Since the 90s DNA micro arrays were the method of choice to monitor differences in RNA levels under various conditions (Schena et al., 1995). In this method, small spots on a solid micro chip surface are coated with DNA oligo nucleotides complementary to the RNAs of interest. Total RNA samples, converted to fluorescently labeled cDNA by reverse transcription (RT), can then be applied to the chip and a specific cDNA will hybridize to its cognate DNA on the spot where it has been coated. After washing a fluorescent scan reveals in which spot high levels of cDNA have bound. In this way, the level of many RNAs can be investigated and easily compared. However, micro arrays are restricted to known RNA candidates.

In recent years, the development of high throughput sequencing has accelerated and diversified research on transcriptomes enormously (Mardis, 2008). In these sequencing methods prepared cDNA libraries are ligated to adapter oligos that can be bound to a solid surface and serve as primers for a stepwise Sanger sequencing reaction. This way almost every molecule of cDNA in a given library can be sequenced, nowadays up to 200 nucleotides in length. The resulting sequencing reads are then aligned to the respective genome and researchers can quantify the amounts of sequencing reads aligned to a particular gene. Next generation sequencing methods allow the identification and relative quantification of all known and unknown RNAs. Strand specific methods of library preparation allow the identification of novel non-coding and antisense RNAs.

However, sequencing methods measure exclusively RNA abundance. As introduced earlier, gene expression is not only regulated by adapting mRNA levels but also involves translational regulation and protein turnover. Only few studies have so far globally compared mRNA levels and the corresponding protein abundance. Intriguingly, they revealed a rather imperfect correlation between transcriptome and translatome (Maier et al., 2009). These studies confirm that alteration of protein production also involves post-transcriptional and translational regulation, as well as protein turnover. Thus, assessing gene expression as a whole one has to take analysis of the translatome into account as well as analysis of the transcriptome.

I.5.2. Methods for translatome analysis

An actively translated mRNA is covered by several 70S ribosomes which simultaneously produce multiple proteins (Miller et al., 1970) thus assembling a so-called polysome. These polysomes are generally used for translatome analysis as they are easy to select and their containing mRNA reflects the portion of translated mRNAs. The state of the art method for such a polysome-based translatome analysis, which has shown the vast extend of translational regulation in yeast, is the so called ribosome profiling (Ingolia et al., 2009). Ingolia and co-workers have shown that quantification of ribosome-associated mRNA correlates significantly better with protein levels than with mRNA abundance alone (Ingolia et al., 2009). Oh and co-workers have developed an adapted system of ribosome profiling in *E. coli* (Oh et al., 2011). In this method translating ribosomes are *in vivo* immobilized on the mRNA by pre-treatment with translation-blocking agents like chloramphenicol and the cells are disrupted by flash freezing in liquid nitrogen and cryogenically pulverizing by mixer milling. Cell lysates are treated with micrococcal nuclease (MNase) and resolved by sucrose density gradients. mRNA stretches which have been protected by ribosomes during digestion are sequenced to obtain the ribosome footprints (see Oh et al., 2011). Thereby the extent of translation on a given mRNA can be relatively quantified.

I.6. Scope of the thesis

As introduced in the previous chapters, stress-induced MazF activity induces a novel post-transcriptional regulatory mechanism upon stressful conditions by generating a new subpopulation of 70SΔ43 ribosomes, which are selectively translating a subset of newly generated lmRNAs. Understanding this mechanism in more detail could help to decipher the physiological reorganizations that lead to persister formation. Hitherto, only few highly abundant proteins have been identified, that remain to be synthesized after *mazF* overexpression employing 2D gel electrophoresis and mass spectrometry (Amitai et al., 2009). As Vesper and co-workers have shown that about 50% of the ribosomes are cleaved by MazF after serine hydroxamate (SHX) treatment, which is mimicking amino acid starvation, it is conceivable that this mechanism targets many more transcripts. So far it is not known how many mRNAs are processed in their 5'-UTR and how many of those are selectively translated as lmRNAs by the 70SΔ43 ribosomes. In the present thesis, I aimed to determine this entity of selectively translated lmRNAs which is termed the 'leaderless mRNA regulon'.

To decipher this 'lmRNA regulon' in order to understand the MazF-induced physiological alterations, I combined sucrose density gradient fractionation and next generation RNA sequencing to isolate intact, full length mRNAs from polysomes. In contrast to the ribosome profiling developed by Ingolia and co-workers (Ingolia et al., 2009), this method enables the concomitant analysis of the translatome and the processing state of the polysomal RNA. Thus, the data presented in this thesis will allow to estimate the linkage between transcription and translation levels and thus provides a snapshot of the altered transcriptional and translational landscape in dependence of MazF activity. These studies are presented in the result chapter 2.1.

The identification of the 'lmRNA regulon' leads consequently to the discovery of many so far unknown distinct MazF targets and thus reveals a potential functionality of these candidates in stress response. In the further course of this study I focused in more detail on a few chosen candidates whose involvement in stress response was either unexpected or of particular interest to us. One of these candidates is *acnB*, the mRNA encoding the TCA cycle enzyme aconitase. The observed cleavage of the *acnB* mRNA at position -24 from the start codon results in the formation of a novel lmRNA with an in-frame AUG start codon seven codons upstream of the original GUG start codon. Translation of this particular mRNA by the 70SΔ43 ribosomes would result in a novel AcnB version with additional seven amino acids at its N-terminus. This modulation could severely interfere with AcnB's regulatory and enzymatic functions. The investigations concerning *acnB* are described in the results chapter 2.2.

Another point of interest is the potential heterogeneity introduced by the MazF-mediated response. First, MazF cleavage of the ribosome results in a heterogeneous population of ribosomes, in which some ribosomes are cleaved and therefore possess a modulated translation activity and others are not. This ribosome heterogeneity comprises a novel level of translational regulation and we further explored the phenomenon of ribosome heterogeneity in pro- and eukaryotes. Our research showed how unexpectedly often ribosome heterogeneity has been reported in recent years and how diverse it is. The underestimated the regulatory potential of ribosome heterogeneity is summarized in the collaborative review article published in December 2014 and here given in chapter 2.4.

Additionally, heterogeneity does not only affect the ribosome themselves. During this study I also wondered if all cells within a bacterial population activate the MazF-mechanism. Do all cells react to a given stress condition in the same way and to the same extend or are only few cells switching the MazF-mediated mechanism on while others don't? Summarizing the question: is a bacterial population homo- or heterogeneous in its stress response? My attempts to investigate this issue by establishing a fluorescent reporter system for MazF-dependent selective translation of lmRNAs are summarized in chapter 2.3.

Taken together, the presented study shows investigations of the MazF-mediated response mechanism which led to the conclusion that activation of MazF during stress triggers an unexpected large spectrum of reactions, which result in very global alterations. With regard to the formation of persister cells, this could comprise exactly the variety of alterations that are necessary for an individual cell to enter into the persister state and further studies on this subject might help to understand persistence.

Additionally, this data provides a broad range of potential future research projects and reveals novel implications of known proteins into stress response and regulation, as shown for AcnB.

II. Results and Discussion

II.1. Comparative transcriptome and translatome analysis of the MazF-mediated stress response

Martina Sauert, Michael Wolfinger, Oliver Vesper, Konstantin Byrgazov and Isabella Moll

Manuscript in preparation. Submission to EMBO Journal or Genome Biology intended.

Contribution of the publication to the overall thesis

In this study the 'leaderless mRNA regulon' of the MazF-mediated stress response was identified. Since MazF was implicated in persister formation, analysis of the 'lmRNA regulon' contributes significantly to the overall understanding of the MazF induced alterations in response to stress and therefore might help to understand the phenomenon of bacterial persistence. Additionally, the data reveals the underestimated significance of translational regulation and ribosome specificity upon stress.

Author's contribution

Martina Sauert contributed all figures and tables presented in this work. The results shown in Figures 2 to 4, Figures S1 to S4, Tables 2 to 4 and Tables S4 were obtained in collaboration with Michael Wolfinger. The results shown in Table 4 were additionally obtained in collaboration with Oliver Vesper and Konstantin Byrgazov. The manuscript was written by Martina Sauert, the paragraph 'Material and Methods – Computational analysis' in collaboration with Michael Wolfinger. The author's contribution to writing this segment was approximately 50%.

Comparative transcriptome and translatome analysis of the MazF-mediated stress response

Martina Sauert, Michael Wolfinger, Oliver Vesper, Konstantin Byrgazov and Isabella Moll

Abstract

Flexible stress adaption is an indispensable key feature for free-living bacteria as they frequently encounter changed environmental conditions. Regulation of the transcriptome as a means to react to various stresses has been well researched, however, evidence is emerging that response at the translational level plays a long underestimated pivotal role in stress adaption. A recently uncovered stress response mechanism is performed at the post-transcriptional level triggered by the toxin-anti toxin module *mazEF*. Upon activation by various stress conditions, the toxin MazF removes the Shine-Dalgarno (SD) sequence containing 5'-untranslated region of a distinct subset of mRNAs, as well as the 3'-terminal part of ribosomal 16S RNA which harbors the anti-SD (aSD) sequence. Hence, these specialized ribosomes are selective for translation of this particular set of "leaderless mRNAs". Thereby, the activation of MazF under diverse stress conditions induces the selective translation of the 'leaderless mRNA regulon' and thus results in the synthesis of a distinct subset of proteins.

As MazF activity has recently been linked to persister cell formation, we aimed to determine the 'leaderless mRNA regulon'. To this end, we developed a method to selectively isolate and identify all mRNAs that are translated after *mazF* overexpression to determine the stress translatome. By this means, we were able to differentiate between the transcriptome and the translatome, and moreover to analyze the MazF-processing state of the respective mRNAs. We identified a set of 223 mRNA candidates that are rendered leaderless by MazF activity and are efficiently and selectively integrated into polysomes in their leaderless form. Examining the functions of the corresponding protein products, we surprisingly found no intriguing functional clustering. The candidates cover all cellular functions indicating the overall importance of the MazF-mediated translation adaption mechanism hereby building a regulatory hub that potentially helps to set the new state for entering into the persister phenotype upon stress. Additionally, comparison of the translatome with the transcriptome upon stress reveals the so far underestimated significance of selective translation as a novel regulatory mechanism in gene expression during stress response.

Introduction

During their lifetime, free-living bacteria have to deal with sudden changes in their environment. These environmental stresses range from changes in temperature, pH, and nutrient availability to the immune response or treatment with antibiotics, when invading a host. A general means to overcome these adverse stress conditions is the stringent response, a bacterial survival mechanism by which the metabolism is reduced to a minimum. During the stringent response the transcriptional program is substantially altered, triggered by synthesis of the alarmones guanosine tetra- and pentaphosphate ((p)ppGpp), leading to shut down of synthesis of DNA, many RNAs, ribosomal proteins and membrane components and to the production of factors that help coping with the stress situation (Potrykus and Cashel, 2008). One of the main mechanisms to alter the transcriptional program during the stringent response is mainly achieved by the use of alternative sigma factors, that guide the RNA polymerase to the respective promoters (reviewed in Sharma and Chatterji, 2010). Another mechanism for transcription regulation involves a variety of factors, which can influence transcription specifically in a positive and negative manner (reviewed by Balleza et al., 2009). Taken together, these mechanisms of transcription alteration in response to stress lead to altered mRNA synthesis and to adapted protein levels. However, some studies have globally compared mRNA levels with the corresponding protein abundance. Intriguingly, they revealed a rather imperfect correlation between transcriptome and translatome (Maier et al., 2009). These studies indicate that alteration of protein production cannot merely be regulated at the transcriptional level by alteration of mRNA abundance but that post-transcriptional and translational regulation, as well as protein turnover, also play pivotal roles in the regulation of protein production. Known mechanisms for translational regulation are differentially strong Shine-Dalgarno (SD) sequences, regulatory small RNAs (sRNAs), riboswitches and translation regulatory proteins.

Recently, an additional post-transcriptional regulatory mechanism upon stress in *E. coli* was identified involving the toxin-antitoxin (TA) module *mazEF* (Vesper et al., 2011). Upon activation by diverse stress conditions, the free toxin MazF cleaves RNAs specifically at single-stranded ACA-sites (Zhang et al., 2003). Hence, bulk mRNA is rapidly degraded upon MazF activation and the cell's overall protein synthesis is severely decreased. Besides this degradation of bulk mRNA, activity of MazF also generates a subset of leaderless mRNAs (lmRNAs) by cleavage of an ACA-sites upstream of the translational start-codon, thereby removing the SD-sequence. Additionally, ribosomal RNA (rRNA) is likewise targeted by MazF. The 16S rRNA is cleaved at position 1500, removing 43 nucleotides from its 3'-end containing the anti-Shine-Dalgarno (aSD) sequence (Vesper et

al., 2011). These so called “stress ribosomes”, herein referred to as 70SΔ43, are incapable to initiate translation on canonical mRNAs containing 5’-untranslated regions (UTRs), since the SD/aSD interaction, required for canonical translation initiation, cannot take place. However, the 70SΔ43 ribosomes selectively translate lmRNAs (Vesper et al., 2011).

Recent studies addressing the physiological significance of the existence of chromosomally encoded TA systems have linked MazF activity to increased persister cell formation (Tripathi et al., 2014). Persisters are supposed to be a metabolically inactive, dormant fraction of a cell population that is -despite being genetically identical to their non-persistent kin- tolerant to lethal concentrations of antibiotics (Lewis, 2010). Thus, the phenomenon of persistence poses a severe problem during antibiotic treatment of pathogenic bacteria but the underlying mechanisms are in general poorly understood.

Taken together, MazF activity induces a novel post-transcriptional regulatory mechanism upon stressful conditions by generating a new subpopulation of 70SΔ43 ribosomes which are selectively translating a subset of newly generated lmRNAs. Understanding this mechanism in more detail could help to decipher the physiological reorganizations that lead to persister formation. Hitherto, only few highly abundant proteins have been identified, that remain to be synthesized after *mazF* overexpression employing 2D gel electrophoresis and mass spectrometry (Amitai et al., 2009). As Vesper and co-workers have shown that about 50% of the ribosomes are cleaved by MazF after serine hydroxamate (SHX) treatment, which is mimicking amino acid starvation, it is conceivable that this mechanism targets many more transcripts. So far it is not known how many mRNAs are processed in their 5’-UTR and how many of those are selectively translated as lmRNAs by the 70SΔ43 ribosomes. Here, we aim to determine this entity of selectively translated lmRNAs which we term the ‘leaderless mRNA regulon’.

To decipher this ‘lmRNA regulon’ in order to understand the MazF-induced physiological alterations, we combined sucrose density gradient fractionation and next generation RNA sequencing to isolate intact, full length mRNAs from polysomes. In contrast to the ribosome profiling developed by Ingolia and co-workers (Ingolia et al., 2009), this method enables the concomitant analysis of the translatome and the processing state of the polysomal RNA. Thus, our data allows an estimation of linkage between transcription and translation levels and provides a snapshot of the altered transcriptional and translational landscape in dependence of MazF activity.

Results

Purification of total and polysome-associated RNAs

Considering the suggested implication of *mazEF* in cell survival and persister formation we aimed to understand the underlying mechanisms which enable a cell to enter into the persister state. Therefore, we employed artificial *mazF* overexpression is an initial point to simultaneously analyze MazF-induced alterations in the transcriptome and the translatome of *E. coli.* We ectopically overexpressed *mazF* for 15 minutes during exponential growth in Luria-Bertani (LB) medium and isolated RNA from those cells and from cells under relaxed conditions in two biological replicates. For transcriptome analysis we isolated total RNA, for the translatome analysis we isolated mRNAs from polysomes as schematically depicted in **Figure 1A**. Mere sequencing of total RNAs after *mazF* overexpression might produce information about the formation of lmRNAs in general but it will not suffice to determine the set of lmRNAs that are actually translated and therefore incorporated into polysomes.

An actively translated mRNA is covered by several 70S ribosomes which simultaneously produce multiple proteins (Miller et al., 1970) thus assembling a so-called polysome. These polysomes are generally used for translatome analysis as they are easy to isolate and their mRNA load reflects the portion of translated mRNAs. The state of the art method for this polysome-based translatome analysis, which has shown the vast extend of translational regulation in yeast, is the so called ribosome profiling (Ingolia et al., 2009). Ingolia and co-workers have shown that quantification of ribosome-associated mRNA correlates significantly better with protein levels than with mRNA abundance alone (Ingolia et al., 2009). Oh and co-workers have developed an adapted system of ribosome profiling in *E. coli* (Oh et al., 2011). In this method translating ribosomes are *in vivo* immobilized on the mRNA by pre-treatment with translation-blocking agents like chloramphenicol and the cells disrupted by flash freezing in liquid nitrogen and cryogenically pulverizing by mixer milling. Cell lysates are treated with micrococcal nuclease (MNase) and resolved by sucrose density gradients. mRNA stretches which have been protected by ribosomes during digestion are sequenced to obtain the ribosome footprints (see Oh et al., 2011). Although a good indicator for translational efficiency, this method cannot be applied to our question as the translated mRNAs are fragmented and results only reveal the sequences that are protected by ribosomes. Information about the 5'-UTRs would not be obtained and therefore no differentiation between leaderless and canonical mRNAs could be made in respect to their translation.

We established a protocol to efficiently isolate full length mRNAs from polysomes. To avoid a bias on the stress response of the cells, we omitted chloramphenicol treatment. We rather "froze" the cells in their current state by harvesting over ice and quickly cooling the cells to 0-4°C. Furthermore, we omitted snap freezing of the cells in liquid nitrogen and disruption by pulverization to avoid shearing of the RNAs and degradation of the non-immobilized polysomes. Instead, we gently disrupted the cells by addition of lysozyme and DNAse I and repeated freeze-and-thaw cycles at -20°C and on ice respectively, always keeping lysates at 0-4°C to prevent ongoing translation.

The ribosomal subunits (30S and 50S), fully assembled 70S ribosomes and polysomes were separated by sucrose density gradient centrifugation of cell lysates (see **Figure 1B**). The overall inhibition of translation after *mazF* induction is mirrored by less pronounced poly-ribosomes peaks (straight line) when compared to ribosomes profiles obtained from cells in exponential growth (dashed line). Nevertheless, we were able to obtain polysomes without antibiotic-induced *in vivo* fixation of the translating ribosomes on the mRNAs by optimizing the harvesting and cell disruption procedure.

The polysome fractions (**Figure 1B**, fractions 20-33) were pooled omitting the 70S monosome peak in order to select only actively translated mRNAs. The respective RNA was isolated and upon depletion of rRNA *via* magnetic beads (Ribozero®, Epicenter; **Table 1**, rows "**P-**" and "**P+**", column "rRNA depletion") subjected to RNA-Seq (see material and methods). **Table 1** summarizes the efficiency and quantity of the individual purifications steps.

The polysomal RNA preparation method allows isolation of canonical and leaderless mRNAs

First, we validated the formation of the 70SΔ43 ribosomes upon *mazF* overexpression. To this end, the rRNA recovered from magnetic beads used for depletion of above mentioned RNA samples was subjected to reverse transcription PCR (RT-PCR). To distinguish between full length (nucleotides 1-1542) and MazF-processed (nucleotides 1-1499) 16S rRNA, two different reverse primers specific for the 16S rRNA sequence upstream (X15) or downstream (Y12) of the MazF cleavage site were used in combination with the forward primer S7, which anneals to a central region of the 16S rRNA (**Figure 1C**). As shown in **Figure 1C**, employing primer pair S7/X15, which anneals to both, full length and truncated 16S rRNA, we obtained the expected product in all samples tested, without treatment (lanes 1 and 3) and upon overexpression of *mazF* (lanes 2 and 4). This result validates that the same amounts of rRNA were used for RT-PCR analysis. However, using primer pair S7/Y12, specific for the full length 16S rRNA, results in the generation of a

significantly lower signal upon *mazF* overexpression (lanes 7 and 9) when compared to samples taken from untreated cells (lanes 6 and 8). Together, this result indicates the formation of 70SΔ43 ribosomes by MazF cleavage in the 16S rRNA. Remarkably, quantification of the RT-PCR analysis reveals that the signal obtained with rRNA extracted from polysomes of MazF-treated cells (**Figure 1C**, lane 9 and **Figure 1D**) is much lower than the signal obtained from total RNA upon *mazF* overexpression (lane 7 and **Figure 1D**). Thus, these results not only prove the formation of 70SΔ43 ribosomes upon *mazF* overexpression in general, they further underline that ribosomes that are still actively translating mRNAs after *mazF* overexpression are predominantly the 70SΔ43 ribosomes, which lack the 3'-terminal 43 nucleotides of the 16S rRNA due to MazF cleavage. Consistent with our previous observations (Vesper et al., 2011) canonical ribosomes still exist (see **Figure 1C**, lane 7). However, translation under these conditions seems to be almost entirely performed by the specialized 70SΔ43 ribosomes (lane 9), which are selectively translating a distinct subset of mRNAs.

Next, the quality of isolated total and polysome-associated RNA was determined *via* RT-PCR on the well-studied candidate mRNA *grcA* (formerly termed *yfiD*; (Vesper et al., 2011). The protein GrcA is the glycine radical cofactor A that reactivates pyruvate formate lyase after oxidative stress. Its corresponding mRNA, *grcA*, has been identified as target for MazF. The active endoribonuclease cleaves at an ACA-site at position -2 relative to the A of the AUG start codon resulting in the selective translation of the leaderless *grcA* mRNA by the 70SΔ43 ribosomes (Vesper et al, 2011). Thus, the *grcA* mRNA was used as a control to confirm the generation of the respective lmRNA by the removal of the 5'-UTR by MazF cleavage. First we validated the cleavage of *grcA* in total RNAs by primer extension, shown in **Figure S3A**The verification in polysomal RNA was performed by RT-PCR as a more sensitive method. For distinction between full length *grcA* mRNA containing the 5'-UTR and the leaderless *grcA* mRNA we performed RT-PCR with the reverse primer G1, annealing within the grcA coding region, in combination with either I3, annealing at the 5'-end of the grcA coding region downstream of the MazF cleavage site, or R1, binding to the 5'-UTR upstream of the MazF cleavage site (see lower panel in **Figure 1E**). The comparable amounts of input RNA were verified by the RT-PCR with primers I3/G1 amplifying the same amounts of a 423 nucleotides long PCR product from full length *grcA* mRNA as well as from leaderless *grcA* (**Figure 1E**, lanes 1-4). Employing primers R1/G1, specific for the full length *grcA* mRNA results in signals of the same intensity in RNA samples extracted from untreated cells (lanes 6 and 8). However, the signal is reduced in total RNA samples from cells after *mazF* overexpression (lane 7) showing that the *grcA* mRNA was cleaved by MazF resulting in the generation of the

lmRNA. In the mRNA samples extracted from polysomes after *mazF* overexpression the signal from the RT-PCR specific for full length *grcA* is even further reduced (lane 9) indicating that the portion of actively translated *grcA* mRNA upon MazF activation is predominantly leaderless.

As *grcA, rpsU* was likewise identified by Vesper and co-workers as a MazF target (Vesper et al, 2011), thus we sought to expand our validation to this candidate. However, checking the cleavage at the ACA site at position -2 from the start codon by primer extension in total RNA and RT-PCR in polysomal RNA, we could not observe the cleavage (shown in **Figure S1**). Comparing the conditions of *mazF* overexpression, we noted, that Vesper and co-worker used a five times higher concentration of IPTG to induce overexpression. It seems that cleavage at the 5'-UTR of *rpsU* requires a very strong expression of *mazF*.

Taken together, the data reveals that the employed polysome purification procedure is appropriate to extract sufficient amounts of intact mRNA for downstream applications like RNA-sequencing. Thus, the polysome-associated RNAs as well as the purified total RNAs were used to generate a cDNA library that was subjected to deep sequencing as described in 'Materials and Methods' to identify transcripts that are selectively translated upon *mazF* overexpression and thus constitute the 'lmRNA Regulon'.

Differential gene expression analysis reveals the extensive effects of the MazF-mediated stress response

For an initial characterization of the MazF-mediated changes in the RNome we employed a differential gene expression (DGE) analysis with *DESeq* (Anders and Huber, 2010) on the read count data obtained from total and polysome-associated RNA-Seq data mapped with the short read aligner *segemehl* (Hoffmann et al., 2009, 2014). We only considered genes with an adjusted p-value (padj) < 0.05 and a fold change > 1.5 or < 0,67 as significantly differentially present between the two conditions (+/- *mazF* overexpression). In Table 2 the numbers of all significantly altered genes is summarized in the last row 'all genes', intersected in total and polysomal RNA, further intersected in up- and down regulated genes. We found a total of 1664 genes significantly differentially regulated in our total RNA analysis, amongst those were 889 down-regulated and 775 up-regulated upon *mazF* overexpression. It appears that MazF induces a vast amount of changes, as this corresponds to 37% of the genome significantly altered after only 15 minutes *mazF* overexpression. This effect is even more pronounced in the polysomal RNA samples, where 2511 genes, representing 56% of the genome, are significantly altered upon *mazF* overexpression. 1296 genes are down-regulated, 1216 up-regulated. This

result goes in line with our hypothesis, that MazF induces a first-level, fast-track stress response by generating the 70SΔ43 ribosomes which can select for lmRNAs. Our data indicates that translational adaption to the stress situation occurs even before mRNA levels are altered to the same extend.

To get an impression of the overall functions assigned to the regulated RNAs we performed functional cluster analysis based on information provided by www.EcoGene.org (Zhou and Rudd, 2013) as specified in detail in 'Materials and Methods'. The supplementary **Table S2** summarizes the functional clusters that were assigned for this study. In **Figure 2A**, the columns "Total down" and "Total up" visualize the portion of functional clusters in the DGE data on total RNA, split in up- and down regulated genes. Compared with the distribution of functional clusters among all genes (**Figure 2A**, column 'all genes') it becomes apparent, that half of the RNAs down-regulated after *mazF* overexpression have a function in general cell metabolism and energy supply. The same is true for DGE analysis of polysome-associated RNA (**Figure 2A**, column 'Poly down'). This observation goes in line with the observations that activation of the toxin MazF leads to down-regulation of cellular metabolism (Tripathi et al., 2014). We also observe that the portion of genes involved in cell structure is particularly high in up-regulated genes (**Figure 2A**, columns 'Total up' and 'Poly up'), and this effect is even more striking in polysomal RNA. Besides this, the differential gene expression does not show any ostentatious cluster-specific effects of *mazF* overexpression which indicates a very broad range of alterations.

In **Figure 2B** we visualized to which extent *mazF* overexpression affects the regulation of the defined clusters in dependence of total (dark shades of gray) and polysome-associated (light shades of gray) RNA and split into overall regulatory effects and down- and up-regulation (second and third column of each set). The first striking observation is that nearly all regulatory effects are more pronounced in the polysomal RNA than in total RNA (**Figure 2B**, first column of each set). In the polysome-associated RNA samples 40-70% of all genes belonging to one particular functional cluster are altered, whereas these effects are 10-30% lower in total RNA. This observation again exemplifies that translational adaption plays a significant functional role in response to the MazF stress.

In some cases the ratio of down- or up-regulation within one cluster is very similar between total RNA and polysomal RNA, as for 'metabolism and energy supply', 'response regulation', and 'not classified'. This ratio however is reverted in the 'cell cycle' cluster, where more genes are up-regulated than down-regulated on the total RNA level but in polysome-associated RNA the bigger portion of regulated genes is down-regulated. This could mean that even when transcriptional regulation reacts to the stress with up-

regulation of cell cycle-specific genes, these RNAs are not efficiently translated and thus not incorporated into polysomes, as other tasks might be of more immediate importance. Exceedingly interesting are the differential ratios between down- and up-regulation in polysomal RNA in the clusters 'protein synthesis' and 'cell structure'. While genes of 'protein synthesis' appear to be only relatively little affected and evenly down- and up-regulated in total RNA samples, there is a strong effect on polysome-associated RNAs. Here, the majority of regulated RNAs are down-regulated and only a minor fraction is up-regulated. It seems that RNAs involved in protein synthesis are selectively excluded from translation during stress. The opposite effect becomes apparent in the 'cell structure' cluster where over 50% of all genes belonging to that cluster are up-regulated in polysomes while this portion is relatively small in total RNA.

When comparing DGE data obtained from total RNA with the data from the RNAs prepared from polysomes it becomes apparent, that the results do not overlap. In **Figure 2C** we plotted the log2foldChange values of the DGE analyses performed on data obtained from total RNA samples and from polysomal RNA samples for each *E.coli* gene significantly found in the one or the other analysis. We find 1244 genes in the second and third quadrant, meaning that these genes overlap in their regulation in total and polysomal RNA. The bisecting line indicates perfect correlation. If the regulatory effects in total RNA and polysomal RNA were correlated, the dots for most of the genes would cluster around that line. However, this is apparently not the case. The majority of dots are not even found in the second and third quadrant, but on the axes or the other quadrants. Dots found on the axes represent genes that are found to be significantly regulated only on the total RNA level (360 genes on the x-axis) or only in polysome-associated RNA (1208 genes on the y-axis). In the first and forth quadrants we find 60 antagonistically regulated genes. 27 genes are down-regulated on the total RNA level but up-regulated in polysomes and *vice versa* for 33 genes. A list of these antagonistically regulated genes can be found in the supplementary material (**Table S3**). Investigating the functions of these genes, it becomes again strikingly apparent that they distribute among all clusters. This antagonistic regulation affects all functions. A peculiar set of genes is a group of five genes encoding ribosomal proteins that are up-regulated in total RNA but down-regulated in polysome-associated RNAs. This is also reflected in supplementary **Figure S2**, which visualizes the extent of genes overlapping or not overlapping in their regulational pattern in the DGE data, in dependence of the functional clusters. Here, the first column of 'all genes' represents the data visualized in **Figure 2C**. In general, only 30-50% of the significantly differentially regulated genes do overlap ('Overlap') and the portion of genes that are exclusively altered in polysomes is exceedingly high ('Poly. only'). Here again, we

witness the more pronounced regulatory effects on the level of polysome-associated RNAs, indicating the high impact of selective translation on the stress response. Having a detailed look on the functional clusters, we basically see rare fluctuations in the distribution of regulatory overlapping and non-overlapping genes. Peculiar are the relative small ratios of genes found significantly up-regulated only in polysomes in the 'cell cycle' and 'protein synthesis' cluster. These functions might play a minor role in the stress reaction and are therefore subjected to translational up-regulation only to minor extent. Contrarily, the ratio of genes significantly up-regulated in polysomes in the 'cell structure' cluster is relative high, which might indicate that these genes are highly affected by translational regulation.

When analyzing the overlap of DGE data obtained from total and polysomal RNA after decreasing the stringency in choosing significant values (DGE padj < 0.05 and fold change factor of only 1.2), the amount of genes being differentially regulated in general increases, but the distribution of overlapping and differentially behaving candidates remains about the same (data not shown).

Differential abundance of RNAs in total and polysomal RNA

To focus in more detail on the differential abundance of RNAs in total and polysome-associated RNA samples, we performed a DGE analysis with *DESeq* (Anders and Huber, 2010) comparing total and polysomal RNA from the same condition ('T-' *versus* 'P-' and 'T+' *versus* 'P+'). We only considered genes with padj < 0.05, and foldChange factor > 1.6 as significantly differentially abundant in either polysomes or total RNA, whereas a foldChange factor of 1.6 means, that the ratio between the one or the other conditions is at least 63% to 37%. The most intrusive observation is that the difference in RNA abundance between total RNA and polysome-associated RNA is much more pronounced after *mazF* overexpression. In this condition we find 805 mRNAs species significantly more abundant in polysomes than in total RNA (**Table 3**, P+) and 762 mRNAs significantly more abundant in total RNA (T+), whereas we only find 251 mRNAs more abundant in polysomes (P-) and 452 more abundant in total RNA (T-) during exponential growth (**Table 3**, black bold numbers). It is remarkable that in non-stressed conditions mRNAs tend to be more abundant in total RNA. It seems that mRNAs are excessively produced during favorable growth conditions and that selectivity of the ribosomes plays only a minor role in regulation of protein synthesis as only 15% of the mRNAs are significantly differentially incorporated into ribosomes compared to their cellular levels. This observation might indicate additional regulatory roles of these mRNAs during stress.

When we compare the RNAs that are differentially abundant in polysomes and total RNA from relaxed conditions and upon *mazF* overexpression, we observe that they only overlap to some extent. Among the 805 RNAs significantly more abundant in polysomes after *mazF* overexpression only 102 show the same differential abundance under non-stressed conditions and *vice versa* 29 RNAs are even more abundant in total RNA (**Table 3**, light gray and dark gray numbers in the second row). **Table 3** shows an overview over the number of significantly differentially abundant mRNAs (bold black numbers) and the comparison between non-stress conditions and upon *mazF* overexpression (gray numbers).

Considering the functional classification of these differentially abundant RNAs some intriguing variability comes to light. First, it is apparent that the distributional pattern of functional clusters from mRNAs significantly more abundant in polysomes (P- and P+) differs vastly from the pattern of RNAs more abundant in total RNA (T- and T+, see **Figure 3**). More precisely, we observe that RNAs with functionality in 'metabolism and energy supply' tend to be – in both conditions – more effectively incorporated into polysomes than others as over 40% of the highly abundant RNAs in polysomes belong to that class. Additionally, we find the portion of RNAs belonging to 'cell structure' being much higher in polysome-abundant RNA species after *mazF* overexpression. It seems that these RNAs are selectively incorporated into polysomes during MazF-induced stress response as they might play an important role in coping with the stress while the portion of RNAs clustering into 'protein synthesis' decreases after the stress and seem to be selectively excluded from ribosomes.

When sorting the mRNAs according to the intensity of the difference in their abundance between total RNA and polysome-associated RNA (foldChange factor > 3, meaning a ratio of 75:25 percent), we find only 6 mRNAs that are intensively more abundant in polysomes under non-stress conditions but 283 RNA more abundant in total RNA. Under *mazF* overexpression conditions however, we find 160 mRNAs high abundant in polysomes as well as 160 mRNA high abundant in total RNA. Again, it seems that selective incorporation of mRNAs into polysome does not play a significant role under normal conditions and many mRNAs seem to be present in the cell in excess. In contrast, during MazF-derived stress selectivity of the ribosomes seems to play an important regulatory role as some mRNAs are selectively incorporated into polysomes and others are avoided.

Analysis of leaderless mRNAs

For the final qualitative analysis of the leaderless state of mRNAs in the polysomes we screened the read count density profiles visualized in the UCSC genome browser (Kent et al., 2002) for variations in the shape of the RNA in dependence of *mazF* overexpression. This screening yielded 335 candidates that show a significant cleavage at an ACA-site upstream of the start-codon and that are in this cleaved state significantly associated to polysomes. The distances of cleaved ACAs to the start codon vary from two to 100 nucleotides. About one third of these candidates (223) are cleaved at an ACA-site in a distance to the start codon of less than 25 nucleotides and can therefore be considered leaderless or short leadered (Vesper et al., 2011). **Table S4** lists these lmRNA candidates, the positions of the respective ACA-sites and the assigned functions of the genes and **Table 4** shows a selection of the most intriguing candidates. When analyzing the functions of the corresponding protein products we observe a very broad distribution (**Table 4,** column 'Main classification').

However, we concede that the RNA-seq approach can not reveal all processed mRNAs and that our list is most likely far from being complete, since the RNA-seq method is in general subjected to restrictions as some sequences tend to be more or less likely to be amplified and subsequently sequenced (Sendler et al., 2011). In some cases the 5'-UTR of an mRNA is not sufficiently covered by sequencing reads in samples from unstressed conditions. Here, we cannot draw any conclusion concerning their leadered or leaderless state after *mazF* overexpression.

We further validated the MazF-cleavage of several of the respective mRNAs by primer extension analysis on total RNA purified from exponentially growing cells and from cells upon *mazF* overexpression. We confirmed the cleavage in the 5'-UTR at the expected ACA-sites for 15 mRNAs, which are indicated in bold in **Table 4** and **Table S4** and shown in **Figure 4** and **Figure S3**. Additionally, we tested two mRNAs that possess an ACA-site in the 5'-UTR but not appear to be cleaved by MazF according to the sequencing data (*erfK*, *infA*) and confirmed that they are not cleaved at the respective positions (data not shown). Likewise, *rpsU* does not appear to be cleaved in the sequencing data as shown in **Figure S1**, confirming our previous observation that *rpsU* was not cleaved in the present study due to a lower concentration of the inducer IPTG.

Discussion

The MazF-mediated stress response mechanism poses a novel example for translational regulation by generating a so far undefined subset of lmRNAs and their selective translation by concomitantly produced specialized 70SΔ43 ribosomes (Vesper et al., 2011). In our attempt to decipher the 'lmRNA Regulon' we established a method to isolate intact, full length mRNAs from polysomes –in contrast to so far published protocols- avoiding physiological interference by translation blocking agents.

Assessing the 'lmRNA Regulon'

Employing our optimized polysome purification procedure we were able to extract intact mRNA, which we subjected to RNA-sequencing analysis (**Figure 1A** and **Table 1**). First, we validated the formation of the specialized 70SΔ43 ribosomes and their enrichment in the polysome fraction, indicating their translational activity (**Figure 1C** and **1D**). Further, we confirmed that *grcA*, an identified MazF target that is translated by the 70SΔ43 ribosomes (Vesper et al., 2011), is enriched in the polysomal fractions after *mazF* overexpression (**Figure 1E**). These results reveal that our method allows the identification of novel lmRNA candidates, as we could confirm the observed cleavages of all tested candidates (**Figure 4** and **S3**). Although we do not claim that this method will reveal all potential processing events, we found a large number (223) of mRNAs rendered leaderless and incorporated into polysomes upon *mazF* overexpression.

Additionally, a few mRNAs are transcribed as leaderless or short leadered mRNAs (reviewed by Moll et al. 2002), usually derived from accessory genetic elements and Romero and co-workers have recently identified a few more lmRNAs in *E.coli* (Romero et al., 2014). Out of these, two are primarily *E. coli* genes (*rhlB*, encoding an ATP dependent RNA helicase, and *pgpA*, encoding the phosphatidyl-glycerophosphatase A). Likewise, *yfbU* possesses a promoter right in front of the start codon resulting in a lmRNA (Vesper et al., 2011). We could validate the leaderless state of these three mRNAs in our sequencing data, as shown in **Figure S4**.

To our surprise, the majority of the MazF-dependent lmRNA candidates does not have specifically assigned functions in stress response, which would have been expected considering that MazF plays a direct role in stress survival or recovery. In contrast to our assumption, the mRNAs cleaved by MazF are involved in a broad range of functions (**Table 4** and **Table S4**) indicating the widespread effects of MazF activity in response to stress.

Interesting MazF targets in the spotlight

Additionally interesting MazF-cleavage candidates are *rho*, *rpoA*, and *zwf* shown in **Figure 4A, B** and **D** and *rtcB* (data not shown). *rho* codes for the transcription termination factor Rho that promotes dissociation of RNA polymerase (RNAP) and the nascent mRNA from the template DNA by binding to so-called *rut* (rho utilization) sites in the nascent mRNA and ATP-dependent helicase activity (Boudvillain et al., 2010; Peters et al., 2011). It has been shown that transcription and translation are coupled by indirect interaction of the ribosome and RNAP under favorable conditions (Burmann et al., 2010; Proshkin et al., 2010). In this situation frequent *rut* sites within coding regions of mRNAs, that would recruit Rho and lead to intragenic transcription termination, are obscured by the ribosome. When translation is shut down due to stress-induced MazF activity, Rho can access these rut sites and promote transcription termination (Boudvillain et al., 2013). It is conceivable that sustained production of Rho *via* selective translation of its lmRNA might link decreased protein synthesis to early transcription termination in order to save resources for the stressed cells. Furthermore, Rho has been linked to additional regulatory functions in gene expression (Boudvillain et al., 2013) which might likewise be important during stress response.

rpoA codes for the α-subunit of RNAP which is essential for assembly of the core RNAP and involved in regulation of transcription initiation as transcription factors bind to the α-subunit. Recently, RNAPα was shown to interact with RP L2 and the authors could show that L2 acts as a transcriptional regulator (Rippa et al., 2010). As *rplB*, the gene coding for L2, was likewise indentified in our screen as a MazF target, one can imagine that the transcriptional regulation *via* L2-RNAPα is important during stress response or stress recovery.

zwf (Zwischenferment) encodes the glucose-6-phosphate 1-dehydrogenase. Interestingly, the residues 199-203 of Zwf encode a NNWDN (Asn-Asn-Trp-Glu-Asn) pentapeptide that can be excised from the protein by ClpPX (Kolodkin-Gal and Engelberg-Kulka, 2008) and is likely to be converted to NNWNN (Asn-Asn-Trp-Asn-Asn) by asparagine synthase A (AsnA) (Kolodkin-Gal et al., 2007). NNWNN represents the quorum sensing molecule Extracellular Death Factor (EDF) which is involved in MazF toxicity and leads to directed bacterial death. Deletion of *zwf* and *asnA* both individually prevented production of active EDF (Kolodkin-Gal et al., 2007). Processing of *zwf* by MazF to a leaderless mRNA might ensure the synthesis of the corresponding protein and thus preserve EDF production (Engelberg-Kulka and Moll, manuscript in preparation).

rtcB codes for the RNA ligase RtcB and we suggest that it is responsible for re-ligation of the aSD-containing 43 nucleotides that have been removed by MazF from the 16S rRNA (Temmel et al, manuscript in preparation).

The underestimated significance of translational regulation and ribosome specificity

Comparative analysis of polysome-associated *versus* total RNA allows us to draw some general conclusions concerning transcriptional and translational regulation of gene expression upon stress. Considering the general stress response, which is mediated at the transcriptional level, one would expect a correlation between the transcriptional regulation of a particular RNA and its translational efficiency as exemplified by its presence in the polysome fraction. However, this assumption is not supported by our results. Interestingly, we observe that the changes in mRNA levels in response to *mazF* overexpression are more pronounced in RNAs associated with polysomes when compared to total RNA (**Figure 2B**). Further, almost 50% of the RNAs differentially incorporated into polysomes upon *mazF* overexpression are not significantly regulated on the total RNA level (**Figures 2C** and **S2**). Taken together, our data indicate that in contrast to relaxed conditions, translational regulation plays a major role in adaptation to stress conditions. This notion was recently strongly supported by Picard and co-workers who have analyzed the translational response of the lactic acid bacterium *Lactococcus lactis* during isoleucine starvation by ribosome profiling coupled with micro array analysis (Picard et al., 2013). The authors present evidence that translational regulation significantly contributes to the stress response. Correspondingly, Taylor and co-workers investigated the extent of translational regulation in protein synthesis of *Shewanella oneidensis MR-1* during oxygen limitation by comparing mRNA-seq and proteome data (Taylor et al., 2013). They report that alteration of translational efficiency contributes to about 75% of the changes in protein levels.

Besides these general observations, we draw our attention to some peculiar groups. The set of genes encoding ribosomal proteins (RPs) proved to be particularly interesting in this study. 46 out of 54 RP-encoding genes are significantly down-regulated in polysomes after *mazF* overexpression, however only 14 out of these are also down-regulated on the total RNA level This is also represented in the ‘protein synthesis’ cluster shown in **Figure 2**, indicating that the proportion of down-regulation is much higher in polysomes than in total RNA (second and third columns in the ‘PS’ cluster). In **Figure S2** it becomes apparent that the portion of genes that is exclusively down-regulated in polysomes is particularly high in the ‘protein synthesis’ functional cluster. Five out of the 46 polysomally down-regulated RP-genes (coding for S17, L20, L21, L27, and L33) are even antagonistically up-

regulated in total RNA as shown in **Table S3**. In addition, eleven RP-coding mRNAs are rendered leaderless and associated to polysomes (S1, S2, S7, S10, S16, S20, L2, L7/L12, L18, L28, and L35, as shown in **Table S4**). However, these lmRNA candidates are not significantly differentially regulated it total or polysomal RNAs (except for S7, L2 and L35 which are polysomally down-regulated). *rpsA*, the mRNA encoding the RP S1 is of particular interest (shown in **Figure 4C**), as S1 is crucial for efficient translation initiation in Gram-negative bacteria (Boni et al., 1991; Qu et al., 2012; de Smit and van Duin, 1994), but is dispensable for the translation of lmRNAs (Moll et al., 2002b; Tedin et al., 1997). As the MazF-mediates stress response mechanism is based on translation of lmRNAs, S1 is not required during the stress. However, continuous synthesis of S1 under these conditions from the leaderless transcript might be crucial to ensure its required presence during recovery from stress when translation of canonical mRNAs becomes prevalent again.

Final conclusions

Taken together, we observe a huge range of alterations in response to *mazF* overexpression. On the one hand we identified diverse MazF targets that are likely to be selectively translated by 70SΔ43 ribosomes; on the other hand we observe widespread regulatory effects, mainly on the translational level. Recently, Tripathy and co-workers have shown that pseudo-physiological activation of MazF by titrating its cognate antitoxin MazE with an enzymatically inactive MazF mutant (E24A) leads to increased persister formation in *E. coli* (Tripathi et al., 2014). Moreover, pretreatment with sub-lethal concentrations of particular antibiotics leads to a higher survival rate during treatment with lethal antibiotic concentrations in dependence of *mazF*. In addition, they observed that basal levels of active MazF are able to induce persistence (Tripathi et al., 2014). Since our study reveals the extent of MazF-induced alterations it is conceivable that MazF is a key regulator in adaption to stress and persister formation. Activation of a single protein inducing such a broad range of alterations might pose a means for individual cells to enter the persistence phenotype. As our study addresses the whole bacterial population, we cannot conclude how transcription and translation are altered in every individual cell. Observing such a broad variation of alterations it is possible that MazF induces heterogeneous effects within the population and this variety could be attributed to the versatility of translational adaptation in single cells. Thus, it remains to be further investigated, if MazF activity induces population heterogeneity and consequently results in the generation of a subset of persister cells.

Additionally, the MazF-mediated mechanism might pose a ‘fast-track’ stress response. Conventional adaption of gene expression involves the differential production and degradation of mRNAs and subsequent translation into the required protein products. As we have shown that the activation of only one protein, namely MazF, induces a pronounced translational regulation, it is conceivable that the MazF-mediated stress response mechanism acts even before the major adjustments by transcriptional regulation have kicked into play as discussed recently (Sauert et al., 2014).

Material and Methods

Bacterial strains and growth conditions used in this study

We used the bacterial strain *E. coli* MC4100 *relA*$^+$ (described by (Engelberg-Kulka et al., 1998) for untreated conditions and MC4100 *relA*$^+$ carrying plasmid pSA1 for IPTG-inducible *mazF* overexpression. Plasmid pSA1 was described by Amitai and co-workers and bears *lacI*^{q} as well as *mazF* under the control of the T5 promoter and the lac operator (Amitai et al., 2009). Bacterial strains were grown at 37°C in LB broth, eventually supplemented with 100 µg/ml ampicillin for plasmid maintenance. Growth was monitored by photometric measurement of an optical density at 600 nm.

Purification of total and polysome-associated RNA upon *mazF* overexpression

To analyze the MazF-mediated stress response in *E. coli*, strains MC4100 *relA*$^+$ and MC4100 *relA*$^+$ pSA1 were grown at 37°C in LB. At OD_{600} of 0.5, both cultures were divided. One half of each culture was treated with 100 µM IPTG, one half was left untreated and all samples were incubated further.

In strain MC4100 *relA*$^+$ pSA1, addition of IPTG induces overexpression of the toxin coding gene *mazF*, leading to severely impaired growth (data not shown). For further analysis, MC4100 *relA*$^+$ pSA1 +IPTG was harvested 15 minutes after IPTG addition (OD_{600} of 0.6), according to the downstream applications. MC4100 *relA*$^+$ was harvested without treatment at an OD_{600} of 0.6.

For total RNA preparation, 50 ml of cell cultures were harvested in 50 ml conical centrifuge tubes (Starlab) by centrifugation for 10 minutes at 4000 rpm and 4°C in an Eppendorf 5810 R centrifuge (Rotor FA 45-6-30) and cell pellets were frozen in liquid nitrogen. Total RNA was isolated using TRIzol®-reagent (Invitrogen) following the manufacturer's protocols.

For preparation of polysome-associated RNA a volume of 1.2 l of cell culture per sample was quickly chilled by pouring into 3x 500 ml centrifuge bottles (Nalgene) containing 100ml fresh ice, while keeping in ice-water-NaCl-bath at approximately -5°C and immediately harvested by centrifugation at 4000 rpm for 10min at 4°C in a Sorvall RC5-C (FiberLite F10S-6x500y rotor, Piramon Technologies). This way we sought to "freeze" ribosomes on translated mRNAs without using translation-blocking antibiotics which would interfere with the general stress response. Cell pellets were always kept on ice and gently resuspended in ice-cold TICO-lysis-buffer (20 mM HEPES, 6 mM MgOAc, 6 mM NH_4OAc, 4 mM β-Mercapto-EtOH, 4 mg/ml Lysozyme) to a final concentration of 200

OD_{600}-units per ml, transferred to a 50 ml conical centrifuge tube (Starlab), and slowly frozen at -20°C to avoid shearing of RNA. For gentle cell disruption the suspension was slowly thawed on ice and slowly refrozen at -20°C for three times. DNAseI (RNAse-free, Roche) was added in a concentration of 0.05 units per OD_{600}-unit and incubated for 10 minutes on ice after each thawing step. The S30 extracts were cleared in aliquots of 1 ml by centrifugation in 1.5 ml reactions tubes (Sarstedt) at 30.000 g for 1 h at 4°C in a Sigma 3K30 centrifuge (rotor 12154) and stored at -80°C.

For separation of ribosomal subunits and 70S ribosomes from polysomes, 50-100 A_{260}-units of S30 extracts (in a maximum of 1 ml) were loaded onto a 10-30% sucrose gradient in TICO-buffer in SW28 tubes (SETON) and separated by centrifugation at 28.000 rpm for 3h at 4°C in a Beckmann L-70 ultracentrifuge (Beckmann SW28 rotor).

Upon fractionation, polysome fractions (see **Figure 1B**, fractions 20-32, approximately 13 ml) were pooled and concentrated to 300 µl in H_2O-DEPC by precipitation with 10% Sodium Acetate (pH 5,2) and 50% 2-propanol over night at -20°C and centrifugation at 13.000 rpm for 1h at 4 °C in a Eppendorf 5810 R centrifuge (Rotor FA 45-6-30). RNA was isolated using TRIzol®-reagent (Invitrogen) following the manufacturer's protocols.

To remove spuriously co-purified genomic DNA from total or polysome derived RNA, the samples were treated with DNAseI (RNAse-free, Roche), extracted again with phenol/chloroform extraction and ethanol-precipitation, and complete digestion was verified by PCR (Primers for chromosomal *grcA*: I3/G1, data not shown). This step was eventually repeated once or twice until last traces of DNA have been degraded. Ribosomal RNA was depleted using Ribo-Zero™ Magnetic Kit (Gram-Negative Bacteria, Epicentre) following the manufacturer's protocol. For further analysis, the depleted rRNA, bound to the magnetic beads, was recovered by phenol/chloroform extraction and ethanol-precipitation. For an overview of the purification process and efficiencies see **Table 1**.

Reverse transcription PCRs

RT-PCR experiments were performed with QIAGEN OneStep RT-PCR Kit according to the manufacturer's protocol. Reactions on extracted rRNA from breads with the primers S7/X15 or S7/Y12 (listed in **Table S5**) were performed with normalized amounts of 25ng rRNA (55°C, 30 minutes for RT; 95°C for 15 minutes for RT inactivation; 21 cycles of 94°C, 45 seconds, 59°C annealing for 45 seconds and 72°C for 30 seconds; 72°C, 5 min). RT-PCR reactions on DNA-digested total RNA and polysome-associated RNA with primers I3/G1 and R1/G1 (listed in **Table S5**) were performed with 25 ng RNA (55°C, 30 minutes for RT;

95°C for 15 minutes for RT inactivation; 30 cycles of 94°C, 45 seconds, 55°C annealing for 45 seconds and 72°C for 30 seconds; 72°C, 5 min). All reactions were performed in duplicates in which one reaction was performed without the initial incubation at 55°C for RT reaction to exclude DNA contamination. These reactions, as well as controls with H_2O as template yielded no signals (data not shown).

***In vitro* transcription and primer extension analysis**

For *in vitro* synthesis of canonical and leaderless variants of *yfiD* mRNAs, the respective genes were amplified by PCR using chromosomal DNA from *E. coli* strain MG1655 as template employing the primers listed in **Table S5**. The PCR products served as templates for *in vitro* transcription reactions using the AmpliScribeTM T7-High Yield transcription kit (Epicenter) according to the manufacturer' protocol. Primer extension analysis was performed as previously described by (Vesper et al., 2011) and (Moll et al., 2004). Briefly, 1 pmol of the respective mRNAs were annealed to the 5'-end-labeled reverse primers (**Table S5**) in 1xRT-buffer by heating for 3 min to 80°C, snap freezing in liquid nitrogen, and slowly thawing on ice. Primer extension reactions were performed in RT-buffer by using the AMV reverse transcriptase (Promega) by incubation at 42°C for 30 min. The samples were separated on an 8% PAA-8M urea gel, and the extension signals were visualized by using a Molecular Dynamics PhosphoImager (GE Healthcare).

Library preparation and sequencing

RNA samples from four samples of the *E. coli* MC4100 RelA+ F' strain were analyzed for this study: Total RNA from untreated cells (T-), total RNA from cells with pSA1 after IPTG-induction leading to *mazF* overexpression (T+), polysome-associated RNA from untreated WT cells (P-) and polysome-associated RNA from cells with pSA1 after IPTG-induction leading to *mazF* overexpression (P+). Libraries from two biological replicates (R1 and R2) were prepared using 50-100 ng of the rRNA-depleted RNA with NEBNext® Ultra Directional RNA Library Prep Kit for Illumina (New England BioLabs), following the manufacturer's protocol. The quality of the resulting adaptor ligated cDNA was checked with Agilent DNA Kit on an Agilent 2100 Bioanalyzer. Library preparation resulted in samples with average fragment sizes of 200-240bp (data not shown). Samples were pooled (one set of four (T-, T+, P-, P+) per replicate for one multiplex) and sequenced on Illumina HiSeq2000 with a single read length of 100 bp (Campus Science Support Facilities GmbH, NGS unit, csf.ac.at). Sequence reads were mapped to the *E. coli* BW2952 MC4100 reference sequence (accession NC_012759).

Computational analysis

The sequencing resulted in a total of approx. 220 million raw reads per multiplex/replicate. Sequencing adapters were removed from the demultiplexed samples with *cutadapt* (Martin, 2011). Quality control before and after adapter removal was performed with *FastQC* (http://www.bioinformatics.babraham.ac.uk/projects/fastqc/). The BW2952 MC4100 reference genome and annotation (accession NC_012759) were obtained from the NCBI FTP server an reads were mapped against the reference genome with *segemehl* (v0.1.7) (Hoffmann et al., 2009, 2014). Uniquely mapped reads were extracted for the downstream analysis and processed for UCSC visualization with the *ViennaNGS* suite (Wolfinger et al., 2014). Read count numbers for each sample were determined with the *htseq-count* utility from the *HTSeq* package (Anders et al., 2014) and differential gene expression analysis was performed with *DESeq* (Anders and Huber, 2010). Cutoff values for considering changes as significant are an adjusted p-value (padj) < 0.05 and log2foldChange < -0.6 for down-regulation and > 0.6 for up-regulation, which corresponds to a fold change of minimal 1.5, meaning an alteration of at least 50%. Visualization of aligned reads and coverage profiles was done with the UCSC genome browser (Kent et al., 2002). Coverage profiles of individual samples were normalized to 10 million reads to allow for intuitive comparison (Wolfinger et al., 2014).

To cluster candidates according to their functions we used the function assignments provided by EcoGene 3.0 (http://www.ecogene.org, (Zhou and Rudd, 2013)). We downloaded a table of gene names, protein products and functions for all 4506 to date annotated genes (dated in December 2014) and used the provided information to cluster the genes into the following functional classes: Metabolism & energy supply (ME), Cell cycle (CC), Protein synthesis(PS), Response regulation(RR), Cell structure (CS), Not classified (NC). See **Table S2** for a detailed list of the defined functional classes and subclasses. The matching of lists of candidates with the classification annotation list was performed with R (R Core Team, 2014).

References

Amitai, S., Kolodkin-Gal, I., Hananya-Meltabashi, M., Sacher, A., and Engelberg-Kulka, H. (2009). Escherichia coli MazF leads to the simultaneous selective synthesis of both “death proteins” and “survival proteins.” PLoS Genet. 5, e1000390.

Anders, S., and Huber, W. (2010). Differential expression analysis for sequence count data. Genome Biol. 11, R106.

Anders, S., Pyl, P.T., and Huber, W. (2014). HTSeq—a Python framework to work with high-throughput sequencing data. Bioinformatics btu638.

Balleza, E., López-Bojorquez, L.N., Martínez-Antonio, A., Resendis-Antonio, O., Lozada-Chávez, I., Balderas-Martínez, Y.I., Encarnación, S., and Collado-Vides, J. (2009). Regulation by transcription factors in bacteria: beyond description. FEMS Microbiol. Rev. 33, 133–151.

Boni, I.V., Isaeva, D.M., Musychenko, M.L., and Tzareva, N.V. (1991). Ribosome-messenger recognition: mRNA target sites for ribosomal protein S1. Nucleic Acids Res. 19, 155–162.

Boudvillain, M., Nollmann, M., and Margeat, E. (2010). Keeping up to speed with the transcription termination factor Rho motor. Transcription 1, 70–75.

Boudvillain, M., Figueroa-Bossi, N., and Bossi, L. (2013). Terminator still moving forward: expanding roles for Rho factor. Curr. Opin. Microbiol. 16, 118–124.

Burmann, B.M., Schweimer, K., Luo, X., Wahl, M.C., Stitt, B.L., Gottesman, M.E., and Rösch, P. (2010). A NusE:NusG complex links transcription and translation. Science 328, 501–504.

Engelberg-Kulka, H., Reches, M., Narasimhan, S., Schoulaker-Schwarz, R., Klemes, Y., Aizenman, E., and Glaser, G. (1998). rexB of bacteriophage lambda is an anti-cell death gene. Proc. Natl. Acad. Sci. U. S. A. 95, 15481–15486.

Hoffmann, S., Otto, C., Kurtz, S., Sharma, C.M., Khaitovich, P., Vogel, J., Stadler, P.F., and Hackermüller, J. (2009). Fast mapping of short sequences with mismatches, insertions and deletions using index structures. PLoS Comput. Biol. 5, e1000502.

Hoffmann, S., Otto, C., Doose, G., Tanzer, A., Langenberger, D., Christ, S., Kunz, M., Holdt, L.M., Teupser, D., Hackermüller, J., et al. (2014). A multi-split mapping algorithm for circular RNA, splicing, trans-splicing and fusion detection. Genome Biol. 15, R34.

Ingolia, N.T., Ghaemmaghami, S., Newman, J.R.S., and Weissman, J.S. (2009). Genome-Wide Analysis in Vivo of Translation with Nucleotide Resolution Using Ribosome Profiling. Science 324, 218–223.

Kent, W.J., Sugnet, C.W., Furey, T.S., Roskin, K.M., Pringle, T.H., Zahler, A.M., and Haussler, D. (2002). The human genome browser at UCSC. Genome Res. 12, 996–1006.

Kolodkin-Gal, I., and Engelberg-Kulka, H. (2008). The extracellular death factor: physiological and genetic factors influencing its production and response in Escherichia coli. J. Bacteriol. 190, 3169–3175.

Kolodkin-Gal, I., Hazan, R., Gaathon, A., Carmeli, S., and Engelberg-Kulka, H. (2007). A linear pentapeptide is a quorum-sensing factor required for mazEF-mediated cell death in Escherichia coli. Science 318, 652–655.

Lewis, K. (2010). Persister cells. Annu. Rev. Microbiol. 64, 357–372.

Maier, T., Güell, M., and Serrano, L. (2009). Correlation of mRNA and protein in complex biological samples. FEBS Lett. 583, 3966–3973.

Martin, M. (2011). Cutadapt removes adapter sequences from high-throughput sequencing reads. EMBnet.journal 17, pp. 10–12.

Miller, O.L., Jr, Hamkalo, B.A., and Thomas, C.A., Jr (1970). Visualization of bacterial genes in action. Science 169, 392–395.

Moll, I., Grill, S., Gualerzi, C.O., and Bläsi, U. (2002a). Leaderless mRNAs in bacteria: surprises in ribosomal recruitment and translational control. Mol. Microbiol. 43, 239–246.

Moll, I., Grill, S., Gründling, A., and Bläsi, U. (2002b). Effects of ribosomal proteins S1, S2 and the DeaD/CsdA DEAD-box helicase on translation of leaderless and canonical mRNAs in Escherichia coli. Mol. Microbiol. 44, 1387–1396.

Moll, I., Hirokawa, G., Kiel, M.C., Kaji, A., and Bläsi, U. (2004). Translation initiation with 70S ribosomes: an alternative pathway for leaderless mRNAs. Nucleic Acids Res. 32, 3354–3363.

Oh, E., Becker, A.H., Sandikci, A., Huber, D., Chaba, R., Gloge, F., Nichols, R.J., Typas, A., Gross, C.A., Kramer, G., et al. (2011). Selective ribosome profiling reveals the cotranslational chaperone action of trigger factor in vivo. Cell 147, 1295–1308.

Peters, J.M., Vangeloff, A.D., and Landick, R. (2011). Bacterial transcription terminators: the RNA 3’-end chronicles. J. Mol. Biol. 412, 793–813.

Picard, F., Loubière, P., Girbal, L., and Cocaign-Bousquet, M. (2013). The significance of translation regulation in the stress response. BMC Genomics 14, 588.

Potrykus, K., and Cashel, M. (2008). (p)ppGpp: still magical? Annu. Rev. Microbiol. 62, 35–51.

Proshkin, S., Rahmouni, A.R., Mironov, A., and Nudler, E. (2010). Cooperation between translating ribosomes and RNA polymerase in transcription elongation. Science 328, 504–508.

Qu, X., Lancaster, L., Noller, H.F., Bustamante, C., and Tinoco, I. (2012). Ribosomal protein S1 unwinds double-stranded RNA in multiple steps. Proc. Natl. Acad. Sci. U. S. A. 109, 14458–14463.

R Core Team (2014). R: A Language and Environment for Statistical Computing (R Foundation for Statistical Computing).

Rippa, V., Cirulli, C., Di Palo, B., Doti, N., Amoresano, A., and Duilio, A. (2010). The ribosomal protein L2 interacts with the RNA polymerase alpha subunit and acts as a transcription modulator in Escherichia coli. J. Bacteriol. 192, 1882–1889.

Romero, D.A., Hasan, A.H., Lin, Y.-F., Kime, L., Ruiz-Larrabeiti, O., Urem, M., Bucca, G., Mamanova, L., Laing, E.E., van Wezel, G.P., et al. (2014). A comparison of key aspects of gene regulation in Streptomyces coelicolor and Escherichia coli using nucleotide-resolution transcription maps produced in parallel by global and differential RNA sequencing. Mol. Microbiol.

Sauert, M., Temmel, H., and Moll, I. (2014). Heterogeneity of the translational machinery: Variations on a common theme. Biochimie.

Sendler, E., Johnson, G.D., and Krawetz, S.A. (2011). Local and global factors affecting RNA sequencing analysis. Anal. Biochem. 419, 317–322.

Sharma, U.K., and Chatterji, D. (2010). Transcriptional switching in Escherichia coli during stress and starvation by modulation of sigma activity. FEMS Microbiol. Rev. 34, 646–657.

De Smit, M.H., and van Duin, J. (1994). Translational initiation on structured messengers. Another role for the Shine-Dalgarno interaction. J. Mol. Biol. 235, 173–184.

Taylor, R.C., Webb Robertson, B.-J.M., Markillie, L.M., Serres, M.H., Linggi, B.E., Aldrich, J.T., Hill, E.A., Romine, M.F., Lipton, M.S., and Wiley, H.S. (2013). Changes in translational efficiency is a dominant regulatory mechanism in the environmental response of bacteria. Integr. Biol. Quant. Biosci. Nano Macro 5, 1393–1406.

Tedin, K., Resch, A., and Bläsi, U. (1997). Requirements for ribosomal protein S1 for translation initiation of mRNAs with and without a 5′ leader sequence. Mol. Microbiol. 25, 189–199.

Tripathi, A., Dewan, P.C., Siddique, S.A., and Varadarajan, R. (2014). MazF-induced growth inhibition and persister generation in Escherichia coli. J. Biol. Chem. 289, 4191–4205.

Vesper, O., Amitai, S., Belitsky, M., Byrgazov, K., Kaberdina, A.C., Engelberg-Kulka, H., and Moll, I. (2011). Selective translation of leaderless mRNAs by specialized ribosomes generated by MazF in Escherichia coli. Cell 147, 147–157.

Wolfinger, M.T., Fallmann, J., Eggenhofer, F., and Amman, F. (2014). ViennaNGS: A toolbox for building efficient next-generation sequencing analysis pipelines. bioRxiv.

Zhang, Y., Zhang, J., Hoeflich, K.P., Ikura, M., Qing, G., and Inouye, M. (2003). MazF cleaves cellular mRNAs specifically at ACA to block protein synthesis in Escherichia coli. Mol. Cell 12, 913–923.

Zhou, J., and Rudd, K.E. (2013). EcoGene 3.0. Nucleic Acids Res. 41, D613–D624.

Figure legends

Figure 1: The polysome purification

A) Schematic depiction of the workflow. *E.coli* MC4100 *relA*$^+$ (light gray) and MC4100 *relA*$^+$ pSA1 (dark gray) were cultured in LB at 37°C to mid-exponential phase and *mazF* overexpression was induced in MC4100 *relA*$^+$ pSA1 (**+**) for 15 minutes by addition of 100 µM IPTG. Both cultures were harvested and on the one hand total RNA extracted („**T-**" for MC4100 *relA*$^+$ and „**T+**" for MC4100 *relA*$^+$ pSA1 +IPTG). On the other hand cell lysates were applied to sucrose gradient density centrifugation to obtain ribosome profiles. The polysome fractions were pooled and the respective mRNAs isolated („**P-**" for MC4100 *relA*$^+$ and „**P+**" for MC4100 *relA*$^+$ pSA1 +IPTG). The four samples were prepared in biological duplicates and all eight samples subjected to RNA-seq. **B) Ribosome profiles.** Cell lysates from *E.coli* MC4100 *relA*$^+$ (dashed line) and MC4100 *relA*$^+$ pSA1 + 100 µM IPTG (straight line) were applied to sucrose density gradient centrifugation after mild cell disruption with lysozyme and DNAse I at 0 – 4°C. **C) RT– PCR detecting 16S rRNA on recovered rRNA from total RNA and from polysome-preparations.** In lanes 1-4 RT-PCRs with primers omitting the potentially cleaved off 43 nucleotides of 16S rRNA (S7 and X15) as an internal control are shown. The signals are equivalent, proving equal input into the analysis. Lanes 6-9 show analogous RT-PCR experiments with primers including the very 3'-end of 16S rRNA (S7 and Y12). In lanes 6 and 8, where rRNA recovered from total RNA or from polysomes, respectively, without *mazF* overexpression were used, the signals corresponds to the internal controls. After *mazF* overexpression, the amount of full length rRNA is significantly reduced in total RNA (lane 7) and barely detectable in polysome RNA (lane 9). Below a schematic drawing depicts the positions of the primers used for RT-PCR on the *16S* rRNA purified from total RNA and from polysome fractions. **D) Quantification of the RT– PCR specific for 16S rRNA.** We normalized the quantified signal intensities of RT-PCRs with primers S7/Y12 which include the very 3'-end of the 16S rRNA to the quantified signal intensities of RT-PCRs with primers S7/X15 omitting the 3'-end. Without *mazF* overexpression (**T-** and **P-**) the 3'-end of 16S rRNA is affected only to a minor extend, possibly resulting from slight RNA degradation events during the purification procedure. However, after *mazF* overexpression (**T+** and **P+**) the 16S rRNA 3'-end is dramatically reduced in total RNAs and even more in rRNA recovered from polysomes. **E) RT– PCR detecting *grcA* mRNA in total and polysomal RNA.** In lanes 1-4 RT-PCRs with primers omitting the potentially cleaved off 5'-UTR of *grcA* (I3 and G1) as an internal control are shown. The signals are equivalent, proving equal input into the analysis. Lanes 6-9 show analogous RT-PCR experiments with primers including the 5'-UTR of *grcA* (R1 and G1). In lanes 6 and 8, where total RNA or mRNA extracted from

polysomes, respectively, without *mazF* overexpression were used, the signals corresponds to the internal controls. After *mazF* overexpression, the amount of full length *grcA* mRNA is significantly reduced in total RNA (lane 7) and even more reduced in polysome-purified mRNA (lane 9). (Primers I3, R1 and G1 add 29, 29 and 10 bp, respectively to the PCR product.) Below a schematic drawing depicts the positions of the primers used for RT-PCR on the *grcA* mRNA within total and polysomal RNA.

Figure 2

A) Distribution of functional clusters within the entity of observed differentially expressed genes. The columns visualize the numbers represented in the first column of the corresponding sections of **Table 2**, normalized to 100% per group (the corresponding numbers are indicated in each sub-column). The last column 'all genes' visualizes the distribution of the functional clusters in the entity of all 4506 *E. coli* genes, that have been considered for cluster analysis, provided by EcoGene.org. **B) Percentage of genes within one cluster differentially affected by *mazF* overexpression.** The columns visualize how many genes within one cluster are relatively affected by *mazF* overexpression (the corresponding numbers are indicated in each sub-column). The first column of each set indicates the total level of regulation, the second and third defines down- and up-regulation, respectively. For each cluster this analysis was separated into genes regulated on the total RNA level (dark shades of gray) and genes regulated in polysomes (light shades of gray). The last set of columns „all genes" visualizes the extent of regulation within the entity of all 4506 *E. coli* genes, that have been considered for cluster analysis, provided by EcoGene.org indicating that 38% of all genes are differentially regulated upon *mazF* overexpression in total RNA samples (black column) and 58% in polysome-associated RNAs (first light gray column). **C) Correlation between regulatory effects by *mazF* overexpression in total and polysome-associated RNA is far from perfect.** The log2foldChange values of the DGE analyses performed on data obtained from total RNA samples and from polysomal RNA samples are plotted for each *E.coli* gene significantly altered according to the one or the other analysis (padj < 0.05; log2foldChange < 0.6 (down-regulation) or > 0.6 (up-regulation)). The black line indicates the bisecting line, on which all points should fall if the regulatory effects in total RNA and polysomal RNA were perfectly correlated. CC = cell cycle, CS = cell structure, NC = not classified, ME = metabolism and energy supply, PS = protein synthesis, RR = response regulation.

Figure 3Distribution of functional clusters within the entity of mRNAs with significantly higher abundance in total or polysomal RNA samples in dependence of *mazF* overexpression.

The columns visualize the distribution into functional clusters of those genes that are more abundant in total or polysomal RNA samples with (T+ and P+) or without (T- and P-) *mazF* overexpression, normalized to 100% per group. The sum of each column corresponds to the numbers in **Table 3**. For comparison, the last column 'all genes' visualizes the distribution of the functional clusters in the entity of all 4506 *E. coli* genes, that have been considered for cluster analysis, provided by EcoGene.org, as already shown in **Figure 2A**.

Figure 4. Verified MazF targets.

Gene loci of the respective genes are schematically depicted by blue arrows. The positions of the primers used for primer extension analysis are indicated by gray arrows. The left panels show the coverage profiles of sequencing reads aligned to the respective gene. The RNA-seq was performed on total RNA (**T**, green and violet) and RNA extracted from polysomes (**P**, blue and red) from *E. coli* cells during exponential growth (**-**, green and blue) or after 15 minutes of *mazF* overexpression (**+**, violet and red). This color code will be used in subsequent figures. The right panels show corresponding primer extension analyses with the respectively indicated primers. Sequencing reactions were obtained from an *in vitro* transcribed *grcA* mRNA. Below excerpts of the nucleotide sequences of the respective genes are given. The coding region is highlighted in blue, the MazF cleavage sites are highlighted in red. Panels **A**, **B**, **C** and **D** summarize the results of the candidates *rho*, *rpoA*, *rpsA* and *zwf*, respectively.

Figure S1. *rpsU* is not targeted by MazF under the conditions used in this study.

A) Primer extension on total RNA extracted from cells with (T+) or without (T-) induction of *mazF* overexpression using primer Y50. The cleavage at position -2 cannot be observed. The sequencing reaction was obtained from an *in vitro* transcribed *grcA* mRNA. **B**) RT-PCR detecting leaderless (H3/C54) and full length (B7/C54) *rpsU* mRNA in polysomal RNA extracted from cells with (P+) or without (P-) induction of *mazF* overexpression. No loss of the 5'-UTR can be detected. (Primers H3, B7 and C54 add 29, 29 and 10 bp, respectively to the PCR product.) **C**) Coverage profiles of sequencing reads aligned to the *rpsU* locus. **D**) Schematic depiction of the positions of the primers used for RT-PCR.

Figure S2. Distribution of overlapping and antagonistic regulatory effects by *mazF* overexpression in total and polysome-associated RNA within functional clusters.

The first column of each set ('all') indicates the total level of regulation, the second and third defines down- and up-regulation, respectively (the corresponding numbers are indicated in each sub-column). The last set of columns „all genes" visualizes the extent of overlap in regulatory effects within the entity of all 4506 *E. coli* genes, that have been considered for cluster analysis, provided by EcoGene.org. The first column of 'all genes' represents the data visualized in **Figure 2C**. CC = cell cycle, CS = cell structure, NC = not classified, ME = metabolism and energy supply, PS = protein synthesis, RR = response regulation.

Figure S3. Additional verified MazF targets.

Gene loci of the respective genes are schematically depicted by blue arrows. The positions of the primers used for primer extension analysis are indicated by gray arrows. The left panels show the coverage profiles of sequencing reads aligned to the respective gene. The RNA-seq was performed on total RNA (**T**, green and violet) and RNA extracted from polysomes (**P**, blue and red) from *E. coli* cells during exponential growth (**-**, green and blue) or after 15 minutes of *mazF* overexpression (**+**, violet and red). This color code will be used in subsequent figures. The right panels show corresponding primer extension analyses with the respectively indicated primers. Sequencing reactions were obtained from an *in vitro* transcribed *grcA* mRNA. Below excerpts of the nucleotide sequences of the respective genes are given. The coding region is highlighted in blue, the MazF cleavage sites are highlighted in red. Panels **A**, **B**, **C**, **D**, **E**, **F,** and **G** summarize the results of the candidates *grcA*, *gapA*, *rpmI*, *rplL*, *rpsP*, *groEL*, and *atpE* respectively.

Figure S4. Verified known leaderless mRNAs.

Coverage profiles of sequencing reads aligned to the respective gene. The RNA-seq was performed on total RNA (**T**, green and violet) and RNA extracted from polysomes (**P**, blue and red) from *E. coli* cells during exponential growth (**-**, green and blue) or after 15 minutes of *mazF* overexpression (**+**, violet and red). Panels **A**, **B**, and **C** show the lmRNAs *rhlB*, *pgpA* and *yfbU*, respectively.

Table legends

Table 1. Summary of RNA preparation. RNA samples from *E. coli* MC4100 *relA*$^+$: Total RNA (**T-)** and polysome-associated RNA (**P-**) from untreated cells and total RNA (**T+**) and polysome-associated RNA (**P+**) from cells carrying pSA1 upon IPTG-induction of *mazF* overexpression. Each sample was prepared in two biological replicates (R1 and R2). See 'Material and Methods' for further information about the purification procedure.

Table 2. Summary of differential gene expression (DGE) data on total and polysomal RNA. Differential gene expression (DGE) analysis was performed with *DESeq* (Anders and Huber 2010). Cut-off values for downstream applications are padj < 0.05 and a foldChange < 0.65 for down-regulated and foldChange > 1.52 for up-regulated genes. Functional cluster analysis was performed based on information provided by EcoGene.org (Zhou and Rudd 2013). In the last row "all genes", the first number (A = number of genes) in each section (bold) indicates the total number of genes altered in the respective group (total and polysomal RNA, each intersected in up- and down-regulated candidates). The entity of these genes was then further differentiated by functional classification into the six classes, represented in the rows above. CC = cell cycle, CS = cell structure, NC = not classified, ME = metabolism and energy supply, PS = protein synthesis, RR = response regulation. Next, these numbers of differentially regulated genes were set into context by assigning corresponding percentages: B = % of genome, C = % of DGE, D = % within cluster.

Table 3. Summary of differential gene expression (DGE) data comparing total and polysomal RNA within the same condition. Differential gene expression (DGE) ('T-' *versus* 'P-' and 'T+' *versus* 'P+') analysis was performed with *DESeq* (Anders and Huber 2010). Cut-off values for downstream applications are padj < 0.05 and a foldChange < 0.65 for down-regulated and foldChange > 1.63 for up-regulated genes. The first entries in rows '**T-**' and '**P-**' (in bold, black) indicate the numbers of mRNAs with significantly higher abundance in total RNA or polysomal RNA, respectively, during exponential growth. The first two entries in the columns '**T+**' and '**P+**' (in bold, balck) indicate the same after *mazF* overexpression. These four numbers are further split in dependence of functional clusters, as shown in **Figure 3**. Numbers in light gray indicate overlapping candidates, whose relative abundance in total RNA or polysomes correlates between the two conditions, the numbers in dark gray indicate antagonistic effects.

Table 4. List of chosen MazF targets. The listed genes are candidates that are cleaved to lmRNAs by MazF and identified in polysome fractions according to the sequencing data. Candidates whose cleavage is experimentally verified by primer extension analysis are indicated in bold. CC = cell cycle, CS = cell structure, ME = metabolism and energy supply, PS = protein synthesis, RR = response regulation, U = unknown.

Table S1. Summary of the processing of sequencing reads. The table summarizes the total numbers of sequencing reads obtained for each sample and the numbers of reads that have been mapped to the reference genome.

Table S2. Summary of functional classes and sub-classes.

Table S3. List of antagonistically regulated genes in total and polysomal RNA. In the first half of the table candidates are listed that are significantly up-regulated (log2fold > 0) in polysomes but down-regulated in total RNA. The second half lists the candidates being regulated *vice versa*. The set of RP-encoding genes is highlighted in bold.

Table S4. Complete list of MazF targets.

The listed genes are candidates that are cleaved to lmRNAs by MazF and identified in polysome fractions according to the sequencing data. Candidates whose cleavage is experimentally verified by primer extension analysis are indicated in bold. CC = cell cycle, CS = cell structure, ME = metabolism and energy supply, PS = protein synthesis, RR = response regulation, U = unknown.

Table S5: Oligonucleotides used in this study. Regions homologous to the *E. coli* genome are underlined.

Figures

Figure 1

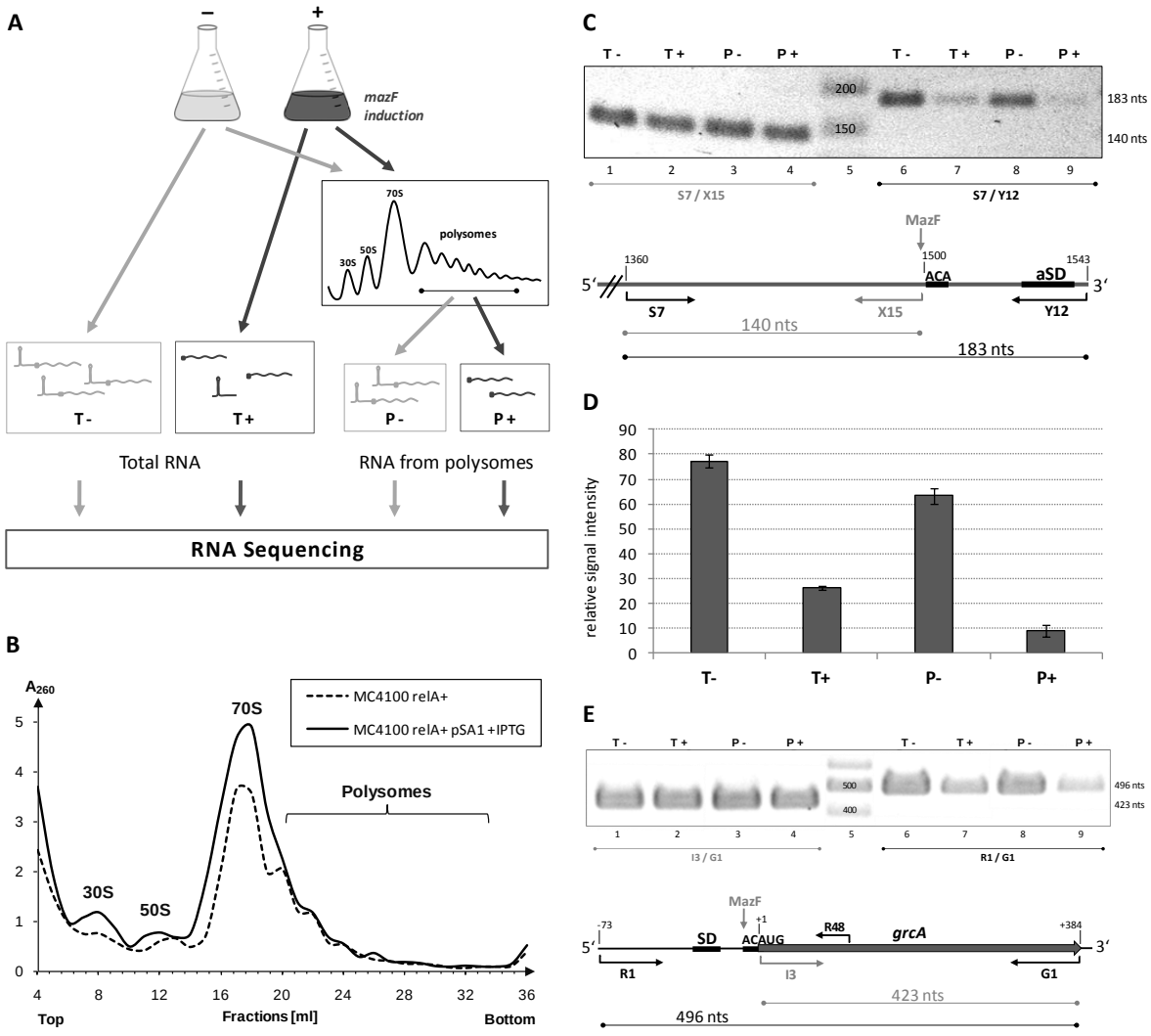

Figure 2

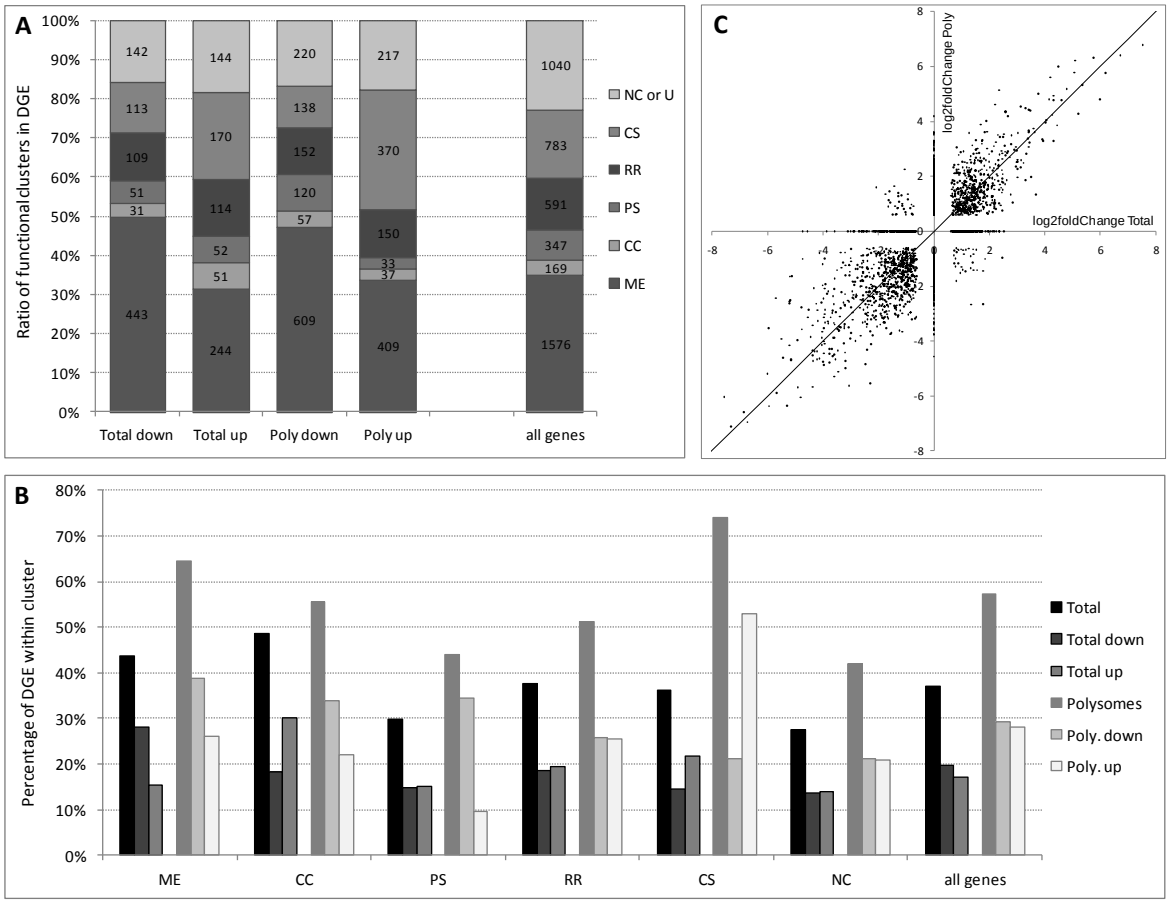

Figure 3

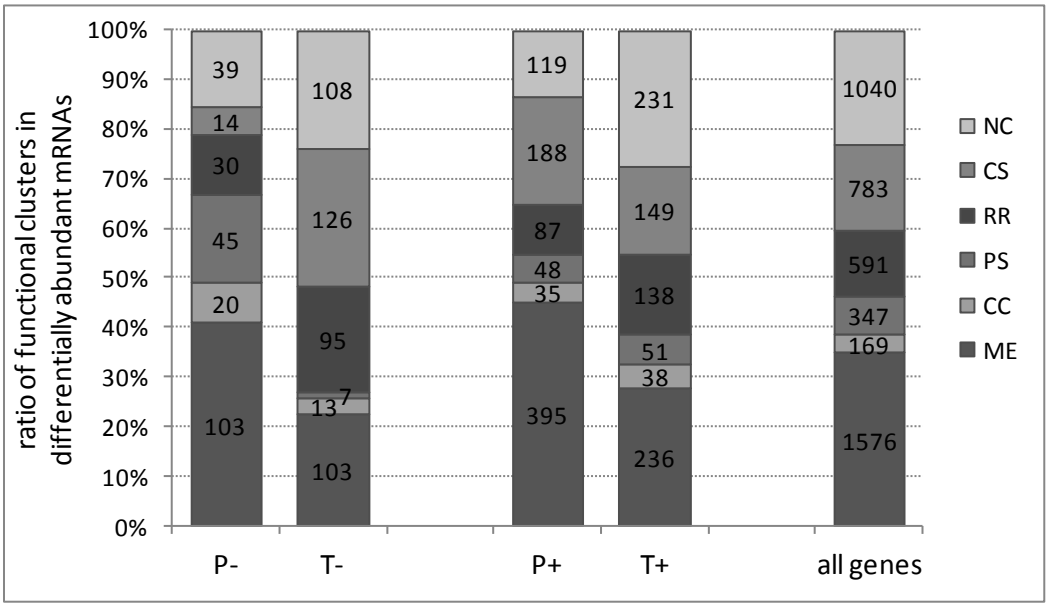

Figure 4

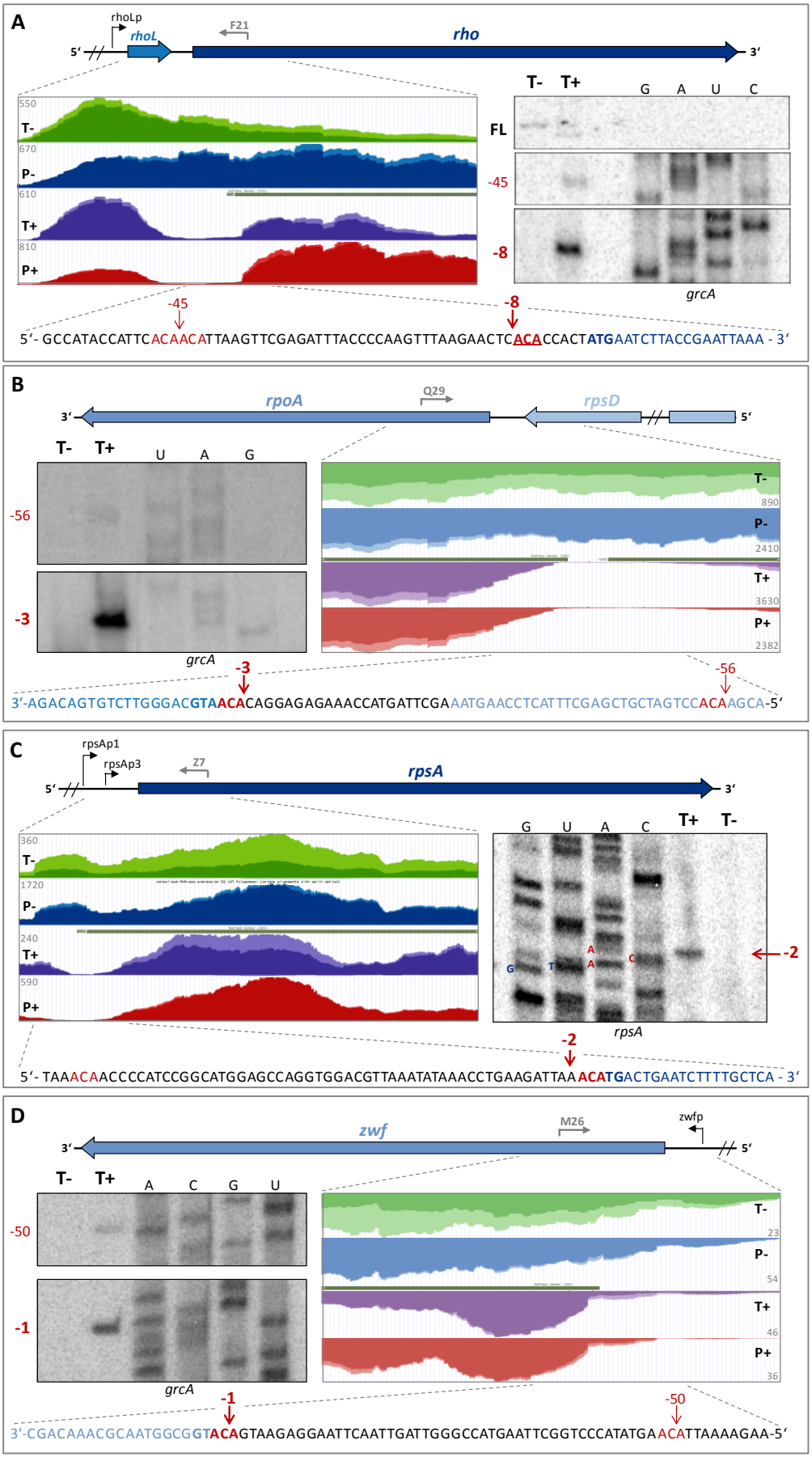
A
rhoLp
rhoL
F21
rho
5'
3'
T- T+ G A U C
550
T-
670
P-
610
T+
810
P+
FL
-45
-8
grcA
-45
-8
5'- GCCATACCATTCACAACATTAAGTTCGAGATTTACCCCAAGTTTAAGAACTCACACCACTATGAATCTTACCGAATTAAA - 3'
B
rpoA
Q29
rpsD
3'
5'
T- T+ U A G
-56
-3
grcA
T-
890
P-
2410
T+
3630
P+
2382
-3
-56
3'-AGACAGTGTCTTGGGACGTAACACAGGAGAGAAACCATGATTCGAAATGAACCTCATTTCGAGCTGCTAGTCCACAAGCA-5'
C
rpsAp1
rpsAp3
Z7
rpsA
5'
3'
G U A C T+ T-
360
T-
1720
P-
240
T+
590
P+
-2
rpsA
-2
5'- TAAACAACCCCATCCGGCATGGAGCCAGGTGGACGTTAAATATAAACCTGAAGATTAAACATGACTGAATCTTTTGCTCA - 3'
D
zwf
M26
zwfp
3'
5'
T- T+ A C G U
-50
-1
grcA
T-
23
P-
54
T+
46
P+
36
-1
-50
3'-CGACAAACGCAATGGCGGTACAGTAAGAGGAATTCAATTGATTGGGCCATGAATTCGGTCCCATATGAACATTAAAAGAA-5'

Figure S1

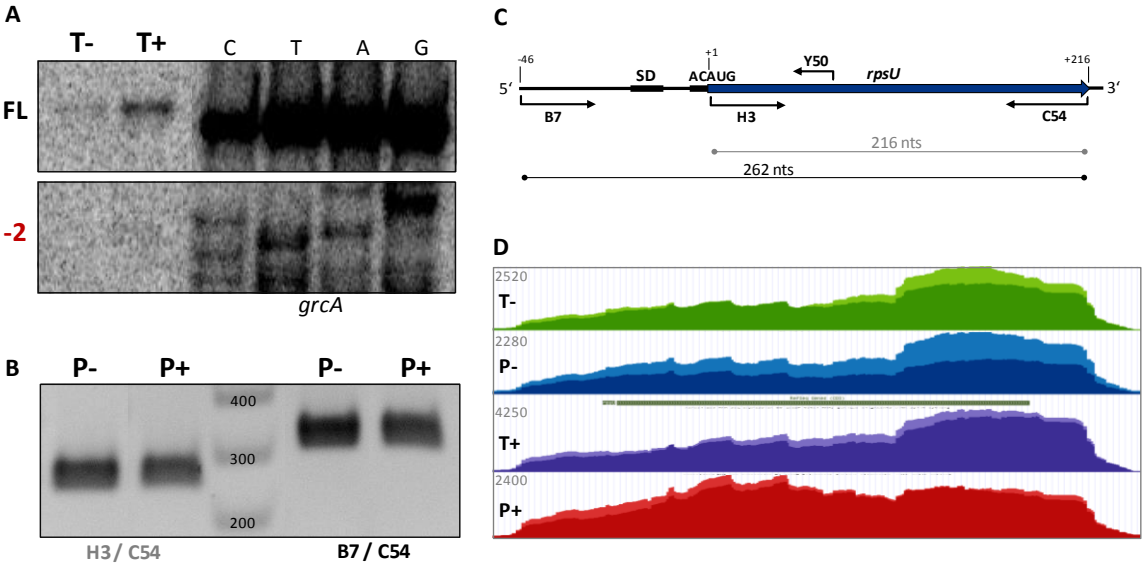

Figure S2

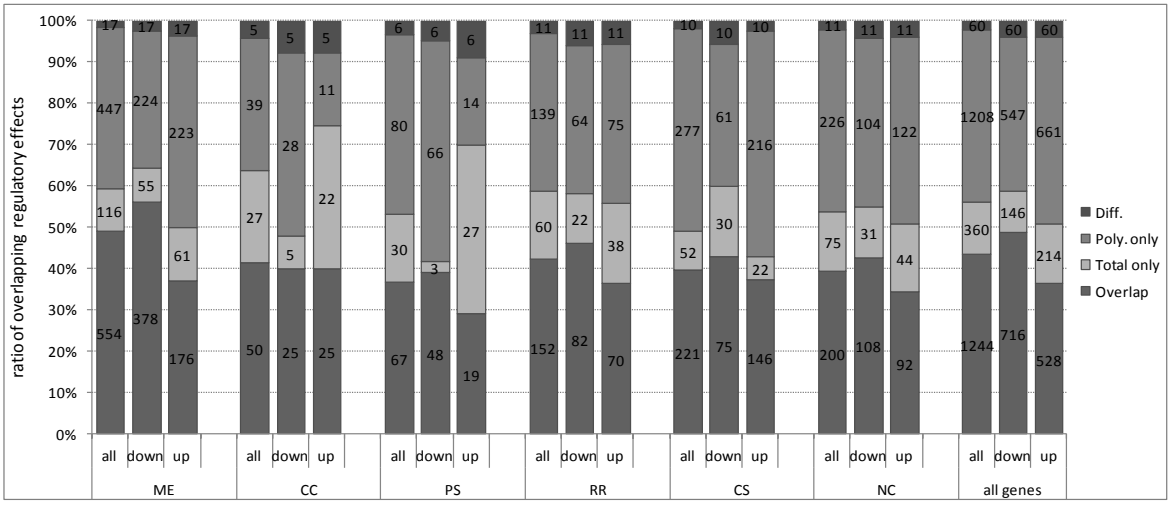

Figure S3

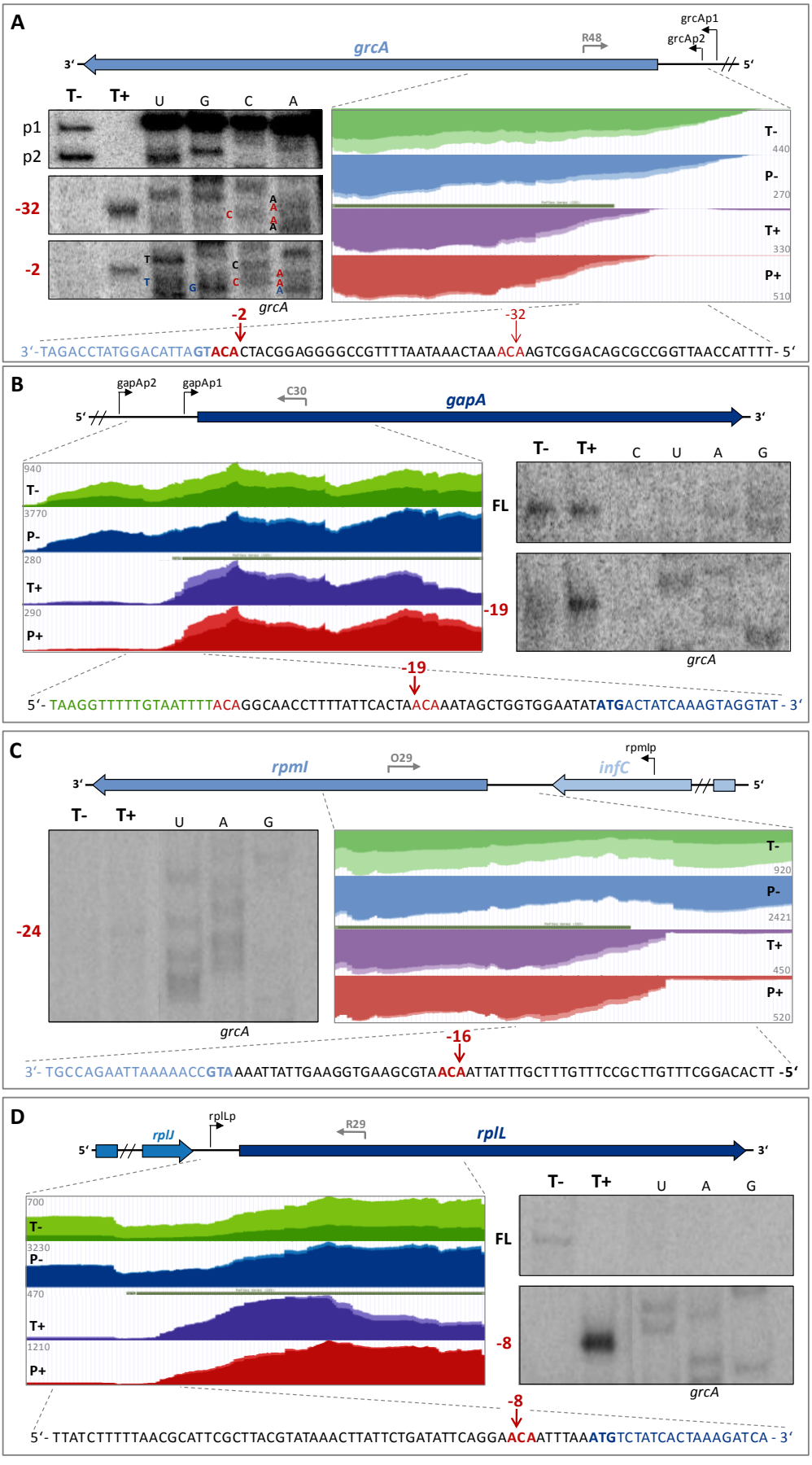
A
grcA
grcAp1
grcAp2
R48
3'
5'
T-
T+
U
G
C
A
p1
p2
-32
-2
T-
P-
T+
P+
440
270
330
510
grcA
-2
-32
3'-TAGACCTATGGACATTAGTACACTACGGAGGGGCCGTTTTAATAAACTAAACAAGTCGGACAGCGCCGGTTAACCATTTT- 5'
B
gapAp2
gapAp1
C30
gapA
5'
3'
T-
T+
C
U
A
G
940
3770
280
290
FL
-19
grcA
-19
5'- TAAGGTTTTTGTAATTTTACAGGCAACCTTTTATTCACTAACAAATAGCTGGTGGAATATATGACTATCAAAGTAGGTAT - 3'
C
rpmI
O29
rpmIp
infC
-24
920
2421
450
520
grcA
-16
3'- TGCCAGAATTAAAAACCGTAAAATTATTGAAGGTGAAGCGTAACAATTATTTGCTTTGTTTCCGCTTGTTTCGGACACTT -5'
D
rplJ
rplLp
R29
rplL
700
3230
470
1210
-8
grcA
-8
5'- TTATCTTTTTAACGCATTCGCTTACGTATAAACTTATTCTGATATTCAGGAACAATTTAAATGTCTATCACTAAAGATCA - 3'

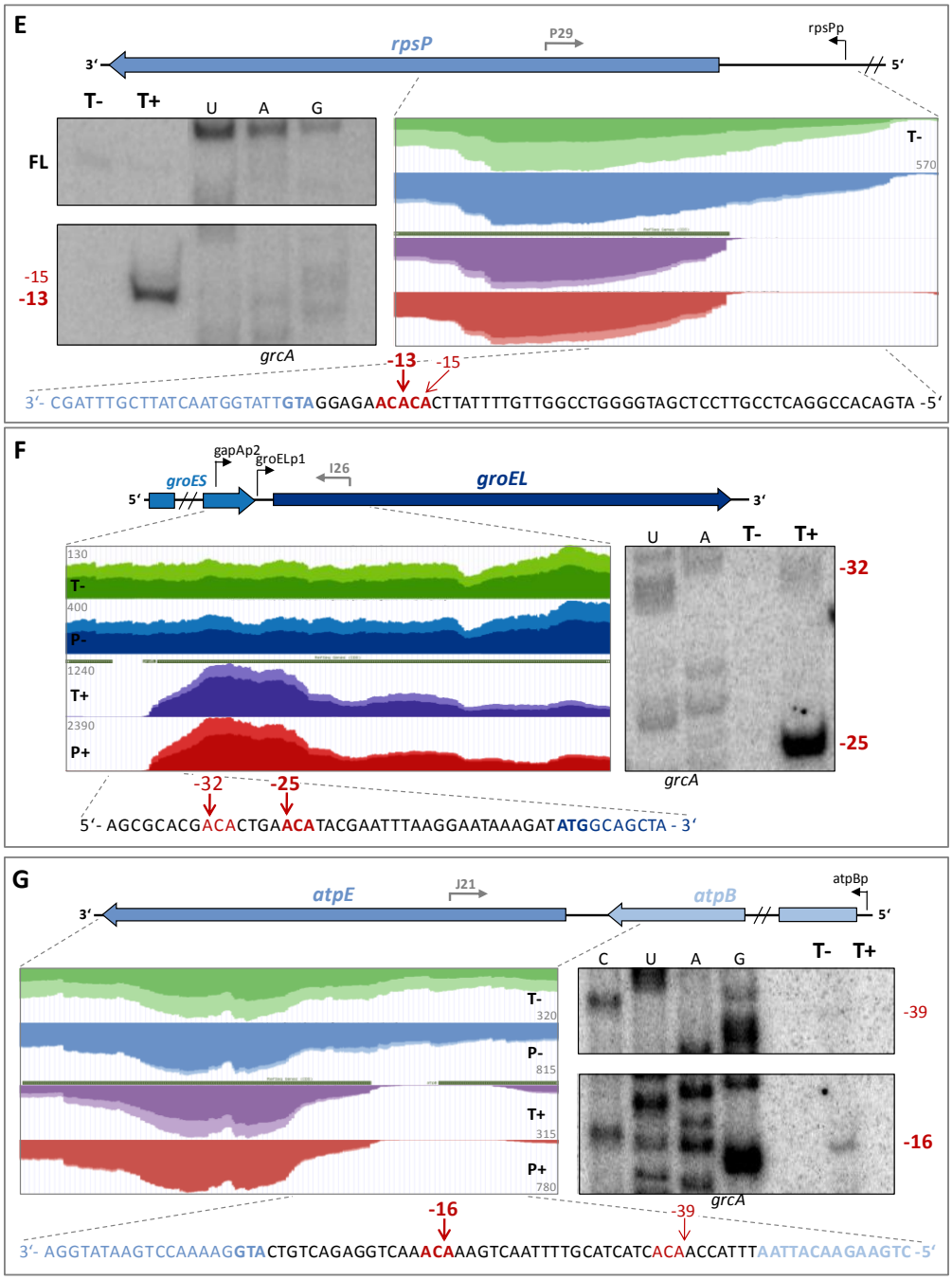
E
rpsP
P29
rpsPp
3'
5'
T-
T+
U
A
G
FL
-15
-13
grcA
T-
570
-13
-15
3'- CGATTTGCTTATCAATGGTATTGTAGGAGAACACACTTATTTTGTTGGCCTGGGGTAGCTCCTTGCCTCAGGCCACAGTA -5'
F
gapAp2
groELp1
I26
groES
groEL
5'
3'
U
A
T-
T+
130
T-
400
P-
1240
T+
2390
P+
-32
-25
grcA
-32
-25
5'- AGCGCACGACACTGAACATACGAATTTAAGGAATAAAGATATGGCAGCTA - 3'
G
atpE
J21
atpB
atpBp
3'
5'
C
U
A
G
T-
T+
T-
320
P-
815
T+
315
P+
780
-39
-16
grcA
-16
-39
3'- AGGTATAAGTCCAAAAGGTACTGTCAGAGGTCAAACAAAGTCAATTTTGCATCATCACAACCATTTAATTACAAGAAGTC -5'

Figure S4

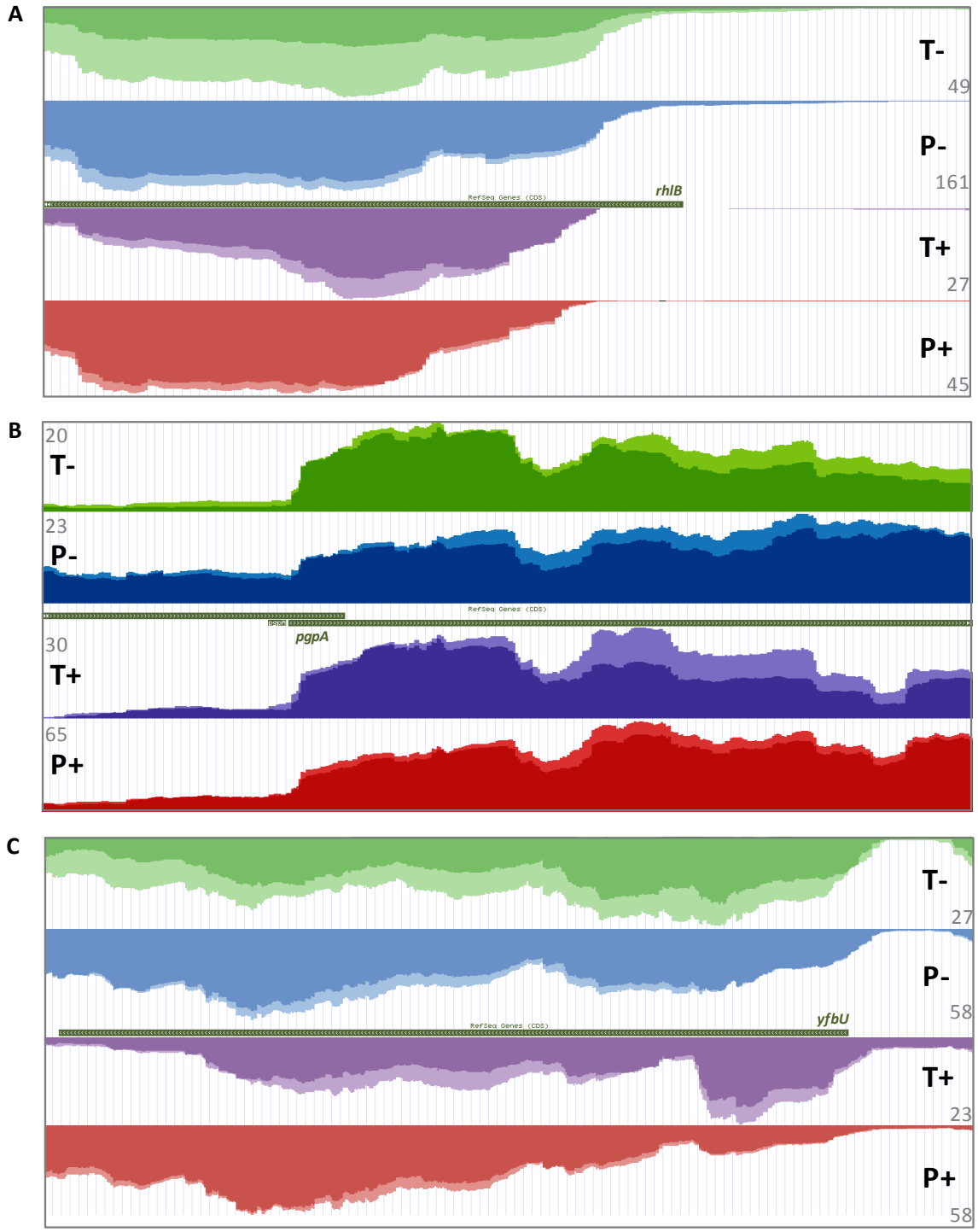
A
T-
49
P-
161
RefSeq Genes (CDS)
rhlB
T+
27
P+
45
B
20
T-
23
P-
RefSeq Genes (CDS)
pgpA
30
T+
65
P+
C
T-
27
P-
58
RefSeq Genes (CDS)
yfbU
T+
23
P+
58

Tables

Table 1

	2-propanol precipitation			TRIzol extraction			DNAseI digestion			rRNA depletion			recovered rRNA		
Sample	Input [µg]	Output [µg]	Efficiency [%]	Input [µg]	Output [µg]	Efficiency [%]	Input [µg]	Output [µg]	Efficiency [%]	Input [µg]	Output [µg]	Efficiency [%]	Input [µg]	Output [µg]	Efficiency [%]
T- R1					203		61	29	48	5	3,8	76	5	1,8	36
T- R2					197		59	30	51	5	3,3	66	5	1,9	38
T+ R1					263		47	24	51	5	1,9	38	5	1,8	36
T+ R2					256		58	29	50	5	3,9	78	5	2,0	40
P- R1	351	238	68	238	181	76	105	91	87	5	0,1	2	5	1,6	32
P- R2	585	276	47	276	241	87	84	80	95	5	0,7	14	5	1,4	28
P+ R1	845	509	60	509	407	80	118	102	86	5	0,4	8	5	1,7	34
P+ R2	780	418	54	418	340	81	119	104	87	5	0,1	2	5	2,0	40

Table 2

	Total				Total down-regulated				Total up-regulated				Poly				Poly down-regulated				Poly up-regulated				All regulated				all genes	
Cluster	**A**	B	C	D	**A**	B	C	D	**A**	B	C	D	**A**	B	C	D	**A**	B	C	D	**A**	B	C	D	**A**	B	C	D	**A**	B
ME	**687**	15	41	44	**443**	10	50	28	**244**	5	31	15	**1017**	23	40	65	**609**	14	47	39	**409**	9	34	26	**1134**	25	39	72	**1576**	35
CC	**82**	2	5	49	**31**	1	3	18	**51**	1	7	30	**94**	2	4	56	**57**	1	4	34	**37**	1	3	22	**121**	3	4	72	**169**	4
PS	**103**	2	6	30	**51**	1	6	15	**52**	1	7	15	**153**	3	6	44	**120**	3	9	35	**33**	1	3	10	**183**	4	6	53	**347**	8
RR	**223**	5	13	38	**109**	2	12	18	**114**	3	15	19	**302**	7	12	51	**152**	3	12	26	**150**	3	12	25	**362**	8	13	61	**591**	13
CS	**283**	6	17	36	**113**	3	13	14	**170**	4	22	22	**508**	11	20	65	**138**	3	11	18	**370**	8	30	47	**560**	12	19	72	**783**	17
NC	**286**	6	17	28	**142**	3	16	14	**144**	3	19	14	**438**	10	17	42	**220**	5	17	21	**217**	5	18	21	**512**	11	18	49	**1040**	23
all genes	**1664**	37	100	37	**889**	20	100	20	**775**	17	100	17	**2512**	**56**	100	56	**1296**	29	100	29	**1216**	27	100	27	**2872**	64	100	64	**4506**	100

Table 3

		P- high	**T-** high	no sign. Diff in **-**
	4506	**251**	**460**	3795
P+ high	**805**	102	**29**	674
T+ high	**762**	**22**	226	514
no sign. Diff in **+**	2939	127	205	2607

Table 4

Gene	cleaved ACA [distance to start]	Protein product	Main classification	Sub-classification
aroG	2	3-deoxy-D-arabino-heptulosonate-7-phosphate synthase, phenylalanine repressible	ME	Amino acids, peptides
cycA	2	D-alanine/D-serine/glycine transporter	ME	Amino acids, peptides
ptrB	2	protease II	ME	Amino acids, peptides
zwf	2	glucose-6-phosphate 1-dehydrogenase	ME	Energy production
amn	2	AMP nucleosidase	ME	Nucleic acids, nucleotides
nrdA	2	ribonucleoside-diphosphate reductase 1, alpha subunit	ME	Nucleic acids, nucleotides
rpmB	2	50S ribosomal subunit protein L28	PS	Ribosomal proteins
rpsA	2	30S ribosomal subunit protein S1	PS	Ribosomal proteins
engA	2	GTPase; multicopy suppressor of ftsJ	RR	Not classified
ygiW	2	hydrogen peroxide and cadmium resistance periplasmic protein; stress-induced OB-fold protein	RR	Stress
yjeI	2	DUF4156 family lipoprotein	U	
mltA	3	membrane-bound lytic murein transglycosylase A	CS	Cell wall
ffh	3	Signal Recognition Particle (SRP) component with 4.5S RNA (ffs)	CS	Transport
kdsC	3	3-deoxy-D-manno-octulosonate 8-phosphate phosphatase	ME	Fatty acids, lipids
rpoA		RNA polymerase, alpha subunit	PS	Transcription
yoaH	3	UPF0181 family protein	U	
ytfK	3	DUF1107 family protein	U	
ftsA	3	ATP-binding cell division protein involved in recruitment of FtsK to Z ring	CC	Cell division
artI	3	arginine transporter subunit	ME	Transport
mdoG	4	OPG biosynthetic periplasmic beta-1,6 branching glycosyltransferase	CS	Cell wall
greA	4	transcript cleavage factor	PS	Translation factors
glnP	4	glutamine transporter subunit	ME	Transport
yhhQ	5	DUF165 family inner membrane protein	CS	Membrane
uxuR	5	fructuronate-inducible hexuronate regulon transcriptional repressor; autorepressor	ME	Carbon compounds
rnd	5	ribonuclease D	PS	tRNA modification
treR	5	trehalose 6-phosphate-inducible trehalose regulon transcriptional repressor	RR	Stress
yacL	5	UPF0231 family protein	U	
yceN	6	putative lipid II flippase	CS	Cell wall
glgB	6	1,4-alpha-glucan branching enzyme	ME	Carbon compounds
vacJ	6	ABC transporter maintaining OM lipid asymmetry, OM lipoprotein component	ME	Fatty acids, lipids
rlmB	6	23S rRNA mG2251 2'-O-ribose methyltransferase, SAM-dependent	PS	Ribosome maturation
rho	8	transcription termination factor	PS	Transcription
ampH	9	D-alanyl-D-alanine-carboxypeptidase/endopeptidase; penicillin-binding protein; weak beta-lactamase	CS	Cell wall
hisQ	9	histidine ABC transporter permease	ME	Amino acids, peptides
ndk	12	multifunctional nucleoside diphosphate kinase and apyrimidinic endonuclease and 3'-phosphodiesterase	ME	Nucleic acids, nucleotides
ydeP	13	putative oxidoreductase	RR	Stress
fliY	15	cystine transporter subunit	CS	Transport
yhcB	16	DUF1043 family inner membrane-anchored protein	U	
seqA	18	negative modulator of initiation of replication	CC	DNA replication
frdA	18	anaerobic fumarate reductase catalytic and NAD/flavoprotein subunit	ME	Energy production
fabI	18	enoyl-[acyl-carrier-protein] reductase, NADH-dependent	ME	Fatty acids, lipids
sstT	19	sodium:serine/threonine symporter	CS	Transport

gapA	20	glyceraldehyde-3-phosphate dehydrogenase A	ME	Energy production
pepP	24	proline aminopeptidase P II	ME	Amino acids, peptides
pdxJ	24	pyridoxine 5'-phosphate synthase	ME	Cofactors
groEL	25	Cpn60 chaperonin GroEL, large subunit of GroESL	RR	Chaperones

Supplementary Table S1

Sample	Tag-#	total raw reads	unmatched reads	unmatch rate	multi mapper	multi rate	uniq mapper	uniq rate
T- R1	4	54.961.257	1.669.609	0,03	33.052.605	0,60	20.239.043	0,37
T- R2	9	49.421.328	1.002.681	0,02	32.389.869	0,66	16.028.778	0,32
P- R1	6	53.527.357	1.843.176	0,03	9.032.410	0,17	42.651.771	0,80
P- R2	10	48.296.955	6.358.635	0,13	4.268.734	0,09	37.669.586	0,78
T+ R1	7	44.944.267	7.087.985	0,16	17.224.310	0,38	20.631.972	0,46
T+ R2	11	42.478.696	2.508.222	0,06	20.486.499	0,48	19.483.975	0,46
P+ R1	8	62.513.502	7.108.432	0,11	14.635.492	0,23	40.769.578	0,65
P+ R2	12	67.839.354	13.579.434	0,20	17.998.850	0,27	36.261.070	0,53

Supplementary Table S2

Classification I	Classification II	Subclassification
Metabolism & energy supply (ME) (1576)	Carbon compounds	Biosynthesis, Catabolism, Transport
	Amino acids, peptides	
	Nucleic acids, nucleotides	
	Fatty acids, lipids	
	Cofactors	
	Energy production	
Cell cycle (CC) (169)	Cell division	
	DNA replication	
	DNA modification	
	DNA repair	
	DNA degradation	
Protein synthesis (PS) (347)	Transcription	
	RNA modification	
	RNA degradation	
	rProteins	
	rRNA	
	tRNA	
	Ribosome maturation	rProtein & rRNA modification
	tRNA modification	
	Translation-factors	
	Protein modification	
Response regulation (RR) (591)	Chemotaxis	
	Quorum sensing	
	sRNA	
	Chaperones	
	Antibiotic resistance	Transport
	Biofilm	
	Toxin-Antitoxins	
	Stress response	Starvation, Stationary phase, Cold shock, Heat shock, Phage shock, Acid stress, Osmotic stress, Oxidative stress, CRISPR, Detoxification, Toxic protein
Cell structure (CS) (783)	Cell wall	Biosynthesis
	Membrane	Inner or outer membrane
	Surface structures	Flagella, Pili, Polysaccharides
	Transport	Ions, Protein- peptide secretion
Not classified (NC) (1040)	Phage or transposon related	
	Unknown	

Supplementary Table S3

Gene	log2FoldChange		Protein	Main classi-fication	Sub-classification
	Total	Poly			
yghB	-1,48	0,62	general envelope maintenance protein; DedA family inner membrane protein	CC	Cell division
mdoH	-1,63	1,13	OPG biosynthetic ACP-dependent transmembrane UDP-glucose beta-1,2 glycosyltransferase; nutrient-dependent cell size regulator, FtsZ assembly antagonist	CS	Cell wall
fsr	-1,31	0,86	putative fosmidomycin efflux system protein	CS	Transport
ccmD	-1,16	1,32	cytochrome c biogenesis protein; heme export ABC transporter holo-CcmE release factor	CS	Transport
yfbS	-1,14	1,00	putative transporter	CS	Transport
yifK	-1,09	0,82	putative APC family amino acid transporter	CS	Transport
ycdZ	-1,03	0,69	DUF1097 family inner membrane protein	CS	Membrane
yejB	-1,01	0,62	microcin C ABC transporter permease	CS	Transport
nikB	-0,95	1,35	nickel ABC transporter permease	CS	Transport
potE	-2,08	1,61	putrescine/proton symporter: putrescine/ornithine antiporter	ME	Amino acids, peptides
nuoN	-1,76	1,35	NADH:ubiquinone oxidoreductase, membrane subunit N	ME	Energy production
cyoB	-1,60	1,46	cytochrome o ubiquinol oxidase subunit I	ME	Energy production
dcuC	-1,44	1,65	anaerobic C4-dicarboxylate transport	ME	Carbon compounds
nagE	-1,35	0,63	N-acetyl glucosamine specific PTS enzyme IIC, IIB, and IIA components	ME	Amino acids, peptides
cydA	-1,25	1,08	cytochrome d terminal oxidase, subunit I	ME	Energy production
rfc	-1,06	2,26	O-antigen polymerase	ME	Fatty acids, lipids
ccmE	-0,95	1,16	periplasmic heme chaperone	ME	Energy production
araH	-0,86	0,85	L-arabinose ABC transporter permease	ME	Carbon compounds
wbbK	-0,74	0,92	lipopolysaccharide biosynthesis protein	ME	Fatty acids, lipids
yeeS	-1,37	0,61	CP4-44 prophage; putative DNA repair protein	NC	Phage or transposon related
chpB	-1,65	0,91	toxin of the ChpB-ChpS toxin-antitoxin system	RR	Toxin-antitoxins
dinQ	-1,57	1,05	UV-inducible membrane toxin, DinQ-AgrB type I toxin-antitoxin system	RR	Toxin-antitoxins
mdtC	-1,14	0,93	multidrug efflux system, subunit C	RR	Antibiotic resistance
emrB	-0,81	0,98	multidrug efflux system protein	RR	Antibiotic resistance
cpxA	-0,77	0,61	sensory histidine kinase in two-component regulatory system with CpxR	RR	Stress
yjjZ	-1,28	1,28	uncharacterized protein	U	
yadH	-0,81	0,64	putative ABC transporter permease	U	
uvrC	0,99	-1,30	excinuclease UvrABC, endonuclease subunit	CC	DNA repair
xerC	1,07	-0,83	site-specific tyrosine recombinase	CC	Cell division
ftsB	1,13	-1,45	cell division protein	CC	Cell division
gspB	1,15	-0,68	part of gsp divergon involved in type II protein secretion	CC	DNA repair
ygiS	0,89	-0,69	putative ABC transporter permease	CS	Transport
ompX	1,43	-0,83	outer membrane protein X	CS	Membrane
pepA	0,72	-0,87	multifunctional aminopeptidase A: a cyteinylglycinase, transcription regulator and site-specific recombination factor	ME	Carbon compounds
sthA	0,74	-1,16	pyridine nucleotide transhydrogenase, soluble	ME	
plsC	0,98	-0,66	1-acyl-sn-glycerol-3-phosphate acyltransferase	ME	Fatty acids, lipids
yeaE	1,05	-0,69	aldo-keto reductase, methylglyoxal to acetol, NADPH-dependent	ME	Carbon compounds
udk	1,41	-0,66	uridine-cytidine kinase	ME	Nucleic acids, nucleotides
menF	1,52	-0,68	isochorismate synthase 2	ME	Cofactors
ntpA	1,84	-1,01	dihydroneopterin triphosphate pyrophosphatase	ME	Cofactors
yciO	0,73	-0,70	putative RNA binding protein	NC	
rnhB	0,78	-1,29	ribonuclease HII, degrades RNA of DNA-RNA hybrids	PS	RNA degradation
rpsQ	0,81	-1,81	**30S ribosomal subunit protein S17**	PS	Ribosomal proteins
rplU	0,86	-0,66	**50S ribosomal subunit protein L21**	PS	Ribosomal proteins
rpmG	1,35	-2,67	**50S ribosomal subunit protein L33**	PS	Ribosomal proteins
rplT	1,78	-2,65	**50S ribosomal subunit protein L20**	PS	Ribosomal proteins

rpmA	2,46	-0,96	**50S ribosomal subunit protein L27**	PS	Ribosomal proteins
ybjN	0,77	-0,99	multicopy suppressor of coaA(Ts); ionizing radiation survival protein; putative chaperone; putative negative regulator of fimbriae and motility	RR	Chemotaxis
gmr	0,88	-1,16	cyclic-di-GMP phosphodiesterase; csgD regulator; modulator of RNase II stability	RR	NC
sspB	0,95	-1,51	ClpXP protease specificity enhancing factor	RR	Stress
yqgF	1,25	-0,63	putative Holliday junction resolvase	RR	NC
ecnA	1,40	-1,13	entericidin A membrane lipoprotein, antidote entericidin B	RR	Toxin-antitoxins
yciT	1,55	-1,41	global regulator of transcription; DeoR family	RR	NC
ycfH	0,80	-0,61	putative DNase	U	
ydcF	0,82	-0,76	DUF218 superfamily protein, SAM-binding	U	
yceD	1,03	-1,40	DUF177 family protein	U	
yjjV	1,32	-0,91	putative DNase	U	
ymjA	1,33	-1,34	DUF2543 family protein	U	
yjjA	1,42	-1,41	putative DUF2501 family periplasmic protein	U	
yneG	1,77	-1,44	DUF4186 family protein	U	

Supplementary Table S4

Gene	cleaved ACA [Distance to start]	Protein product	Main classi-fication	Sub-classification
mutH	2	methyl-directed mismatch repair protein	CC	DNA repair
mscL	2	mechanosensitive channel protein, high conductance	CS	Transport
tatC	2	TatABCE protein translocation system subunit	CS	Transport
amn	2	AMP nucleosidase	ME	Nucleic acids, nucleotides
aroG	2	3-deoxy-D-arabino-heptulosonate-7-phosphate synthase, phenylalanine repressible	ME	Amino acids, peptides
cycA	2	D-alanine/D-serine/glycine transporter	ME	Amino acids, peptides
fabD	2	malonyl-CoA-[acyl-carrier-protein] transacylase	ME	Fatty acids, lipids
gatZ	2	D-tagatose 1,6-bisphosphate aldolase 2, subunit	ME	Energy production
glpK	2	glycerol kinase	ME	Energy production
ispD	2	4-diphosphocytidyl-2C-methyl-D-erythritol synthase	ME	Fatty acids, lipids
nadC	2	quinolinate phosphoribosyltransferase	ME	Cofactors
nrdA	2	ribonucleoside-diphosphate reductase 1, alpha subunit	ME	Nucleic acids, nucleotides
nupG	2	nucleoside transporter	ME	Nucleic acids, nucleotides
pdxY	2	pyridoxamine kinase	ME	Cofactors
proS	2	prolyl-tRNA synthetase	ME	Nucleic acids, nucleotides
ptrB	2	protease II	ME	Amino acids, peptides
sppA	2	protease IV (signal peptide peptidase)	ME	Amino acids, peptides
srlB	2	glucitol/sorbitol-specific enzyme IIA component of PTS	ME	Carbon compounds
grcA	2	autonomous glycyl radical cofactor A	ME	Energy production
yggG	2	Phe-Phe periplasmic metalloprotease, OM lipoprotein; low salt-inducible; Era-binding heat shock protein	ME	Amino acids, peptides
zwf	2	glucose-6-phosphate 1-dehydrogenase	ME	Energy production
mltD	2	predicted membrane-bound lytic murein transglycosylase D	ME	Energy production
yajG	2	putative lipoprotein	NC	
ybgL	2	UPF0271 family protein	NC	
rpmB	2	50S ribosomal subunit protein L28	PS	Ribosomal proteins
rpoN	2	RNA polymerase, sigma 54 (sigma N) factor	PS	Transcription
rpsA	2	30S ribosomal subunit protein S1	PS	Ribosomal proteins
rsuA	2	16S rRNA pseudouridine(516) synthase	PS	Ribosome maturation
srmB	2	ATP-dependent RNA helicase	PS	Transcription
engA	2	GTPase; multicopy suppressor of ftsJ	RR	NC
uspD	2	stress-induced protein	RR	Stress
ygiW	2	hydrogen peroxide and cadmium resistance periplasmic protein; stress-induced OB-fold protein	RR	Stress
yjeI	2	DUF4156 family lipoprotein	U	
ftsE	3	cell division ATP-binding protein	CC	Cell division
ftsA	3	ATP-binding cell division protein involved in recruitment of FtsK to Z ring	CC	Cell division
exbB	3	membrane spanning protein in TonB-ExbB-ExbD complex	CS	Transport
ffh	3	Signal Recognition Particle (SRP) component with 4.5S RNA (ffs)	CS	Transport
mltA	3	membrane-bound lytic murein transglycosylase A	CS	Cell wall
yadS	3	UPF0126 family inner membrane protein	CS	Membrane
ynaI	3	mechanosensitive channel protein, very small conductance	CS	Transport
btuB	3	vitamin B12/cobalamin outer membrane transporter	CS	Membrane
kdsC	3	3-deoxy-D-manno-octulosonate 8-phosphate phosphatase	ME	Fatty acids, lipids
ptsH	3	phosphohistidinoprotein-hexose phosphotransferase component of PTS system (Hpr)	ME	Carbon compounds
srlA	3	glucitol/sorbitol-specific enzyme IIC component of PTS	ME	Carbon compounds
visC	3	2-octaprenylphenol hydroxylase, FAD-dependent	ME	Cofactors
yqjH	3	putative siderophore interacting protein	ME	Energy production
artI	3	arginine transporter subunit	ME	Transport
trmJ	3	tRNA mC32,mU32 2'-O-methyltransferase, SAM-dependent	PS	tRNA modification
rplB	3	50S ribosomal subunit protein L2	PS	Ribosomal proteins
rpoA	3	RNA polymerase, alpha subunit	PS	Transcription
cpxR	3	response regulator in two-component regulatory system with CpxA	RR	Stress
grxD	3	glutaredoxin-4	U	
yeaQ	3	UPF0410 family protein	U	
yoaH	3	UPF0181 family protein	U	
ytfK	3	DUF1107 family protein	U	
mdoG	4	OPG biosynthetic periplasmic beta-1,6 branching glycosyltransferase	CS	Cell wall
ydeE	4	putative transporter	CS	Transport
glnP	4	glutamine transporter subunit	ME	Transport
wecH	4	O-acetyltransferase for enterobacterial common antigen (ECA)	ME	
lgt	4	phosphatidylglycerol-prolipoprotein diacylglyceryl transferase	ME	Fatty acids, lipids
yqaE	4	cyaR sRNA-regulated protein	NC	

greA	4	transcript cleavage factor	PS	Translation factors
ilvL	5	ilvG operon leader peptide	ME	Amino acids, peptides
tig	5	peptidyl-prolyl cis/trans isomerase (trigger factor)	CC	Cell division
yhhQ	5	DUF165 family inner membrane protein	CS	Membrane
ynaJ	5	DUF2534 family putative inner membrane protein	CS	Membrane
yafV	5	putative NAD(P)-binding C-N hydrolase family amidase	ME	Energy production
radA	5	DNA repair protein	ME	Amino acids, peptides
uxuR	5	fructuronate-inducible hexuronate regulon transcriptional repressor; autorepressor	ME	Carbon compounds
yfcF	5	glutathione S-transferase	ME	
ydcJ	5	putative metalloenzyme	NC	
ppiD	5	periplasmic folding chaperone, has an inactive PPIase domain	NC	
rtcB	5	RNA-splicing ligase	PS	rRNA modification
rnd	5	ribonuclease D	PS	tRNA modification
rplR	5	50S ribosomal subunit protein L18	PS	Ribosomal proteins
emrA	5	multidrug efflux system	RR	Antibiotic resistance
treR	5	trehalose 6-phosphate-inducible trehalose regulon transcriptional repressor	RR	Stress
yacL	5	UPF0231 family protein	U	
yeaO	5	DUF488 family protein	U	
ytfJ	5	putative transcriptional regulator	U	
yhdV	5	putative outer membrane protein	U	
yceA	5	putative rhodanese-related sulfurtransferase	U	
yceN	6	putative lipid II flippase	CS	Cell wall
ynjC	6	putative ABC transporter permease	CS	Transport
thrL	6	thr operon leader peptide	ME	Amino acids, peptides
gsk	6	inosine/guanosine kinase	ME	Nucleic acids, nucleotides
apt	6	adenine phosphoribosyltransferase	ME	Nucleic acids, nucleotides
caiC	6	putative crotonobetaine/carnitine-CoA ligase	ME	Energy production
glgB	6	1,4-alpha-glucan branching enzyme	ME	Carbon compounds
nrdB	6	ribonucleoside-diphosphate reductase 1, beta subunit, ferritin-like protein	ME	Nucleic acids, nucleotides
vacJ	6	ABC transporter maintaining OM lipid asymmetry, OM lipoprotein component	ME	Fatty acids, lipids
rlmB	6	23S rRNA mG2251 2'-O-ribose methyltransferase, SAM-dependent	PS	Ribosome maturation
katG	6	catalase-peroxidase HPI, heme b-containing	RR	Stress
yddM	6	putative DNA-binding transcriptional regulator	RR	NC
yjhU	6	putative DNA-binding transcriptional regulator; KpLE2 phage-like element	RR	NC
ydfZ	6	selenoprotein, function U	U	
ygiB	6	DUF1190 family protein	U	
ygaZ	7	putative L-valine exporter, norvaline resistance protein	ME	Amino acids, peptides
mukE	7	chromosome condensin MukBEF, MukE localization factor	U	
pflA	8	pyruvate formate-lyase 1-activating enzyme; [formate-C-acetyltransferase 1]-activating enzyme; PFL activase	ME	Energy production
fadH	8	2,4-dienoyl-CoA reductase, NADH and FMN-linked	ME	Energy production
coaA	8	pantothenate kinase	ME	Cofactors
pgm	8	phosphoglucomutase	ME	Carbon compounds
uhpA	8	response regulator in two-component regulatory system wtih UhpB	ME	Carbon compounds
rho	8	transcription termination factor	PS	Transcription
rplL	8	50S ribosomal subunit protein L7/L12	PS	Ribosomal proteins
htrG	8	SH3 domain protein	U	
ampH	9	D-alanyl-D-alanine-carboxypeptidase/endopeptidase; penicillin-binding protein; weak beta-lactamase	CS	Cell wall
yidC	9	membrane protein insertase	CS	Membrane
ugpQ	9	glycerophosphodiester phosphodiesterase, cytosolic	ME	Energy production
glmM	9	phosphoglucosamine mutase	ME	Carbon compounds
lrp	9	leucine-responsive global transcriptional regulator	ME	
hisQ	9	histidine ABC transporter permease	ME	Amino acids, peptides
ycbZ	9	putative peptidase	NC	
yeaT	9	transcriptional activator of dmlA	RR	NC
murA	10	UDP-N-acetylglucosamine 1-carboxyvinyltransferase	CS	Cell wall
sohA	10	antitoxin of the SohA(PrlF)-YhaV toxin-antitoxin system	RR	Toxin-antitoxins
atpE	11	F0 sector of membrane-bound ATP synthase, subunit c	ME	Energy production
yhcM	11	divisome ATPase	CC	Cell division
shiA	11	shikimate transporter	CS	Transport
rbsK	11	ribokinase	ME	Carbon compounds
yjcE	11	putative cation/proton antiporter	U	
zipA	12	FtsZ stabilizer	CC	Cell division
ivbL	12	ilvB operon leader peptide	ME	Amino acids, peptides
ndk	12	multifunctional nucleoside diphosphate kinase and apyrimidinic endonuclease and 3'-phosphodiesterase	ME	Nucleic acids, nucleotides
yhiR	12	23S rRNA m(6)A2030 methyltransferase, SAM-dependent	PS	Ribosome maturation
phoB	12	response regulator in two-component regulatory system with PhoR	RR	NC

yjgJ	12	transcriptional repressor for divergent bdcA	RR	NC
fpr	13	ferredoxin-NADP reductase; flavodoxin reductase	ME	Energy production
gnd	13	6-phosphogluconate dehydrogenase, decarboxylating	ME	Energy production
iadA	13	isoaspartyl dipeptidase	ME	Amino acids, peptides
metL	13	Bifunctional aspartokinase/homoserine dehydrogenase 2	ME	Amino acids, peptides
yhhK	13	PanD autocleavage accelerator, panothenate synthesis	ME	Cofactors
yjjG	13	dUMP phosphatase	ME	Nucleic acids, nucleotides
rpsP	13	30S ribosomal subunit protein S16	PS	Ribosomal proteins
ydeP	13	putative oxidoreductase	RR	Stress
dipZ	14	thiol:disulfide interchange protein and activator of DsbC	ME	Energy production
fdoG	14	formate dehydrogenase-O, large subunit	ME	Energy production
hcaR	14	hca operon transcriptional regulator	ME	Carbon compounds
rhsC	14	Rhs protein with putative toxin domain; putative neighboring cell growth inhibitor	RR	Stress
dnaQ	15	DNA polymerase III epsilon subunit	CC	DNA replication
fimE	15	tyrosine recombinase/inversion of on/off regulator of fimA	CS	Surface structures
fliY	15	cystine transporter subunit	CS	Transport
dcuA	15	C4-dicarboxylate antiporter	ME	Carbon compounds
murP	15	N-acetylmuramic acid permease, EIIBC component, PTS system	ME	Carbon compounds
yciO	15	putative RNA binding protein	NC	
bdm	15	biofilm-dependent modulation protein	RR	Biofilm
yadH	15	putative ABC transporter permease	U	
yfiB	16	OM lipoprotein putative positive effector of YfiN activity	CS	Membrane
ydcS	16	putative ABC transporter periplasmic binding protein	CS	Transport
btuE	16	glutathione peroxidase	ME	Amino acids, peptides
sixA	16	phosphohistidine phosphatase	ME	
yjfJ	16	PspA/IM30 family protein	NC	
rpsG	16	30S ribosomal subunit protein S7	PS	Ribosomal proteins
lepA	16	back-translocating elongation factor EF4, GTPase	PS	Translation factors
lexA	16	transcriptional repressor of SOS regulon	RR	Stress
yggE	16	oxidative stress defense protein	RR	Stress
yeiS	16	DUF2542 family protein	U	
yhcB	16	DUF1043 family inner membrane-anchored protein	U	
yjbR	16	DUF419 family protein	U	
yfjD	17	UPF0053 family inner membrane protein	CS	Membrane
yjiY	17	putative transporter	CS	Transport
ptsI	17	PEP-protein phosphotransferase of PTS system (enzyme I)	ME	Carbon compounds
imp	17	LPS assembly OM complex LptDE, beta-barrel component	RR	Stress
yniA	17	fructosamine kinase family protein	U	
seqA	18	negative modulator of initiation of replication	CC	DNA replication
fabI	18	enoyl-[acyl-carrier-protein] reductase, NADH-dependent	ME	Fatty acids, lipids
frdA	18	anaerobic fumarate reductase catalytic and NAD/flavoprotein subunit	ME	Energy production
nlpC	18	putative C40 clan peptidase lipoprotein	ME	Fatty acids, lipids
rpsT	18	30S ribosomal subunit protein S20	PS	Ribosomal proteins
feaR	18	transcriptional activator for tynA and feaB	RR	NC
dnaN	19	DNA polymerase III, beta subunit	CC	DNA replication
nepI	19	putative transporter	CS	Transport
sstT	19	sodium:serine/threonine symporter	CS	Transport
cysQ	19	3'(2'),5'-bisphosphate nucleotidase	ME	Energy production
nuoM	19	NADH:ubiquinone oxidoreductase, membrane subunit M	ME	Energy production
fbp	19	fructose-1,6-bisphosphatase I	ME	Carbon compounds
galU	19	glucose-1-phosphate uridylyltransferase	ME	Carbon compounds
gatB	19	galactitol-specific enzyme IIB component of PTS	ME	Carbon compounds
thyA	19	thymidylate synthetase	ME	Nucleic acids, nucleotides
wbbK	19	lipopolysaccharide biosynthesis protein	ME	Fatty acids, lipids
pepB	19	aminopeptidase B	ME	
infC	19	translation initiation factor IF-3	PS	Translation factors
efp	19	polyproline-specific translation elongation factor EF-P	PS	Translation factors
prfA	19	peptide chain release factor RF-1	PS	Translation factors
nagZ	19	beta N-acetyl-glucosaminidase	RR	Antibiotic resistance
marA	19	multiple antibiotic resistance transcriptional regulator	RR	Antibiotic resistance
yobA	19	CopC family protein	RR	Stress
mdtK	20	multidrug efflux system transporter	CS	Transport
ilvD	20	dihydroxyacid dehydratase	ME	Amino acids, peptides
mtlA	20	mannitol-specific PTS enzyme: IIA, IIB and IIC components	ME	Carbon compounds
gapA	20	glyceraldehyde-3-phosphate dehydrogenase A	ME	Energy production
rsd	20	stationary phase protein, binds sigma 70 RNA polymerase subunit	RR	NC
rfaB	21	lipopolysaccharide 1,6-galactosyltransferase; UDP-D-galactose:(glucosyl)lipopolysaccharide-1,6-D-galactosyltransferase	CS	Surface structures
aroH	21	3-deoxy-D-arabino-heptulosonate-7-phosphate synthase, tryptophan repressible	ME	Amino acids, peptides

kefG	22	potassium-efflux system ancillary protein for KefB, glutathione-regulated	CS	Transport
aroP	22	aromatic amino acid transporter	ME	Amino acids, peptides
clpX	22	ATPase and specificity subunit of ClpX-ClpP ATP-dependent serine protease	ME	Amino acids, peptides
accB	22	acetyl CoA carboxylase, BCCP subunit	ME	Cofactors
araF	22	L-arabinose ABC transporter periplasmic binding protein	ME	Carbon compounds
fadD	22	acyl-CoA synthetase (long-chain-fatty-acid--CoA ligase)	ME	Fatty acids, lipids
folE	22	GTP cyclohydrolase I	ME	Cofactors
lepB	23	leader peptidase (signal peptidase I)	CS	Transport
garR	23	tartronate semialdehyde reductase	ME	Energy production
glpF	23	glycerol facilitator	ME	Carbon compounds
metF	23	5,10-methylenetetrahydrofolate reductase	ME	Energy production
yebZ	23	inner membrane protein	RR	Antibiotic resistance
yjcZ	23	YjcZ family protein; yhjH motility defect suppressor	U	
clcB	24	H(+)/Cl(-) exchange transporter	CS	Transport
acnB	24	aconitate hydratase 2; aconitase B; 2-methyl-cis-aconitate hydratase	ME	Energy production
panC	24	pantothenate synthetase	ME	Cofactors
pdxJ	24	pyridoxine 5'-phosphate synthase	ME	Cofactors
pepP	24	proline aminopeptidase P II	ME	Amino acids, peptides
ynjH	24	DUF1496 family protein	NC	
frr	24	ribosome recycling factor	PS	Translation factors
yfiH	24	UPF0124 family protein	U	
ygdD	25	UPF0382 family inner membrane protein	CS	Membrane
aphA	25	acid phosphatase/phosphotransferase, class B, non-specific	ME	Nucleic acids, nucleotides
napB	25	nitrate reductase, small, cytochrome C550 subunit, periplasmic	ME	Energy production
pabC	25	4-amino-4-deoxychorismate lyase component of para-aminobenzoate synthase multienzyme complex	ME	Cofactors
rpmI	25	50S ribosomal subunit protein L35	PS	Ribosomal proteins
groEL	25	Cpn60 chaperonin GroEL, large subunit of GroESL	RR	Chaperones
ytfB	25	OapA family protein	U	

Table S5

ID	Description	Sequence
G1	grcA-3'-end_rev	AACAGGATCCTTACAGGCTTTCAGTAAAGGTAC
R1	T7-canonical-grcA_fwd	AAATTCTAGA**GTAATACGACTCACTATAG**CAAGCAACAATGGTTTTACCAATTG
I3	T7-ll-grcA_fwd	AAATTCTAGA**GTAATACGACTCACTATAG**CATGATTACAGGTATCCAGATTA
S7	16SrRNA_fwd	AGAATGCCACGGTGAATACG
Y12	16SrRNA-3'-end_rev	TAAGGAGGTGATCCAACCGC
X15	16SrRNAΔ43_rev	TACGACTTCACCCCAGT
H3	T7-ll-rpsU_fwd	AAATTCTAGA**GTAATACGACTCACTATAG**CATGCCGGTAATTAAAGTAC
C54	rpsU-3'-end_rev	AACAGGATCCTTAGTACAGACGAGTGCG
B7	T7-canonical-rpsU_fwd	AAATTCTAGA**GTAATACGACTCACTATAG**GCGTTGATGCCAGCGG
Y50	RpsU91-110_rev (RT)	AACTCACGACGACGAACTTC
R48	grcA80-96_rev (RT)	GATGCAACGCGCTTCGC
M26	Zwf_rev81-98 (RT)	AGTTGATACAGGGAAGGC
Z7	rpsA85-103_rev (RT)	CGTCTTTGTCGATAGCAAC
O29	rpmI_rev (RT)	ATGTGACGCAGGTTAGCG
P29	rpsP_rev (RT)	CGACCGTTGCGTGCAT
Q29	rpoA_rev (RT)	GCGTCGAACTCACTTGCT
R29	RplL_rev (RT)	AGATCAGTTCTACAACGTCC
J21	atpE51-72_rev (RT)	AGCACCGATTGCCGCCAGACCC
F21	rho44-67_rev (RT)	GCCCCATATTTTCGCCGAGAGTGA

Acknowledgements

This work was supported within the framework of the Special Research Program `RNA-REG` on 'RNA regulation of the translatome' (F4316-B09) and the Doctoral Program Plus: RNA Biology (W1207-B09) and by grant P22249-B20 from the Austrian Science Fund to I.M.

II.2. AcnB is involved in the MazF-mediated stress response in *Escherichia coli*.

Martina Sauert, Hannes Temmel, Paul Kollmann, Oliver Vesper, Konstantin Byrgazov and Isabella Moll

Manuscript in preparation. Submission to Molecular Microbiology intended.

Contribution of the publication to the overall thesis

The *acnB* mRNA was identified as a target for MazF in the previous study assessing the 'leaderless mRNA regulon'. Here, we demonstrate that MazF activity can contribute to regulation of cellular processes in response to stress in two additional ways. First, MazF cleavage of the *acnB* mRNA creates an alternative translational start resulting in production of an alternative protein variant. Second, the freed 5'-UTR can play regulatory roles by acting as a small RNA.

Author's contribution

Martina Sauert contributed all figures and tables presented in this munscript, with exception of Figures 3C and 4A, which were contributed by Paul Kollmann. The manuscript was written by Martina Sauert, the paragraphs 'Introduction' and 'Discussion' were written in collaboration with Isabella Moll. The author's contribution to writing these segments was 50%.

Abstract

Aconitase B (AcnB) is a bifunctional enzyme involved in the central metabolism of *Escherichia coli*. It catalyzes the reversible isomerisation of citrate and isocitrate in the citric acid cycle and glyoxylate cycle during exponential growth phase. The enzyme contains an unstable [4Fe-4S] cluster, which is required for its catalytic activity. In addition, the N-terminal region of AcnB serves as a Fe^{2+} sensor mediating the dimerization of the protein in the presence of iron which is required for its catalytic activity. Under iron deprivation the monomeric AcnB takes on a new role as an iron-responsive element binding protein (IRE-BP), thereby acting as post-transcriptional regulator of gene expression. Thus, the iron responsive dimerization allows switching between the catalytic and regulatory role of AcnB. Here, we provide evidence for a novel mechanism leading to inhibition of AcnB dimerization even under iron-replete conditions, which likewise promotes its regulatory function. We show that during stress the endoribonuclease MazF, the toxin-component of the toxin-antitoxin (TA) system *mazEF*, cleaves the *acnB* mRNA 24 nucleotides upstream of the canonical GUG start codon. As a result an AUG codon, located in frame with the *acnB* open reading frame, is present at the novel 5´-terminus of the mRNA. As stress-ribosomes generated likewise by MazF selectively translate leaderless mRNAs harboring a 5´-terminal AUG start codon, translation of the truncated *acnB* mRNA initiates at the upstream AUG codon resulting in the synthesis of an alternative AcnB protein harboring seven additional N-terminal amino acid residues (MRARRTV) including three positively charged arginines. As the N-terminus is involved in dimerization, the addition of polar residues could interfere with the formation of the catalytically active form of AcnB even under iron replete conditions and thus might provide an alternative mechanism to switch the AcnB function from an enzymatic catalyst to a post-transcriptional regulator without the need of iron release. Additionally, our data indicate that the freed, stable 5'-UTR of *acnB* might play a regulatory role affecting the functionality of cell surface structures.

Introduction

Bacteria frequently have to respond and adapt to changes in environmental conditions, like shifts in temperature or pH, oxidative and osmotic stress or nutrient deprivation. In particular, pathogenic bacteria are subjected to rapidly changing environments when they invade their host. In order to survive, bacteria have developed several strategies to alter gene expression and protein activity, which allow a fast adaptation to environmental cues (Hengge 2008; Marles-Wright and Lewis 2007). In contrast to the alteration of the transcriptional program, we recently observed a post-transcriptional response mechanism, which leads to the alteration of the translational program (Vesper et al. 2011). Under stress conditions as antibiotic treatment, the endoribonuclease MazF -the toxin component of the toxin-antitoxin (TA) module *mazEF* (Aizenman, Engelberg-Kulka, and Glaser 1996; Engelberg-Kulka et al. 2006)- cleaves at single-stranded ACA-sites at or closely upstream of the AUG start codon of specific transcripts and thereby generates leaderless mRNAs (lmRNAs) (Vesper et al. 2011; Sauert et al, manuscript in preparation). Concomitantly, MazF targets the 16S rRNA at an ACA triplet in the 3'-terminal region of the 16S rRNA located upstream of helix 45. Thus, the cleavage leads to the loss of the 3´-terminus of the 16S rRNA, including helix 45 and the anti-Shine-Dalgarno (aSD) sequence (Vesper et al. 2011). Consequently, this sub-population of 'stress-ribosomes', herein referred to as 70SΔ43 ribosomes, selectively translates the lmRNAs generated by MazF, entailing expression of a particular group of genes, the 'lmRNA regulon', that might be substantial for bacteria to sustain stress (Sauert et al., manuscript in preparation).

Aconitases are major bifunctional enzymes of the central metabolism as they catalyze the isomerization of citrate to isocitrate *via* cis-aconitate in the citric acid cycle and glyoxylate cycle. The catalytically active form of the enzymes contains an unstable [4Fe-4S] cluster located at the active site which is formed by four structurally conserved domains (Williams et al. 2002). Under iron starvation or oxidative stress conditions aconitases take on a new role as post-transcriptional regulators of gene expression as they bind to specific mRNAs thereby affecting their stability and/or translation (Tang and Guest 1999; Tang et al. 2002). *E. coli* has two aconitases, AcnA, the stress induced stationary phase enzyme (Gruer and Guest 1994; Cunningham, Gruer, and Guest 1997) and AcnB, the major aconitase during exponential growth (Bradbury et al. 1996). Structurally these two enzymes are distinct as AcnB contains an additional 160 residue N-terminal HEAT-like domain (Domain 5) that is unique and has no counterpart in other members of the aconitase protein superfamily (Williams et al. 2002). This characteristic N-terminal domain was suggested to play a particular function in channeling substrates to

or from the AcnB active site (Williams et al. 2002). Further analyses revealed that the N-terminal region of AcnB consisting of domains 5 and 4 is pivotal for the iron-dependent formation of the catalytically active AcnB dimer. Noteworthy, not the iron-sulfur cluster but domain 4 serves as sensor for Fe^{2+} availability, which mediates switching between the dimeric catalytic form and the monomeric mRNA binding form (Tang et al. 2005). Moreover, it was shown that the N-terminal region is necessary and sufficient for the regulatory activity of AcnB as it binds AcnB-regulated transcripts and displays regulatory function (Tang et al. 2005).

Here, we present an alternative post-transcriptional mechanism which might inhibit AcnB dimerization uncoupled from iron deficiency. Sequence analysis revealed the presence of an ACA site in the 5´-UTR of the *acnB* transcript, which is followed by an in-frame AUG codon. Under stress conditions, MazF-mediated cleavage at this ACA places the AUG codon at the novel 5´-terminus of the truncated *acnB* mRNA. Since the AUG is in frame with the *acnB* open reading frame (ORF) and stress-ribosomes selectively translate mRNAs harboring a 5´-terminal AUG start codon (Vesper et al. 2011), translation of the truncated *acnB* mRNA can initiate at the upstream AUG codon resulting in the synthesis of an alternative AcnB protein, herein referred to as AcnB*, harboring seven additional N-terminal amino acid residues (MRARRTV) including three positively charged arginines. As the N-terminus is involved in dimerization (Tang et al. 2005), the addition of polar residues could interfere with the formation of the catalytically active form of AcnB even under iron replete conditions and we hypothesizes that the regulatory activity of the protein is promoted. We show that the truncated *acnB* mRNA starting at the AUG codon is translated, albeit with a lower efficiency when compared to canonical *acnB*. Thus, the levels of the alternative AcnB* are expected to be low. However, we present evidence that MazF cleavage is not only of importance to stimulate the synthesis of the AcnB* variant. In addition, the cleavage sets the 5'-UTR of *acnB* free which might itself perform additional regulatory functions during stress response and modulation of cell surface structures by acting as small regulatory RNA.

Thus, our findings suggest two additional aspects of the post-transcriptional stress response mediated by MazF: (i) the generation of alternative translational start sites to produce protein variants and (ii) excision of small regulatory RNAs. These mechanisms provide opportunities for fast adaptation to changed environments by altering protein activity at the level of translation and generation of small regulatory RNAs at post-transcriptional level.

Results

The *acnB* mRNA is cleaved by MazF

We recently analyzed the MazF-mediated alterations of the transcriptome and translatome of *E. coli* by RNA sequencing of total RNA and mRNAs extracted from polysomes during exponential growth and in response to *mazF* overexpression (Sauert et. al, manuscript in preparation). In the subsequent screen for MazF targets we identified *acnB* as one of many mRNAs that are cleaved by MazF in the 5'-UTR creating a lmRNA which can be selectively translated by 70SΔ43 ribosomes likewise generated by MazF (Sauert, et al, manuscript in preparation). **Figure 1B** presents the coverage of sequencing reads aligned to the *acnB* gene. The *acnB* mRNA is truncated after *mazF* overexpression and the most pronounced cleavage is located in the 5'-UTR (T+, violet). Interestingly, the 5'-UTR is still present in total RNA (T+, violet) but lost in polysomal RNA (P+, red). Together, this data indicates that the *acnB* 5'-UTR is stable in the cell but not associated to polysomes and that the leaderless version of *acnB* is translated by the 70SΔ43. The MazF cleavage corresponds to the ACA-site at position -24 relative to the canonical GUG start codon (**Figure 1D** and **C**). This ACA-site is directly followed by an AUG codon at position -21, which is in frame with the *acnB* open reading frame (ORF). MazF cleavage at this position thus results in a lmRNA with a 5'-terminal AUG start codon and its translation by the 70SΔ43 ribosomes would consequently result in an elongated protein variant of AcnB with additional seven amino acids (M R A R R T V) at the N-terminus, (**Figure 1D**).

Next, we verified the cleavage of the *acnB* transcript by MazF *in vivo via* primer extension analysis on total RNA extracted from *E. coli* MG1655 strain before and after 15, 30, 60, and 120 minutes of *mazF* overexpression and after 120 minutes under relaxed conditions. The primer extension shown in **Figure 3A** reveals the cleavage at position -23 (A/CA) already after 15 minutes upon induction of *mazF* overexpression (middle panel, lane 2) with a further increase in intensity after 30 and 60 minutes (lanes 3 and 4). Before induction of *mazF* overexpression and after 120 minutes growth under relaxed conditions this signal is absent (lanes 1 and 6), indicating that this is a MazF-dependent cleavage event. Additionally, we observe two weak primer extension abortion signals in dependence of *mazF* overexpression. One is located within the *acnB* coding region at position +13 (GAA/TAC) and appears with a delay of about 30 minutes to the primary MazF cleavage. The second, very minor abortion signal is located at position -38 (CG/CC). Both sites have no resemblance to potential MazF cleavage sites and it remains to be elucidated how these mRNA truncations are achieved.

The role of AcnB in stress response

To investigate if AcnB plays a role in the MazF-mediated stress response, we generated the strain MG1655Δ*acnB* as described in Material and Methods. Upon induction of *mazF* overexpression during early exponential growth in Luria-Bertani (LB) growth of both strains, MG1655 and MG1655Δ*acnB* is severely inhibited (**Figure 2A**). However, without *mazF* overexpression strain MG1655 enters the stationary phase earlier when compared to MG1655Δ*acnB*. To further investigate, if the *acnB* deletion has an impact on recovery from stress, we induced *mazF* overexpression during early exponential growth in LB for 30 minutes and upon re-inoculation in fresh LB the recovery of both strains was monitored. F**igure 2B** shows that the Δ*acnB* strain is severely compromised in the outgrowth after *mazF* overexpression, when compared to the wild type (WT) strain. This observation reveals that AcnB might play a significant role in stress recovery.

Additionally, we aimed to examine, if the MazF cleavage at position -23 of the *acnB* mRNA is crucial for the observed defect in stress recovery. To this end we created an MG1655 mutant strain carrying a single chromosomal point mutation at position -23, changing the ACA to an ATA site(*acnB*_C(-23)→T). This mutation had no apparent effect on growth under relaxed conditions. In contrast, the *acnB*_C(-23)→T mutation appears to pose an advantage during outgrowth from stress, i. e. *mazF* overexpression, especially at low concentrations of the inducer of *mazF* overexpression IPTG (**Figure 2C**). We next checked if the cleavage at position -23 still occurs in MG1655*acnB*_C(-23)→T. **Figure 3A** reveals that in contrast to the WT *acnB* mRNA (panel 2, lanes 1-6), no cleavage at position -23 occurred upon *mazF* overexpression, when total RNA purified from strain MG1655*acnB*_C(-23)→T before (panel 2, lane 17) and upon *mazF* overexpression (lanes 18-21) was used as template for primer extension analysis. However, the signals at positions +13 and -38 are slightly visible in total RNA extracted from cells after 120 minutes of *mazF* overexpression (panels 1 and 3, lane 20).

Translation of the leaderless *acnB* transcript

Employing toeprinting analysis we further show that 70S ribosomes (**Figure 3C** lane 2, third panel) as well as 70SΔ43 (**Figure 3C** lane 10, third panel) form a ternary complex (TC) on the AUG codon of the *in vitro* synthesized leaderless version of *acnB* indicating that translation can initiate at the AUG start codon when located at 5'-terminus. In striking contrast, translation cannot initiate at this AUG codon when the 5'-UTR is present, indicated by the lack of the corresponding signal when the canonical *acnB* mRNA was used for toeprinting analysis (**Figure 3C**, lanes 1 and 9, panel 3). In addition, 70S ribosomes also form a TC on the internal GUG start codon on the leaderless *acnB* mRNA

(lane 2, panel 4) but to a minor extend compared to the binding to the 5'-terminal AUG. Peculiarly, ribosome binding at the 5'-terminal AUG results in a double band indicating that the TC formed on that lmRNA is unstable or/and not perfectly positioned. This might result in low translation efficiency of the generated lmRNA.

Further, we aimed to validate the production of the N-terminal elongated AcnB protein variant which would result from translation of the leaderless *acnB* mRNA starting at the 5'-terminal AUG codon. Due to the size of the AcnB protein of 93 kDa, it is difficult to distinguish the protein from the alternative AcnB* protein, which harbors seven additional amino acids. However, considering the additional positive charges, we employed native polyacrylamide gel electrophoresis (PAGE) to distinguish between the two variants (**Figure 4A**), as shown by artificial expression of the variants from plasmids pBAD*acnB*_GUG and pBAD-*acnB*_AUG (**Figure 4A**, lanes 12 and 13, and **Figure 4B**). Native cell lysates from strain MG1655 harboring pSA1 were prepared with and without induction of *mazF* overexpression by addition of 10 µM IPTG at several time points and used for western blot analysis upon native PAGE. However, we were not able to detect the AcnB* variant at any time point upon *mazF* overexpression (**Figure 4A**, lanes 12 and 13) which could be attributed to the expected low efficiency of translation starting at the 5'-terminal AUG (**Figure 3C**). This hypothesis is supported by the fact that even in the presence of a Shine-Dalgarno (SD) sequence upstream of the AUG codon, less AcnB* is synthesized (**Figure 4A**, lane 13) when compared to the canonical *acnB* mRNA (**Figure 4A**, lane 12). Thus, we cannot exclude that the protein variant is produced in low amounts which we cannot detect due to limitations in sensitivity.

The sedimentation phenotype of the *acnB*_C(-23)→T mutant

Surprisingly, during our studies we observed that the *acnB*_C(-23)→T mutant strain tends to sediment when compared to the WT strain. This phenotype is unique for the *acnB*_C(-23)→T mutant strain and has not been observed for the *acnB* deletion or the WT strain (see **Figure 5A** and **B**), and moreover, strains with similar point mutations of ACA→ATA in the 5'-UTRs of other MazF candidate transcripts did not show this phenotype (data not shown). To further investigate this phenotype we performed sedimentation assays as described in Material and Methods. In **Figure 5A** the effect of fast sedimentation of MG1655*acnB*_C(-23)→T becomes strikingly apparent. Further, we have not observed any temperature dependence of this effect (data not shown).

Discussion

AcnB, the major aconitase during exponential growth (Bradbury et al., 1996), has two distinct functions. Besides its catalytic role in the TCA cycle where it catalyzes the reversible isomerisation of citrate to isocitrate, it is involved in post-transcriptional regulation of gene expression by directly interacting with specific mRNAs. Here, we provide evidence that the *acnB* gene is additionally involved in the MazF-mediated stress response pathway.

The *acnB* mRNA: A peculiar target of the stress-induced endoribonuclease MazF

Recently, we performed an RNA-Seq analysis to determine the entity of transcripts that are targeted by the stress induced endoribonuclease MazF when *E. coli* encounters adverse conditions (Sauert et al., manuscript in preparation). Interestingly, this screen revealed that MazF cleaves the *acnB* mRNA at position -23 with respect to the G of the genuine GUG start codon, thereby generating a lmRNA that contains a 5'-terminal AUG codon that is in frame with the *acnB* ORF (**Figure 1** and **3A**). This peculiar feature of the *acnB* transcript tempted us to speculate that upon MazF cleavage the specialized ribosomes selectively initiate translation at the 5´-terminal AUG thus synthesizing an alternative AcnB* protein that contains seven additional amino acids at the N-terminus, which are highly positively charged. Given that the N-terminus is involved in dimerization of the protein essential for its catalytical activity, it is conceivable that this alteration might impair dimer formation and thus favor the regulatory activity of the protein. As expected, toeprinting analysis performed on the canonical and leaderless *acnB* transcripts strongly support this notion (**Figure 3C**). The TC is formed at the AUG codon exclusively when it is located at the 5´-terminus, indicating that indeed the translation of the lmRNA can result in the synthesis of AcnB*. However, we were not able to detect the AcnB* protein *in vivo*. This fact could be attributed to an inefficient translation of the leaderless *acnB* mRNA. Moreover, even in the presence of a strong ribosome binding site translation starting at the AUG codon yields a lower amount of the AcnB* protein upon ectopic expression (**Figure 4A**, lane 13) when compared to AcnB (**Figure 4A**, lane 12), translation of which starts at the authentic start codon. This phenomenon can be explained by the fact that positively charged residues located at the N-terminus are considered to interact with the negatively charged ribosome exit tunnel, thereby slowing down ribosomal movement and translation (Lu and Deutsch, 2008; Lu et al., 2007). Moreover, considering that AcnB* could be possibly targeted by the methionine aminopeptidase (Map) that removes the N-terminal methionine (Gloge et al., 2014), one could further envisage that

the positively charged residue Arg (R) at the N-terminus likewise contributes to the low protein abundance by stimulating proteolytic degradation *via* channeling the protein to the ClpAP protease according to the N-end rule (Tasaki et al., 2012).

Additionally, primer extension analysis performed on total RNAs purified upon *mazF* expression indicate additional processing of the *acnB* mRNA, which cannot be directly attributed to MazF (**Figure 3A**). These could either represent additional cleavage events or the generation of strong alternative mRNA structures that lead to abortion of the extending reverse transcriptase or might even indicate alternative transcriptional start sites. The signal obtained at position +13 (**Figure 3A**, panel 3, lane 20) might indicate the subsequent activation of an additional endoribonuclease delayed by 30 to 60 minutes in response to MazF activation. Likewise, it is conceivable that the truncated *acnB* mRNA folds into an alternative structure that might create an RNase III cleavage site, which cleaves double-stranded RNA (Lamontagne et al., 2001). The weak signal upstream of the MazF cleavage site appears two hours after *mazF* induction and might result from transcription starting at an alternative promoter in order to rescue the loss of full length *acnB* mRNA. As these two additional signals can also be detected in total RNA extracted from the *acnB*_C(-23)→T mutant 120 minutes after induction of *mazF* expression, they seem to be independent of the MazF-mediated *acnB* cleavage at position -23. This commends the hypothesis of activation of secondary endoribonucleases, which could result in the degradation of the *acnB* mRNA. Taken together with the low abundance of the AcnB* protein, these results support the idea that the alternative AcnB* protein does not pose the sole regulatory element but that the removed 5'-UTR might play an additional regulatory role in stress response.

The *acnB* 5´-UTR: A novel regulatory RNA?

Our growth analysis shows that the *acnB* deletion mutant has severe defects in recovery after *mazF* overexpression (**Figure 2B**). This data underpins the observation by Tang and colleagues (2002) that an *acnB* deletion mutant is sensitive to oxidative stress, which has been shown to induce the *mazEF* TA system (Hazan et al., 2004). Moreover, the *acnB*_C(-23)→T mutation, which interferes with MazF cleavage at this position, stimulates outgrowth from *mazF* overexpression, especially at low concentrations of the inductor IPTG (**Figure 2**). In contrast, this point mutation does not affect growth under relaxed conditions. Together, these results raise the question whether the generation of the leaderless *acnB* mRNA, and its selective translation by 70SΔ43 ribosomes resulting in the synthesis of AcnB* are of importance for the post-transcriptional stress response

pathway mediated by MazF. Considering the low abundance of the AcnB* protein mentioned above and the stability of the cleaved *acnB* 5´-UTR as revealed by the RNA-Seq analysis (**Figure 1**) and further underlined by the strong hairpin structure (**Figure 6**), our data strongly suggest that besides the AcnB* protein the free 5'-UTR (5'-UTR$_{acnB}$) might play a pivotal role as regulatory RNA under these conditions. This hypothesis is further supported by the sedimentation phenotype observed for strain MG1655*acnB*_C(-23)→T (**Figure 5**). In contrast, strain MG1655Δ*acnB* does not show this sedimentation phenotype. However, despite the replacement of the *acnB* gene with the Kan^R cassette (see Materials and Methods), the *acnB* deletion strain still harbors the promoter as well as the 5'-UTR sequence of *acnB*. Thus, this strain is still able to generate the free 5'-UTR$_{acnB}$, which might play a significant role during stationary phase indicated by the sedimentation of the cells unable to generate this 5'-UTR$_{acnB}$ regulatory RNA.

It was generally accepted that the bacterial stress response is primarily controlled at the level of transcription by specific protein regulators (Hengge-Aronis, 2002). However, post-transcriptional systems can offer rapid response mechanisms for modulating mRNA stability and translational efficiency, like it was shown for the AcnB-mediated response to oxidative stress and iron starvation (Tang and Guest, 1999). Conversion of the active holo-enzyme harboring an [4Fe-4S] cluster into a site-specific mRNA binding apo-protein upon oxidative stress provides a fast molecular mechanism to respond to stress conditions. Accordingly, an *acnB* mutant is more sensitive to oxidative stress (Tang et al., 2002). In sharp contrast, an *acnA* mutant shows only a slight increase in stress sensitivity when challenged with H_2O_2 (Tang et al., 2002). This differential sensitivity of the *acn* mutants was attributed to the antagonistic effects of both aconitases, AcnA and AcnB on the levels of the *sodA* transcript and on SodA synthesis, which is involved in detoxifying superoxide (Tang et al., 2002). Binding of AcnB to the *sodA* transcript strongly reduces its half-life, and thus negatively affects SodA synthesis. Thus, in the absence of *acnB* the SodA levels are increased thereby mimicking oxidative stress conditions.

The reported MazF-mediated system offers a faster response mechanism by modulating translation and generation of regulatory RNAs from existing mRNAs. Thus, this mechanisms may be of much greater general significance than simply controlling.

Material and Methods

Bacterial strains and growth conditions

In this study we used the bacterial strains *E. coli* MG1655 and MG1655Δ*acnB.* MG1655Δ*acnB* was generated by ΦP1 transduction (Lennox, 1955) using BW25113Δ*acnB* (Keio collection, (Baba et al., 2006) as donor and MG1655 as acceptor. Bacterial strains are grown at 37°C in LB broth and growth is monitored by photometric measurement of optical density at 600 nm (OD_{600}).

For outgrowth experiments, bacterial strains harboring plasmid pSA1 for IPTG-inducible *mazF* overexpression were cultured at 37°C in LB supplemented with 100 µM ampicillin (Amp) and *mazF* overexpression was induced for 30 minutes by addition of 10, 30 or 100 µM IPTG during exponential growth at an OD_{600} around 0,3-0,4. Then, cultures were harvested by centrifugation at 37°C, 4.000 rpm for 5 minutes, resuspended in fresh LB supplemented with 100 µM Amp to an OD_{600} of exactly 0,2 and cultured again at 37°C.

Overexpression of artificial *acnB* constructs on pBAD33 backbones was induced by addition of 0,4% L-arabinose during exponential growth at an OD_{600} around 0,3-0,4 for one hour. Cells were harvested by centrifugation at 5.000 rpm for 5 minutes and supernatant-free cell pellets were frozen in $N_{2\ aq}$ and stored at -20°C for further analysis.

In vitro transcription and primer extension analysis

Leaderless and canonical *acnB* mRNAs were produced using AmpliScribe™ T7 High Yield Transcription Kit (Epicenter) with 1 µg of PCR products on chromosomal DNA from MG1655 using primers P18/Z32 and I17/Z32, respectively (listed in **Table S1**) following the manufacturer's protocol. The resulting RNA was extracted by phenol chloroform extraction. Primer extension analysis was performed as described in (Vesper et al. 2011) using primer M16 for detection of MazF-cleavage in the 5'-UTR and primer K34 for detection of internal cleavage at position 290 (see **Table S1**). Briefly, 1 pmol of the respective mRNAs were annealed to the 5'-end-labeled reverse primers in 1xRT-buffer by heating for 3 min to 80°C, snap freezing in liquid nitrogen, and slowly thawing on ice. Primer extension reactions were performed in RT-buffer by using the AMV reverse transcriptase (Promega) by incubation at 42°C for 30 min. The samples were separated on an 8% PAA-8M urea gel, and the extension signals were visualized by using a Molecular Dynamics PhosphoImager (GE Healthcare).

Toeprinting reaction

For ribosome binding assays 1 pmol of radioactively labeled oligo nucleotide M16 (listed in **Table S1**) is mixed with 0.5 pmol of the *in vitro* transcribed *acnB* RNA in 1x VD-buffer in a total volume of 20 µl. The oligo nucleotide is annealed by heating the mixture to 80°C for 3 minutes and immediate snap freezing in $N_{2\,aq}$. The mixture is gently thawed on ice and 5 µl of 50 µM MgOAc in 1x VD+ are added to increase the Mg^{2+} concentration for the subsequent RT reaction. To 2 µl of the annealing mix 4 pmol of 30S or 70S ribosomes and 16 pmol tRNA-fMet are added in a total volume of 10 µl in 1x VD+. This reaction is incubated at 37°C for 10 minutes to allow binding of the ribosomes to the mRNA 5'-end. Then 2 µl of MMLV-mix are added and incubated again for 10 minutes at 37°C to perform the RT reaction. The reaction is stopped by addition 1.5 volumes of MMLV loading dye. 8 µl of that mixture are loaded onto a pre-warmed 30 cm long 8% PAA-urea gel and electrophoresis performed at 18-24 mA for 2-3 hours. The resulting gel is dried on Whatman paper and radioactivity detected by a phosphor screen and Typhoon imager.

Insertion of a 'scarless' point mutation in the chromosome of *E. coli*

To create an *E. coli* mutant with a single chromosomal point mutation disrupting the MazF cleavage site at position -23 we used a 'two-step' mutagenesis developed by Datsenko and Wanner, based on the modified 'one-step' gene inactivation protocol (Datsenko and Wanner, 2000). To this end, we amplified a cassette containing the kanamycin resistance (Kan^R) gene including the *kana* promoter and the CcdB toxin coding gene under control of the rhamnose (Rha) promoter from the template plasmid pKILL45 (derived from pKD45 (Datsenko and Wanner, personal communication), obtained from Susann Fragel, Schnetz laboratory Cologne) with primers G34 and H34 (see **Table S1**). The primers contain each 50 nucleotides overhangs that are homologous to the *acnB* 5'-UTR. Using pKD46, the λ red helper plasmid (temperature sensitive replication), we inserted the cassette into the chromosome of MG1655 by selection on kanamycin containing LB agar plates according to the describes procedure (Datsenko and Wanner, 2000). Subsequently, we exchanged this cassette with a 100 bp long DNA, corresponding to the homologous regions of the primers G34 and H34, but including the desired point mutation at position -23 (A<u>C</u>A → A<u>T</u>A). The 100 bp DNA carrying the point mutation was obtained *via* a two-step PCR approach, employing a overlap PCR on the two PCR products resulted from PCRs with primers Z30/A31 and B31/C31 on genomic DNA of MG1655. This second step was likewise performed with the use of pKD46, however, here selection was

performed on M9 minimal media plate with 0,4% L-rhamnose to select for the loss of the rhamnose-regulated *ccdB* gene, which has been inserted into the chromosome in the previous step. Cells still carrying the Kan^R-*ccdB* cassette do not survive due to the expression of the toxic gene *ccdB* in the presence of L-rhamnose. The stably inserted point mutation was verified by amplification of the acnB gene from the resulting mutants with the primers.

Non-denaturing protein analysis

For non-denaturing PAGE analysis of protein samples melted cell pellets were resuspended in appropriate volumes of 1mg lysozyme/ml 1xTE (10 mM Tris-HCl, pH 8.0, 1 mM EDTA) buffer resulting in 10 OD/ml (lysozyme from chicken egg white, Fluka, in a final concentration of 0,2mg/OD) and incubated on ice for 10 minutes. The mixture was shock frozen in $N_{2\ aq}$ and thawed at room temperature for 3 times. The cell debris was pelleted by centrifugation at 4°C and 30.000 rpm for 10 min and the supernatant was treated with RNase I and DNAse I (both Thermo Scientific) for 1 hour at 37°C and subsequently used for downstream analysis. Native cell lysates were mixed in a 1:1 ratio with 2x native sample buffer (0.175 mM Tris-HCl, pH 6.8, 20% glycerol, 0.2% bromo phenol blue) and immediately loaded onto native PAA gels (8% acrylamide/bisacrylamide (37.5:1, Roth), 0.25 M Tris-HCl, pH 8.8). Electrophoresis is performed in 250 mM Tris-HCl, pH 8.8, 0.19 M glycine in Biorad Protean II electrophoresis cells. Proteins separated on PAA gels are transferred to a nitrocellulose membrane (Amersham Protan 0.2 µm) by semi-dry transfer in transfer buffer (48 mM Tris, pH 8.3, 39 mM glycine, 0.037% SDS, 20% methanol) in a Biorad Trans-Blot® SD Semi-Dry Transfer Cell. Membranes are blocked by incubation in 1x PBS, 5% milk powder for 1 h at room temperature or over night at 4°C. The primary antibody α-AcnB (obtained from Jeff Green, Sheffield University) is applied for 1 h at room temperature or over night at 4°C. After washing the secondary antibody (α-rabbit-IgG-IRDye800®, Rockland) is applied for 45 minutes at room temperature and the signals are scanned in an Odyssee scanner.

Sedimentation assays

To qualitatively quantify the sedimentation phenotype observed in MG1655 *acnB*_C(-23)→T, we prepared overnight cultures of the strains MG1655 WT, MG1655 Δ*acnB* and *acnB*_C(-23)→T in three biological replicates. Upon termination of shaking we carefully took samples from very top of the culture and measured the OD_{600}. All values were normalized to the respective starting OD_{600}.

References

Aizenman, E, H Engelberg-Kulka, and G Glaser. 1996. “An Escherichia Coli Chromosomal ‘Addiction Module’ Regulated by Guanosine [corrected] 3’,5’-Bispyrophosphate: A Model for Programmed Bacterial Cell Death.” Proceedings of the National Academy of Sciences of the United States of America 93 (12): 6059–63.

Baba, Tomoya, Takeshi Ara, Miki Hasegawa, Yuki Takai, Yoshiko Okumura, Miki Baba, Kirill A Datsenko, Masaru Tomita, Barry L Wanner, and Hirotada Mori. 2006. “Construction of Escherichia Coli K-12 in-Frame, Single-Gene Knockout Mutants: The Keio Collection.” Molecular Systems Biology 2 (February): 2006.0008. doi:10.1038/msb4100050.

Bradbury, A. J., M. J. Gruer, K. E. Rudd, and J. R. Guest. 1996. “The Second Aconitase (AcnB) of Escherichia Coli.” Microbiology (Reading, England) 142 (Pt 2) (February): 389–400.

Cunningham, L., M. J. Gruer, and J. R. Guest. 1997. “Transcriptional Regulation of the Aconitase Genes (acnA and acnB) of Escherichia Coli.” Microbiology (Reading, England) 143 (Pt 12) (December): 3795–3805.

Datsenko, K. A., and B. L. Wanner. 2000. “One-Step Inactivation of Chromosomal Genes in Escherichia Coli K-12 Using PCR Products.” Proceedings of the National Academy of Sciences of the United States of America 97 (12): 6640–45. doi:10.1073/pnas.120163297.

Engelberg-Kulka, Hanna, Shahar Amitai, Ilana Kolodkin-Gal, and Ronen Hazan. 2006. “Bacterial Programmed Cell Death and Multicellular Behavior in Bacteria.” PLoS Genetics 2 (10): e135. doi:10.1371/journal.pgen.0020135.

Gloge, Felix, Annemarie H. Becker, Günter Kramer, and Bernd Bukau. 2014. “Co-Translational Mechanisms of Protein Maturation.” Current Opinion in Structural Biology 24 (February): 24–33. doi:10.1016/j.sbi.2013.11.004.

Gruer, M. J., and J. R. Guest. 1994. “Two Genetically-Distinct and Differentially-Regulated Aconitases (AcnA and AcnB) in Escherichia Coli.” Microbiology (Reading, England) 140 (Pt 10) (October): 2531–41.

Hazan, Ronen, Boaz Sat, and Hanna Engelberg-Kulka. 2004. “Escherichia Coli mazEF-Mediated Cell Death Is Triggered by Various Stressful Conditions.” Journal of Bacteriology 186 (11): 3663–69. doi:10.1128/JB.186.11.3663-3669.2004.

Hengge-Aronis, Regine. 2002. “Recent Insights into the General Stress Response Regulatory Network in Escherichia Coli.” Journal of Molecular Microbiology and Biotechnology 4 (3): 341–46.

Hengge, Regine. 2008. “The Two-Component Network and the General Stress Sigma Factor RpoS (sigma S) in Escherichia Coli.” Advances in Experimental Medicine and Biology 631: 40–53. doi:10.1007/978-0-387-78885-2_4.

Lamontagne, B., S. Larose, J. Boulanger, and S. A. Elela. 2001. “The RNase III Family: A Conserved Structure and Expanding Functions in Eukaryotic dsRNA Metabolism.” Current Issues in Molecular Biology 3 (4): 71–78.

Lennox, E. S. 1955. “Transduction of Linked Genetic Characters of the Host by Bacteriophage P1.” Virology 1 (2): 190–206.

Lu, Jianli, and Carol Deutsch. 2008. “Electrostatics in the Ribosomal Tunnel Modulate Chain Elongation Rates.” Journal of Molecular Biology 384 (1): 73–86. doi:10.1016/j.jmb.2008.08.089.

Lu, Jianli, William R. Kobertz, and Carol Deutsch. 2007. “Mapping the Electrostatic Potential within the Ribosomal Exit Tunnel.” Journal of Molecular Biology 371 (5): 1378–91. doi:10.1016/j.jmb.2007.06.038.

Marles-Wright, Jon, and Richard J Lewis. 2007. “Stress Responses of Bacteria.” Current Opinion in Structural Biology 17 (6): 755–60. doi:10.1016/j.sbi.2007.08.004.

Tang, Y., and J. R. Guest. 1999. “Direct Evidence for mRNA Binding and Post-Transcriptional Regulation by Escherichia Coli Aconitases.” Microbiology (Reading, England) 145 (Pt 11) (November): 3069–79.

Tang, Yue, John R. Guest, Peter J. Artymiuk, and Jeffrey Green. 2005. “Switching Aconitase B between Catalytic and Regulatory Modes Involves Iron-Dependent Dimer Formation.” Molecular Microbiology 56 (5): 1149–58. doi:10.1111/j.1365-2958.2005.04610.x.

Tang, Yue, Michael A. Quail, Peter J. Artymiuk, John R. Guest, and Jeffrey Green. 2002. “Escherichia Coli Aconitases and Oxidative Stress: Post-Transcriptional Regulation of sodA Expression.” Microbiology (Reading, England) 148 (Pt 4): 1027–37.

Tasaki, Takafumi, Shashikanth M. Sriram, Kyong Soo Park, and Yong Tae Kwon. 2012. “The N-End Rule Pathway.” Annual Review of Biochemistry 81: 261–89. doi:10.1146/annurev-biochem-051710-093308.

Vesper, Oliver, Shahar Amitai, Maria Belitsky, Konstantin Byrgazov, Anna Chao Kaberdina, Hanna Engelberg-Kulka, and Isabella Moll. 2011. “Selective Translation of Leaderless mRNAs by Specialized Ribosomes Generated by MazF in Escherichia Coli.” Cell 147 (1): 147–57. doi:10.1016/j.cell.2011.07.047.

Williams, Colin H., Timothy J. Stillman, Vladimir V. Barynin, Svetlana E. Sedelnikova, Yue Tang, Jeffrey Green, John R. Guest, and Peter J. Artymiuk. 2002. “E. Coli Aconitase B Structure Reveals a HEAT-like Domain with Implications for Protein–protein Recognition.” Nature Structural & Molecular Biology 9 (6): 447–52. doi:10.1038/nsb801.

Figure and Table legends

Figure 1: MazF cleavage of the *acnB* mRNA. **A**) Schematic depiction of the *acnB* gene locus. The two promoters *acnB*p1 (-96) and *acnB*p2 (-51) are indicated by black arrows. The position of the binding site of the primer M16 used for primer extension analysis shown in Figure 3 is indicated. **B**) Sequencing read coverage along the *acnB* gene. RNA-seq was performed on total RNA (**T**, green and violet) and RNA extracted from polysomes (**P**, blue and red) from *E. coli* cells during exponential growth (**-**, green and blue) or after 15 minutes of *mazF* overexpression (**+**, violet and red) (Sauert et al, manuscript in preparation). The coding region of *acnB* is represented by a dark green bar, annotating the orientation on the plus strand by white arrowheads from left to right. **C**) The region of -100 to +330 nucleotides relative to the *acnB* start codon is enlarged for *mazF* overexpression conditions. **D**) The nucleotide sequence of *acnB* around the canonical GUG start codon (green) and the MazF cleavage site (red) is shown. The canonical Shine-Dalgarno sequence is underlined and the AUG codon in frame with the coding region is depicted in red and underlined. Translation initiation at the AUG of the lmRNA would result in translation of additional seven amino acids (red) preceeding the canonical sequence starting at GUG (green).

Figure 2. Growth curves of MG1655, MG1655Δ*acnB* and MG1655*acnB*_C(-23)→T in dependence of *mazF* overexpression. The WT is depicted by a black line and the *acnB* mutants by a dashed line. Induction of *mazF* overexpression during early exponential growth phase from plasmid pSA1 by addition of 100µM IPTG is indicated by triangles. **A**) Growth of WT and Δ*acnB* upon induction of *mazF* overexpression. Relaxed conditions are indicated by circles. **B**) Outgrowth of WT and Δ*acnB* in fresh LB after 30 minutes of *mazF* overexpression. Untreated cultures are indicated by circles. C) Outgrowth of WT and *acnB*_C(-23)→T in fresh LB after 30 minutes of *mazF* overexpression. Circles indicate induction of *mazF* overexpression with only 10 µM IPTG.

Figure 3. MazF cleavage and ribosome binding. A) Primer extension analysis on total RNA extracted from MG1655 and MG1655*acnB*_C(-23)→T under relaxed conditions and upon *mazF* overexpression. **B**) The positions of verified MazF cleavage events (red arrows) and toeprints on the canonical GUG start codon (green, bold arrow) and on the alternative AUG start codon (red, bold arrow). **C**) Toeprint assays on *in vitro* transcribed full length and leaderless *acnB* mRNAs with canonical 70S and MazF-derived 70SΔ43 ribosomes. All primer extension reactions were performed with primer M16 (**Table S1**).

The sequencing reactions were obtained from an *in vitro* transcribed full length *acnB* mRNA.

Figure 4. The alternative AcnB variant is not detectable. A) Western blot detecting AcnB in cell lysates from MG1655 WT under relaxed conditions and upon *mazF* overexpression over a duration of 4,5 hours separated on a 8% native PAA gel. The control samples pBAD-*acnB*_GUG and _AUG were obtained from MG1655Δ*acnB* carrying pBAD-*acnB*_GUG or _AUG upon one hour of induction of *acnB* overexpression by addition of 0,4 % L-arabinose. **B**) Schematic depiction of the artificial *acnB* constructs in pBAD33.

Figure 5. Sedimentation of MG1655*acnB*_C(-23)→T. A) Sedimentation assay with MG1655, MG1655Δ*acnB* and MG1655*acnB*_C(-23)→T. **B**) The respective overnight cultures after 5 hours motionless conditions.

Figure 6. Depiction of the 2D structure of the *acnB* 5'-UTR. The sequence of *acnB* from position -96 to +15 was submitted to RNAfold within the Vienna RNA package (http://rna.tbi.univie.ac.at, Lorenz et al., 2011) for folding into a 2D structure, based on predicted minimum free energy structures and base pair probabilities and the output was visualized with Varna (http://varna.lri.fr, Darty et al., 2009).

Table S1. Primers used in this study. Regions homologous to the *E.coli* chromosome are underlined.

Table S2. Plasmids used in this study. For the pBAD33-acnB plasmids the nucleotide sequences of the artificial 5'-UTR are given. The XhoI restriction site for cloning into pBAD33 is underlined and the AG-rich region serving as SD sequence is highlighted in gray. The repective initial ORFs are highlighted bold and the canonical translational start site is additionally underlined. pBAD-*acnB*_GUG encodes the canonical ORF of *acnB* with a nucleotide change from GTG to ATG to increase artificial overexpression. pBAD-*acnB*_AUG encodes the alternative *acnB* ORF with the additional 21 nucleotides, starting with the ATG and with a mutation in the canonical start codon GTG to GTT to exclude canonical translation on this construct.

Figures

Figure 1

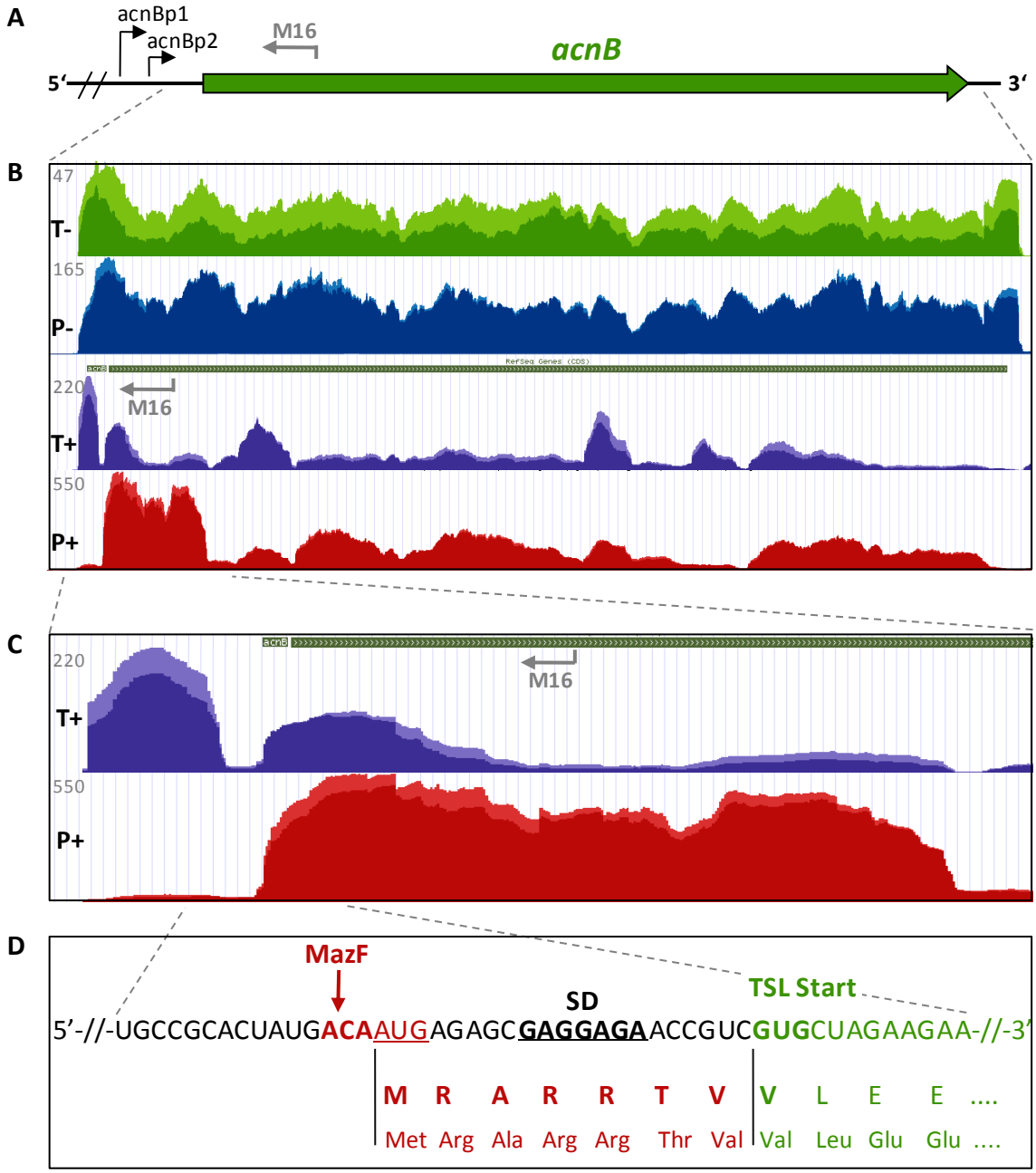

Figure 2

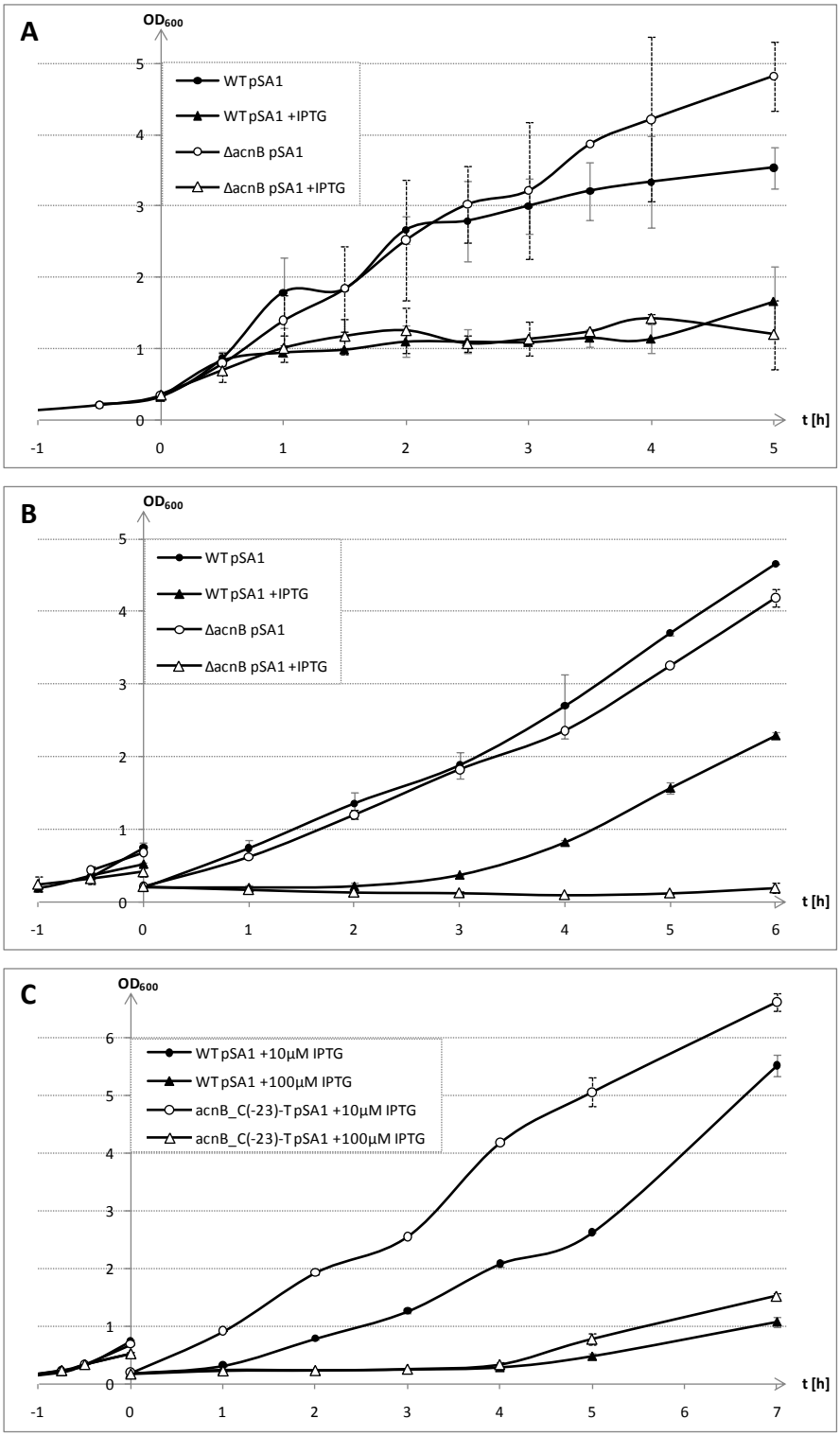
A
OD600
WT pSA1
WT pSA1 +IPTG
ΔacnB pSA1
ΔacnB pSA1 +IPTG
t [h]
B
OD600
WT pSA1
WT pSA1 +IPTG
ΔacnB pSA1
ΔacnB pSA1 +IPTG
t [h]
C
OD600
WT pSA1 +10µM IPTG
WT pSA1 +100µM IPTG
acnB_C(-23)-T pSA1 +10µM IPTG
acnB_C(-23)-T pSA1 +100µM IPTG
t [h]

Figure 3

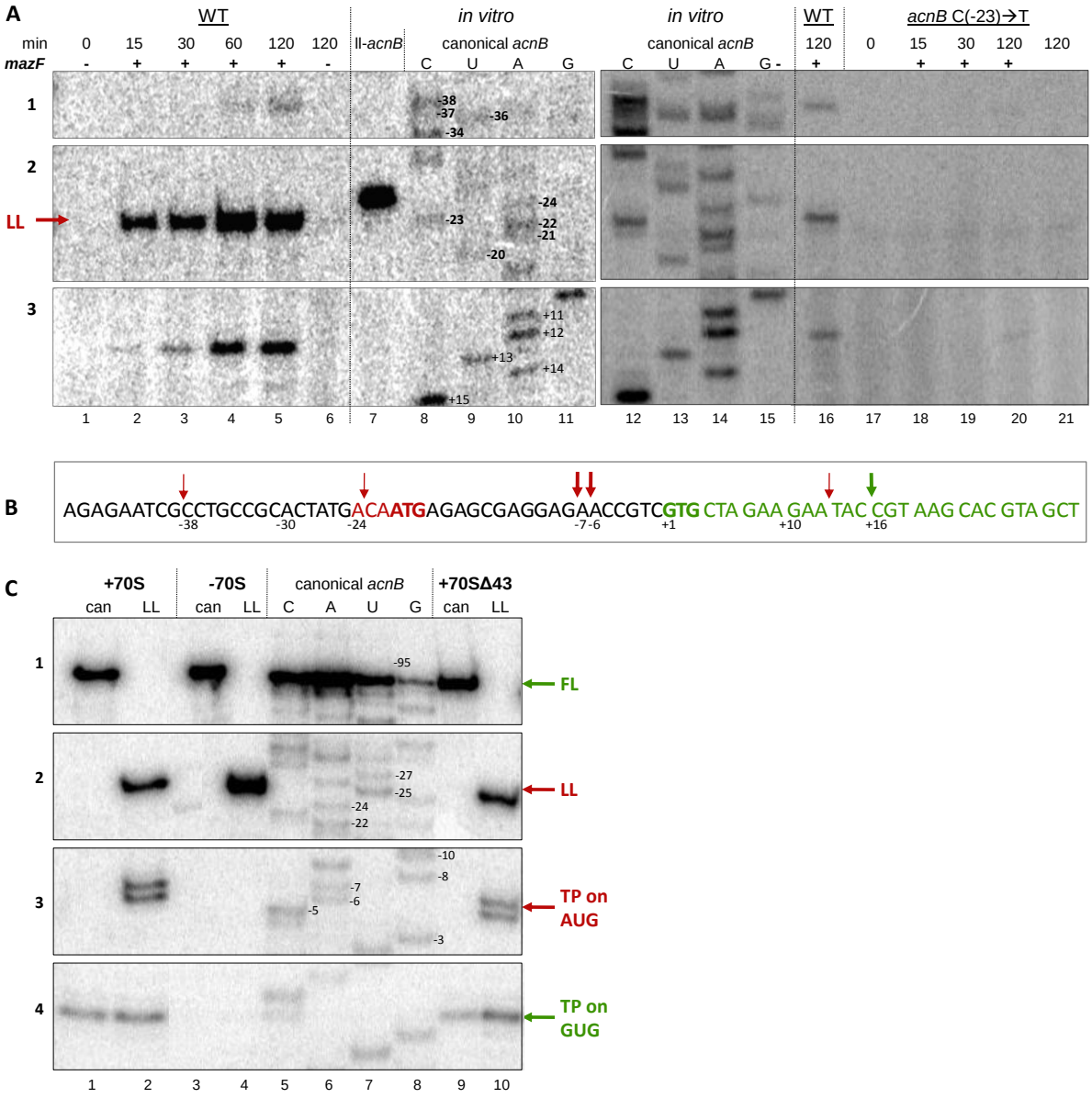
A
WT
in vitro
in vitro
WT
acnB C(-23)→T
min 0 15 30 60 120 120 II-acnB canonical acnB C U A G canonical acnB C U A G - 120 0 15 30 120 120
mazF - + + + + - + + + + +
1
2
LL
3
-38 -37 -36 -34 -24 -23 -22 -21 -20 +11 +12 +13 +14 +15
1 2 3 4 5 6 7 8 9 10 11 12 13 14 15 16 17 18 19 20 21
B
AGAGAATCGCCTGCCGCACTATGACAATGAGAGCGAGGAGAACCGTCGTG CTA GAA GAA TAC CGT AAG CAC GTA GCT
-38 -30 -24 -7 -6 +1 +10 +16
C
+70S -70S canonical acnB +70SΔ43
can LL can LL C A U G can LL
1
2
3
4
-95 -27 -25 -24 -22 -10 -8 -7 -6 -5 -3
FL
LL
TP on AUG
TP on GUG
1 2 3 4 5 6 7 8 9 10

Figure 4

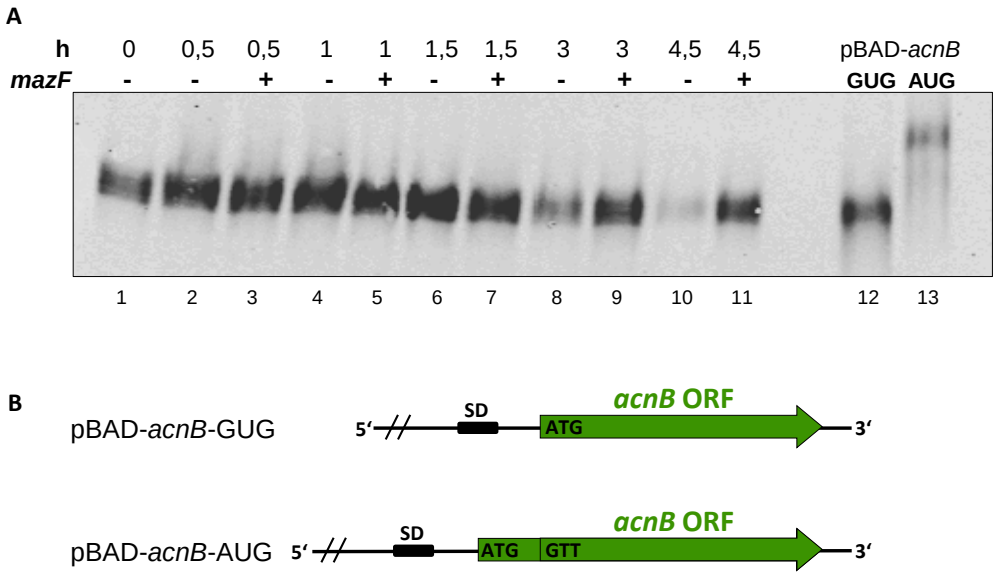

Figure 5

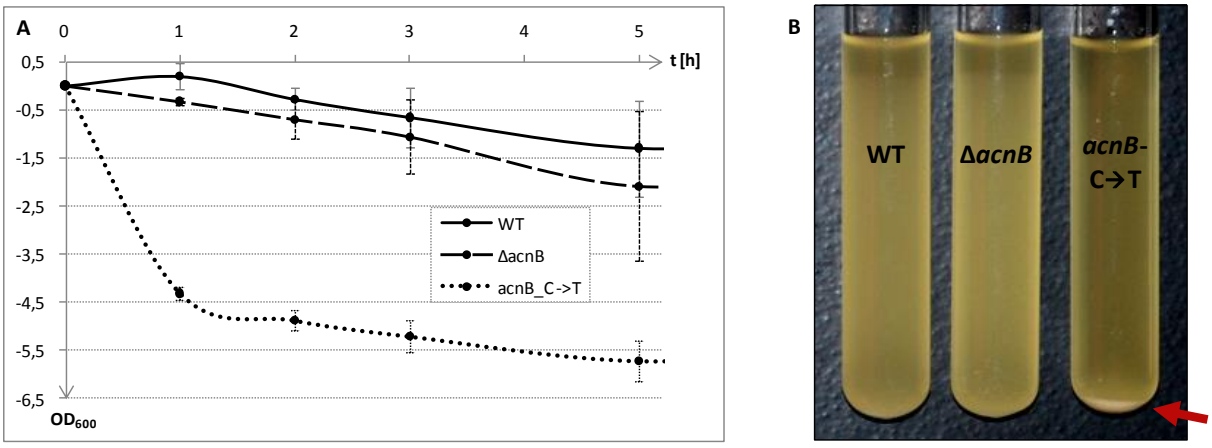

Figure 6

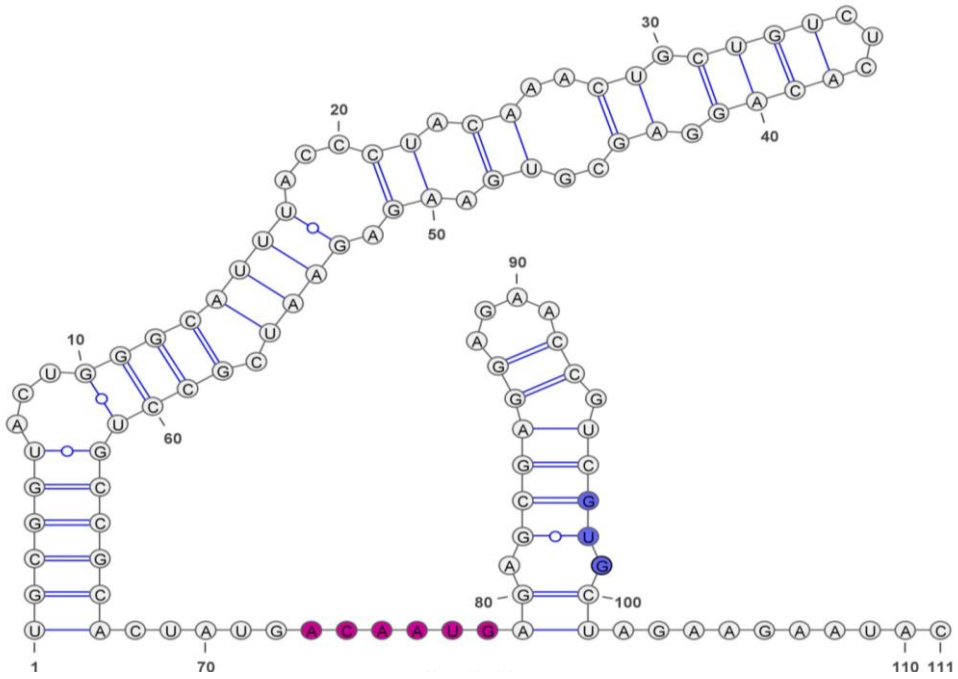

Tables

Table S1

ID	Description	Sequence
M16	acnB_rev48-63 (RT)	GGGTTTGGGCGCAATC
K34	acnB_rev333-353 (RT)	GCTTTGGCAGCAATAGGTGC
F16	acnB-5'-UTR_fwd	TATAAAGCTTCATCCTTAACGATTCAGCCAC
G16	acnB-3'-UTR_rev	TATAGGATCCCGGAACGGCGATGGTTTAG
R48	grcA_rev80-96 (RT)	GATGCAACGCGCTTCGC
G34	IM_G34_acnB-neo_fwd	AAACTGCTGTCTCACAGGAGCGTGAAGAGAATCGCCTGCCGCACTATGACTCAGAAGAACTCGTCAAGAAGG
H34	IM_H34_acnB-ccdB_rev	CTACGTGCTTACGGTATTCTTCTAGCACGACGGTTCTCCTCGCTCTCATTCCGGATATTATCGTGAGGATG
Z30	acnB_ACA1_fwd	AAACTGCTGTCTCACAGGAG
A31	acnB_ACA1-mut_rev	CGCTCTCATTATCATAGTGCG
B31	acnB_ACA2-mut_fwd	CGCACTATGATAATGAGAGCG
C31	acnB_ACA2_rev	CTACGTGCTTACGGTATTCTTC

Table S2

Name	Content	origin
pSA1	pQE30-*mazF*	Amitai et al., 2009
pKD46	λ red helper plasmid (temperature sensitive replication, Amp^R)	Datsenko and Wanner, 2000)
pKILL45	Template for amplification of the $Kana^R$-ccdB cassettes is derived from pKD45 (Datsenko and Wanner, unpublished)	Susann Fragel (Schnetz laboratory Cologne, unpublished)
pBAD-*acnB*_GUG	TCTAGAAATAATTTTGTTTAACTTTAAGAAGGAGATATACAT**ATGCTAGAA**	This work
pBAD-*acnB*_AUG	TCTAGAAATAATTTTGTTTAACTTTAAGAAGGAGATATACAT**ATGAGAGCGAGGAGAACCGTCGTTCTAGAA**	This work

Acknowledgement

This work was supported within the framework of the Special Research Program `RNA-REG` on 'RNA regulation of the translatome' (F4316-B09) and the Doctoral Program Plus: RNA Biology (W1207-B09) and by grant P22249-B20 from the Austrian Science Fund to I.M.

We thank Dr. Jeff Green, Sheffield University, UK, for providing antibodies directed against AcnB. and Katharina Otto for performing the experiments shown in **Figure2B** and **C** and for her contribution to the experiments shown in **Figure 3A**.

II.3. ΔACA-EmGFP reporter

Fluorescent reporter for MazF-dependent selective translation of leaderless mRNAs

I aimed to develop a quick assay to monitor MazF-dependent selective lmRNA translation in response to stress. With the objective to screen for stress conditions that induce the MazF-mediated response mechanism. Additionally, we aimed to study the MazF-mediated response on the single cell level to investigate whether the whole population reacts in the same way to a given stress condition or if individual cells turn the MazF-dependent mechanism on while others don't. In this respect, we chose a fluorescent assay in order to allow observation in a fluorescent microscope and eventually FACS sorting of cells that show selective translation of lmRNAs upon *mazF* overexpression or other physiological stress conditions.

II.3.1. Reporter design

I constructed a *gfp* reporter gene free of ACA-sites to guarantee mRNA stability during MazF activity. The GFP variant chosen is derived from the so called Emerald–GFP (EmGFP, pRSET-*em-gfp*, Invitrogen), which is the brightest available GFP variant with very fast folding kinetics and distinct excitation and emission peaks of 487nm and 509nm respectively (Tsien, 1998). The nucleotide sequence of *em-gfp* is shown below in triplets, with the previous ACA sites marked in red and the changed nucleic acid bold.

ATG GTG AGC AAG GGC GAG GAG CTG TTC ACC GGG GTG GTG CCC ATC
CTG GTC GAG CTG GAC GGC GAC GTA AAC GGC C**A**T AAG TTC AGC GTG
TCC GGC GAG GGC GAG GGC GAT GCC ACC TAC GGC AAG CTG ACC CTG
AAG TTC ATC TGC ACC ACC GGC AAG CTG CCC GTG CCC TGG CCC ACC
CTC GTG ACC ACC TTG ACC TAC GGC GTG CAG TGC TTC GCC CGC TAC
CCC GAC C**A**T ATG AAG CAG CAC GAC TTC TTC AAG TCC GCC ATG CCC
GAA GGC TAC GTC CAG GAG CGC ACC ATC TTC TTC AAG GAC GAC GGC
AAC T**A**T AAG ACC CGC GCC GAG GTG AAG TTC GAG GGC G**A**T ACC CTG
GTG AAC CGC ATC GAG CTG AAG GGC ATC GAC TTC AAG GAG GAC GGC
A**A**T ATC CTG GGG C**A**T AAG CTG GAG T**A**T AAC T**A**T **AA**T AGC C**A**T AAG
GTC TAT ATC ACC GCC G**A**T AAG CAG AAG AAC GGC ATC AAG GTG AAC
TTC AAG ACC CGC C**A**T **AA**T ATC GAG GAC GGC AGC GTG CAG CTC GCC
GAC CAC TAC CAG CAG A**A**T ACC CCC ATC GGC GAC GGC CCC GTG CTG
CTG CCC G**A**T AAC CAC TAC CTG AGC ACC CAG TCC GCC CTG AGC AAA
GAC CCC AAC GAG AAG CGC GAT C**A**T ATG GTC CTG CTG GAG TTC GTG
ACC GCC GCC GGG ATC ACT CTC GGC ATG GAC GAG CTG T**A**T AAG TAA

To study the lmRNA translation under a given stress condition, I designed four different types of 5'-UTRs preceding the *em-gfp* coding region. As positive control served

a construct with an ACA-free canonical 5'-UTR including a strong SD sequence ("can", Figure II.3.1A). This mRNA should not be affected by stress conditions and the *em-gfp* reporter should be constitutively translated under relaxed conditions. A negative control is an *em-gfp* construct with a strong stem loop structure closely upstream of the AUG start codon ("ΔTIR" – no translation initiation region, Figure II.3.1D). This structural feature is expected to sterically hinder ribosomes to initiate translation of this *em-gfp* reporter mRNA. The leaderless *em-gfp* reporter has no 5'-UTR at all, starting directly with the start codon AUG ("ll" - leaderless, Figure II.3.1C). The last construct serves as an indicator for MazF cleavage and subsequent translation of the resulting leaderless *em-gfp* mRNA. It is constructed like the negative control reporter (ΔTIR) with an inhibiting stem loop structure, however, it contains with an ACA cleavage site directly upstream of the start codon AUG ("cll" – conditional leaderless, Figure II.3.1B). This reporter mRNA should be translated only upon MazF cleavage at this particular ACA-site. Figure II.3.1 gives a graphical overview over the constructed reporters and Table II.3.1 shows the corresponding nucleotide sequences.

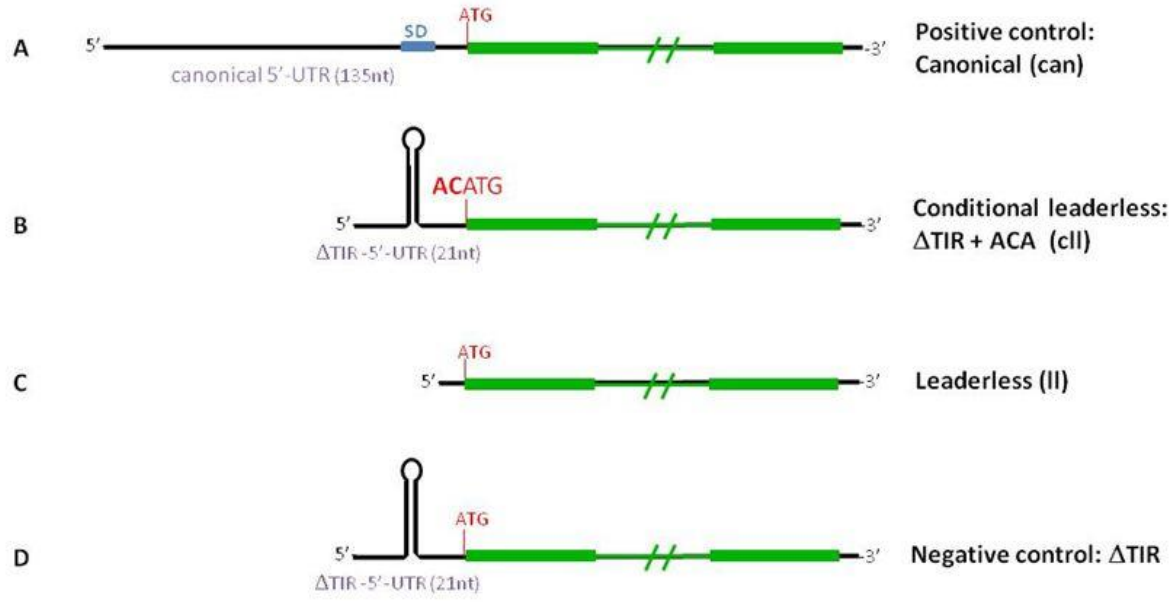

Figure II.3.1: GFP reporter constructs for detection MazF-dependent selective lmRNA translation

These constructs were cloned into the high-copy vector pUH-C, providing a strong lac promoter and a terminator sequence. Additionally, the entire cassettes, comprising the promoter region, reporter genes and the terminator were cloned into the low-copy vector pACYC177. A summary of the plasmids and cloning procedures can be found in 'Material and Methods'.

construct	5'-UTR sequence
can	TTGACTTGTGAGCGGATAACAATGATACTTAGATTCAGAATTCTCGCCAG GGGTGCTCGGCATAAGCCGAAGATATCGGTAGAGTTAATATTGAGCAGA TCCCCCGGTGAAGGATTTAACCGTGTTATCTCGTTGGAGATATTCATGGC GTATTTTGGATCCTAACGAGGCGCAAAAA**ATG**
cII	TTGACTTGTGAGCGGATAACAATGATACTTAGATTCAAGAATTCGGCCGC AGCGGCCAA**ACA**TG
II	TTGACTTGTGAGCGGATAACAATGATACTTAGATTC**ATG**
ΔTIR	TTGACTTGTGAGCGGATAACAATGATACTTAGATTCAAGAATTCGGCCGC AGCGGCCAAAA**ATG**

Table II.3.1: Nucleotide sequences of the 5'-UTRs of the respective *em-gfp* reporters. The AUG start codon of *em-gfp* is shown in bold, the lac promoter region, derived from pUH-C, is indicated in gray. In the canonical reporter is the SD sequence indicated in red. The stem loop structures in the conditional leaderless and the ΔTIR reporters are underlined and the ACA site in the conditional leaderless reporter is highlighted in bold red.

II.3.2. Results

II.3.2.a) Verification of MazF cleavage

To initially verify that the conditional leaderless *em-gfp* reporter mRNA is cleaved by MazF *in vivo*, total RNA was extracted from *E. coli* MC4100 *relA+* carrying plasmids pACYC177 harboring the four reporters, in the case of cII and ΔTIR also in combination with pBAD-*mazF* for arabinose (Ara)-inducible *mazF* overexpression, with and without 30 minutes of induction. 10 µg of the extracted total RNA was used for primer extension analysis using the reverse primer IM_Z10, annealing at nucleotides 60-76 of *em-gfp.* As controls primer extension analysis on *in vitro* transcribed canonical (from PCR product IM_X10/N9) and leaderless *em-gfp* (from PCR product IM_Y10/N9) RNAs was likewise performed.

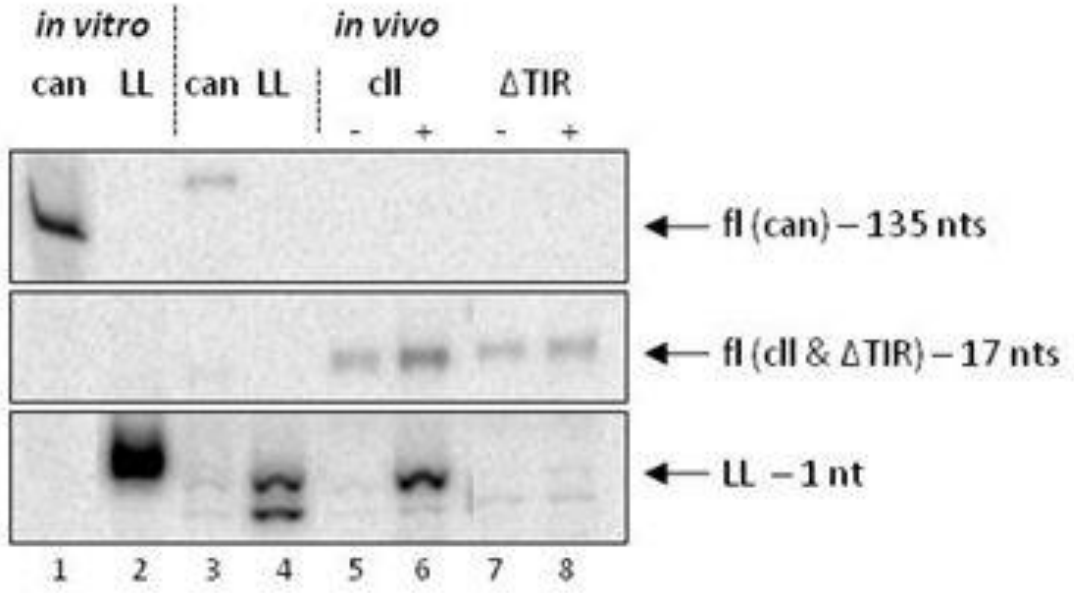

Figure II.3.2: Primer extension analysis of *em-gfp* mRNAs. Total RNA for analysis was extracted after *em-gfp* expression in MC4100 *relA*$^{+}$ from pAYCY177 and –for the cII and ΔTIR reporters- in combination with or without *mazF* overexpression driven from pBAD-*mazF* by induction with 0,4% Ara.

The results shown in Figure II.3.2 unambiguously reveal the cleavage of the conditional leaderless *em-gfp* mRNA at position -1 after *mazF* overexpression (lane 6). The ΔTIR construct is not cleaved at that position and only the signal indicating the 5'-terminal end is detectable (lane 8).

II.3.2.b) Analysis of fluorescent EmGFP signals

A measure for translation efficiency is the fluorescent signal of EmGFP. As detection of fluorescence directly in the medium proofed to be inaccurate due to auto-fluorescence of the LB medium, cell lysates were subjected to native polyacrylamide gel electrophoresis (PAGE) and the fluorescence of GFP bands in the gel was determined. As a loading control these gels were subsequently transferred to nitrocellulose membranes and the levels of RP S2, which should be constant during all conditions, were detected by immuno staining.

First, we established the detection of EmGFP fluorescent signals after native PAGE. In Figure II.3.3 lysates from MC4100 *relA*$^+$ cells carrying the low copy plasmid pACYC177 with the four EmGFP reporters were loaded in comparative amounts on native polyacrylamide (PAA) gels. The cultures with the cII and ΔTIR constructs additionally harbored the plasmid pBAD-*mazF.* Over expression of *mazF* was induced by addition of 0,4% Ara for 30 minutes.

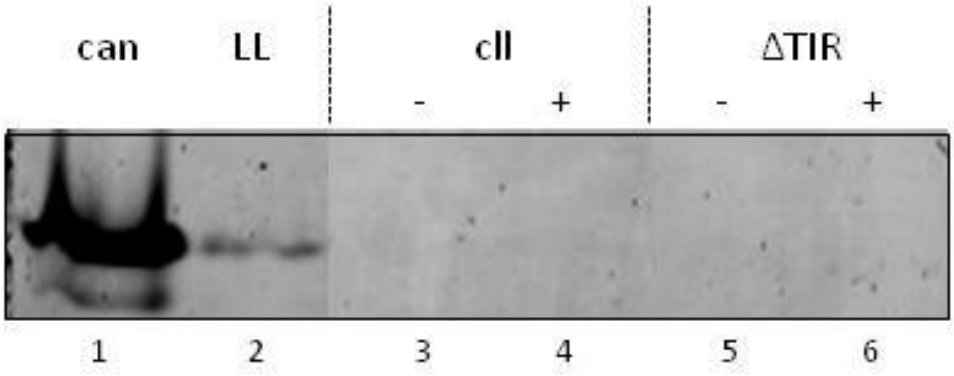

Figure II.3.3: Fluorescent scan of EmGFP reporter variants. Cell lysates from MC4100 *relA*$^+$ with *em-gfp* expression from pAYCY177 and –for the cII and ΔTIR reporters- in combination with or without *mazF* overexpression driven from pBAD-*mazF* by induction with 0,4% Ara on native PAA gel. 0,05 OD_{600}-units of cell lysates were loaded for each sample.

As shown in Figure II.3.3 the canonical *em-gfp* reporter yields a very intense signal (lane 1), whereas the signal obtained by using the leaderless *em-gfp* reporter is ten times weaker (lane 2). This reflects the relatively poor efficiency of translation of lmRNAs under normal conditions. No signals were detected for the conditional leaderless and the ΔTIR reporters, neither under normal conditions (lanes 3 and 5) nor after *mazF* overexpression (lanes 4 and 6). Furthermore, in subsequent experiments the detection of the cII reporter was never possible under any condition tested. Thus we hypothezised that expression from the low copy vector pACYC177 is not sufficient. Therefore, we continued the experiments with the constructs encoded on the high copy vector pUH-C and subsequent optimization additionally revealed that strain MG1655 was more suitable for the experiments.

Finally, we analyzed EmGFP fluorescent signal intensities upon expression of the cII and II reporter from plasmid pUH-C in strain MG1655 in dependence of *mazF* overexpression, stationary growth phase or growth in minimal medium (M9). Figure II.3.4A shows the growth of MG1655 harboring pUH-C_cII (red) or _II (blue) in LB with (triangles) or without (circles) induction of *mazF* overexpression from pBAD-*mazF* by addition of 0,5% Ara during exponential growth at OD_{600} 0,4 to 0,5. *mazF* overexpression induces equal inhibition of growth in both strains. Samples for cell lysis were taken before and 1, 2, 4 and 6 hours after induction from induced as well as from uninduced cultures. In Figure II.3.4B fluorescent scans and subsequently performed western blot analyses on native PAA gels are shown. The results reveal that translation of the cII-*em-gfp* is only induced after four to six hours *mazF* overexpression (lanes 8 and 9). Translation of the II reporter seems to be induced by entry into stationary growth phase (lanes 13 and 14) and even more pronounced upon four to six hours after induction of *mazF* overexpression (lanes 17 and 18).

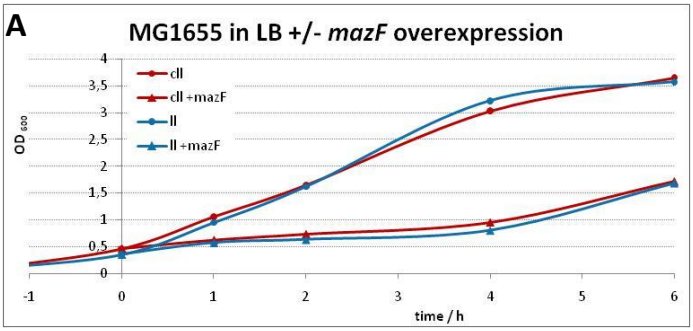

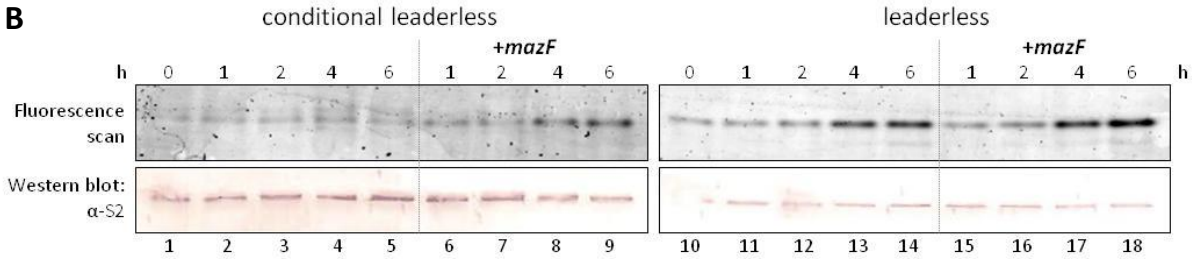

Figure II.3.4: A) Growth of MG1655 pUH-C_cII (red) or _II (blue) in LB with (triangles) or without (circles) induction of *mazF* overexpression from pBAD-*mazF* by addition of 0,5% Ara during exponential growth at OD_{600} 0,4 to 0,5. B) Fluorescent scans and western blot analyses with α-S2 antibodies of cell lysates from samples taken from A) on native PAA gels.

Similarly, the same strains were cultured until mid-exponential growth phase (OD_{600} of about 0,5) and shifted to M9 minimal medium. Growth analysis shown in Figure II.3.5A indicate the decelerated growth of both cultures in M9 (triangles). Considering the EmGFP levels in Figure II.3.5B it seems that translation of the cII reporter is slightly induced after four to six hours upon *mazF* overexpression (lanes 8 and 9) and translation of the II reporter is again induced by entry into stationary growth phase (lanes 13 and 14) and even stronger upon four to six hours after *mazF* overexpression (lanes 17 and 18).

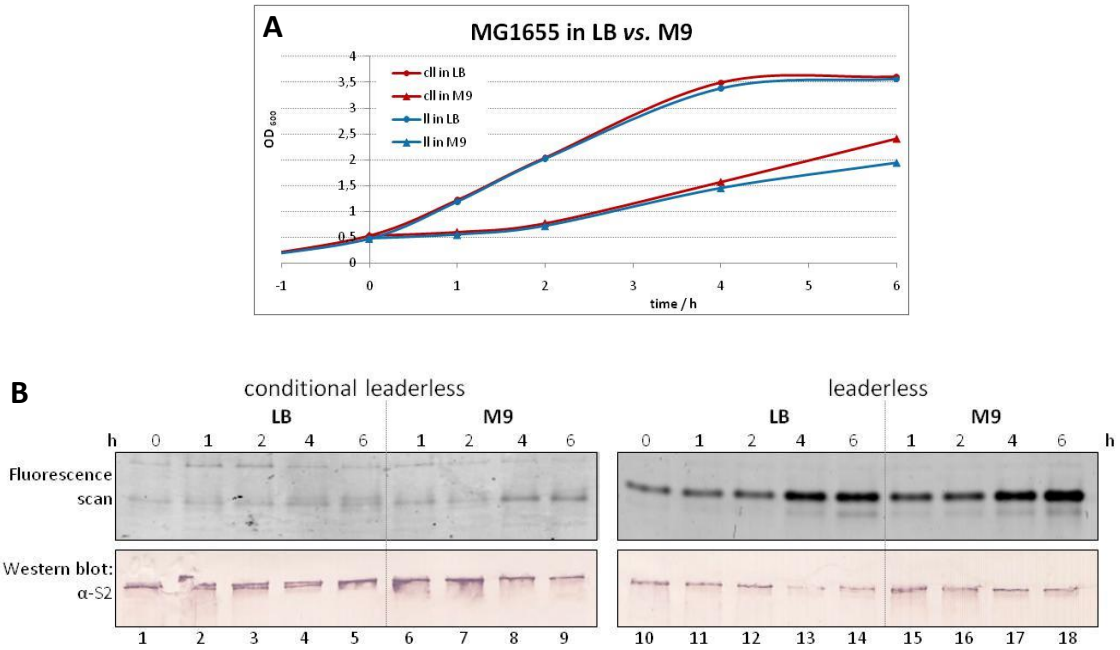

Figure II.3.5: A) Growth of MG1655 pUH-C_cII (red) or _II (blue) in LB (triangles) or upon shift to M9 at OD_{600} 0,5 (circles). **B**) Fluorescent scans and western blot analyses using α-S2 antibodies of cell lysates from samples taken from A) on native PAA gels.

The elevated ll-EmGFP levels upon entry into stationary growth phase, *mazF* overexpression or shift to M9 were well reproducible and very promising. However, performing similar experiments with a *mazF* deletion strain we observed the same increased EmGFP levels at late time points Figure II.3.6B, lanes 13 and 14) or upon slight stress induction by addition very low concentrations (1 µg/ml) of the translation blocking antibiotic chloramphenicol (Cam) (lanes 18 and 19). In a *mazF* deletion strain we would not expect such result. However, further studies in the lab revealed that additional TA systems might play similar roles as *mazEF*. For instance, we observed that overexpression of the *mazF*-related toxin gene *chpB* leads to a depletion of RPs S6 and S18 which could comprise an alternative way to stimulate lmRNA translation (Vesper et al. unpublished data).

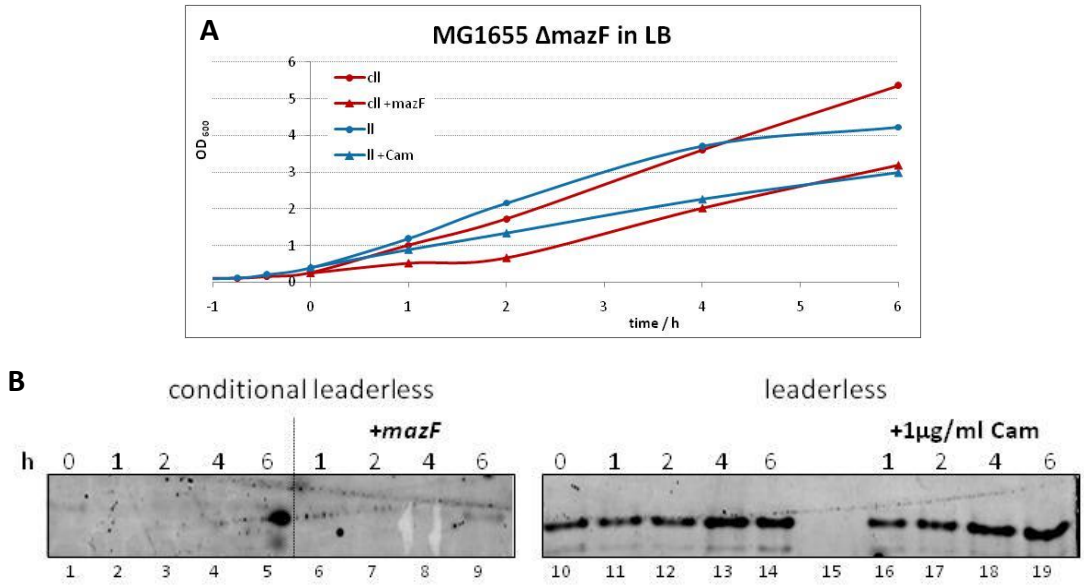

Figure II.3.6: A) Growth of MG1655 Δ*mazF* pUH-C_cll (red) in LB with (triangles) or without (circles) induction of *mazF* overexpression from pBAD-*mazF* by addition of 0,5% Ara during exponential growth at OD_{600} 0,4 to 0,5 and MG1655 Δ*mazF* pUH-C_ll (blue) with (triangles) or without (circles) addition of 1 µg/ml chloramphenicol (Cam). **B**) Fluorescent scans of cell lysates from samples separated on native PAA gels in A).

Moreover, expression of cll-*em-gfp* in combination with *mazF* overexpression from pBAD-*mazF* in a *mazF* deletion strain hardly yielded any fluorescence signal for EmGFP (figure xxx, lanes 1 to 9). In general, detection of the cll-EmGFP proved to be very difficult due to generally very low fluorescence signals and detection limits. Taken together, the use of the cll-*em-gfp* construct as a reporter for MazF-mediated selective translation of leaderless mRNAs is very limited and for that reason not suitable for screening purposes. Nevertheless, the ACA-free EmGFP constructs are still in use for single cell studies currently performed in the lab.

II.4. Heterogeneity of the translational machinery: Variations on a common theme.

Review

Martina Sauert[1], Hannes Temmel[1], and Isabella Moll

[1] equal contribution

Biochimie. 2014 Dec 24. pii: S0300-9084(14)00395-2. doi: 10.1016/j.biochi.2014.12.011

Contribution of the publication to the overall thesis

This review collects evidence for heterogeneity in the translational machinery throughout all organisms. The broad variation in the composition of the ribosome and modifications of translation factors in response to environmental signals is highlighted. This level of adaptation and specialization leads to the immediate implementation of environmental information.

Author's contribution

Martina Sauert contributed Figure 1 and Figure 2 was obtained in collaboration with Hannes Temmel. The paragraphs 'Introduction', 'Translation in pro- and eukaryotes', 'Heterogeneity of the translation machinery', 'Heterogeneity of translation factors', 'Heterogeneity of tRNAs' and 'Extra-translational functions of ribosomal proteins and translation factors' were written by Martina Sauert. Further, Martina Sauert contributed ideas discussion and revisions for entire manuscript.

ARTICLE IN PRESS

Biochimie xxx (2014) 1–9

Contents lists available at ScienceDirect

Biochimie

journal homepage: www.elsevier.com/locate/biochi

Review

Heterogeneity of the translational machinery: Variations on a common theme

Martina Sauert [1], Hannes Temmel [1], Isabella Moll*

Department of Microbiology, Immunobiology and Genetics, Max F. Perutz Laboratories, Centre for Molecular Biology, University of Vienna, Dr. Bohrgasse 9/4, 1030 Vienna, Austria

ARTICLE INFO

Article history:
Received 1 October 2014
Accepted 16 December 2014
Available online xxx

Keywords:
Protein synthesis
Ribosome heterogeneity
Gene expression regulation
Translation regulation
Stress response

ABSTRACT

In all organisms the universal process of protein synthesis is performed by the ribosome, a complex multi-component assembly composed of RNA and protein elements. Although ribosome heterogeneity was observed already more than 40 years ago, the ribosome is still traditionally viewed as an unchangeable entity that has to be equipped with all ribosomal components and translation factors in order to precisely accomplish all steps in protein synthesis. In the recent years this concept was challenged by several studies highlighting a broad variation in the composition of the translational machinery in response to environmental signals, which leads to its adaptation and functional specialization. Here, we summarize recent reports on the variability of the protein synthesis apparatus in diverse organisms and discuss the multiple mechanisms and possibilities that can lead to functional ribosome heterogeneity. Collectively, these results indicate that all cells are equipped with a remarkable toolbox to fine tune gene expression at the level of translation and emphasize the physiological importance of ribosome heterogeneity for the immediate implementation of environmental information.

1. Introduction

According to the central dogma of molecular biology, in all living cells the genetic information is stored at the level of DNA and transcribed into messenger RNA (mRNA), which subsequently serves as a template for the translation of the encoded information into the amino acid sequence of proteins. This latter step is performed by the ribosome, a sophisticated cellular machinery composed of RNA and protein elements. In order to allow all organisms to respond and adapt protein synthesis to environmental cues, the coordinated regulation of gene expression is crucial to ensure the establishment of a productive metabolic network. Hitherto, the main scientific focus in the regulation of gene expression has been directed on the alteration of the transcriptional program. Thus, the role of adjustment at the translational level has been underestimated. However, in the past decades, this perception changed dramatically and it became widely accepted that mRNA levels do not necessarily correspond to the amount of proteins being made. Together, these observations implicate a profound regulation at the post-transcriptional level, which has mostly been attributed to features intrinsic to the mRNA or a variety of non-ribosomal protein and RNA factors that modulate diverse steps in protein synthesis like small RNAs, mRNA binding proteins, and *cis*- or *trans*-acting regulators [1,2]. However, still it was generally believed that the assembly of all ribosomal components is required and mandatory for the process of protein synthesis.

In striking contrast to this perception, in the recent years several lines of evidence strongly underpin the notion that the ribosome as well as genuine translation factors are likewise key players in post-transcriptional regulation. In this review we will focus on the intrinsic alteration of the translational program by the formation of distinct ribosomal subpopulations that differ in their protein or RNA complement, or which are equipped with differentially modified translation factors. Collectively, these results strongly underline the great potential of the translational machinery to serve as a hub for signal integration at the post-transcriptional level in a variety of different organisms.

2. Translation in pro- and eukaryotes

The ribosome is a highly conserved molecular machinery. In all organisms it is composed of two unequal subunits, which consist of

* Corresponding author. Tel.: +43 1 4277 54606; fax: +43 1 4277 9546.
E-mail address: Isabella.Moll@univie.ac.at (I. Moll).
[1] Equal contribution.

http://dx.doi.org/10.1016/j.biochi.2014.12.011
0300-9084/

Please cite this article in press as: M. Sauert, et al., Heterogeneity of the translational machinery: Variations on a common theme, Biochimie (2014), http://dx.doi.org/10.1016/j.biochi.2014.12.011

a distinct set of ribosomal RNA (rRNA) and ribosomal protein (RP) components and perform a specific function during translation, as outlined below. The ribosome harbors three different tRNA binding sites: The A-site, where decoding occurs and the correct aminoacyl-tRNA (aa-tRNA) is selected on the basis of the mRNA codon displayed, the P-site, which carries the peptidyl-tRNA, and the E-site, which binds exclusively deacetylated tRNAs that are exiting the ribosome [3]. Thus, during translation the tRNA moves from the A-site through the P- and E-site, where it leaves the ribosome [4]. Conceptionally, the complexity of the ribosome structure is reflected in the process of protein synthesis, which can be intersected into three major steps: initiation, elongation and termination/recycling.

In prokaryotic translation initiation, the small ribosomal (30S) subunit binds the mRNA *via* direct interaction between the anti-Shine-Dalgarno (aSD) sequence located at the 3′-terminus of the 16S rRNA and the Shine-Dalgarno (SD) sequence in the 5′-untranslated region (5′-UTR) closely upstream of the start codon of the mRNA. The initiator tRNA fMet-tRNA^{fMet} (tRNAi) is recruited by initiation factor 2 (IF2) to the ribosomal P-site where it interacts with the start codon, thus forming the 30S pre-initiation complex (PIC). The accuracy of the codon–anticodon recognition is controlled by IF3, while IF1 stimulates the activity of IF2. Subsequently, the large (50S) ribosomal subunit joins the PIC to result in the 70S initiation complex (IC) [5]. Interestingly, the exact chronological order of the PIC assembly is still a matter of debate and seems not to be strictly determined.

Contrary, eukaryotic translation initiation is mediated primarily *via* protein–protein interactions. First, the tRNAi is recruited to the small ribosomal subunit (40S) to form a ternary complex (TC) with the GTP-bound eukaryotic initiation factor 2 (eIF2) [6]. Formation of this 43S pre-initiation complex (PIC) is strongly enhanced by additional factors, such as eIF3 [7]. In contrast to the bacterial translation initiation complex, which is assembled directly at internal ribosome binding sites, the 43S PIC generally binds to the capped 5′-end of a eukaryotic mRNA and scans along the transcript in 5′–3′-direction until it encounters a start codon [8]. After recognition of the start codon, the large ribosomal subunit (60S) assembles to form the 80S initiation complex, which is ready for elongation. The diverse phases are assisted by 12 eIFs and additional auxiliary factors [6,9]. Alternatively, under distinct conditions or on certain transcripts internal initiation can occur in a cap-independent manner at so called internal ribosome entry sites (IRES) [10].

The step of translation elongation is well conserved in pro- and eukaryotes [11]. The aa-tRNA is recruited to the ribosome by elongation factor Tu (EF-Tu) in prokaryotes, or the ortholog eEF1A in eukaryotes. Subsequently, the growing peptide chain is transferred to the newly bound aa-tRNA in the peptidyl-transferase center (PTC) that is exclusively formed by rRNA of the large subunit. Then the ribosome translocates one codon downstream on the mRNA assisted by the orthologs EF-G and eEF2 in prokaryotes and eukaryotes, respectively [12,13]. When the elongating ribosome encounters a stop codon in its A-site, termination and recycling are initiated. In bacteria, either release factor 1 (RF1) or RF2 recognizes the stop codon and triggers hydrolysis of the ester-bond in the peptidyl-tRNA situated in the P-site resulting in the release of the synthesized polypeptide chain from the ribosome. Next, RF3 stimulates the rapid dissociation of RF1 or RF2 from the ribosome [14]. In eukaryotes the structurally different proteins eRF1 and eRF3 trigger these reactions [15]. The two subunits and the mRNA of the post-termination complex are then disassembled with the help of the ribosome recycling factor (RRF) together with IF3 in prokaryotes. In eukaryotes, where no such factor exists, the recycling process is more complex and involves the ATPase ABCE1 [16].

3. Heterogeneity of the translation machinery

As translation initiation is the rate-limiting step in protein synthesis, it is therefore the predominant target for regulation. As mentioned above, hitherto translational regulation was attributed to *cis*- and *trans*-acting non-ribosomal RNA and protein factors, which modulate the accessibility of the SD-sequence for the SD-aSD interaction in prokaryotes [17]. In eukaryotes, protein- or micro RNA (miRNA)-mediated translation regulation is more commonly involving the 3′-UTRs of mRNAs [9]. Additionally, mRNA structures like the 5′-cap, the 3′-poly(A)-tail, IRESs and upstream open reading frames (uORFs) play crucial roles in eukaryotic translation regulation [18].

In contrast to these regulatory mechanisms mediated by extra-ribosomal factors, in this review we will summarize and discuss the current scientific understanding concerning the functional heterogeneity of the translational apparatus, a concept that is considered to represent an accessory layer of gene expression regulation. We aim to emphasize that the translation machinery, built of the ribosome itself but also involving the essential factors that assist in the translation process, is not an inevitably unchangeable entity. In the recent years, a paradigm shift has taken place with increasing evidence that the ribosome is not one determined complex, but that its components can be altered resulting in translational fine-tuning to follow changing cellular needs.

Ribosome heterogeneity has been observed already in the 1970s, where ribosomes purified from bacteria grown under different conditions were shown to lack certain RPs without losing their translational functions [19–21]. However, these observations have been neglected for a long time and the term 'ribosome heterogeneity' has not been established in the scientific community (Fig. 1). Over the years, many studies performed in eukaryotes presented evidence that ribosomes can vary in their protein and rRNA complement between different cell types and developmental states. These observations culminated in the postulation of the 'ribosome filter hypothesis' by Mauro and Edelman in the year 2002 [22]. The authors propose that the ribosome composition functions as translation determination factor. Depending on the RPs and rRNA sequences represented in the respective ribosome, the complex acts like a filter that selects for specific mRNAs and hence modulates translation [22,23]. A few years later, the Silver lab reported that different RP paralogs are functionally distinct and contribute to translational selectivity in *Saccharomyces cerevisiae* [24], which led to the proposal of the 'ribosome code', analogous to

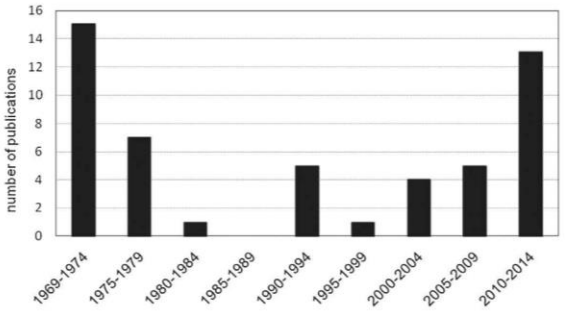

Fig. 1. Scientific publications addressing 'ribosome heterogeneity' since 1969. The graph depicts that despite being already observed more than 40 years ago, ribosome heterogeneity as a means to regulate translation was not a scientific subject till the dawn of the new millennium.

Please cite this article in press as: M. Sauert, et al., Heterogeneity of the translational machinery: Variations on a common theme, Biochimie (2014), http://dx.doi.org/10.1016/j.biochi.2014.12.011

the 'histone code' that affects transcription. Subsequently, this theory that goes in line with the ribosome filter hypothesis was extended to the formation of specialized ribosomes *via* the incorporation of different forms or modifications of rRNA, or by post-translational modifications of RPs that allow regulated translation of specific mRNAs.

In the following chapters we aim to give a brief update on the recent progress in understanding functional heterogeneity of the translational machinery. Due to its complex nature there are different routes for potential modifications: on the ribosome itself, affecting either the rRNA or the RPs; *via* alteration of translation factors; or *via* modification of tRNAs (Fig. 2). Moreover, all components of the translation machinery can additionally have ancillary functions in non-translational processes.

3.1. Variation in the ribosomal protein complement

3.1.1. Stoichiometry of ribosomal proteins on the ribosome

The simplest way to modify a multi-subunit assembly is to alter the relative abundance of its individual components. Since the rRNA molecules are functionally indispensable for the active translation machinery, the RPs pose the sole ribosomal building blocks whose abundance on the complex can possibly be adapted. One mechanism to alter the RP complement is the differential expression of the respective genes. Previously, it was accepted that ribosomal proteins are produced in a coordinated manner to ensure that each ribosome contains a full complement of all components, which was considered to be mandatory for correct protein synthesis. However, this assumption was challenged by multiple observations that under distinct conditions as well as in diverse cell types some RPs are present in substoichiometric amounts on the ribosomes [21,25,26], indicative for an alteration of the translational activity and specificity by a heterogeneous RP complement. This notion is supported by the observed replacement of damaged RPs on *Escherichia coli* ribosomes that results in the repair of the multicomponent complex [27]. This phenomenon points towards the possibility to specifically re-equip the heterogeneous protein-depleted ribosomes.

In prokaryotes, the ribosomal protein complement was shown to differ with respect to the encountered environmental conditions or the growth phase [19–21,26,28]. Furthermore, antibiotic treatment can be added to the list of factors modifying the RP complement. In *E. coli*, the ribosome targeting antibiotic Kasugamycin was shown to mediate the formation of a specific ribosomal subclass, the so-called 61S ribosomes that lack the RPs S1, S2, S6, S12, S18, and S21 [29]. Due to the lack of protein S1 that is essential for translation initiation on canonical mRNAs [30] but is dispensable for translation of leaderless mRNAs (lmRNAs) harboring a 5′-terminal start codon [31], the 61S ribosomes are likewise selective for lmRNAs [29]. These findings tempted us to formulate a hypothesis that the presence or absence of a specific RP can modulate the translatome. In this context, the specific translation initiation on lmRNAs by a ribosomal subpopulation lacking protein S1 might pose a significant contribution to the post-transcriptional regulation in bacteria. This concept is further supported by findings that suggest the presence of ribosomes lacking S1 even under relaxed growth conditions [32]. Moreover, the relatively small boundary between protein S1 and the ribosome, which was recently determined at atomic resolution [33], opens the potential to modulate the affinity of protein S1 for the ribosome by post-translational protein modification.

A heterogeneous RP content as a means to remodel the translatome is not limited to prokaryotes. Already in the 1980s, work performed in *Dictyostelium discoideum* suggested that different sets of RPs assembled to the ribosome result in an alteration of the translational specificity [25]. This study indicates that the protein complement of ribosomes from vegetative amoeboid cells substantially differs when compared to the RPs present on ribosomes derived from spores. Besides the developmental stage, cell type dependent variations in the synthesis of several RPs have been

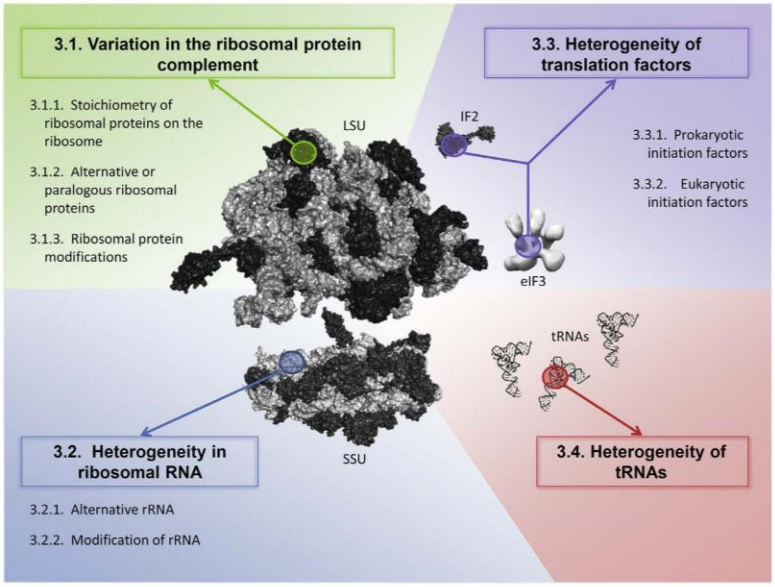

Fig. 2. Components of the translation machinery that have the potential to contribute to functional heterogeneity. Structures were visualized with Polyview 3D software [125] using the following maps: *E. coli* large ribosomal subunit (LSU; pdb accession code: 3d5a [126], rRNA in light gray, proteins in dark gray); small ribosomal subunit (SSU; pdb accession code: 3d5b [126]); *E. coli* IF2 (pdb accession code: 1g7r [127]); human eIF3 (EMD-2166 [128]); yeast $tRNA^{Phe}$ (pdb accession code: 6tna [129]).

reported in six different human tissues and several regions of the mouse embryo [34,35], which might likewise affect the composition of the ribosome. However, analyses of a selection of RNA sequencing data obtained from various organisms with a major focus on mammalian tissues and cell lines showed that the molar ratios of 80%–90% of RP transcripts vary less than threefold with little tissue specificity [36]. These results suggest that a post-transcriptional mechanism is required for the regulation of the expression of RP-coding genes either affecting mRNA translation or stability.

Nevertheless, several studies underline the presence of this regulatory pathway in eukaryotes, exemplified by the observation that overexpression of the *parkin* gene in a human cell line leads to a specific decrease in abundance of protein RPSA [37]. The observed down-regulation of RPSA in response to *parkin* gene expression may explain Parkin's proposed tumor suppressor activity, since RPSA was implicated in being enriched in cancer tissues and is considered to promote tumor progression *via* an unknown mechanism [38,39]. Along the same lines, the expression of the oncogene *v-erbA* in chicken erythrocytic progenitor cells was shown to affect the transcription of specific RP encoding genes and hence results in the formation of heterogeneous ribosomes that lack RPL11 [40]. Interestingly, proteomic analysis revealed that consequently the abundance of nine proteins was altered, suggesting that the modulation of the ribosome composition results in an alteration of the translatome. Moreover, it has been shown that in contrast to bulk mRNA translation the vesicular stomatitis virus specific cap-dependent translation requires RpL40 [41]. This study again exemplifies that the absence of certain RPs can have a very specific impact on translational properties. Collectively, the functional specialization of ribosomes by the alteration of their protein complement can be found in all domains of life. However, it is important to note that some results require a careful interpretation as they are based on the analysis of whole cell protein content, which does not necessarily reflect the actual ribosome composition and may neglect the fraction of free RPs. This is particularly relevant since described phenotypes can be likewise attributed to extra-ribosomal functions of RPs, which were reviewed in detail by Warner and McIntosh [42].

3.1.2. Alternative or paralogous ribosomal proteins

Several studies describing ribosome heterogeneity discuss the model of employing alternative RPs. This hypothesis is strengthened by the fact that many different prokaryotes and eukaryotes harbor multiple paralogs of RP coding genes [24,43,44], which are synthesized simultaneously or in response to certain environmental conditions [44]. In the Gram-positive soil bacterium *Bacillus subtilis* for example, the genes encoding ribosomal proteins L31 and S14 are duplicated, and the respective RP paralogs differ in the presence of a zinc-binding motif [45]. The authors hypothesize that incorporation of the protein variants into the ribosome is zinc-dependent. During zinc limitation, the zinc-bound variant is functionally replaced by the zinc-independent paralog. However, since hitherto no alteration of the translational specificity was described upon protein exchange, this mechanism could solely contribute to zinc storage and its mobilization under zinc-limiting conditions.

In yeast approximately 70% of all duplicated RP genes are asymmetrically expressed [44], potentially implying that the paralogous proteins are not merely functionally equivalent substitutes. Komili and co-workers underscored this hypothesis by reporting that the translation of localized mRNAs in *S. cerevisiae* is affected in a paralog-specific manner [24]. Besides, the analysis of cells lacking specific RP paralogs indicated functional differences between the paralogs that extend beyond mRNA localization [24]. Alongside, diploid yeast strains deficient in one or the other copy of RP genes, harbored distinct populations of specialized ribosomes with individual translational properties [46]. Interestingly, in *S. cerevisiae*, the ribosomal stalk protein paralogs P1a, P1b, P2a and P2b, form two heterodimers that preferentially bind to sites A and B of the P0 protein, respectively [47]. Each of the four possible P1/P2 combinations results in a specific phenotype indicating that they perform non-identical physiological roles. Moreover, the absence of one heterodimer reduced cell growth and hindered the synthesis of the 60S ribosomal subunit [47].

An exceptional example for the presence of RP paralogs are plants. In *Arabidopsis thaliana*, each ribosomal protein is encoded by two to seven genes [48], and recently 429 genes coding for potential RPs have been identified [49]. Many paralogs display sequence variations and are differentially expressed during development [50,51]. In addition, nearly half of the RPs identified in a proteomic approach are represented by two or more distinct spots in 2D gel analyses indicating different protein isoforms that are post-translationally modified [52]. In the same model organism, Zsögön and co-workers report that the levels of the two RPL27a paralogs with redundant function, RPL27aC and RPL27aB, influence the ovule development [53]. The reduction of the expression levels of one or the other has a distinct effect on fertility revealing a function of RPL27a in the coordination of ovule development.

Most genes coding for ribosomal proteins in mammals are represented in a single copy, with a few exceptions like RPS4 [54] or RPL39l [55], which was found to be highly expressed in differentiating mouse embryonic stem cells. Interestingly, the enrichment of RPL39l has been observed likewise in human hepatocellular carcinoma tumor (HCC) cells and cancer cell lines with high tumor grading and alpha-fetoprotein levels [55]. Moreover, the expression pattern of all RPs and their paralogs in mouse was tested across 22 different tissues indicating a high level of tissue-specific expression [55]. This finding goes in line with a proteomic survey of ribosomes in *Mus musculus*, revealing the testis-specific synthesis of the proteins RPL10-like and RPL39-like [56], which are paralogs of the X-linked ribosomal proteins RPL10 and RPL39, respectively. The same laboratory recently identified a new paralog of X-linked RPS4 [57]. They show that the autosomal, intronless gene was expressed predominantly in testis similar to RPL10-like and RPL39-like. However, in contrast to the paralog RPL10-like, the RPS4 paralog shows a partially different expression pattern in spermatogenic cells [57].

3.1.3. Ribosomal protein modifications

An alternative mechanism to alter the properties of the translational machinery is the modification of ribosomal components incorporated in the mature and active ribosome. Considering the energy demanding processes of *de novo* synthesis and assembly of alternative RPs to ribosomes, this mechanism might constitute a direct and energy effective option of adaptation.

In prokaryotes, comparative proteome analysis revealed the differential acetylation and phosphorylation of several RPs in the exponential or stationary growth phase [58,59]. Interestingly, the interaction of proteins L7/L12 with the ribosome is likewise affected by a growth phase dependent acetylation [60]. During stationary phase or growth in minimal medium the N-terminal acetylated protein L7 is the predominant form on the ribosome, resulting in stabilization of the ribosomal stalk complex during adverse conditions. Together, these findings strongly underscore the idea that protein modification might provide a powerful mechanism to fine tune protein synthesis. Nevertheless, no direct functional specialization has been attributed to RP modification in bacteria so far.

Correspondingly, methylation, acetylation, and hydroxylation of RPs were observed in yeast [61]. Some of these substitutions were

Please cite this article in press as: M. Sauert, et al., Heterogeneity of the translational machinery: Variations on a common theme, Biochimie (2014), http://dx.doi.org/10.1016/j.biochi.2014.12.011

found to appear in a growth phase dependent manner, for example the proteins RPS1B and RPS2 [62]. Interestingly, the dimethylation of protein RPS2 plays an additional role in processing and nuclear export of rRNA [63], and the hydroxylation of protein RPS23 was shown to affect translational accuracy in a stop codon context-dependent manner and determines the viability as a consequence of nonsense codon suppression under certain conditions [64]. Another example for ribosome heterogeneity based on RP modification was described by Ramagopal already in 1991, when differential ribosomal protein phosphorylation and methylation patterns were identified in ribosomes from different phases of the *D. discoideum* lifecycle [65]. This modulation is considered to facilitate the unique translational needs of the cell during the respective life phase.

Again, an exceptional high number of modifications in RPs was determined in plants. In *A. thaliana*, 23 of the 80 RP families were shown to contain at least one covalent modification that represent potential differential modification sites [66]. Moreover, UV-B exposure and the associated ribosome damage was described to lead to an increase of *de novo* synthesis of some RPs and phosphorylation of RPS6 and an S6 kinase in *Zea mays* leaves [67]. A similar response to UV-B light exposure was described for mammalian cells [68], making it tempting to envisage that ribosome damage induces a feedback-loop, which favors RP mRNA translation for *de novo* ribosome biogenesis in order to replace damaged ribosomes. This hypothesis is strengthened by recent observations that the expression of genes encoding mitoribosomal proteins in *A. thaliana* respond to the silencing of the mitochondrial gene encoding protein RPL10 [69]. This specific gene silencing leads to the formation of unstable small ribosomal subunits and consequently to a misbalance between the ribosomal subunits. Notably, these misregulated ribosomes display a translational selectivity as they preferentially translate mRNAs coding for mitochondrial RPs.

3.2. Heterogeneity in the rRNA

3.2.1. Alternative rRNA

The concept, that incorporation of alternative rRNA molecules into ribosomes might change the specificity of the translational machinery in response to external signals, was strengthened by the presence of multiple rRNA gene (*rrn*) copies in the genomes of a variety of organisms in all domains of life. The *Streptomyces coelicolor* genome harbors for example six copies of divergent large subunit (LSU) rRNA genes that constitute five LSU rRNA species in a cell, which are differentially transcribed during the morphological development [70]. Similarly, *B. subtilis* harbors ten *rrn* operons and their reduction to one copy increased the doubling time as well as the sporulation frequency and the motility [71]. Notably, mutants that carried different combinations of two *rrn* operons revealed a wide range of growth rates and sporulation frequencies, indicating distinct functional roles for all *rrn* operons.

An alternative mechanism for the adaptation of the translational machinery to environmental conditions has been shown for the halophilic archaeon *Haloarcula marismortui*, which harbors three rRNA operons [72]. Here, the *rrnB* operon, which is GC-rich in contrast to the *rrnA* and *rrnC* operons, is selectively transcribed at high temperatures. By this means, heat-stable ribosomes are generated during temperature stress. However, no specific functional differences can be attributed to the presence of the specific rRNA variants.

The parasite *Plasmodium berghei* has two structurally distinct genes that code for cytoplasmatic small subunit (SSU) rRNAs [73]. The expression of one rRNA gene was almost exclusively found when living in the mosquito host, while the alternative transcript arises when the parasite infects the mammalian host, becoming the predominant SSU rRNA species. Interestingly, no structural differences between the ribosomes containing one or the other rRNA were detected and parasites lacking the mosquito specific rRNA gene were able to complete their development in both hosts, declining the hypothesis of functionally distinct ribosome subspecies and rather indicating a dose dependent role for the prevalence of two distinct rRNA genes [74]. Similarly, the sea urchin *Paracentrotus lividus* harbors three different 5S rRNA clusters, the transcription of which leads to several 5S rRNA variants that are incorporated in functional ribosomes resulting in a high heterogeneity in animal ribosomes [75].

3.2.2. Modification of rRNA

The rRNA is heavily modified in particular at functionally relevant positions, mainly by 2-hydroxyl methylation and the conversion of uridine to pseudouridine [76]. In general, these modifications occur during rRNA maturation in the process of riboneogenesis, and are considered as check points during ribosome assembly. In eukaryotes, the modifications are facilitated by snoRNAs and their tissue specific expression might be a source for ribosome specialization [77]. Recently, a new method was established to determine pseudouridinylated positions in RNA using next generation sequencing that allows to test whether specific sites in rRNA are differently modified in response to environmental cues representing translational adaptation [78,79]. Nevertheless, Yoon and co-workers already showed that altering the pseudouridylation-state of rRNA affects translation and moreover, that reduced rRNA pseudouridylation led to a pathological syndrome and deficiencies in IRES-dependent translation [80]. However, the next generation sequencing based methodology allows to globally identify functional heterogeneity mediated by alternative pseudouridylation.

In contrast to the above mentioned modifications that occur during assembly, an intriguing mechanism of rRNA processing occurs on already translationally active ribosomes in *E. coli* [81]. When *E. coli* cells encounter stress conditions, the endoribonuclease MazF, the toxin component of the toxin–antitoxin module *mazEF*, becomes activated [82]. Subsequently, MazF targets the 16S rRNA within 30S ribosomal subunits at the decoding center, thereby removing the 3′-terminal 43 nucleotides [81]. As this region comprises the aSD sequence that is required for translation initiation on canonical mRNAs, a subpopulation of ribosomes is engendered that selectively translates lmRNAs both *in vivo* and *in vitro*. Concomitantly, MazF generates lmRNAs by removing the 5′-UTRs of distinct transcripts. Collectively, the translational program is remodeled in response to stressful conditions [81].

Considering that rRNA interacts with a variety of different proteins, it is obvious that rRNA modifications have the potential to modulate the respective affinities and consequently alter ribosomal properties. The erythromycin resistance methyltransferases (Erm), for example, dimethylate nucleotide A2058 in the LSU rRNA [83,84]. Despite conferring resistance to macrolide antibiotics, this modification reduces cell fitness, as it mediates abnormal interactions of the nascent peptide with the modified rRNA in the peptide exit tunnel. These findings depict the two-edged nature of this ribosome modification and explain the necessity why *erm* genes have evolved to be inducible [83].

In *S. cerevisiae*, a variation in ribose methylation was described within the 18S rRNA. 32% of molecules incorporated in ribosomes are not methylated at 2′-O-ribose of the A100 residue, however, both 40S ribosomal subunits, with and without A_m100, participate in translation [85]. A different study showed a more severe impact of the lack of an rRNA modification. Ribosomes isolated from a yeast strain, which harbors a catalytically impaired rRNA pseudouridine synthase, display decreased affinities for tRNAs as well as for the

Please cite this article in press as: M. Sauert, et al., Heterogeneity of the translational machinery: Variations on a common theme, Biochimie (2014), http://dx.doi.org/10.1016/j.biochi.2014.12.011

cricket paralysis virus IRES [86]. In general, these ribosomes reveal a decreased translational fidelity and IRES-dependent translational initiation [86].

3.3. Heterogeneity of translation factors

As protein synthesis is assisted by several genuine translation factors, it is obvious to envision regulatory mechanisms by virtue of modified translation factors. In this chapter we want to summarize and discuss heterogeneity within translation factors and their possible impacts on translation regulation.

3.3.1. Prokaryotic initiation factors

In bacteria, there is ample evidence that the ratio between the individual IFs and the ribosomes play crucial roles in selective translation of certain mRNAs. This mechanism was described in *E. coli* by Giuliodori and co-workers [87]. The authors observed the preferential translation of distinct mRNAs that encode proteins important for cold-shock and cold-tolerance under cold-shock conditions. Their results further indicate that this selectivity can be attributed to a stoichiometric imbalance of the IF to ribosome ratio, contradicting the dogma of equimolar ratios between ribosome and IFs by Howe and Hershey [88]. Interestingly, increased amounts of IF3, together with IF1, preferentially stimulate translation of cold-shock mRNAs [87]. Alternatively, IF2, which recruits the tRNAi to the PIC, has been shown to selectively stimulate translation initiation on lmRNAs [89]. This result clearly suggests that recognition of the 5′-terminally AUG start codon *via* codon–anticodon interaction is crucial for translation initiation on lmRNAs. In contrast, IF3 appears to antagonize start codon selection on lmRNAs by destabilizing the translation initiation complex assembled at the 5′-end of the transcript [90]. These results were confirmed in a subsequent study indicating that the ratio between IF2 and IF3 is crucial for efficient translation initiation on 5′-terminal AUG start codons of lmRNAs in *E. coli* [91]. Together, these studies exemplify that alterations of the IF stoichiometry have the potential to affect the selectivity of the translational machinery in bacteria resulting in the preferred translation of a subset of mRNAs.

3.3.2. Eukaryotic initiation factors

The alteration of the translational specificity by means of variation or modification of translation factors is a well-established mechanism in eukaryotes. For example the stress-induced phosphorylation of the α-subunit of eIF2, which recruits the tRNAi to the 40S ribosome, leads to a general inhibition of translation [92]. However, in hepatitis C virus (HCV) infections, an alternative tRNAi-binding protein, eIF2A, has been reported to guide translation initiation to HCV IRES sites [93]. By this means the viral mRNA is selectively translated and overcomes the general translation inhibition by eIF2α phosphorylation during stress induced by the virus infection itself. Interestingly, eIF2A seems likewise to be involved in translation initiation with elongator tRNAs as shown for Leu-tRNA initiation on CUG-start codons [94]. This mechanism has been exemplified by Liang and co-workers, who have shown the synthesis of an N-terminal elongated variant of the human tumor suppressor PTEN, by translation initiation at an upstream and in-frame CUG-start codon [95]. Another alternative eIF2 initiation factor, namely eIF2D, acts in a GTP-independent manner and guides translation initiation to unconventional mRNAs like HCV IRES or lmRNAs [96]. Employing an alternative initiation mechanism, eIF2D recruits tRNAi to the 40S ribosome after the AUG start codon has been positioned at the P-site. Collectively, eIF2 and its alternatives appear to add another regulatory level to translation initiation, as the choice of the one or the other variant guides initiation towards different classes of mRNAs. This mechanism appears to be conceptionally similar to the regulation of transcription, where the use of alternative sigma factors guides the RNA polymerase to another set of promoters upon encountering external stimuli.

eIF3 is the largest initiation factor, consisting of 13 different subunits in mammals, of which only 6 build the functional core complex [97]. It generally plays a regulatory role in translation initiation as it stimulates the formation of the TC and the 43S PIC. eIF3 is also involved in cap-independent translation initiation as on IRES-mediated initiation of protein synthesis. The diverse roles of eIF3 might in part be explained by its heterogeneous composition. Already in the 1970s, researchers have described heterogeneity in association of eIF3 to the ribosomes in rat liver homogenates [98]. The results suggested that eIF3 was preferentially bound to newly synthesized 40S ribosomes, but not to recycled ribosomes. However, eIF3 is not only involved in the association of the TC eIF2-GTP-tRNAi to the 40S ribosome, but acts likewise as a ribosome-dissociation factor after termination and hinders re-association of the free 40S and 60S subunits [99,100]. Kolupaeva and co-workers have proposed that the ability of eIF3 to bind the 40S subunit and to prevent its re-association with 60S subunits is dependent on the presence of the subunit eIF3j in mammals [101]. As observed more recently in a mammalian cell line, the subunit eIF3a shows oscillating levels within the cell cycle and appears to be a translational regulator for the S-phase entrance [102]. The subunits eIF3e and eIF3g have been reported to associate with translational regulators like p56 or poly(A)-binding proteins, respectively, thereby stimulating or inhibiting translation initiation [103,104]. For other eIF3 subunits a role in cancer cells was suggested. The mRNA levels encoding the subunits eIF3a, -b, -c, -h, and -I are increased in a wide variety of human tumors and moreover, their overexpression was shown to induce oncogenic malignancy [105]. In contrast, eIF3f seems to have tumor suppressive activity by affecting cap-dependent and cap-independent translation initiation [106]. In addition, the factor is involved in translation inhibition during apoptosis ([107] and references therein). Intriguingly, eIF3 also is remarkably heterogeneous in terms of localization: nuclear eIF3 has a different subunit composition than cytosolic eIF3, which is lacking the subunits eIF3a and -f [108]. The authors suggest that the cytosolic eIF3f is phosphorylated during apoptosis, which results in a stronger association of eIF3f to the eIF3 core complex leading to translation inhibition. The pro-apoptotic function of eIF3f seems furthermore to be regulated by direct interaction with the anti-apoptotic factor Mss4 [109]. Thus, eIF3 is an intriguing example for regulation of protein synthesis mediated by modified translation factors, as induced heterogeneity of a single IF can adapt the translational program to a vast variety of conditions.

3.4. Heterogeneity of tRNAs

During translation, tRNAs act as the adaptor molecules in decoding of the base triplets on the mRNA into the corresponding amino acids. But their role is not merely mechanistical and – although highly conserved – they show remarkable structural diversity amongst species [110]. In the recent years, it has been shown that tRNAs do not only exist in their aminoacylated or uncharged full length form, but also short fragments of tRNAs or tRNA halves have been observed (reviewed in Ref. [111]). The stress-induced 5′-tRNA halves inhibit translation in mammalian cells by interfering with initiation factors eIF4E/G/A [112], and tRNA fragments can bind to the ribosome and inhibit translation as it was shown for the archaeon *Haloferax volcanii* [113].

However, in correspondence to genes encoding RPs, there are also several copies for tRNA genes. The *E. coli* genome encodes four copies for the tRNAi. Samhita and co-workers found that one of these genes (*metY*) appeared to be dispensable [114]. However, in

Please cite this article in press as: M. Sauert, et al., Heterogeneity of the translational machinery: Variations on a common theme, Biochimie (2014), http://dx.doi.org/10.1016/j.biochi.2014.12.011

nutrient-rich conditions the presence of all four genes is advantageous over only three. On the other hand, the lack of one tRNAi-gene has been shown to be beneficial during nutrient-deprived conditions and during long-term growth [114]. These findings strongly imply that different variants of tRNAi are used for translation initiation under different environmental conditions. It is important to note that ribosomes derived from an *E. coli* strain lacking three tRNAi genes (*metZVW*) are slightly depleted of ribosomal protein S1 [115], which is required for translation initiation on canonical mRNAs [30,116]. Also higher eukaryotes harbor multiple tRNA gene copies coding for so-called isodecoders, different tRNA-bodies with the same anti-codon. The function of these isodecoders appears not to be redundant as loss of one particular tRNA ($tRNA^{Arg}UCU$) cannot be compensated by its isodecoders in mice [117].

Several lines of evidence indicate that tRNAs can also be targeted by bacterial stress-dependent toxins. VapC is an endoribonuclease of the toxin–antitoxin system *vapBC*. Upon activation it cleaves the tRNAi at the anticodon stem-loop thus resulting in the inhibition of translation [118]. Besides, VapC activation stimulates translation initiation on elongation codons of the *dksA* mRNA, however, the underling mechanism still remains elusive. Taken together, these findings indicate an alternative mechanism of stress-induced adaptation of the translational program by tRNA intrinsic variations.

3.5. Extra-translational functions of ribosomal proteins and translation factors

As mentioned above, heterogeneous expression of RPs can result in the formation of specialized ribosomes, and has been observed in prokaryotes and eukaryotes in dependence of growth conditions and cell type [34,119]. Considering the extra-ribosomal functions of several RPs (summarized in Ref. [42]) and translation factors, one is tempted to speculate that these extra-ribosomal functions could likewise represent a means to reduce the amount of RPs or factors available for the translational machinery. For example, the largest RP present in Gram-negative bacteria, namely protein S1, is, besides its important mRNA-binding function in translation initiation, a subunit of the RNA-directed RNA polymerase of the bacteriophage Qβ [120]. In this context, S1 plays a role in the termination of the polymerase reaction. Moreover, the mammalian RPS3 acts additionally as an endonuclease and can become part of the nuclear NFκB complex, thereby interfering with transcription regulation (reviewed in Ref. [42]).

Likewise, translation factors have been implicated with non-translational functions, like eIF3f, which has been proposed to create a link between translation and RNA degradation during stress [106]. During apoptosis, eIF3f might interact with heterogeneous nuclear ribonucleoprotein K blocking its RNA protective function. Additionally, eIF3f possesses a de-ubiquitinase activity by itself, which links it to Notch signaling pathways [121] and moreover, it seems to be a regulatory factor in the balance between muscle atrophy and hypertrophy [122]. Another factor involved in several extra-ribosomal functions is eEF1A, which besides the delivery of aa-tRNAs to the ribosomal A-site is responsible for non-canonical processes like quality control of newly synthesized proteins, apoptosis, and viral propagation [123]. Moreover, it was shown recently that a methylated version of eEF1A is required for nodavirus RNA replication in yeast [124]. Taken together, these results add significant weight to the audacious hypothesis that extra-translational functions could withdraw RPs or translation factors from the translational machinery and thus result in an adjustment of translation.

4. The multifaceted translational machinery: a perspective

In light of the increasing evidence, ribosome heterogeneity, though still far from being entirely understood, proves to be an integral mechanism to modulate and fine tune protein synthesis in response to environmental signals in all organisms. Considering the time and energy consuming steps of the transcriptional stress response mechanisms, which involve the synthesis of alternative sigma factors followed by the selective transcription and translation of regulatory factors, it is conceivable that the strategies summarized here provide a novel 'fast-track reaction' for the cell to cope with the immediate changes in external conditions. Thus, the alteration of the transcriptional program would constitute the second level of stress response required for the mid- and long-term adjustment of the metabolic network.

Despite the multitude of examples for ribosome heterogeneity available, there is still ample need for further studies to gain comprehensive insights into the functional reprogramming of the translational machinery. Nevertheless, the above mentioned studies dramatically object the long-cherished tenet that the ribosome is the unchangeable operating unit of protein synthesis and strongly favor the conception that multifaceted ribosomes represent a central hub for signal integration in cellular physiology.

Conflict of interest

The authors declare no conflict of interest.

Acknowledgments

The authors would like to thank all colleagues and past and present members of the Moll group who contributed to our studies on ribosome heterogeneity. The work was supported by grants W1207-B09, P20112-B03, P22249-B20, F4316-B09, P26946-B20, and P27043-B20 from the Austrian Science Fund to I.M.

References

[1] T. Glisovic, J.L. Bachorik, J. Yong, G. Dreyfuss, RNA-binding proteins and post-transcriptional gene regulation, FEBS Lett. 582 (2008) 1977–1986.
[2] S. Kuersten, A. Radek, C. Vogel, L.O. Penalva, Translation regulation gets its 'omics' moment, Wiley Interdiscip. Rev. RNA 4 (2013) 617–630.
[3] N. Burkhardt, R. Junemann, C.M. Spahn, K.H. Nierhaus, Ribosomal tRNA binding sites: three-site models of translation, Crit. Rev. Biochem. Mol. Biol. 33 (1998) 95–149.
[4] B.S. Laursen, H.P. Sorensen, K.K. Mortensen, H.U. Sperling-Petersen, Initiation of protein synthesis in bacteria, Microbiol. Mol. Biol. Rev. 69 (2005) 101–123.
[5] A. Simonetti, S. Marzi, L. Jenner, A. Myasnikov, P. Romby, et al., A structural view of translation initiation in bacteria, Cell. Mol. Life Sci. 66 (2009) 423–436.
[6] A.G. Hinnebusch, J.R. Lorsch, The mechanism of eukaryotic translation initiation: new insights and challenges, Cold Spring Harb. Perspect. Biol. 4 (2012).
[7] T.V. Pestova, V.G. Kolupaeva, The roles of individual eukaryotic translation initiation factors in ribosomal scanning and initiation codon selection, Genes Dev. 16 (2002) 2906–2922.
[8] I.B. Lomakin, T.A. Steitz, The initiation of mammalian protein synthesis and mRNA scanning mechanism, Nature 500 (2013) 307–311.
[9] R.J. Jackson, C.U. Hellen, T.V. Pestova, The mechanism of eukaryotic translation initiation and principles of its regulation, Nat. Rev. Mol. Cell Biol. 11 (2010) 113–127.
[10] S.K. Jang, Internal initiation: IRES elements of picornaviruses and hepatitis c virus, Virus Res. 119 (2006) 2–15.
[11] M.V. Rodnina, W. Wintermeyer, Recent mechanistic insights into eukaryotic ribosomes, Curr. Opin. Cell Biol. 21 (2009) 435–443.
[12] T.E. Dever, R. Green, The elongation, termination, and recycling phases of translation in eukaryotes, Cold Spring Harb. Perspect. Biol. 4 (2012) a013706.
[13] X. Agirrezabala, J. Frank, Elongation in translation as a dynamic interaction among the ribosome, tRNA, and elongation factors EF-G and EF-Tu, Q. Rev. Biophys. 42 (2009) 159–200.
[14] A.V. Zavialov, R.H. Buckingham, M. Ehrenberg, A posttermination ribosomal complex is the guanine nucleotide exchange factor for peptide release factor RF3, Cell 107 (2001) 115–124.

Please cite this article in press as: M. Sauert, et al., Heterogeneity of the translational machinery: Variations on a common theme, Biochimie (2014), http://dx.doi.org/10.1016/j.biochi.2014.12.011

[15] A.A. Korostelev, Structural aspects of translation termination on the ribosome, RNA 17 (2011) 1409–1421.
[16] E. Nurenberg, R. Tampe, Tying up loose ends: ribosome recycling in eukaryotes and archaea, Trends Biochem. Sci. 38 (2013) 64–74.
[17] P. Romby, M. Springer, Bacterial translational control at atomic resolution, Trends Genet. TIG 19 (2003) 155–161.
[18] F. Gebauer, M.W. Hentze, Molecular mechanisms of translational control, Nat. Rev. Mol. Cell Biol. 5 (2004) 827–835.
[19] J. Van Duin, C.G. Kurland, Functional heterogeneity of the 30S ribosomal subunit of *E. coli*, Mol. Gen. Genet. 109 (1970) 169–176.
[20] C.G. Kurland, P. Voynow, S.J. Hardy, L. Randall, L. Lutter, Physical and functional heterogeneity of E. coli ribosomes, Cold Spring Harb. Symp. Quant. Biol. 34 (1969) 17–24.
[21] E. Deusser, Heterogeneity of ribosomal populations in *Escherichia coli* cells grown in different media, Mol. Gen. Genet. 119 (1972) 249–258.
[22] V.P. Mauro, G.M. Edelman, The ribosome filter hypothesis, Proc. Natl. Acad. Sci. U. S. A. 99 (2002) 12031–12036.
[23] V.P. Mauro, G.M. Edelman, The ribosome filter redux, Cell Cycle 6 (2007) 2246–2251.
[24] S. Komili, N.G. Farny, F.P. Roth, P.A. Silver, Functional specificity among ribosomal proteins regulates gene expression, Cell 131 (2007) 557–571.
[25] S. Ramagopal, H.L. Ennis, Regulation of synthesis of cell-specific ribosomal proteins during differentiation of Dictyostelium discoideum, Proc. Natl. Acad. Sci. U. S. A. 78 (1981) 3083–3087.
[26] E. Deusser, H.G. Wittmann, Ribosomal proteins: variation of the protein composition in Escherichia coli ribosomes as function of growth rate, Nature 238 (1972) 269–270.
[27] A. Pulk, A. Liiv, L. Peil, U. Maivali, K. Nierhaus, et al., Ribosome reactivation by replacement of damaged proteins, Mol. Microbiol. 75 (2010) 801–814.
[28] T.A. Bickle, G.A. Howard, R.R. Traut, Ribosome heterogenecity. The nonuniform distribution of specific ribosomal proteins among different functional classes of ribosomes, J. Biol. Chem. 248 (1973) 4862–4864.
[29] A.C. Kaberdina, W. Szaflarski, K.H. Nierhaus, I. Moll, An unexpected type of ribosomes induced by kasugamycin: a look into ancestral times of protein synthesis? Mol. Cell 33 (2009) 227–236.
[30] M.A. Sorensen, J. Fricke, S. Pedersen, Ribosomal protein S1 is required for translation of most, if not all, natural mRNAs in *Escherichia coli in vivo*, J. Mol. Biol. 280 (1998) 561–569.
[31] I. Moll, A. Resch, U. Blasi, Discrimination of 5′-terminal start codons by translation initiation factor 3 is mediated by ribosomal protein S1, FEBS Lett. 436 (1998) 213–217.
[32] F. Delvillani, G. Papiani, G. Deho, F. Briani, S1 ribosomal protein and the interplay between translation and mRNA decay, Nucleic Acids Res. 39 (2011) 7702–7715.
[33] K. Byrgazov, I. Grishkovskaya, S. Arenz, N. Coudevylle, H. Temmel, D.N. Wilson, K. Djinovic-Carugo, I. Moll, Structural basis for the flexible interaction of protein S1 with the *Escherichia coli* ribosome, Nucleic Acids Res. (2014), http://dx.doi.org/10.1093/nar/gku1314.
[34] S. Bortoluzzi, F. d'Alessi, C. Romualdi, G.A. Danieli, Differential expression of genes coding for ribosomal proteins in different human tissues, Bioinformatics 17 (2001) 1152–1157.
[35] N. Kondrashov, A. Pusic, C.R. Stumpf, K. Shimizu, A.C. Hsieh, et al., Ribosome-mediated specificity in Hox mRNA translation and vertebrate tissue patterning, Cell 145 (2011) 383–397.
[36] V. Gupta, J.R. Warner, Ribosome-omics of the human ribosome, RNA 20 (2014) 1004–1013.
[37] D.G. Song, Y.S. Kim, B.C. Jung, K.J. Rhee, C.H. Pan, Parkin induces upregulation of 40S ribosomal protein SA and posttranslational modification of cytokeratins 8 and 18 in human cervical cancer cells, Appl. Biochem. Biotechnol. 171 (2013) 1630–1638.
[38] J. Nelson, N.V. McFerran, G. Pivato, E. Chambers, C. Doherty, et al., The 67 kDa laminin receptor: structure, function and role in disease, Biosci. Rep. 28 (2008) 33–48.
[39] D. Li, J. Chen, Z. Gao, X. Li, X. Yan, et al., 67-kDa laminin receptor in human bile duct carcinoma, Eur. Surg. Res. 42 (2009) 168–173.
[40] A.T. Nguyen-Lefebvre, G. Leprun, V. Morin, J. Vinuelas, Y. Coute, et al., V-erbA generates ribosomes devoid of RPL11 and regulates translational activity in avian erythroid progenitors, Oncogene 33 (2014) 1581–1589.
[41] A.S. Lee, R. Burdeinick-Kerr, S.P. Whelan, A ribosome-specialized translation initiation pathway is required for cap-dependent translation of vesicular stomatitis virus mRNAs, Proc. Natl. Acad. Sci. U. S. A. 110 (2013) 324–329.
[42] J.R. Warner, K.B. McIntosh, How common are extraribosomal functions of ribosomal proteins? Mol. Cell 34 (2009) 3–11.
[43] M. Kellis, B.W. Birren, E.S. Lander, Proof and evolutionary analysis of ancient genome duplication in the yeast Saccharomyces cerevisiae, Nature 428 (2004) 617–624.
[44] J. Parenteau, M. Durand, G. Morin, J. Gagnon, J.F. Lucier, et al., Introns within ribosomal protein genes regulate the production and function of yeast ribosomes, Cell 147 (2011) 320–331.
[45] Y. Natori, H. Nanamiya, G. Akanuma, S. Kosono, T. Kudo, et al., A fail-safe system for the ribosome under zinc-limiting conditions in *Bacillus subtilis*, Mol. Microbiol. 63 (2007) 294–307.
[46] J.W. Bauer, C. Brandl, O. Haubenreisser, B. Wimmer, M. Weber, et al., Specialized yeast ribosomes: a customized tool for selective mRNA translation, PLoS One 8 (2013) e67609.
[47] D. Cardenas, J. Revuelta-Cervantes, A. Jimenez-Diaz, H. Camargo, M. Remacha, et al., P1 and P2 protein heterodimer binding to the P0 protein of Saccharomyces cerevisiae is relatively non-specific and a source of ribosomal heterogeneity, Nucleic Acids Res. 40 (2012) 4520–4529.
[48] A. Barakat, K. Szick-Miranda, I.F. Chang, R. Guyot, G. Blanc, et al., The organization of cytoplasmic ribosomal protein genes in the Arabidopsis genome, Plant Physiol. 127 (2001) 398–415.
[49] R. Sormani, C. Masclaux-Daubresse, F. Daniel-Vedele, F. Chardon, Transcriptional regulation of ribosome components are determined by stress according to cellular compartments in Arabidopsis thaliana, PLoS One 6 (2011) e28070.
[50] M.L. Falcone Ferreyra, A. Pezza, J. Biarc, A.L. Burlingame, P. Casati, Plant L10 ribosomal proteins have different roles during development and translation under ultraviolet-B stress, Plant Physiol. 153 (2010) 1878–1894.
[51] D. Weijers, M. Franke-van Dijk, R.J. Vencken, A. Quint, P. Hooykaas, et al., An Arabidopsis minute-like phenotype caused by a semi-dominant mutation in a RIBOSOMAL PROTEIN S5 gene, Development 128 (2001) 4289–4299.
[52] P. Giavalisco, D. Wilson, T. Kreitler, H. Lehrach, J. Klose, et al., High heterogeneity within the ribosomal proteins of the Arabidopsis thaliana 80S ribosome, Plant Mol. Biol. 57 (2005) 577–591.
[53] A. Zsogon, D. Szakonyi, X. Shi, M.E. Byrne, Ribosomal protein RPL27a promotes female gametophyte development in a dose-dependent manner, Plant Physiol. 165 (2014) 1133–1143.
[54] A.M. Lopes, R.N. Miguel, C.A. Sargent, P.J. Ellis, A. Amorim, et al., The human RPS4 paralogue on Yq11.223 encodes a structurally conserved ribosomal protein and is preferentially expressed during spermatogenesis, BMC Mol. Biol. 11 (2010) 33, http://dx.doi.org/10.1186/1471-2199-11-33.
[55] Q.W. Wong, J. Li, S.R. Ng, S.G. Lim, H. Yang, et al., RPL39L is an example of a recently evolved ribosomal protein paralog that shows highly specific tissue expression patterns and is upregulated in ESCs and HCC tumors, RNA Biol. 11 (2014) 33–41.
[56] Y. Sugihara, H. Honda, T. Iida, T. Morinaga, S. Hino, et al., Proteomic analysis of rodent ribosomes revealed heterogeneity including ribosomal proteins L10-like, L22-like 1, and L39-like, J. Proteome Res. 9 (2010) 1351–1366.
[57] Y. Sugihara, E. Sadohara, K. Yonezawa, M. Kugo, K. Oshima, et al., Identification and expression of an autosomal paralogue of ribosomal protein S4, X-linked, in mice: potential involvement of testis-specific ribosomal proteins in translation and spermatogenesis, Gene 521 (2013) 91–99.
[58] B. Macek, F. Gnad, B. Soufi, C. Kumar, J.V. Olsen, et al., Phosphoproteome analysis of *E. coli* reveals evolutionary conservation of bacterial Ser/Thr/Tyr phosphorylation, Mol. Cell. Proteomics 7 (2008) 299–307.
[59] B.J. Yu, J.A. Kim, J.H. Moon, S.E. Ryu, J.G. Pan, The diversity of lysine-acetylated proteins in *Escherichia coli*, J. Microbiol. Biotechnol. 18 (2008) 1529–1536.
[60] Y. Gordiyenko, S. Deroo, M. Zhou, H. Videler, C.V. Robinson, Acetylation of L12 increases interactions in the *Escherichia coli* ribosomal stalk complex, J. Mol. Biol. 380 (2008) 404–414.
[61] S.W. Lee, S.J. Berger, S. Martinovic, L. Pasa-Tolic, G.A. Anderson, et al., Direct mass spectrometric analysis of intact proteins of the yeast large ribosomal subunit using capillary LC/FTICR, Proc. Natl. Acad. Sci. U. S. A. 99 (2002) 5942–5947.
[62] D.T. Ladror, B.L. Frey, M. Scalf, M.E. Levenstein, J.M. Artymiuk, et al., Methylation of yeast ribosomal protein S2 is elevated during stationary phase growth conditions, Biochem. Biophys. Res. Commun. 445 (2014) 535–541.
[63] R.S. Lipson, K.J. Webb, S.G. Clarke, Rmt1 catalyzes zinc-finger independent arginine methylation of ribosomal protein Rps2 in Saccharomyces cerevisiae, Biochem. Biophys. Res. Commun. 391 (2010) 1658–1662.
[64] C. Loenarz, R. Sekirnik, A. Thalhammer, W. Ge, E. Spivakovsky, et al., Hydroxylation of the eukaryotic ribosomal decoding center affects translational accuracy, Proc. Natl. Acad. Sci. U. S. A. 111 (2014) 4019–4024.
[65] S. Ramagopal, Covalent modifications of ribosomal proteins in growing and aggregation-competent Dictyostelium discoideum: phosphorylation and methylation, Biochem. Cell Biol. 69 (1991) 263–268.
[66] A.J. Carroll, J.L. Heazlewood, J. Ito, A.H. Millar, Analysis of the Arabidopsis cytosolic ribosome proteome provides detailed insights into its components and their post-translational modification, Mol. Cell. Proteomics 7 (2008) 347–369.
[67] P. Casati, V. Walbot, Crosslinking of ribosomal proteins to RNA in maize ribosomes by UV-B and its effects on translation, Plant Physiol. 136 (2004) 3319–3332.
[68] P. Brenneisen, J. Wenk, M. Wlaschek, T. Krieg, K. Scharffetter-Kochanek, Activation of p70 ribosomal protein S6 kinase is an essential step in the DNA damage-dependent signaling pathway responsible for the ultraviolet B-mediated increase in interstitial collagenase (MMP-1) and stromelysin-1 (MMP-3) protein levels in human dermal fibroblasts, J. Biol. Chem. 275 (2000) 4336–4344.
[69] M. Kwasniak, P. Majewski, R. Skibior, A. Adamowicz, M. Czarna, et al., Silencing of the nuclear RPS10 gene encoding mitochondrial ribosomal protein alters translation in Arabidopsis mitochondria, Plant Cell 25 (2013) 1855–1867.
[70] H.L. Kim, W.S. Song, K. Kim, K. Lee, Characterization of heterogeneous LSU rRNA profiles in Streptomyces coelicolor under different growth stages and conditions, Curr. Microbiol. 57 (2008) 537–541.
[71] K. Yano, T. Wada, S. Suzuki, K. Tagami, T. Matsumoto, et al., Multiple rRNA operons are essential for efficient cell growth and sporulation as well as outgrowth in *Bacillus subtilis*, Microbiology 159 (2013) 2225–2236.

Please cite this article in press as: M. Sauert, et al., Heterogeneity of the translational machinery: Variations on a common theme, Biochimie (2014), http://dx.doi.org/10.1016/j.biochi.2014.12.011

[72] A. Lopez-Lopez, S. Benlloch, M. Bonfa, F. Rodriguez-Valera, A. Mira, Intragenomic 16S rDNA divergence in *Haloarcula marismortui* is an adaptation to different temperatures, J. Mol. Evol. 65 (2007) 687–696.

[73] J.H. Gunderson, M.L. Sogin, G. Wollett, M. Hollingdale, V.F. de la Cruz, et al., Structurally distinct, stage-specific ribosomes occur in Plasmodium, Science 238 (1987) 933–937.

[74] R.M. van Spaendonk, J. Ramesar, A. van Wigcheren, W. Eling, A.L. Beetsma, et al., Functional equivalence of structurally distinct ribosomes in the malaria parasite, *Plasmodium berghei*, J. Biol. Chem. 276 (2001) 22638–22647.

[75] E. Dimarco, E. Cascone, D. Bellavia, F. Caradonna, Functional variants of 5S rRNA in the ribosomes of common sea urchin Paracentrotus lividus, Gene 508 (2012) 21–25.

[76] W.A. Decatur, M.J. Fournier, rRNA modifications and ribosome function, Trends Biochem. Sci. 27 (2002) 344–351.

[77] J.C. Castle, C.D. Armour, M. Lower, D. Haynor, M. Biery, et al., Digital genome-wide ncRNA expression, including SnoRNAs, across 11 human tissues using polyA-neutral amplification, PLoS One 5 (2010) e11779.

[78] T.M. Carlile, M.F. Rojas-Duran, B. Zinshteyn, H. Shin, K.M. Bartoli, et al., Pseudouridine profiling reveals regulated mRNA pseudouridylation in yeast and human cells, Nature 515 (7525) (2014) 143–146, http://dx.doi.org/10.1038/nature13802.

[79] S. Schwartz, D.A. Bernstein, M.R. Mumbach, M. Jovanovic, R.H. Herbst, et al., Transcriptome-wide mapping reveals widespread dynamic-regulated pseudouridylation of ncRNA and mRNA, Cell 159 (2014) 148–162.

[80] A. Yoon, G. Peng, Y. Brandenburger, O. Zollo, W. Xu, et al., Impaired control of IRES-mediated translation in X-linked dyskeratosis congenita, Science 312 (2006) 902–906.

[81] O. Vesper, S. Amitai, M. Belitsky, K. Byrgazov, A.C. Kaberdina, et al., Selective translation of leaderless mRNAs by specialized ribosomes generated by MazF in *Escherichia coli*, Cell 147 (2011) 147–157.

[82] E. Aizenman, H. Engelberg-Kulka, G. Glaser, An *Escherichia coli* chromosomal "addiction module" regulated by guanosine [corrected] 3′,5′-bispyrophosphate: a model for programmed bacterial cell death, Proc. Natl. Acad. Sci. U. S. A. 93 (1996) 6059–6063.

[83] P. Gupta, S. Sothiselvam, N. Vazquez-Laslop, A.S. Mankin, Deregulation of translation due to post-transcriptional modification of rRNA explains why *erm* genes are inducible, Nat. Commun. 4 (2013) 1984.

[84] A.L. Starosta, V.V. Karpenko, A.V. Shishkina, A. Mikolajka, N.V. Sumbatyan, et al., Interplay between the ribosomal tunnel, nascent chain, and macrolides influences drug inhibition, Chem. Biol. 17 (2010) 504–514.

[85] M. Buchhaupt, S. Sharma, S. Kellner, S. Oswald, M. Paetzold, et al., Partial methylation at Am100 in 18S rRNA of baker's yeast reveals ribosome heterogeneity on the level of eukaryotic rRNA modification, PLoS One 9 (2014) e89640.

[86] K. Jack, C. Bellodi, D.M. Landry, R.O. Niederer, A. Meskauskas, et al., rRNA pseudouridylation defects affect ribosomal ligand binding and translational fidelity from yeast to human cells, Mol. Cell 44 (2011) 660–666.

[87] A.M. Giuliodori, A. Brandi, C.O. Gualerzi, C.L. Pon, Preferential translation of cold-shock mRNAs during cold adaptation, RNA 10 (2004) 265–276.

[88] J.G. Howe, J.W. Hershey, Initiation factor and ribosome levels are coordinately controlled in *Escherichia coli* growing at different rates, J. Biol. Chem. 258 (1983) 1954–1959.

[89] S. Grill, C.O. Gualerzi, P. Londei, U. Blasi, Selective stimulation of translation of leaderless mRNA by initiation factor 2: evolutionary implications for translation, EMBO J. 19 (2000) 4101–4110.

[90] K. Tedin, I. Moll, S. Grill, A. Resch, A. Graschopf, et al., Translation initiation factor 3 antagonizes authentic start codon selection on leaderless mRNAs, Mol. Microbiol. 31 (1999) 67–77.

[91] S. Grill, I. Moll, D. Hasenohrl, C.O. Gualerzi, U. Blasi, Modulation of ribosomal recruitment to 5′-terminal start codons by translation initiation factors IF2 and IF3, FEBS Lett. 495 (2001) 167–171.

[92] E. Schmitt, M. Naveau, Y. Mechulam, Eukaryotic and archaeal translation initiation factor 2: a heterotrimeric tRNA carrier, FEBS Lett. 584 (2010) 405–412.

[93] J.H. Kim, S.M. Park, J.H. Park, S.J. Keum, S.K. Jang, eIF2A mediates translation of hepatitis C viral mRNA under stress conditions, EMBO J. 30 (2011) 2454–2464.

[94] S.R. Starck, V. Jiang, M. Pavon-Eternod, S. Prasad, B. McCarthy, et al., Leucine-tRNA initiates at CUG start codons for protein synthesis and presentation by MHC class I, Science 336 (2012) 1719–1723.

[95] H. Liang, S. He, J. Yang, X. Jia, P. Wang, et al., PTENalpha, a PTEN isoform translated through alternative initiation, regulates mitochondrial function and energy metabolism, Cell Metab. 19 (2014) 836–848.

[96] S.E. Dmitriev, I.M. Terenin, D.E. Andreev, P.A. Ivanov, J.E. Dunaevsky, et al., GTP-independent tRNA delivery to the ribosomal P-site by a novel eukaryotic translation factor, J. Biol. Chem. 285 (2010) 26779–26787.

[97] M. Masutani, N. Sonenberg, S. Yokoyama, H. Imataka, Reconstitution reveals the functional core of mammalian eIF3, EMBO J. 26 (2007) 3373–3383.

[98] R.H. Hinton, B.M. Mullock, Differences between newly formed and recycled free small ribosome subunits in liver cytoplasm, Biochem. J. 158 (1976) 97–103.

[99] H. Trachsel, T. Staehelin, Initiation of mammalian protein synthesis. The multiple functions of the initiation factor eIF-3, Biochim. Biophys. Acta 565 (1979) 305–314.

[100] H.A. Thompson, I. Sadnik, J. Scheinbuks, K. Moldave, Studies on native ribosomal subunits from rat liver. Purification and characterization of a ribosome dissociation factor, Biochemistry 16 (1977) 2221–2230.

[101] V.G. Kolupaeva, A. Unbehaun, I.B. Lomakin, C.U. Hellen, T.V. Pestova, Binding of eukaryotic initiation factor 3 to ribosomal 40S subunits and its role in ribosomal dissociation and anti-association, RNA 11 (2005) 470–486.

[102] Z. Dong, Z. Liu, P. Cui, R. Pincheira, Y. Yang, et al., Role of eIF3a in regulating cell cycle progression, Exp. Cell Res. 315 (2009) 1889–1894.

[103] Y. Martineau, M.C. Derry, X. Wang, A. Yanagiya, J.J. Berlanga, et al., Poly(A)-binding protein-interacting protein 1 binds to eukaryotic translation initiation factor 3 to stimulate translation, Mol. Cell. Biol. 28 (2008) 6658–6667.

[104] J. Guo, D.J. Hui, W.C. Merrick, G.C. Sen, A new pathway of translational regulation mediated by eukaryotic initiation factor 3, EMBO J. 19 (2000) 6891–6899.

[105] L. Zhang, X. Pan, J.W. Hershey, Individual overexpression of five subunits of human translation initiation factor eIF3 promotes malignant transformation of immortal fibroblast cells, J. Biol. Chem. 282 (2007) 5790–5800.

[106] F. Wen, R. Zhou, A. Shen, A. Choi, D. Uribe, et al., The tumor suppressive role of eIF3f and its function in translation inhibition and rRNA degradation, PLoS One 7 (2012) e34194.

[107] R. Marchione, S.A. Leibovitch, J.L. Lenormand, The translational factor eIF3f: the ambivalent eIF3 subunit, Cell. Mol. Life Sci. 70 (2013) 3603–3616.

[108] J. Shi, J.W. Hershey, M.A. Nelson, Phosphorylation of the eukaryotic initiation factor 3f by cyclin-dependent kinase 11 during apoptosis, FEBS Lett. 583 (2009) 971–977.

[109] B.M. Walter, C. Nordhoff, G. Varga, G. Goncharenko, S.W. Schneider, et al., Mss4 protein is a regulator of stress response and apoptosis, Cell Death Dis. 3 (2012) e297.

[110] K. Fujishima, A. Kanai, tRNA gene diversity in the three domains of life, Front. Genet. 5 (2014) 142.

[111] J. Gebetsberger, N. Polacek, Slicing tRNAs to boost functional ncRNA diversity, RNA Biol. 10 (2013) 1798–1806.

[112] P. Ivanov, M.M. Emara, J. Villen, S.P. Gygi, P. Anderson, Angiogenin-induced tRNA fragments inhibit translation initiation, Mol. Cell 43 (2011) 613–623.

[113] J. Gebetsberger, M. Zywicki, A. Kunzi, N. Polacek, tRNA-derived fragments target the ribosome and function as regulatory non-coding RNA in *Haloferax volcanii*, Archaea 2012 (2012) 260909.

[114] L. Samhita, V. Nanjundiah, U. Varshney, How many initiator tRNA genes does *Escherichia coli* need? J. Bacteriol. 196 (2014) 2607–2615.

[115] L. Samhita, K. Virumae, J. Remme, U. Varshney, Initiation with elongator tRNAs, J. Bacteriol. 195 (2013) 4202–4209.

[116] K. Tedin, A. Resch, U. Blasi, Requirements for ribosomal protein S1 for translation initiation of mRNAs with and without a 5′ leader sequence, Mol. Microbiol. 25 (1997) 189–199.

[117] R. Ishimura, G. Nagy, I. Dotu, H. Zhou, X.L. Yang, et al., RNA function. Ribosome stalling induced by mutation of a CNS-specific tRNA causes neurodegeneration, Science 345 (2014) 455–459.

[118] K.S. Winther, K. Gerdes, Enteric virulence associated protein VapC inhibits translation by cleavage of initiator tRNA, Proc. Natl. Acad. Sci. U. S. A. 108 (2011) 7403–7407.

[119] A.N. Milne, W.W. Mak, J.T. Wong, Variation of ribosomal proteins with bacterial growth rate, J. Bacteriol. 122 (1975) 89–92.

[120] N.N. Vasilyev, Z.S. Kutlubaeva, V.I. Ugarov, H.V. Chetverina, A.B. Chetverin, Ribosomal protein S1 functions as a termination factor in RNA synthesis by Qbeta phage replicase, Nat. Commun. 4 (2013) 1781.

[121] J. Moretti, P. Chastagner, S. Gastaldello, S.F. Heuss, A.M. Dirac, et al., The translation initiation factor 3f (eIF3f) exhibits a deubiquitinase activity regulating Notch activation, PLoS Biol. 8 (2010) e1000545.

[122] A. Csibi, M.P. Leibovitch, K. Cornille, L.A. Tintignac, S.A. Leibovitch, MAFbx/Atrogin-1 controls the activity of the initiation factor eIF3-f in skeletal muscle atrophy by targeting multiple C-terminal lysines, J. Biol. Chem. 284 (2009) 4413–4421.

[123] A.N. Sasikumar, W.B. Perez, T.G. Kinzy, The many roles of the eukaryotic elongation factor 1 complex, Wiley Interdiscip. Rev. RNA 3 (2012) 543–555.

[124] Z. Li, P.A. Gonzalez, Z. Sasvari, T.G. Kinzy, P.D. Nagy, Methylation of translation elongation factor 1A by the METTL10-like See1 methyltransferase facilitates tombusvirus replication in yeast and plants, Virology 448 (2014) 43–54.

[125] A. Porollo, J. Meller, Versatile annotation and publication quality visualization of protein complexes using POLYVIEW-3D, BMC Bioinform. 8 (2007) 316.

[126] M. Laurberg, H. Asahara, A. Korostelev, J. Zhu, S. Trakhanov, et al., Structural basis for translation termination on the 70S ribosome, Nature 454 (2008) 852–857.

[127] A. Roll-Mecak, C. Cao, T.E. Dever, S.K. Burley, X-Ray structures of the universal translation initiation factor IF2/eIF5B: conformational changes on GDP and GTP binding, Cell 103 (2000) 781–792.

[128] J. Querol-Audi, C. Sun, J.M. Vogan, M.D. Smith, Y. Gu, et al., Architecture of human translation initiation factor 3, Structure 21 (2013) 920–928.

[129] J.L. Sussman, S.R. Holbrook, R.W. Warrant, G.M. Church, S.H. Kim, Crystal structure of yeast phenylalanine transfer RNA. I. Crystallographic refinement, J. Mol. Biol. 123 (1978) 607–630.

Please cite this article in press as: M. Sauert, et al., Heterogeneity of the translational machinery: Variations on a common theme, Biochimie (2014), http://dx.doi.org/10.1016/j.biochi.2014.12.011

III. Conclusion and future prospects

In this work I aimed to decipher the 'lmRNA regulon' in order to define the consequences of the MazF-mediated stress response mechanism in *E. coli*. I established a method to isolate full length mRNAs from polysomes for RNA sequencing providing information about the processing state of individual mRNAs as well as their transcriptional and translational regulation. Hereby, I identified 223 targets of the MazF-mediated stress response mechanism. Surprisingly, the corresponding protein products of these targets have no common functions in stress response, but are involved in all cellular processes. Thus, my data reveal an unexpected diversity of MazF targets. In the light of persister cell formation which has been qualitatively linked to MazF activity further analysis of the identified MazF targets might bridge the knowledge gap between MazF activity and entry of single cells within a population into the persister phenotype. In particular, single cell studies of the MazF-mediated stress response in the future might uncover if all the identified MazF targets are processed in every cell in order to reprogram every cell's translational program to this extent or if a different set of mRNAs is targeted in every single cell to increase population heterogeneity. Augmented population heterogeneity consequently multiplies the possibility that individual cells develop a persister phenotype.

Alongside the multitude of MazF targets my comparative transcriptome and translatome studies reveal the underestimated significance of translational regulation in response to stress. Comparing differential gene expression analyses performed on the total RNA level (the transcriptome) with differential gene expression analyses performed on RNAs extracted from polysomes (the translatome) the regulatory effects are consistently more pronounced on the level of the translatome. Thus, analysis of the translatome reveals regulatory effects that would have been missed by conventional transcriptome analysis. On the other hand, I also observe significant regulations in the transcriptome which are not reflected or even antagonistically regulated in the translatome. This observation underlines the further importance of ribosome specificity and selective translation during stress.

Acting so diversely on the translational level, the MazF-mediated mechanism might pose a 'fast-track' stress response. Conventional adaption of gene expression by alteration of the transcriptome involves the differential production and degradation of mRNAs and subsequent translation into the required protein products. As we have shown that the activation of only one protein, namely MazF, induces such a pronounced translational regulation, it is conceivable that the MazF-mediated stress response

mechanism acts even before the major adjustments by transcriptional regulation have kicked into play.

In addition to direct translation regulation, my data also point toward further potential levels of post-transcriptional regulation. Some of the removed 5'-UTRs of cleaved MazF targets appear to be very stable and they might act as regulatory small RNAs, once freed from their corresponding mRNA. Concomitantly, MazF cleavage of mRNAs can affect their translational efficiency in many manners. The loss of the mRNAs 5'-terminus can result in alternatively folded mRNAs with increased or decreased translation efficiency. Moreover, cleavage of the mRNA might even create an alternative translational start site resulting in production of alternative protein variants, as discussed for *acnB*. The mechanism, conceptional similar to mRNA slicing in eukaryotes would open new doors in post-transcriptional regulation of gene expression.

IV. Material and Methods

IV.1. Buffers, solutions, media

IV.1.1. Media for bacterial growth

LB medium	10 g tryptone/peptone 5 g yeast extract 10 g NaCl Add to 1l with H_2O dest., adjust pH to 7.2 with NaOH Eventually supplemented with 0,5% glucose
10x M9 salts	452 mM Na_2HPO_4 x $7H_2O$ 219 mM KH2PO4 85.5 mM NaCl 187 mM NH4Cl adjust pH 7.0 with KOH
M9 minimal medium	1x M9 salts 0,4 % glucose or glycerol 0.2 mM $CaCl_2$ 2 mM $MgSO_4$ x $7H_2O$ 1 µg/ml Vit B1 (thiamine) 20 µg/ml CasAminoAcids or 1 µg/ml per single amino acid
Antibiotics If not otherwise indicated, antibiotics were used in following final concentrations.	100 µg/ml ampicillin (30 µg/ml for low copy plasmids) 30 µg/ml chloramphenicol (15 µg/ml for low copy plasmids) 50 µg/ml kanamycin (25 µg/ml for chromosomally encoded resistance) 15 µg/ml tetracycline (for chromosomally encoded resistance) 30 µg/ml spectinomycin 100 µg/ml streptomycin

IV.1.2. Solutions for nucleic acid analysis

DEPC water	1 ml DEPC (Diethylpyrocarbonat) 1l $H_2O_{millipore}$ Mix → incubate at 37°C over night Autoclave twice
10x RT +/- Mg^{2+}	0.5 M Tris-HCl, pH 8.3 0.6 M NaCl (0.06 M $MgCl_2$) 0.1 M DTT
5x dNTPs in RT+	3.75 mM dNTPs each (Fermentas, Promega) 1x RT+

5x ddNTPs in RT+	1 mM ddNTP (Fermentas, Promega) 1x RT+
AMV-RT-Mix (per reaction)	3x dNTPs (in RT+) 1x RT+ 1 U AMV-RT (avian myeloblastosis virus reverse transcriptase, Promega, 10 U/µl)
MMLV-loading dye	9.4 M Urea 1x TBE 0.04% bromo phenol blue + xylene cyanol 15 mM EDTA
10x TBE	890 mM Tris, pH 8.0 890 mM boric acid 40 mM EDTA
PAA-urea gel buffer	6-15% Acrylamide/bisacrylamide mixture (19:1, Serva) 1x TBE 8 M urea
10x VD +/- Mg^{2+}	0.05 M Tris-Cl pH 7.4 0.3 M NH_4Cl 30 mM β-Mercapto-EtOH (0.05 M MgOAc)
4x dNTPs in VD+	3.75 mM dNTPs each (Fermentas, Promega) 1x VD+
MMLV-RT-Mix	1x dNTPs (in VD+) 1x VD+ 0.25 mg/ml BSA 400 U M-MLV-RT (moloney murine leukemia virus reverse transcriptase, Promega, 200 U/µl)

IV.1.1. Solutions for protein analysis

TE buffer	10 mM Tris-HCl, pH 8.0 1 mM EDTA
native sample buffer	0.175 mM Tris-HCl, pH 6.8 20% glycerol 0.2% bromo phenol blue
Native resolving gel buffer	8-15% Acrylamide/bisacrylamide mixture (37.5:1, Roth) 0.25 M Tris-HCl, pH 8.8
Native stacking gel buffer	4.5% Acrylamide/bisacrylamide mixture (37.5:1, Roth) 0.125 M Tris-HCl, pH 6.8
10x Native running buffer	0.25 M Tris-HCl, pH 8.8 1.9 M glycine

4x SDS sample buffer	0.2 M Tris-HCl pH 6.8 40% glycerol 8% SDS 0.4 M DTT 0.2% bromo phenol blue
SDS resolving gel buffer	8-15% Acrylamide/bisacrylamide mixture (37.5:1, Roth) 0.375 M Tris-HCl pH 8,8 0.1% SDS
SDS stacking gel buffer	4.5% Acrylamide/bisacrylamide mixture (37.5:1, Roth) 0.125 M Tris-HCl pH 6,8 0.1% SDS
10x SDS running buffer	0.25 M Tris-HCl, pH 8.8 1.9 M glycine 0.1% SDS
Coomassie stain	40% methanol 10% acetic acid 0.1% Coomassie Brilliant Blue G250
destain solution	40% methanol 10% acetic acid
1x transfer buffer	48 mM Tris, pH 8.3 39 mM glycine 0.037% SDS 20% methanol
10x PBS	1,37 M NaCl 26,8 mM KCl 0,1 M Na_2HPO_4 17,6 mM KH_2PO_4 pH 7.4
PBS-T	1x PBS 0,2% Tween
Blocking buffer	1x PBS 5% milk powder 0.02% NaN_3
AP buffer	100 mM NaCl 100 mM Tris-Cl 5 mM $MgCl_2$
AP-developer solution	10ml AP-buffer +33µl BCIP + 66µl NBT

IV.1.2. Antibodies

IV.1.2.a) Primary antibodies

Antibody	species	dilution	supplier
α-S2$_{\alpha 2}$	rabbit	1:5.000	Lab stocks
α-GFP	mouse	1:5.000 / 1:10.000	New England Biolabs
α-S1	goat	1:2.000	Lab Stocks
α-AcnB	rabbit	1:5.000	Jeff Green, Sheffield University
α-HA	rabbit	1:10.000	Novus Biological
α-FLAG	goat	1:5.000	New England Biolabs

IV.1.2.b) Secondary antibodies

Antibody	dilution	supplier
α-rabbit-IgG-IRDye800®	1:15.000	Rockland
α-goat- IgG-IRDye800®	1:15.000	Rockland
α-mouse- IgG-IRDye800®	1:15.000	Rockland
α-rabbit-IgG Alkaline phosphatase	1:10.000	Sigma
α-goat- IgG Alkaline phosphatase	1:10.000	Sigma
α-mouse- IgG Alkaline phosphatase	1:10.000	Sigma

IV.2. Plasmids, oligo nucleotides

IV.2.1. Plasmids

Name	**Content**	**cloning**	**origin**
pSA1	pQE30-*mazF*		
pBAD-*mazF*	pBAD33-*mazF*		
pUH-C	pUH21-2_wo Cam		This work
GFP plasmids			
pMS2_111	pMA-T_ΔACA-EmGFP	from GeneArt	GeneArt
pMS2_112	pMA-T_ΔACA-EmGFP_BamHI	BamHI inserted in ompA-5'-UTR by cloning overlap PCR product (preceding PCRs: X15+IM_E10 and IM_F10+IM_N9) XbaI/PstI	This work
pMS2_225	pUH21-2_ΔACA-EmGFP_cII	PCR on pMS2_222 with IM_R13/N9 --> clone EcoRI/PstI into pUH21-2	This work
pMS2_245	pUH21-2_ΔACA-	PCR on pMS2_222 with IM_S13/N9 -->	This

	EmGFP_ΔTIR	clone EcoRI/PstI into pUH21-2	work
pMS2_413	pACYC177_ΔACA-EmGFP	from pMS2_212 (XhoI/NheI), cloned XhoI/NheI into pACYC177	This work
pMS2_433	pACYC177_ΔACA-EmGFP_II	from pMS2_23 (XhoI/NheI), cloned XhoI/NheI into pACYC177	This work
pMS2_4253	pACYC177_ΔACA-EmGFP_cII	from pMS2_225 (XhoI/NheI), cloned XhoI/NheI into pACYC177	This work
pMS2_4453	pACYC177_ΔACA-EmGFP_ΔTIR	from pMS2_245 (XhoI/NheI), cloned XhoI/NheI into pACYC177	This work
pMS2_512	pUH-C_ΔACA-EmGFP	from pMS2_212 (XbaI/NheI) --> sticky end ligation	This work
pMS2_53	pUH-C_ΔACA-EmGFP_II	from pMS2_23 (XbaI/NheI) --> sticky end ligation	This work
pMS2_525	pUH-C_ΔACA-EmGFP_cII	from pMS2_225 (XbaI/NheI) --> sticky end ligation	This work
pMS2_545	pUH-C_ΔACA-EmGFP_ΔTIR	from pMS2_245 (XbaI/NheI) --> sticky end ligation	This work
pMS2_612	pUH-C-2.Op_ΔACA-EmGFP	invers PCR on pMS2_512 with IM_G19/H19 (each phosphorylated) --> blunt end ligation (DpnI digest)	This work
pMS2_625	pUH-C-2.Op_ΔACA-EmGFP_cII	invers PCR on pMS2_525 with IM_E19/H19 (each phosphorylated) --> blunt end ligation (DpnI digest)	This work
pMS2_645	pUH-C-2.Op_ΔACA-EmGFP_ΔTIR	invers PCR on pMS2_545 with IM_F19/H19 (each phosphorylated) --> blunt end ligation (DpnI digest)	This work
pPK_111	pACYC184 acnB wt	pPK1 (acnB wt) = F/G16 (genom. DNA) --> HindIII/BamHI in pACYC184	Paul Kollmann
pPK_113	pACYC184 acnB mut 1	pPK1 (_CTATGAtAATG) (acnB ΔM) (potential cleavage site ACU-->A deleted) --> invers PCR on pPK_111 with H/I16, coincidental deletion of A	Paul Kollmann
pPK_112	pACYC184 acnB mut 3	pPK1 (AtAATG) (acnB M) --> invers PCR on pPK_111 with H/I16	Paul Kollmann
pPK_115	pACYC184 acnB wt +GTt	pPK1 GTt = invers PCR L/M19 on pACYC184 acnB wt	Paul Kollmann
pPK_113+5	pACYC184 acnB mut 1 +GTt	pPK1 mut1 GTt= invers PCR L/M19 on pACYC184 acnB mut 1	Paul Kollmann
pPK_112+5	pACYC184 acnB mut 3 +GTt	pPK1 mut3 GTt = invers PCR L/M19 on pACYC184 acnB mut 3	Paul Kollmann

pPK_211	pXG-0 acnB wt	acnB wt = L/P16 on pACYC184_acnB-WT --> XbaI --> in pXG-0 (XbaI/HincII)	Paul Kollmann
pPK_212	pXG-0 acnB mut3	ACA -> AtAATG = L/P16 on pACYC184_acnB-mut3 --> XbaI --> in pXG-0 (XbaI/HincII)	Paul Kollmann
pPK_3112	pET22b ll-acnB can.GTG	ll-acnB starting at can. GTG = W/X18 on pPK1 --> NdeI/XhoI in pET22b	Paul Kollmann
pPK_3212	pET22b ll-acnB ACAATG	ll-acnB starting at ACAATG = V/X18 on pPK1 --> NdeI/XhoI in pET22b	Paul Kollmann
pPK_3252	pET22b ll-acnB ACAATG+GTt	ll-acnB starting at ACAATG = and GUG(start) --> GUU mutation = invers PCR L/M19 on pET22b ll-acnB ACAATG	Paul Kollmann
pPK_4113	pBAD33 acnB GTG	ll acnB starting at can. GTG (with SD) = P16/R19 on pET22b-acnB_GTG --> XbaI/HindIII in pBAD33	Paul Kollmann
pPK_4213	pBAD33 acnB ACATG	ll acnB starting at ACAATG (with SD) = P16/R19 on pET22b-acnB_ACATG --> XbaI/HindIII in pBAD33	Paul Kollmann
pPK_4253	pBAD33 acnB ACAATG+GTt	ll acnB starting at ACAATG (with SD) and GUG(start) --> GUU mutation = invers PCR L/M19 on pBAD33 acnB ACATG	Paul Kollmann

IV.2.2. Oligonucleotides

Name	Function	Nucleotide sequence
UB_X15	T7-XbaI_fwd	GGGCTCTAGAGTAATACGACTCACTATAG
IM_E10	pMA-T-ΔACA-EmGFP_insert BamHI_1st-rev	CC ATT TTT TGC GCC TCG TTA GGA TCC AAA ATACGCC
IM_F10	pMA-T-ΔACA-EmGFP_insert BamHI_2nd-fwr	GAGATATTCATGGCGTATTTTGGATCCTAACGAGG
IM_N9	EmGFP-3'-end_rev, PstI, SmaI	TTACCCGGGTTACTGCAGTTACTTATACAGCTCGTC
IM_R13	cll-EmGFP-fwd_3	ATAGAATTCGGCCGCAGCGGCCAAACATGGTGAGC AAGGGCGAGGAGCTGTTCA

IM_S13	cll-EmGFP-ΔACA-fwd_3	ATAGAATTCGGCCGCAGCGGCCAAAAATGGTGAGC AAGGGCGAGGAGCTGTTCA
IM_E19	cll-stem-GFP_fwd	[phos]AGAATTCGGCCGCAGCGGCCAAACATG
IM_F19	ΔTIR-stem-GFP_fwd	[phos]AGAATTCGGCCGCAGCGGCCAAAAATG
IM_G19	ΔTIR-stem-GFP_fwd	[phos]GAATTCTCGCCAGGGGTGCTCGGC
IM_H19	pUH-C_op1_rev	[phos]TGAATCTAAGTATCATTGTTATCCGCTCACA
IM_X10	T7-gfp_fwd	AAATTCTAGAGTAATACGACTCACTATAGGCATGGT GAGCAAGGGCG
IM_Y10	T7-ll-EmGFP_GATG_fwd	AAATTCTAGAGTAATACGACTCACTATAGGATGGTG AGCAAGGGCG
IM_Z10	GFP_rev 60-76 nts	GGCCGTTTACGTCGCC

IV.3. *Escherichia coli* strains

Name	Genotype
Top 10	*mcr*A, Δ(*mrr-hsd*RMS-*mcr*BC), Δ*lac*X74, *deo*R, *rec*A1, *ara*D139Δ(*ara-leu*)7697, *gal*K, *rps*L, *end*A1, *nup*G
Top 10 F'	identical to TOP10. Additional F´ episome (tetracycline-R, lacI^q repressor)
MC4100 *relA*$^+$ *F'*	F$^-$, [*araD*139]$_{B/r}$, Δ(*argF*-lac)169* &lambda$^-$, e14- *flhD*5301, Δ(*fruK-yeiR*)725 (*fruA*25)‡, *relA*1, *rpsL*150(strR), *rbsR*22, Δ(*fimB-fimE*)632(::IS1), *deoC*1
MG1655	F$^-$, λ$^-$, *ilvG-*, *rfb*-50, *rph*-1
MG1655 Δ*mazF*	F$^-$, λ$^-$, *ilvG-*, *rfb*-50, *rph*-1, Δ*mazF*

IV.4. Methods for RNA analysis

IV.4.1. RNA extraction

IV.4.1.a) RNA extraction from E. coli cells with TRIzol® (Invitrogen)

A medium-free cell pellet from 20-50 ml of *E. coli* cells is resuspended in 800 µl of TRIzol® (Invitrogen) and incubated at room temperature for 5 minutes. Then 200 µl of chloroform are added and vigorously mixed by vortexing. The phases are separated by centrifugation at 13000 rpm for 5 minutes and the upper aqueous phase is transferred into a fresh 1.5 ml reaction tube. The extraction is repeated by vigorous mixing with 500 µl chloroform and phases separated by centrifugation at 13000 rpm for 2 minutes. The RNA from the upper aqueous phase is precipitated by addition of 3 volumes ethanol (96%), 1/10 volume 3M sodium acetate, pH 5.2 (NaOAc) and 2 µg glycerol (RNA-grade, Thermo Scientific) and incubation at -20°C for at least 1 hour. The precipitated RNA is collected by centrifugation at 13000 rpm at 4 °C for 30 minutes and subsequent washing with 70% ethanol. The dried RNA pellet is resuspended in 50-100 µl DEPC water.

IV.4.1.b) RNA extraction from aqueous solutions

The volume of the RNA to be extracted is adjusted to 300 µl in DEPC water and 300 µl of phenol/chloroform/isoamyl alcohol (25:24:1, pH 7) added and vigorously mixed by vortexing. The phases are separated by centrifugation at 13000 rpm for 5 minutes and the procedure as described in IV.4.1.a) continued.

IV.4.1. *In vitro* transcription

In vitro transcriptions were performed using AmpliScribe™ T7 High Yield Transcription Kit (Epicenter) with 1 µg of linearized plasmid template or PCR product in a total volume of 20 µl following the manufacturer's protocol. Additional DNAse I digestion was performed by addition of 1 µl DNAse I (RNAse-free, Roche) and incubation at 37°C for 15 minutes. The resulting RNA was extracted was described in IV.4.1.b).

IV.4.2. Radioactive labeling of oligo nucleotides

100 pmol of oligo nucleotide are mixed with 1x PNK buffer A (provided by Thermo Scientific), 3 µl ^{32}P-γ-ATP (Hartman Analytics, 10 mCi/ml) and 10 U of T4 polynucleotide kinase (T4 PNK, Thermo Scientific) in a total volume of 20 µl and incubated at 37°C for 30 minutes. The remaining nucleotides are removed by applying the mixture to QUIAGEN nucleotide removal spin column according to the manufacturer's protocol and eluting the labeled oligo nucleotides in 100 µl to gain a 1 pmol/µl solution.

IV.4.3. Primer extension

10 µg of total RNA are mixed with 1 pmol of the labeled oligo nucleotide in 1x RT-buffer in a total volume of 15 µl. The oligo nucleotide is annealed by heating the mixture to 80°C for 3 minutes and immediate snap freezing in $N_{2\,aq}$. The mixture is gently thawed on ice and 3 µl of 36 µM $MgCl_2$ in 1x RT+ are added to increase the Mg^{2+} concentration for the subsequent reverse transcription (RT) reaction. For extension reactions of *in vitro* transcribed RNA 0.5 pmol of specific RNA are used for the annealing reaction. To perform Sanger sequencing the annealing mix of a specific RNA is aliquoted into four different tubes containing each 5 µl of one kind of di-desoxynucleotide (5x ddNTPs). 5 µl of AMV-mix are added to each annealing mix and the reaction incubated at 42°C for 30 minutes. The reaction is stopped by addition 1.5 volumes of MMLV loading dye and the resulted cDNA denatured by heating at 95°C for 10 minutes. 8 µl of that mixture are loaded onto a pre-warmed 30 cm long 8% PAA-urea gel and electrophoresis performed at 18-24 mA for 2-3 hours. The resulting gel is dried on Whatman paper and radioactivity detected by a phosphor screen and Typhoon imager.

IV.4.4. Toeprinting reaction

For ribosome binding assays 1 pmol of radioactively labeled oligo nucleotide is mixed with 0.5 pmol of the *in vitro* transcribed RNA of interest in 1x VD- buffer in a total volume of 20 µl. The oligo nucleotide is annealed by heating the mixture to 80°C for 3 minutes and immediate snap freezing in $N_{2\,aq}$. The mixture is gently thawed on ice and 5 µl of 50 µM MgOAc in 1x VD+ are added to increase the Mg^{2+} concentration for the subsequent RT reaction. To 2 µl of the annealing mix 4 pmol of 30S ribosomes and 16 pmol tRNA-fMet are added in a total volume of 10 µl in 1x VD+. This reaction is incubated at 37°C for 10 minutes to allow binding of 30S ribosomes to the mRNA 5'-end. Then 2 µl of MMLV-mix are added and incubated again for 10 minutes at 37°C to perform the RT reaction. The reaction is stopped by addition 1.5 volumes of MMLV loading dye. 8 µl of that mixture are loaded onto a pre-warmed 30 cm long 8% PAA-urea gel and electrophoresis performed at 18-24 mA for 2-3 hours. The resulting gel is dried on Whatman paper and radioactivity detected by a phosphor screen and Typhoon imager.

IV.5. Methods for protein analysis

IV.5.1. Native cell disruption for native PAGE

Melted cell pellets were resuspended in appropriate volumes of 1mg lysozyme/ml 1xTE buffer resulting in 10 OD/ml (lysozyme from chicken egg white, Fluka, in a final concentration of 0,2mg/OD) and incubated on ice for 10 minutes. The mixture was shock frozen in $N_{2\,aq}$ and thawed at room temperature for 3 times. The cell debris was pelleted by centrifugation at 4°C and 30.000 rpm for 10 min and the supernatant used for downstream analysis (e.g. native PAGE, next chapter).

IV.5.2. Native PAGE

Native cell lysates are mixed in a 1:1 ratio with 2x native sample buffer and immediately loaded onto native PAA gels (if necessary in appropriate dilutions). Electrophoresis is performed in 1x native running buffer at 30 mA per gel in Biorad Protean II electrophoresis cells. For detection of GFP signals the gels are scanned in Typhoon scanner. For immuno staining western blot protocol is continued.

IV.5.3. SDS PAGE

Medium-free cell pellets are resuspended in 1.5x SDS sample buffer to result in 5 OD/ml mixtures. Cells are disrupted by heating at 95°C for 10 minutes and subsequently cell debris pelleted by centrifugation at 13000 rpm for 10 minutes. The supernatant can be loaded directly (for Coomassie staining) or in appropriate dilutions in 1x SDS sample buffer (for subsequent Western blot) to SDS-PAA gels. Electrophoresis is performed in 1x SDS running buffer at 30 mA per gel in Biorad Protean II electrophoresis cells. Gels can be stained with coomassie stain for 30 minutes and destained in destain solution until the desired contrast is achieved or continue with western blot protocol.

IV.5.4. Western blot

Proteins separated on native or SDS PAA gels are transferred to a nitrocellulose membrane (Amersham Protan 0.2 µm) by semi-dry transfer in 1x transfer buffer in a Biorad Trans-Blot® SD Semi-Dry Transfer Cell. Membranes are blocked by incubation in blocking buffer for 1 h at room temperature or over night at 4°C. The primary antibody in blocking buffer is applied and incubated for 1 h at room temperature or over night at 4°C. Subsequently, membranes are washed three times in 1x PBS-T for 10 minutes and the secondary antibody is applied for 45 minutes at room temperature. If the secondary

antibody is infra red (IR)-coupled the signals are directly scanned in an Odyssee scanner. If the secondary antibody is coupled with alkaline phosphatase (AP) the protein intensities are detected on the membrane by incubation with AP-buffer for 10 minutes and subsequent application of AP-developer solution until signals are visible.

V. References

Agirrezabala, X., and Frank, J. (2009). Elongation in translation as a dynamic interaction among the ribosome, tRNA, and elongation factors EF-G and EF-Tu. Q. Rev. Biophys. *42*, 159–200.

Aizenman, E., Engelberg-Kulka, H., and Glaser, G. (1996). An Escherichia coli chromosomal "addiction module" regulated by guanosine [corrected] 3',5'-bispyrophosphate: a model for programmed bacterial cell death. Proc. Natl. Acad. Sci. U. S. A. *93*, 6059–6063.

Akashi, H., and Gojobori, T. (2002). Metabolic efficiency and amino acid composition in the proteomes of Escherichia coli and Bacillus subtilis. Proc. Natl. Acad. Sci. U. S. A. *99*, 3695–3700.

Amitai, S., Kolodkin-Gal, I., Hananya-Meltabashi, M., Sacher, A., and Engelberg-Kulka, H. (2009). Escherichia coli MazF leads to the simultaneous selective synthesis of both "death proteins" and "survival proteins." PLoS Genet. *5*, e1000390.

Anders, S., and Huber, W. (2010). Differential expression analysis for sequence count data. Genome Biol. *11*, R106.

Anders, S., Pyl, P.T., and Huber, W. (2014). HTSeq—a Python framework to work with high-throughput sequencing data. Bioinformatics btu638.

Arnold, R.J., and Reilly, J.P. (1999). Observation of Escherichia coli ribosomal proteins and their posttranslational modifications by mass spectrometry. Anal. Biochem. *269*, 105–112.

Arsène, F., Tomoyasu, T., and Bukau, B. (2000). The heat shock response of Escherichia coli. Int. J. Food Microbiol. *55*, 3–9.

Baba, T., Ara, T., Hasegawa, M., Takai, Y., Okumura, Y., Baba, M., Datsenko, K.A., Tomita, M., Wanner, B.L., and Mori, H. (2006). Construction of Escherichia coli K-12 in-frame, single-gene knockout mutants: the Keio collection. Mol. Syst. Biol. *2*, 2006.0008.

Balakin, A.G., Skripkin, E.A., Shatsky, I.N., and Bogdanov, A.A. (1992). Unusual ribosome binding properties of mRNA encoding bacteriophage lambda repressor. Nucleic Acids Res. *20*, 563–571.

Balleza, E., López-Bojorquez, L.N., Martínez-Antonio, A., Resendis-Antonio, O., Lozada-Chávez, I., Balderas-Martínez, Y.I., Encarnación, S., and Collado-Vides, J. (2009). Regulation by transcription factors in bacteria: beyond description. FEMS Microbiol. Rev. *33*, 133–151.

Beckwith, J.R. (1967). Regulation of the lac operon. Recent studies on the regulation of lactose metabolism in Escherichia coli support the operon model. Science *156*, 597–604.

Beinert, H., Kennedy, M.C., and Stout, C.D. (1996). Aconitase as Ironminus signSulfur Protein, Enzyme, and Iron-Regulatory Protein. Chem. Rev. *96*, 2335–2374.

Benjamin, J.-A.M., and Massé, E. (2014). The iron-sensing aconitase B binds its own mRNA to prevent sRNA-induced mRNA cleavage. Nucleic Acids Res. *42*, 10023–10036.

Bernstein, J.A., Khodursky, A.B., Lin, P.-H., Lin-Chao, S., and Cohen, S.N. (2002). Global analysis of mRNA decay and abundance in Escherichia coli at single-gene resolution using two-color fluorescent DNA microarrays. Proc. Natl. Acad. Sci. U. S. A. *99*, 9697–9702.

Blaha, G., Stanley, R.E., and Steitz, T.A. (2009). Formation of the first peptide bond: the structure of EF-P bound to the 70S ribosome. Science *325*, 966–970.

Blank, L., Green, J., and Guest, J.R. (2002). AcnC of Escherichia coli is a 2-methylcitrate dehydratase (PrpD) that can use citrate and isocitrate as substrates. Microbiol. Read. Engl. *148*, 133–146.

Blower, T.R., Pei, X.Y., Short, F.L., Fineran, P.C., Humphreys, D.P., Luisi, B.F., and Salmond, G.P.C. (2011). A processed noncoding RNA regulates an altruistic bacterial antiviral system. Nat. Struct. Mol. Biol. *18*, 185–190.

Boni, I.V., Isaeva, D.M., Musychenko, M.L., and Tzareva, N.V. (1991). Ribosome-messenger recognition: mRNA target sites for ribosomal protein S1. Nucleic Acids Res. *19*, 155–162.

Borukhov, S., and Severinov, K. (2002). Role of the RNA polymerase sigma subunit in transcription initiation. Res. Microbiol. *153*, 557–562.

Boudvillain, M., Nollmann, M., and Margeat, E. (2010). Keeping up to speed with the transcription termination factor Rho motor. Transcription *1*, 70–75.

Boudvillain, M., Figueroa-Bossi, N., and Bossi, L. (2013). Terminator still moving forward: expanding roles for Rho factor. Curr. Opin. Microbiol. *16*, 118–124.

Bradbury, A.J., Gruer, M.J., Rudd, K.E., and Guest, J.R. (1996). The second aconitase (AcnB) of Escherichia coli. Microbiol. Read. Engl. *142 (Pt 2)*, 389–400.

Brantl, S. (2007). Regulatory mechanisms employed by cis-encoded antisense RNAs. Curr. Opin. Microbiol. *10*, 102–109.

Bravo, A., de Torrontegui, G., and Díaz, R. (1987). Identification of components of a new stability system of plasmid R1, ParD, that is close to the origin of replication of this plasmid. Mol. Gen. Genet. MGG *210*, 101–110.

Breaker, R.R. (2012). Riboswitches and the RNA world. Cold Spring Harb. Perspect. Biol. *4*.

Brock, J.E., Pourshahian, S., Giliberti, J., Limbach, P.A., and Janssen, G.R. (2008). Ribosomes bind leaderless mRNA in Escherichia coli through recognition of their 5'-terminal AUG. RNA N. Y. N *14*, 2159–2169.

Brock, M., Maerker, C., Schütz, A., Völker, U., and Buckel, W. (2002). Oxidation of propionate to pyruvate in Escherichia coli. Involvement of methylcitrate dehydratase and aconitase. Eur. J. Biochem. FEBS *269*, 6184–6194.

Buck, M., Gallegos, M.T., Studholme, D.J., Guo, Y., and Gralla, J.D. (2000). The bacterial enhancer-dependent sigma(54) (sigma(N)) transcription factor. J. Bacteriol. *182*, 4129–4136.

Budde, P.P., Davis, B.M., Yuan, J., and Waldor, M.K. (2007). Characterization of a higBA toxin-antitoxin locus in Vibrio cholerae. J. Bacteriol. *189*, 491–500.

Bukowski, M., Rojowska, A., and Wladyka, B. (2011). Prokaryotic toxin-antitoxin systems--the role in bacterial physiology and application in molecular biology. Acta Biochim. Pol. *58*, 1–9.

Burgess, R.R., Travers, A.A., Dunn, J.J., and Bautz, E.K. (1969). Factor stimulating transcription by RNA polymerase. Nature *221*, 43–46.

Burkhardt, N., Jünemann, R., Spahn, C.M., and Nierhaus, K.H. (1998). Ribosomal tRNA binding sites: three-site models of translation. Crit. Rev. Biochem. Mol. Biol. *33*, 95–149.

Burmann, B.M., Schweimer, K., Luo, X., Wahl, M.C., Stitt, B.L., Gottesman, M.E., and Rösch, P. (2010). A NusE:NusG complex links transcription and translation. Science *328*, 501–504.

Byrgazov, K., Manoharadas, S., Kaberdina, A.C., Vesper, O., and Moll, I. (2012). Direct interaction of the N-terminal domain of ribosomal protein S1 with protein S2 in Escherichia coli. PloS One *7*, e32702.

Byrgazov, K., Grishkovskaya, I., Arenz, S., Coudevylle, N., Temmel, H., Wilson, D.N., Djinovic-Carugo, K., and Moll, I. (2015). Structural basis for the interaction of protein S1 with the Escherichia coli ribosome. Nucleic Acids Res. *43*, 661–673.

Cannon, W.R. (2014). Concepts, Challenges, and Successes in Modeling Thermodynamics of Metabolism. Front. Bioeng. Biotechnol. *2*.

Carpousis, A.J. (2007). The RNA degradosome of Escherichia coli: an mRNA-degrading machine assembled on RNase E. Annu. Rev. Microbiol. *61*, 71–87.

Casino, P., Rubio, V., and Marina, A. (2010). The mechanism of signal transduction by two-component systems. Curr. Opin. Struct. Biol. *20*, 763–771.

Celesnik, H., Deana, A., and Belasco, J.G. (2007). Initiation of RNA decay in Escherichia coli by 5’ pyrophosphate removal. Mol. Cell *27*, 79–90.

Christensen, S.K., and Gerdes, K. (2003). RelE toxins from Bacteria and Archaea cleave mRNAs on translating ribosomes, which are rescued by tmRNA. Mol. Microbiol. *48*, 1389–1400.

Culver, G.M. (2003). Assembly of the 30S ribosomal subunit. Biopolymers *68*, 234–249.

Culver, G.M., and Noller, H.F. (1999). Efficient reconstitution of functional Escherichia coli 30S ribosomal subunits from a complete set of recombinant small subunit ribosomal proteins. RNA N. Y. N *5*, 832–843.

Cunningham, L., Gruer, M.J., and Guest, J.R. (1997). Transcriptional regulation of the aconitase genes (acnA and acnB) of Escherichia coli. Microbiol. Read. Engl. *143 (Pt 12)*, 3795–3805.

Darty, K., Denise, A., and Ponty, Y. (2009). VARNA: Interactive drawing and editing of the RNA secondary structure. Bioinforma. Oxf. Engl. *25*, 1974–1975.

Datsenko, K.A., and Wanner, B.L. (2000). One-step inactivation of chromosomal genes in Escherichia coli K-12 using PCR products. Proc. Natl. Acad. Sci. U. S. A. *97*, 6640–6645.

Decatur, W.A., and Fournier, M.J. (2002). rRNA modifications and ribosome function. Trends Biochem. Sci. *27*, 344–351.

Dennis, P.P., Ehrenberg, M., and Bremer, H. (2004). Control of rRNA synthesis in Escherichia coli: a systems biology approach. Microbiol. Mol. Biol. Rev. MMBR *68*, 639–668.

Deutscher, M.P. (2003). Degradation of stable RNA in bacteria. J. Biol. Chem. *278*, 45041–45044.

Dever, T.E., and Green, R. (2012). The elongation, termination, and recycling phases of translation in eukaryotes. Cold Spring Harb. Perspect. Biol. *4*, a013706.

Doerfel, L.K., Wohlgemuth, I., Kothe, C., Peske, F., Urlaub, H., and Rodnina, M.V. (2013). EF-P is essential for rapid synthesis of proteins containing consecutive proline residues. Science *339*, 85–88.

Engelberg-Kulka, H., Reches, M., Narasimhan, S., Schoulaker-Schwarz, R., Klemes, Y., Aizenman, E., and Glaser, G. (1998). rexB of bacteriophage lambda is an anti-cell death gene. Proc. Natl. Acad. Sci. U. S. A. *95*, 15481–15486.

Engelberg-Kulka, H., Amitai, S., Kolodkin-Gal, I., and Hazan, R. (2006). Bacterial programmed cell death and multicellular behavior in bacteria. PLoS Genet. *2*, e135.

Van Etten, W.J., and Janssen, G.R. (1998). An AUG initiation codon, not codon-anticodon complementarity, is required for the translation of unleadered mRNA in Escherichia coli. Mol. Microbiol. *27*, 987–1001.

Fineran, P.C., Blower, T.R., Foulds, I.J., Humphreys, D.P., Lilley, K.S., and Salmond, G.P.C. (2009). The phage abortive infection system, ToxIN, functions as a protein-RNA toxin-antitoxin pair. Proc. Natl. Acad. Sci. U. S. A. *106*, 894–899.

Flynn, J.M., Neher, S.B., Kim, Y.I., Sauer, R.T., and Baker, T.A. (2003). Proteomic discovery of cellular substrates of the ClpXP protease reveals five classes of ClpX-recognition signals. Mol. Cell *11*, 671–683.

Fozo, E.M., Hemm, M.R., and Storz, G. (2008). Small Toxic Proteins and the Antisense RNAs That Repress Them. Microbiol. Mol. Biol. Rev. *72*, 579–589.

Gardner, P.R., and Fridovich, I. (1991). Superoxide sensitivity of the Escherichia coli aconitase. J. Biol. Chem. *266*, 19328–19333.

Gardner, P.R., and Fridovich, I. (1992). Inactivation-reactivation of aconitase in Escherichia coli. A sensitive measure of superoxide radical. J. Biol. Chem. *267*, 8757–8763.

Gardner, P.R., Costantino, G., Szabó, C., and Salzman, A.L. (1997). Nitric oxide sensitivity of the aconitases. J. Biol. Chem. *272*, 25071–25076.

Genschik, P., Drabikowski, K., and Filipowicz, W. (1998). Characterization of the Escherichia coli RNA 3'-terminal phosphate cyclase and its sigma54-regulated operon. J. Biol. Chem. *273*, 25516–25526.

Gerdes, K., Christensen, S.K., and Løbner-Olesen, A. (2005). Prokaryotic toxin-antitoxin stress response loci. Nat. Rev. Microbiol. *3*, 371–382.

Germain, E., Castro-Roa, D., Zenkin, N., and Gerdes, K. (2013). Molecular mechanism of bacterial persistence by HipA. Mol. Cell *52*, 248–254.

Gloge, F., Becker, A.H., Kramer, G., and Bukau, B. (2014). Co-translational mechanisms of protein maturation. Curr. Opin. Struct. Biol. *24*, 24–33.

Görke, B., and Vogel, J. (2008). Noncoding RNA control of the making and breaking of sugars. Genes Dev. *22*, 2914–2925.

Gottesman, S. (2003). Proteolysis in bacterial regulatory circuits. Annu. Rev. Cell Dev. Biol. *19*, 565–587.

Grill, S., Gualerzi, C.O., Londei, P., and Bläsi, U. (2000). Selective stimulation of translation of leaderless mRNA by initiation factor 2: evolutionary implications for translation. EMBO J. *19*, 4101–4110.

Grill, S., Moll, I., Hasenöhrl, D., Gualerzi, C.O., and Bläsi, U. (2001). Modulation of ribosomal recruitment to 5'-terminal start codons by translation initiation factors IF2 and IF3. FEBS Lett. *495*, 167–171.

Grønlund, H., and Gerdes, K. (1999). Toxin-antitoxin systems homologous with relBE of Escherichia coli plasmid P307 are ubiquitous in prokaryotes. J. Mol. Biol. *285*, 1401–1415.

Gruer, M.J., and Guest, J.R. (1994). Two genetically-distinct and differentially-regulated aconitases (AcnA and AcnB) in Escherichia coli. Microbiol. Read. Engl. *140 (Pt 10)*, 2531–2541.

Gruer, M.J., Bradbury, A.J., and Guest, J.R. (1997a). Construction and properties of aconitase mutants of Escherichia coli. Microbiol. Read. Engl. *143 (Pt 6)*, 1837–1846.

Gruer, M.J., Artymiuk, P.J., and Guest, J.R. (1997b). The aconitase family: three structural variations on a common theme. Trends Biochem. Sci. *22*, 3–6.

Hazan, R., Sat, B., and Engelberg-Kulka, H. (2004). Escherichia coli mazEF-mediated cell death is triggered by various stressful conditions. J. Bacteriol. *186*, 3663–3669.

Hengge, R. (2008). The two-component network and the general stress sigma factor RpoS (sigma S) in Escherichia coli. Adv. Exp. Med. Biol. *631*, 40–53.

Hengge-Aronis, R. (2002). Recent insights into the general stress response regulatory network in Escherichia coli. J. Mol. Microbiol. Biotechnol. *4*, 341–346.

Hennelly, S.P., Antoun, A., Ehrenberg, M., Gualerzi, C.O., Knight, W., Lodmell, J.S., and Hill, W.E. (2005). A time-resolved investigation of ribosomal subunit association. J. Mol. Biol. *346*, 1243–1258.

Hentze, M.W., and Kühn, L.C. (1996). Molecular control of vertebrate iron metabolism: mRNA-based regulatory circuits operated by iron, nitric oxide, and oxidative stress. Proc. Natl. Acad. Sci. U. S. A. *93*, 8175–8182.

Herold, M., and Nierhaus, K.H. (1987). Incorporation of six additional proteins to complete the assembly map of the 50 S subunit from Escherichia coli ribosomes. J. Biol. Chem. *262*, 8826–8833.

Herr, A.J., Jensen, M.B., Dalmay, T., and Baulcombe, D.C. (2005). RNA polymerase IV directs silencing of endogenous DNA. Science *308*, 118–120.

Hinnebusch, A.G., and Lorsch, J.R. (2012). The mechanism of eukaryotic translation initiation: new insights and challenges. Cold Spring Harb. Perspect. Biol. *4*.

Hoffmann, S., Otto, C., Kurtz, S., Sharma, C.M., Khaitovich, P., Vogel, J., Stadler, P.F., and Hackermüller, J. (2009). Fast mapping of short sequences with mismatches, insertions and deletions using index structures. PLoS Comput. Biol. *5*, e1000502.

Hoffmann, S., Otto, C., Doose, G., Tanzer, A., Langenberger, D., Christ, S., Kunz, M., Holdt, L.M., Teupser, D., Hackermüller, J., et al. (2014). A multi-split mapping algorithm for circular RNA, splicing, trans-splicing and fusion detection. Genome Biol. *15*, R34.

Hughes, K.T., and Mathee, K. (1998). The anti-sigma factors. Annu. Rev. Microbiol. *52*, 231–286.

Ingolia, N.T., Ghaemmaghami, S., Newman, J.R.S., and Weissman, J.S. (2009). Genome-Wide Analysis in Vivo of Translation with Nucleotide Resolution Using Ribosome Profiling. Science *324*, 218–223.

Jackson, R.J., Hellen, C.U.T., and Pestova, T.V. (2010). The mechanism of eukaryotic translation initiation and principles of its regulation. Nat. Rev. Mol. Cell Biol. *11*, 113–127.

Jacques, J.-F., Jang, S., Prévost, K., Desnoyers, G., Desmarais, M., Imlay, J., and Massé, E. (2006). RyhB small RNA modulates the free intracellular iron pool and is essential for normal growth during iron limitation in Escherichia coli. Mol. Microbiol. *62*, 1181–1190.

Jang, S.K. (2006). Internal initiation: IRES elements of picornaviruses and hepatitis c virus. Virus Res. *119*, 2–15.

Jay, G., and Kaempfer, R. (1974). Sequence of events in initiation of translation: a role for initiator transfer RNA in the recognition of messenger RNA. Proc. Natl. Acad. Sci. U. S. A. *71*, 3199–3203.

Jensen, R.B., and Gerdes, K. (1995). Programmed cell death in bacteria: proteic plasmid stabilization systems. Mol. Microbiol. *17*, 205–210.

Jiang, Y., Pogliano, J., Helinski, D.R., and Konieczny, I. (2002). ParE toxin encoded by the broad-host-range plasmid RK2 is an inhibitor of Escherichia coli gyrase. Mol. Microbiol. *44*, 971–979.

Jishage, M., Iwata, A., Ueda, S., and Ishihama, A. (1996). Regulation of RNA polymerase sigma subunit synthesis in Escherichia coli: intracellular levels of four species of sigma subunit under various growth conditions. J. Bacteriol. *178*, 5447–5451.

Jørgensen, M.G., Pandey, D.P., Jaskolska, M., and Gerdes, K. (2009). HicA of Escherichia coli Defines a Novel Family of Translation-Independent mRNA Interferases in Bacteria and Archaea. J. Bacteriol. *191*, 1191–1199.

Kaczanowska, M., and Rydén-Aulin, M. (2007). Ribosome Biogenesis and the Translation Process in Escherichia coli. Microbiol. Mol. Biol. Rev. MMBR *71*, 477–494.

Kamada, K., Hanaoka, F., and Burley, S.K. (2003). Crystal structure of the MazE/MazF complex: molecular bases of antidote-toxin recognition. Mol. Cell *11*, 875–884.

Kasari, V., Mets, T., Tenson, T., and Kaldalu, N. (2013). Transcriptional cross-activation between toxin-antitoxin systems of Escherichia coli. BMC Microbiol. *13*, 45.

Kent, W.J., Sugnet, C.W., Furey, T.S., Roskin, K.M., Pringle, T.H., Zahler, A.M., and Haussler, D. (2002). The human genome browser at UCSC. Genome Res. *12*, 996–1006.

Keren, I., Kaldalu, N., Spoering, A., Wang, Y., and Lewis, K. (2004). Persister cells and tolerance to antimicrobials. FEMS Microbiol. Lett. *230*, 13–18.

Kolodkin-Gal, I., and Engelberg-Kulka, H. (2008). The extracellular death factor: physiological and genetic factors influencing its production and response in Escherichia coli. J. Bacteriol. *190*, 3169–3175.

Kolodkin-Gal, I., Hazan, R., Gaathon, A., Carmeli, S., and Engelberg-Kulka, H. (2007). A linear pentapeptide is a quorum-sensing factor required for mazEF-mediated cell death in Escherichia coli. Science *318*, 652–655.

Korostelev, A.A. (2011). Structural aspects of translation termination on the ribosome. RNA N. Y. N *17*, 1409–1421.

Kuroda, A., Nomura, K., Ohtomo, R., Kato, J., Ikeda, T., Takiguchi, N., Ohtake, H., and Kornberg, A. (2001). Role of inorganic polyphosphate in promoting ribosomal protein degradation by the Lon protease in E. coli. Science *293*, 705–708.

Laalami, S., Zig, L., and Putzer, H. (2014). Initiation of mRNA decay in bacteria. Cell. Mol. Life Sci. *71*, 1799–1828.

Lake, J.A. (1976). Ribosome structure determined by electron microscopy of Escherichia coli small subunits, large subunits and monomeric ribosomes. J. Mol. Biol. *105*, 131–139.

Lamontagne, B., Larose, S., Boulanger, J., and Elela, S.A. (2001). The RNase III family: a conserved structure and expanding functions in eukaryotic dsRNA metabolism. Curr. Issues Mol. Biol. *3*, 71–78.

Langklotz, S., Baumann, U., and Narberhaus, F. (2012). Structure and function of the bacterial AAA protease FtsH. Biochim. Biophys. Acta BBA - Mol. Cell Res. *1823*, 40–48.

Lehnherr, H., Maguin, E., Jafri, S., and Yarmolinsky, M.B. (1993). Plasmid addiction genes of bacteriophage P1: doc, which causes cell death on curing of prophage, and phd, which prevents host death when prophage is retained. J. Mol. Biol. *233*, 414–428.

Lennox, E.S. (1955). Transduction of linked genetic characters of the host by bacteriophage P1. Virology *1*, 190–206.

Leplae, R., Geeraerts, D., Hallez, R., Guglielmini, J., Dreze, P., and Van Melderen, L. (2011). Diversity of bacterial type II toxin-antitoxin systems: a comprehensive search and functional analysis of novel families. Nucleic Acids Res. *39*, 5513–5525.

Lewis, K. (2010). Persister cells. Annu. Rev. Microbiol. *64*, 357–372.

Liu, M., Zhang, Y., Inouye, M., and Woychik, N.A. (2008). Bacterial addiction module toxin Doc inhibits translation elongation through its association with the 30S ribosomal subunit. Proc. Natl. Acad. Sci. U. S. A. *105*, 5885–5890.

Lomakin, I.B., and Steitz, T.A. (2013). The initiation of mammalian protein synthesis and mRNA scanning mechanism. Nature *500*, 307–311.

Lorenz, R., Bernhart, S.H., Höner Zu Siederdissen, C., Tafer, H., Flamm, C., Stadler, P.F., and Hofacker, I.L. (2011). ViennaRNA Package 2.0. Algorithms Mol. Biol. AMB *6*, 26.

Lu, J., and Deutsch, C. (2008). Electrostatics in the ribosomal tunnel modulate chain elongation rates. J. Mol. Biol. *384*, 73–86.

Lu, J., Kobertz, W.R., and Deutsch, C. (2007). Mapping the electrostatic potential within the ribosomal exit tunnel. J. Mol. Biol. *371*, 1378–1391.

Mackie, G.A. (1998). Ribonuclease E is a 5'-end-dependent endonuclease. Nature *395*, 720–723.

Maier, T., Güell, M., and Serrano, L. (2009). Correlation of mRNA and protein in complex biological samples. FEBS Lett. *583*, 3966–3973.

Maisonneuve, E., Shakespeare, L.J., Jørgensen, M.G., and Gerdes, K. (2011). Bacterial persistence by RNA endonucleases. Proc. Natl. Acad. Sci. U. S. A. *108*, 13206–13211.

Mardis, E.R. (2008). Next-Generation DNA Sequencing Methods. Annu. Rev. Genomics Hum. Genet. *9*, 387–402.

Marianovsky, I., Aizenman, E., Engelberg-Kulka, H., and Glaser, G. (2001). The regulation of the Escherichia coli mazEF promoter involves an unusual alternating palindrome. J. Biol. Chem. *276*, 5975–5984.

Markovski, M., and Wickner, S. (2013). Preventing bacterial suicide: A novel toxin-antitoxin strategy. Mol. Cell *52*, 611–612.

Marles-Wright, J., and Lewis, R.J. (2007). Stress responses of bacteria. Curr. Opin. Struct. Biol. *17*, 755–760.

Martin, M. (2011). Cutadapt removes adapter sequences from high-throughput sequencing reads. EMBnet.journal *17*, pp. 10–12.

Massé, E., and Gottesman, S. (2002). A small RNA regulates the expression of genes involved in iron metabolism in Escherichia coli. Proc. Natl. Acad. Sci. U. S. A. *99*, 4620–4625.

Massé, E., Escorcia, F.E., and Gottesman, S. (2003). Coupled degradation of a small regulatory RNA and its mRNA targets in Escherichia coli. Genes Dev. *17*, 2374–2383.

Masuda, Y., Miyakawa, K., Nishimura, Y., and Ohtsubo, E. (1993). chpA and chpB, Escherichia coli chromosomal homologs of the pem locus responsible for stable maintenance of plasmid R100. J. Bacteriol. *175*, 6850–6856.

Meinhart, A., Alings, C., Sträter, N., Camacho, A.G., Alonso, J.C., and Saenger, W. (2001). Crystallization and preliminary X-ray diffraction studies of the epsilonzeta addiction system encoded by Streptococcus pyogenes plasmid pSM19035. Acta Crystallogr. D Biol. Crystallogr. *57*, 745–747.

Van Melderen, L. (2010). Toxin–antitoxin systems: why so many, what for? Curr. Opin. Microbiol. *13*, 781–785.

Metzger, S., Dror, I.B., Aizenman, E., Schreiber, G., Toone, M., Friesen, J.D., Cashel, M., and Glaser, G. (1988). The nucleotide sequence and characterization of the relA gene of Escherichia coli. J. Biol. Chem. *263*, 15699–15704.

Miki, T., Park, J.A., Nagao, K., Murayama, N., and Horiuchi, T. (1992). Control of segregation of chromosomal DNA by sex factor F in Escherichia coli. Mutants of DNA gyrase subunit A suppress letD (ccdB) product growth inhibition. J. Mol. Biol. *225*, 39–52.

Miller, O.L., Jr, Hamkalo, B.A., and Thomas, C.A., Jr (1970). Visualization of bacterial genes in action. Science *169*, 392–395.

Mizuno, T., Chou, M.Y., and Inouye, M. (1984). A unique mechanism regulating gene expression: translational inhibition by a complementary RNA transcript (micRNA). Proc. Natl. Acad. Sci. U. S. A. *81*, 1966–1970.

Moll, I., and Bläsi, U. (2002). Differential inhibition of 30S and 70S translation initiation complexes on leaderless mRNA by kasugamycin. Biochem. Biophys. Res. Commun. *297*, 1021–1026.

Moll, I., Resch, A., and Bläsi, U. (1998a). Discrimination of 5'-terminal start codons by translation initiation factor 3 is mediated by ribosomal protein S1. FEBS Lett. *436*, 213–217.

Moll, I., Resch, A., and Bläsi, U. (1998b). Discrimination of 5'-terminal start codons by translation initiation factor 3 is mediated by ribosomal protein S1. FEBS Lett. *436*, 213–217.

Moll, I., Grill, S., Gualerzi, C.O., and Bläsi, U. (2002a). Leaderless mRNAs in bacteria: surprises in ribosomal recruitment and translational control. Mol. Microbiol. *43*, 239–246.

Moll, I., Grill, S., Gründling, A., and Bläsi, U. (2002b). Effects of ribosomal proteins S1, S2 and the DeaD/CsdA DEAD-box helicase on translation of leaderless and canonical mRNAs in Escherichia coli. Mol. Microbiol. *44*, 1387–1396.

Moll, I., Grill, S., Gründling, A., and Bläsi, U. (2002c). Effects of ribosomal proteins S1, S2 and the DeaD/CsdA DEAD-box helicase on translation of leaderless and canonical mRNAs in Escherichia coli. Mol. Microbiol. *44*, 1387–1396.

Moll, I., Hirokawa, G., Kiel, M.C., Kaji, A., and Bläsi, U. (2004). Translation initiation with 70S ribosomes: an alternative pathway for leaderless mRNAs. Nucleic Acids Res. *32*, 3354–3363.

Moore, P.B., and Steitz, T.A. (2003). The structural basis of large ribosomal subunit function. Annu. Rev. Biochem. *72*, 813–850.

Moore, S.D., and Sauer, R.T. (2007). The tmRNA System for Translational Surveillance and Ribosome Rescue. Annu. Rev. Biochem. *76*, 101–124.

Mutschler, H., Gebhardt, M., Shoeman, R.L., and Meinhart, A. (2011). A novel mechanism of programmed cell death in bacteria by toxin-antitoxin systems corrupts peptidoglycan synthesis. PLoS Biol. *9*, e1001033.

Nie, L., Wu, G., and Zhang, W. (2006). Correlation of mRNA expression and protein abundance affected by multiple sequence features related to translational efficiency in Desulfovibrio vulgaris: a quantitative analysis. Genetics *174*, 2229–2243.

Nürenberg, E., and Tampé, R. (2013). Tying up loose ends: ribosome recycling in eukaryotes and archaea. Trends Biochem. Sci. *38*, 64–74.

O'Donnell, S.M., and Janssen, G.R. (2002). Leaderless mRNAs bind 70S ribosomes more strongly than 30S ribosomal subunits in Escherichia coli. J. Bacteriol. *184*, 6730–6733.

Ogura, T., and Hiraga, S. (1983). Mini-F plasmid genes that couple host cell division to plasmid proliferation. Proc. Natl. Acad. Sci. U. S. A. *80*, 4784–4788.

Oh, E., Becker, A.H., Sandikci, A., Huber, D., Chaba, R., Gloge, F., Nichols, R.J., Typas, A., Gross, C.A., Kramer, G., et al. (2011). Selective ribosome profiling reveals the cotranslational chaperone action of trigger factor in vivo. Cell *147*, 1295–1308.

Onodera, Y., Haag, J.R., Ream, T., Costa Nunes, P., Pontes, O., and Pikaard, C.S. (2005). Plant nuclear RNA polymerase IV mediates siRNA and DNA methylation-dependent heterochromatin formation. Cell *120*, 613–622.

Osada, Y., Saito, R., and Tomita, M. (1999). Analysis of base-pairing potentials between 16S rRNA and 5' UTR for translation initiation in various prokaryotes. Bioinforma. Oxf. Engl. *15*, 578–581.

Paget, M.S.B., and Helmann, J.D. (2003). The sigma70 family of sigma factors. Genome Biol. *4*, 203.

Pandey, D.P., and Gerdes, K. (2005). Toxin-antitoxin loci are highly abundant in free-living but lost from host-associated prokaryotes. Nucleic Acids Res. *33*, 966–976.

Pedersen, K., and Gerdes, K. (1999). Multiple hok genes on the chromosome of Escherichia coli. Mol. Microbiol. *32*, 1090–1102.

Pedersen, K., Christensen, S.K., and Gerdes, K. (2002). Rapid induction and reversal of a bacteriostatic condition by controlled expression of toxins and antitoxins. Mol. Microbiol. *45*, 501–510.

Pestova, T.V., and Kolupaeva, V.G. (2002). The roles of individual eukaryotic translation initiation factors in ribosomal scanning and initiation codon selection. Genes Dev. *16*, 2906–2922.

Peters, J.M., Vangeloff, A.D., and Landick, R. (2011). Bacterial transcription terminators: the RNA 3'-end chronicles. J. Mol. Biol. *412*, 793–813.

Picard, F., Loubière, P., Girbal, L., and Cocaign-Bousquet, M. (2013). The significance of translation regulation in the stress response. BMC Genomics *14*, 588.

Pontes, O., Costa-Nunes, P., Vithayathil, P., and Pikaard, C.S. (2009). RNA polymerase V functions in Arabidopsis interphase heterochromatin organization independently of the 24-nt siRNA-directed DNA methylation pathway. Mol. Plant *2*, 700–710.

Potrykus, K., and Cashel, M. (2008). (p)ppGpp: still magical? Annu. Rev. Microbiol. *62*, 35–51.

Proshkin, S., Rahmouni, A.R., Mironov, A., and Nudler, E. (2010). Cooperation between translating ribosomes and RNA polymerase in transcription elongation. Science *328*, 504–508.

Pullinger, G.D., and Lax, A.J. (1992). A Salmonella dublin virulence plasmid locus that affects bacterial growth under nutrient-limited conditions. Mol. Microbiol. *6*, 1631–1643.

Qu, X., Lancaster, L., Noller, H.F., Bustamante, C., and Tinoco, I. (2012). Ribosomal protein S1 unwinds double-stranded RNA in multiple steps. Proc. Natl. Acad. Sci. U. S. A. *109*, 14458–14463.

R Core Team (2014). R: A Language and Environment for Statistical Computing (R Foundation for Statistical Computing).

Régnier, P., and Hajnsdorf, E. (2009). Poly(A)-assisted RNA decay and modulators of RNA stability. Prog. Mol. Biol. Transl. Sci. *85*, 137–185.

Rentmeister, A., Mayer, G., Kuhn, N., and Famulok, M. (2007). Conformational changes in the expression domain of the Escherichia coli thiM riboswitch. Nucleic Acids Res. *35*, 3713–3722.

Rippa, V., Cirulli, C., Di Palo, B., Doti, N., Amoresano, A., and Duilio, A. (2010). The ribosomal protein L2 interacts with the RNA polymerase alpha subunit and acts as a transcription modulator in Escherichia coli. J. Bacteriol. *192*, 1882–1889.

Rodnina, M.V., and Wintermeyer, W. (2009). Recent mechanistic insights into eukaryotic ribosomes. Curr. Opin. Cell Biol. *21*, 435–443.

Romero, D.A., Hasan, A.H., Lin, Y.-F., Kime, L., Ruiz-Larrabeiti, O., Urem, M., Bucca, G., Mamanova, L., Laing, E.E., van Wezel, G.P., et al. (2014). A comparison of key aspects of gene regulation in Streptomyces coelicolor and Escherichia coli using nucleotide-resolution transcription maps produced in parallel by global and differential RNA sequencing. Mol. Microbiol.

Sauert, M., Temmel, H., and Moll, I. (2014). Heterogeneity of the translational machinery: Variations on a common theme. Biochimie.

Schena, M., Shalon, D., Davis, R.W., and Brown, P.O. (1995). Quantitative monitoring of gene expression patterns with a complementary DNA microarray. Science *270*, 467–470.

Schumacher, M.A., Piro, K.M., Xu, W., Hansen, S., Lewis, K., and Brennan, R.G. (2009). Molecular mechanisms of HipA-mediated multidrug tolerance and its neutralization by HipB. Science *323*, 396–401.

Schuwirth, B.S., Borovinskaya, M.A., Hau, C.W., Zhang, W., Vila-Sanjurjo, A., Holton, J.M., and Cate, J.H.D. (2005). Structures of the bacterial ribosome at 3.5 A resolution. Science *310*, 827–834.

Selmer, M., Dunham, C.M., Murphy, F.V., Weixlbaumer, A., Petry, S., Kelley, A.C., Weir, J.R., and Ramakrishnan, V. (2006). Structure of the 70S ribosome complexed with mRNA and tRNA. Science *313*, 1935–1942.

Sendler, E., Johnson, G.D., and Krawetz, S.A. (2011). Local and global factors affecting RNA sequencing analysis. Anal. Biochem. *419*, 317–322.

Shah, D., Zhang, Z., Khodursky, A., Kaldalu, N., Kurg, K., and Lewis, K. (2006). Persisters: a distinct physiological state of E. coli. BMC Microbiol. *6*, 53.

Sharma, U.K., and Chatterji, D. (2010). Transcriptional switching in Escherichia coli during stress and starvation by modulation of sigma activity. FEMS Microbiol. Rev. *34*, 646–657.

Ben-Shem, A., Garreau de Loubresse, N., Melnikov, S., Jenner, L., Yusupova, G., and Yusupov, M. (2011). The structure of the eukaryotic ribosome at 3.0 Å resolution. Science *334*, 1524–1529.

Shi, W., Zhou, Y., Wild, J., Adler, J., and Gross, C.A. (1992). DnaK, DnaJ, and GrpE are required for flagellum synthesis in Escherichia coli. J. Bacteriol. *174*, 6256–6263.

Shinagawa, H. (1996). SOS response as an adaptive response to DNA damage in prokaryotes. EXS *77*, 221–235.

Shine, J., and Dalgarno, L. (1974). The 3'-terminal sequence of Escherichia coli 16S ribosomal RNA: complementarity to nonsense triplets and ribosome binding sites. Proc. Natl. Acad. Sci. U. S. A. *71*, 1342–1346.

Simonetti, A., Marzi, S., Jenner, L., Myasnikov, A., Romby, P., Yusupova, G., Klaholz, B.P., and Yusupov, M. (2009). A structural view of translation initiation in bacteria. Cell. Mol. Life Sci. CMLS *66*, 423–436.

De Smit, M.H., and van Duin, J. (1994). Translational initiation on structured messengers. Another role for the Shine-Dalgarno interaction. J. Mol. Biol. *235*, 173–184.

Smith, E., and Morowitz, H.J. (2004). Universality in intermediary metabolism. Proc. Natl. Acad. Sci. U. S. A. *101*, 13168–13173.

Starosta, A.L., Lassak, J., Peil, L., Atkinson, G.C., Virumäe, K., Tenson, T., Remme, J., Jung, K., and Wilson, D.N. (2014). Translational stalling at polyproline stretches is modulated by the sequence context upstream of the stall site. Nucleic Acids Res. *42*, 10711–10719.

Tan, Q., Awano, N., and Inouye, M. (2011). YeeV is an Escherichia coli toxin that inhibits cell division by targeting the cytoskeleton proteins, FtsZ and MreB. Mol. Microbiol. *79*, 109–118.

Tanaka, N., Meineke, B., and Shuman, S. (2011). RtcB, a novel RNA ligase, can catalyze tRNA splicing and HAC1 mRNA splicing in vivo. J. Biol. Chem. *286*, 30253–30257.

Tang, Y., and Guest, J.R. (1999). Direct evidence for mRNA binding and post-transcriptional regulation by Escherichia coli aconitases. Microbiol. Read. Engl. *145 (Pt 11)*, 3069–3079.

Tang, Y., Quail, M.A., Artymiuk, P.J., Guest, J.R., and Green, J. (2002). Escherichia coli aconitases and oxidative stress: post-transcriptional regulation of sodA expression. Microbiol. Read. Engl. *148*, 1027–1037.

Tang, Y., Guest, J.R., Artymiuk, P.J., Read, R.C., and Green, J. (2004). Post-transcriptional regulation of bacterial motility by aconitase proteins. Mol. Microbiol. *51*, 1817–1826.

Tang, Y., Guest, J.R., Artymiuk, P.J., and Green, J. (2005). Switching aconitase B between catalytic and regulatory modes involves iron-dependent dimer formation. Mol. Microbiol. *56*, 1149–1158.

Tasaki, T., Sriram, S.M., Park, K.S., and Kwon, Y.T. (2012). The N-end rule pathway. Annu. Rev. Biochem. *81*, 261–289.

Taylor, R.C., Webb Robertson, B.-J.M., Markillie, L.M., Serres, M.H., Linggi, B.E., Aldrich, J.T., Hill, E.A., Romine, M.F., Lipton, M.S., and Wiley, H.S. (2013). Changes in translational efficiency is a dominant regulatory mechanism in the environmental response of bacteria. Integr. Biol. Quant. Biosci. Nano Macro *5*, 1393–1406.

Tedin, K., Resch, A., and Bläsi, U. (1997). Requirements for ribosomal protein S1 for translation initiation of mRNAs with and without a 5′ leader sequence. Mol. Microbiol. *25*, 189–199.

Tedin, K., Moll, I., Grill, S., Resch, A., Graschopf, A., Gualerzi, C.O., and Bläsi, U. (1999). Translation initiation factor 3 antagonizes authentic start codon selection on leaderless mRNAs. Mol. Microbiol. *31*, 67–77.

Tian, Q.B., Ohnishi, M., Tabuchi, A., and Terawaki, Y. (1996). A new plasmid-encoded proteic killer gene system: cloning, sequencing, and analyzing hig locus of plasmid Rts1. Biochem. Biophys. Res. Commun. *220*, 280–284.

Tomoyasu, T., Gamer, J., Bukau, B., Kanemori, M., Mori, H., Rutman, A.J., Oppenheim, A.B., Yura, T., Yamanaka, K., and Niki, H. (1995). Escherichia coli FtsH is a membrane-bound, ATP-dependent protease which degrades the heat-shock transcription factor sigma 32. EMBO J. *14*, 2551–2560.

Tripathi, A., Dewan, P.C., Siddique, S.A., and Varadarajan, R. (2014). MazF-induced growth inhibition and persister generation in Escherichia coli. J. Biol. Chem. *289*, 4191–4205.

Tsien, R.Y. (1998). The green fluorescent protein. Annu. Rev. Biochem. *67*, 509–544.

Tsilibaris, V., Maenhaut-Michel, G., and Van Melderen, L. (2006). Biological roles of the Lon ATP-dependent protease. Res. Microbiol. *157*, 701–713.

Udagawa, T., Shimizu, Y., and Ueda, T. (2004). Evidence for the translation initiation of leaderless mRNAs by the intact 70 S ribosome without its dissociation into subunits in eubacteria. J. Biol. Chem. *279*, 8539–8546.

Unterholzner, S.J., Poppenberger, B., and Rozhon, W. (2013). Toxin-antitoxin systems. Mob. Genet. Elem. *3*.

Varghese, S., Tang, Y., and Imlay, J.A. (2003). Contrasting sensitivities of Escherichia coli aconitases A and B to oxidation and iron depletion. J. Bacteriol. *185*, 221–230.

Vázquez-Laslop, N., Lee, H., and Neyfakh, A.A. (2006). Increased persistence in Escherichia coli caused by controlled expression of toxins or other unrelated proteins. J. Bacteriol. *188*, 3494–3497.

Vecerek, B., Moll, I., and Bläsi, U. (2005). Translational autocontrol of the Escherichia coli hfq RNA chaperone gene. RNA N. Y. N *11*, 976–984.

Vecerek, B., Moll, I., and Bläsi, U. (2007). Control of Fur synthesis by the non-coding RNA RyhB and iron-responsive decoding. EMBO J. *26*, 965–975.

Vesper, O., Amitai, S., Belitsky, M., Byrgazov, K., Kaberdina, A.C., Engelberg-Kulka, H., and Moll, I. (2011). Selective translation of leaderless mRNAs by specialized ribosomes generated by MazF in Escherichia coli. Cell *147*, 147–157.

Wang, X., Lord, D.M., Cheng, H.-Y., Osbourne, D.O., Hong, S.H., Sanchez-Torres, V., Quiroga, C., Zheng, K., Herrmann, T., Peti, W., et al. (2012). A new type V toxin-antitoxin system where mRNA for toxin GhoT is cleaved by antitoxin GhoS. Nat. Chem. Biol. *8*, 855–861.

Wassarman, K.M. (2007). 6S RNA: a regulator of transcription. Mol. Microbiol. *65*, 1425–1431.

Waters, L.S., and Storz, G. (2009). Regulatory RNAs in Bacteria. Cell *136*, 615–628.

Wawrzynow, A., Wojtkowiak, D., Marszalek, J., Banecki, B., Jonsen, M., Graves, B., Georgopoulos, C., and Zylicz, M. (1995). The ClpX heat-shock protein of Escherichia coli, the ATP-dependent substrate specificity component of the ClpP-ClpX protease, is a novel molecular chaperone. EMBO J. *14*, 1867–1877.

Williams, J.J., and Hergenrother, P.J. (2012). Artificial activation of toxin-antitoxin systems as an antibacterial strategy. Trends Microbiol. *20*, 291–298.

Williams, C.H., Stillman, T.J., Barynin, V.V., Sedelnikova, S.E., Tang, Y., Green, J., Guest, J.R., and Artymiuk, P.J. (2002). E. coli aconitase B structure reveals a HEAT-like domain with implications for protein–protein recognition. Nat. Struct. Mol. Biol. *9*, 447–452.

Winther, K.S., and Gerdes, K. (2011). Enteric virulence associated protein VapC inhibits translation by cleavage of initiator tRNA. Proc. Natl. Acad. Sci. U. S. A. *108*, 7403–7407.

Wolfinger, M.T., Fallmann, J., Eggenhofer, F., and Amman, F. (2014). ViennaNGS: A toolbox for building efficient next-generation sequencing analysis pipelines. bioRxiv.

Wu, C.-J., and Janssen, G.R. (1996). Translation of vph mRNA in Streptomyces lividans and Escherichia coli after removal of the 5' untranslated leader. Mol. Microbiol. *22*, 339–355.

Yamaguchi, Y., and Inouye, M. (2011). Regulation of growth and death in Escherichia coli by toxin–antitoxin systems. Nat. Rev. Microbiol. *9*, 779–790.

Yonath, A., Leonard, K.R., and Wittmann, H.G. (1987). A tunnel in the large ribosomal subunit revealed by three-dimensional image reconstruction. Science *236*, 813–816.

Youderian, P., and Arvidson, D.N. (1994). Direct recognition of the trp operator by the trp holorepressor--a review. Gene *150*, 1–8.

Yusupova, G., and Yusupov, M. (2014). High-resolution structure of the eukaryotic 80S ribosome. Annu. Rev. Biochem. *83*, 467–486.

Zavialov, A.V., Buckingham, R.H., and Ehrenberg, M. (2001). A posttermination ribosomal complex is the guanine nucleotide exchange factor for peptide release factor RF3. Cell *107*, 115–124.

Zhang, A., Wassarman, K.M., Rosenow, C., Tjaden, B.C., Storz, G., and Gottesman, S. (2003a). Global analysis of small RNA and mRNA targets of Hfq. Mol. Microbiol. *50*, 1111–1124.

Zhang, Y., Zhang, J., Hoeflich, K.P., Ikura, M., Qing, G., and Inouye, M. (2003b). MazF cleaves cellular mRNAs specifically at ACA to block protein synthesis in Escherichia coli. Mol. Cell *12*, 913–923.

Zhang, Y., Zhu, L., Zhang, J., and Inouye, M. (2005). Characterization of ChpBK, an mRNA interferase from Escherichia coli. J. Biol. Chem. *280*, 26080–26088.

Zhou, J., and Rudd, K.E. (2013). EcoGene 3.0. Nucleic Acids Res. *41*, D613–D624.

Zielenkiewicz, U., and Ceglowski, P. (2005). The toxin-antitoxin system of the streptococcal plasmid pSM19035. J. Bacteriol. *187*, 6094–6105.

Appendix

Abbreviations and Symbols

AAA^+ proteases	ATPases associated with various cellular activities
aa-tRNA	aminoacyl-tRNA
Acn	aconitase
Acn	aconitase
Amp	ampiciline
Ara	arabinose
Arg	arginine
aSD	anti Shine-Dalgarno
A-site	aminoacyl site
Asp	aspartate
ATP	adenosine triphosphate
bp	baise pairs
Cam	chloramphenicol
can	canonical
Ccd	coupled cell division
Chp	chromosomal homologs for plasmid-encoded genes
Clp	caseinolytic protease
CP	central protuberance
Dks	DnaK supressor
DNA	desoxy-ribonucleic acid
Dna	DNA binding protein
Doc	death on curing
DS	double strand
eEF	eukaryotic elongation factor
EF	elongation factor
EF-Tu	elongation factor thermo unstable
eIF	eukaryotic initiation factor
EmGFP	Emerald GFP
eRF	eukaryotic release factor
E-site	exit site
Fe^{2+}	iron (divalent ion)
fl	full length
fli	flagellin
fMet-$tRNA_i^{fMet}$	$tRNA_i$ coupled with a formylated methionine
Fts	Filamentation, temperature sensitive
GDP	guanosine diphosphate
GFP	green fluorescent protein
Gho	Ghost cells
GltX	glumamyl-tRNA-synthetase

Gro	Growth of phage
Grp	Growth after phage induction
GTP	guanosine triphosphate
GTP	guanosine triphosphate
HEAT	Huntingtin, EF3, protein phosphatase 2A (PP2A), and yeast kinase TOR1
Hfq	Host factor for Q beta
Hic	HIF contiguous
Hig	host inhibition of growth
Hip	high in persistence
HK	histidine kinase
Hok	host killing
IC	initiation complex
IF	initiation factor
IRE	iron responsive element
IRES	internal ribosome entry sites
IRP	iron regulatory protein
LB	*Luria-Bertani*
ll	leaderless
lmRNA	leaderless mRNA
LSU	large ribosomal subunit
Met-tRNA$_i^{Met}$	initiator tRNA coupled with methionine
min	minutes
miRNA	micro RNA
Mn^{2+}	manganese (divalent ion)
MNase	micrococcal nuclease
Mqs	Motility quorum-sensing
Mre	mecillinam resistance
mRNA	messenger RNA
$NADP^+$/NADPH	nicotinamide adenine dinucleotide phosphate
ncRNA	non-coding RNA
nts	nucleotides
-OH	hydroxyl group
PAA	polyacrylamide
PAGE	polyacrylamide gel electrophoresis
PAP I	poly(A) polymerase
Par	partitioning
PCD	programmed cell death
Phd	prevent host death
P_i	inorganic phosphate
PIC	pre-initiation complex
PNPase	polynucleotide phosphorylase
poly(A)	poly-adenosine
ppGpp	guanosine 3',5'-bis(diphosphate)

PP_i	inorganic pyrophosphate
pppGpp	guanosine 3’-diphosphate, 5’-triphosphate
P-site	peptidyl site
PTC	peptidyl-transferase center
RBS	ribosome binding site
Rel	relaxed
RF	release factor
RNA	ribonucleic acid
RNAP	RNA polymerase
RP	ribosomal protein
RR	response regulator
RT	reverse transcription
Rtc	RNA terminal phosphate cyclase
S	Sverdberg, a unit for sedimentation rate
SD	Shine-Dalgarno
SHX	serine hydroxamate
siRNA	small interfering RNA
SmpB	small protein B
Sok	suppressor of host killing
sRNA	small RNA
ssrA	short stable RNA A
SSU	small ribosomal subunit
TA	toxin-antitoxin
TC	ternary complex
TCA	tricarboxylic acid cycle
TCS	two-component system
TIR	translation initiation region
tmRNA	transfer messenger RNA
TPP	thiamine pyrophosphate
tRNA	transfer RNA
$tRNA_i$	initiator tRNA
UDP-Glc-NAC	uridine diphosphate-N-acetylglucosamine
UTR	untranslated region
Vap	virulent associated protein
ΔTIR	lack of a translation iniitation region

Å	angstrom, a unit of length equal to 10−10 m
α	alpha
β	beta
ω	omega
σ	sigma, used for RNAP subunit
ψ	Phi, used for pseudouridine
ε	epsilon
ζ	zeta

Curriculum vitae

Martina Sauert

martina.sauert@univie.ac.at

EDUCATION

Since 11/2010 **PhD-student** at the Max F. Perutz Laboratories, University of Vienna, Vienna, Austria

PhD-project: "Selective translation of leaderless mRNAs by specialized ribosomes upon MazF-mediated stress in *Escherichia coli*.", Department for Microbiology, Assoz. Prof. Dr. Isabella Moll

10/2005-09/2010 **Studies of Biochemistry** (German Diplom) at University of Regensburg, Regensburg, Bavaria, Germany

Final grade: 1,2 (Excellent)

Diploma-Thesis: "Studies concerning the assembly of the large ribosomal subunit in *S. cerevisiae*", Department for Biochemistry III, Dr. Philipp Milkereit and Prof. Dr. Herbert Tschochner

06/2005 **High School Degree** (German Abitur) at Heinrich-Heine-Gymnasium, Ostfildern-Nellingen, Baden-Württemberg, Germany

Final grade: 1,4 (Excellent)

SCIENTIFIC INTERNSHIPS

11/2008-03/2009 INSERM, Prof. Dr. Gérard Mauco, **Université de Poitiers**, Poitiers, France

"Ischemia reperfusion in renal transplantation"

08/2008-09/2008 Department of Biochemistry and Molecular Biology, Prof. Dr. Ming-Shi Chang , **National Cheng Kung University, Tainan**, Taiwan

"Regulation of IL-20 by hypoxia-inducible factor"

08/2006-09/2006 Department of Physiology, Prof. Dr. Tak-Ming Wong, **University of Hong Kong**, Hong Kong, China

"Ischemia and reperfusion in rat hearts"

SCHOLARSHIPS

11/09/2013 A.T.Kearney Scholarship for the Falling Walls Conference

11/2008-03/2009 Scholarship by the German Academic Exchange Service for internships in European non-ERASMUS institutions

08/2008-09/2008 Scholarship by the Taiwanese National Science Council and the German Academic Exchange Service for the Taiwan Summer School Program

07/2007 Oskar-Karl-Forster Fellowship by the Bavarian Ministry of State

06/2005-06/2006 e-fellows.net fellowship

CAREER-RELATED ACTIVITIES

2014 & 2015	**Falling Walls Lab Vienna:** Organizer Organization of a regional one-day conference with about 50 participants in collaboration with the Falling Walls Foundation, Berlin, Germany
09/26/2014 & 06/06/2014	**"Töne & Moleküle"**, Centre for Molecular Biology and University of Music and Performing Arts, Vienna, Austria Short, unconstrained lectures about science to a non-scientific audience and musical performances
12/05-06/2013	**"WIRE" – Boston Consulting Group**, Berlin, Germany Interdisciplinary workshop for strategy development
2013	**MFPL-CareerDay:** Head of organizing committee Organization of an internal one-day event with workshops and round-table discussions with invited guests for about 100 participants
2011 – 2013	**MFPL-PhD & PostDoc Retreat:** Organizing committee and treasurer
10/2007-07/2010	Elected **students council** and member of the Committee for the Degree Program of Biochemistry at the Faculty for Biology and Medicine, University of Regensburg, Bavaria, Germany

TEACHING

04/2015	Teacher for "Übung IIIA", University of Vienna Conception and preparation of an advanced laboratory course in molecular biology for 16-20 students, including examination
03/2015	Teacher for "Übung IB", University of Vienna Conception and preparation of a basic laboratory course in molecular biology for 16-20 students, including examination
10/2014-	Supervision of a Master thesis, University of Vienna
07/17-08/02/2014	Teacher at **'Deutsche SchülerAkademie'**, Rostock, Mecklenburg-Vorpommern, Germany Teaching a class of 16-18 year old school students in advanced microbiology and antibiotics during a summer school program
04-06/2014	Supervision of a Bachelor thesis, University of Vienna
03 & 11/2014	Tutor for "Übung IIIA" , University of Vienna Conception, preparation and execution of an advanced laboratory course in molecular biology for 16-20 students, including examination
Since 2011	Supervision of altogether 11 students at all levels and from different backgrounds during their laboratory internships

LANGUAGES

German	Native language
English	Fluent, spoken and written
French	Fluent, spoken and written
Spanish	Intermediate level
Chinese	Basic (Mandarin)

CONTRIBUTIONS TO SCIENTIFIC CONFERENCES

11/08/2013	**Falling Walls Lab Finale**, Berlin, Germany Talk: "Breaking the wall of bacterial persister cell formation"
10/10-12/2013	Symposium: RNP Biogenesis and Function, Regensburg, Germany Posters: "Selective translation of the 'leaderless mRNA Regulon' by specialized ribosomes in *E. coli*" "Rrp5p, Noc1p and Noc2p form a protein module which is part of early large ribosomal subunit precursors in *S. cerevisiae*" "Comparative analyses on yeast pre-ribosomal particles to identify and characterize major ribosomal protein assembly events"
07/09-12/2013	ZING Ribosome Conference, Napa Valley, California, USA Poster: "Spotlights on the MazF-mediated modulation of the RNome"
04/24-28/2012	International Symposium on RNA-based Regulation & Ribosome Biogenesis, Frankfurt, Germany Talk and Poster: "Selective translation of leaderless mRNAs by specialized ribosomes generated by MazF in *E. coli*"
09/07-11/2011	EMBO Conference Series on Protein Synthesis and Translational Control, EMBL ATC, Heidelberg, Germany Poster: "Selective translation of leaderless mRNAs by specialized ribosomes generated by MazF in *E. coli*"

SKILLS

Informatics	Microsoft Office, R – biostatistic programming, Illustrator, bibliography, diverse image quantification tools, basic bioinformatics (BLAST, PDB)
RNA methods	RNA-Seq, RNA-seq analysis, ribosome profiling, primer extension, toeprinting, northern, RT-PCR, RNAi, random SELEX
DNA methods	molecular cloning, qPCR, EMSA
Protein methods	western, Co-IP, (semi-quantitative) mass spectrometry, GFP reporter assays, FACS
Model organisms	*E. coli*, *S. cerevisiae*, insect cell culture, diverse mammalian cell cultures, HPV
Social and management skills	presentations, organization, event planning, teamwork, team leadership, project management, teaching, science communication to public

EXTRACURRICULAR ACTIVITIES

Long distance running - half marathon

Rock climbing and hiking

VoiceClub and choir at the University of Vienna

Actress at the Vienna BioCenter – Amateur Dramatic Club

Acoustic guitar

Ballroom dancing

MANUSCRIPTS IN PREPARATION

Sauert, M, Wolfinger, MT, Vesper, O, and Moll, I
"Comparative transcriptome and translatome analysis of the MazF-mediated stress response in *Escherichia coli*."

Sauert, M, Temmel, H, Kollmann, P, Vesper, O, Byrgazov, K, and Moll, I
"A novel AcnB isoform is synthesized in a MazF-dependent manner during stress in *Escherichia coli*."

Temmel, H, **Sauert, M,** Vesper, O, Reiss, A, Martinez, J, and Moll, I
"The *Escherichia coli* RNA ligase RtcB recovers functionally specific ribosomes upon stress release."

Temmel, H, **Sauert, M**, Vesper, O, Reiss, A, Martinez, J, and Moll, I
"The RNA ligase RtcB is involved in the regulation of carbohydrate metabolism and motility in *Escherichia coli*."

PUBLICATIONS

Sauert M, Temmel H, Moll I. (2014)
"Heterogeneity of the translational machinery: Variations on a common theme." *Biochimie. 2014 Dec 24.* Review

Fieber, C, Gratz, N, Koestler, T, Li, XD, Castiglia, V, Janos, M, Aberle, M, **Sauert, M**, Wegner, M, Alexopoulou, L, Kirschning, CJ, Chen, ZJ, von Haesseler, A, Kovarik, P (2015)
"Combined activation of TLR13 and TLR2 is required for protective innate response to *Streptococcus pyogenes* in mice." *PLoS One. In press*

Ohmayer U, Gamalinda M, **Sauert M,** Ossowski J, Pöll G, Linnemann J, Hierlmeier T, Perez-Fernandez J, Kumcuoglu B, Leger-Silvestre I, Faubladier M, Griesenbeck J, Woolford J, Tschochner H, Milkereit P (2013)
"Studies on the assembly characteristics of large subunit ribosomal proteins in *S. cerevisiae*". *PLoS One. 2013 Jul 10;8(7)*

Hierlmeier T, Merl J, **Sauert M** Perez-Fernandez J, Schultz P, Bruckmann A, Hamperl S, Ohmayer U, Rachel R, Jacob A, Hergert K, Deutzmann R, Griesenbeck J, Hurt E, Milkereit P, Baßler J, Tschochner H (2013)
„Rrp5p, Noc1p and Noc2p form a protein module which is part of early large ribosomal subunit precursors in *S. cerevisiae." Nucleic Acids Res. 2013 Jan;41(2):1191-210.*

Tang WH, Kravtsov GM, **Sauert M** Tong XY, Hou XY, Wong TM, Chung SK, Man Chung SS (2010)
"Polyol pathway impairs the function of SERCA and RyR in ischemic-reperfused rat hearts by increasing oxidative modifications of these proteins." *J Mol Cell Cardiol. 2010 Jul;49(1):58-69.*

REFERENCES

MSC MBA Fabien Martins	Administrative director at Max F. Perutz Laboratories, Dr.-Bohr-Gasse 9/6, A-1030 Wien, Austria, phone: +43 14277 24010, email: fabien.martins@mfpl.ac.at
Assoz. Prof. Dr. Isabella Moll	Associate professor at Department for Microbiology, Immunology and Genetics at University of Vienna, Max F. Perutz Laboratories, Dr.-Bohr-Gasse 9/4, A-1030 Wien, Austria, phone: +43 14277 54606, email: isabella.moll@univie.ac.at
Prof. Dr. Herbert Tschochner	Head of Department for Biochemistry III at Universität Regensburg, Universitätsstr. 31, D-93053 Regensburg, Germany, phone: +49 941 9432471, email: herbert.tschochner@vkl.uni-regensburg.de

List of Publications

Sauert M, Temmel H, Moll I. (2014)

"Heterogeneity of the translational machinery: Variations on a common theme." *Biochimie*. *2014 Dec 24.* Review

Fieber C, Gratz N, Koestler T, Li XD, Castiglia V, Janos M, Aberle M, **Sauert M**, Wegner M, Alexopoulou L, Kirschning CJ, Chen ZJ, von Haesseler A, Kovarik P (2015)

"Combined activation of TLR13 and TLR2 is required for protective innate response to *Streptococcus pyogenes* in mice." *PLoS One. In press*

Planned publications

Sauert M, Wolfinger MT, Vesper O, and Moll I

"Comparative transcriptome and translatome analysis of the MazF-mediated stress response in *Escherichia coli*."

Sauert M, Temmel H, Kollmann P, Vesper O, Byrgazov K, and Moll I

"A novel AcnB isoform is synthesized in a MazF-dependent manner during stress in *Escherichia coli*."

Temmel H, **Sauert M,** Vesper O, Reiss A, Martinez J, and Moll I

"The *Escherichia coli* RNA ligase RtcB recovers functionally specific ribosomes upon stress release."

Temmel H, **Sauert M**, Vesper O, Reiss A, Martinez J, and Moll I

"The RNA ligase RtcB is involved in the regulation of carbohydrate metabolism and motility in *Escherichia coli.*"

Acknowledgements

I want to thank Isabella Moll for this very exciting and interesting project she entrusted me with and this great opportunity to work in her lab. Furthermore, Isabella was a great teacher and mentor. She strongly encouraged me in everything I aimed to do (scientifically and non-scientifically) and supported me tremendously by putting a lot of confidence in me. I am very grateful for the time we spent together and looking forward to even more.

In this context I likewise want to thank the whole Moll lab as well as the entire microbiology community on the fourth floor, built by the Bläsi, Görke and Witte labs. Special thanks go to my long-term lab colleagues Oliver Vesper and Hannes Temmel, to Olli for teaching me basically all the lab essentials that I built my work on and to Hannes for a great time in lab that never lacked excitement. I also want to thank Yvonne Göpel for sharing inspiring lunch times and fun free time.

A big thanks is addressed to the RNA community on campus: the DK RNA and the SFB. These communities provided a great platform for scientific discussions during Tuesday seminars or annual retreats, organized workshops and allowed me to travel to several conferences to present my work. Here, I especially want to thank Nicola Wiskocil for her never-ending efforts to support us PhD students with every administrative issue we might come up with. Likewise I want to thank Gerlinde Aschauer for her support in every bureaucratic detail concerning my thesis submission. I also want to thank Michael Wolfinger for his share in all my bioinformatics analyses and especially for the time he took to explain the ‘electrical things’.

Additionally, I thank the MFPL and the University of Vienna not only for hosting me and my thesis but also for supporting many on- and off-campus extracurricular activities, like dragon boat racing, skiing, relay running, the VBC Amateur Dramatic Club, the Voice Club, the Falling Walls Lab, MFPL career day, MFPL PhD and PostDoc retreats, which all together made my time on campus very satisfying.

Now I want to thank my family. First in line, I particularly want to thank my Mom. She has always supported me in my dreams, made me trust in myself, assured me that I can achieve whatever I take up and primarily, she was always proud of me. Now I am very proud myself to proof worthy of this life-long faith. I also want to thank my grandparents and my aunt, uncle and cousins for their support in the last nine years of my education. Special thanks go to my ‘aunt’ Gudrun for so quickly proof reading my introduction!

And finally, thanks to my friends Sophia, Vicky, Thomas, and Volker. Your friendship has ever since been an important anchor in my life and will hopefully accompany me for many more years. The fact that I could always put my faith in you and our friendship helped me through difficult times and thus also supported my thesis.